A Musculoskeletal Model-based Assistance-As-Needed Paradigm for Assistive Robotics

Marc G. Carmichael

Submitted in fulfillment of the requirement
for the degree of Doctor of Philosophy

2013

The Faculty of Engineering and Information Technology
Mechatronics and Intelligent Systems Group

www.uts.edu.au

Supervisor : Prof. Dikai Liu
Co-Supervisor : Prof. Kenneth J. Waldron

Certificate

I, Marc G. Carmichael, declare that this thesis entitled *A Musculoskeletal Model-based Assistance-As-Needed Paradigm for Assistive Robotics* and the work presented in it are my own. I confirm that:

- This work was done wholly or mainly while in candidature for a research degree at this University.
- Where any part of this thesis has previously been submitted for a degree or any other qualification at this University or any other institution, this has been clearly stated.
- Where I have consulted the published work of others, this is always clearly attributed.
- Where I have quoted from the work of others, the source is always given. With the exception of such quotations, this thesis is entirely my own work.
- I have acknowledged all main sources of help.
- Where the thesis is based on work done by myself jointly with others, I have made clear exactly what was done by others and what I have contributed myself.

Signed: Production Note:
Signature removed prior to publication.

Date: 07/01/2013

Acknowledgements

This work would not have been possible without the encouragement and support of many, many others around me.

I would firstly like to thank my supervisor Prof. Dikai Liu for the opportunity to work on this topic and the support you provided throughout. Your direction, motivation and the perfect amount of pressure allowed me to accomplish this significant milestone in my life.

To my co-supervisor Prof. Kenneth Waldron, and to Dr. Gabriel Aguirre-Ollinger for all of your advice and expertise. It was an immense help and contributed greatly to the completion of this work.

To all the professors, researchers, engineers and students at the Centre for Autonomous Systems. I am glad to have had the opportunity to work in an environment surrounded by such clever and motivated people. You made my time a whole lot more enjoyable, and your support assured me that everything was going to work out, eventually.

Lastly to my friends, family, and loved ones. This commitment has occupied the majority of my life over the past years. Even with the little time I have been able to give you, I continued to receive encouragement, support and understanding throughout it all. For that I am extremely thankful.

Contents

List of Tables

List of Figures

Nomenclature

Formatting Style

Formatting	Description
$[\cdots]^T$	Vector or matrix transpose
$\|\cdots\|$	Vector norm
$\|\cdot\|$	Scalar absolute value

Subscript and Numbering

Symbol	Description
k	Number of degrees of freedom in the musculoskeletal system
m	Number of MTU models in the musculoskeletal system
$\mathbb{N}_1$	Set of natural numbers $\{1, 2, 3, 4, \dots\}$

Symbol Usage

Symbol	Description	Units
α	Muscle fibre pennation angle	rad
α_0	Muscle fibre pennation angle at optimal length L_0^m	rad
ε^t	Tendon strain	-
σ	Standard deviation	-
$\boldsymbol{\theta}$	Robot measured joint position vector	rad
$\dot{\boldsymbol{\theta}}$	Robot measured joint velocity vector	rad/s
$\boldsymbol{\theta}_r$	Robot reference joint position vector	rad
$\dot{\boldsymbol{\theta}}_r$	Robot reference joint velocity vector	rad/s
a	MTU activation	-
$\mathbf{a}$	MTU activation column vector	-
A	Robot assistance parameter	-
b	Robot admittance gain	$\mathrm{m.s^{-1}/N}$
$\mathbf{C}$	Coriolis and centripetal effects	N.m
f_A^m	Active force component in muscle fiber	N
f_P^m	Passive force component in muscle fiber	N
f^t	Tendon force	N
f^M	MTU force	N
$\mathbf{f}$	MTU force column vector	N
$\mathbf{f}^A$	MTU active force column vector	N
$\mathbf{f}^P$	MTU passive force column vector	N
$\tilde{f}_A^m(\cdot)$	Normalised MTU fiber active force-length function	-
$\tilde{f}_P^m(\cdot)$	Normalised MTU fiber passive force-length function	-
$\tilde{f}_V^m(\cdot)$	Normalised MTU fiber force-velocity function	-
$\tilde{f}^t(\cdot)$	Normalised MTU tendon force-strain function	-

F_0^m	Maximum isometric muscle fiber force	N
F^E	Scalar magnitude of external force	N
$\mathbf{F}_H$	Measured force vector between robot and human operator	N
$\mathbf{F}_E$	Measured force vector between robot and the task	N
$\mathbf{H}$	Mass matrix of the musculoskeletal dynamic system	kg.m^2
$\mathbf{J}$	Robot kinematic Jacobian matrix	-
$\mathbf{J}_v$	Musculoskeletal kinematic Jacobian matrix	-
$\mathbf{K}_A$	Activation-to-force gain matrix	N
K_D	Derivative gain in robot PD controller	-
K_P	Proportional gain in robot PD controller	-
$\mathbf{K}_\tau$	Activation-to-torque gain matrix	N.m
$\mathbf{K}_{\tau i}$	The i-th row of matrix $\mathbf{K}_\tau$	N.m
l^M	MTU length	m
$\dot{l}^M$	MTU velocity	m/s
$\mathbf{l}$	MTU length column vector	m
$\dot{\mathbf{l}}$	MTU velocity column vector	m/s
l^m	MTU fiber length	m
$\tilde{l}^m$	Normalised MTU fiber length	-
$\dot{l}^m$	MTU fiber velocity	m/s
$\tilde{\dot{l}}^m$	Normalised MTU fiber velocity	-
l^t	Tendon length	m
L_0^m	MTU fiber optimal length (coinciding with F_0^m)	m
L_s^t	MTU tendon slack length	m
$\mathbf{L}$	MTU Jacobian matrix	-
$\mathbf{M}$	Mass matrix of the robot dynamic system	kg.m^2
q	Generalised coordinate position	rad

$\dot{q}$	Generalised coordinate velocity	rad/s
$\ddot{q}$	Generalised coordinate acceleration	rad/s^2
$\mathbf{q}$	Generalised coordinate position column vector	rad
$\dot{\mathbf{q}}$	Generalised coordinate velocity column vector	rad/s
$\ddot{\mathbf{q}}$	Generalised coordinate acceleration column vector	rad/s^2
r_i	The i-th element of vector $\mathbf{r}$	m
$\mathbf{r}$	External force moment-arm column vector	m
s	MTU activation upper bound	-
$\mathbf{s}$	MTU activation upper bound column vector	-
S_P	Strength capability of a human operator	N
$S_P^{\max}$	Strength upper bound used to limit S_P	N
S_T	Strength requirement of a task	N
τ^M	Muscular joint torque	N.m
$\boldsymbol{\tau}^M$	Muscular joint torque column vector	N.m
$\boldsymbol{\tau}^A$	Active muscular joint torque column vector	N.m
τ_i^P	The i-th element of vector $\boldsymbol{\tau}^P$	N.m
$\boldsymbol{\tau}^P$	Passive muscular joint torque column vector	N.m
τ_i^B	The i-th element of vector $\boldsymbol{\tau}^B$	N.m
$\boldsymbol{\tau}^B$	Dynamic and gravity load torque column vector	N.m
$\boldsymbol{\tau}^G$	Gravity load torque column vector	N.m
$\boldsymbol{\tau}^E$	External load torque column vector	N.m
$\mathbf{u}$	Unit vector representing external force direction	-
V_0^m	MTU fiber maximum contractile velocity	m/s

Abbreviations

AAN	Assistance As Needed
ADL	Activities of Daily Living
CV	Coefficient of Variation
EMG	Electromyography
IAD	Intelligent Assist Device
MM	Musculoskeletal Model
MSD	Musculoskeletal Disorder
MTU	Musculo-Tendon Unit
MVC	Maximum Voluntary Contraction
SM	Strength Model
TM	Task Model

Abstract

A Musculoskeletal Model-based Assistance-As-Needed Paradigm for Assistive Robotics

Robotic systems which operate collaboratively with their human operators to provide assistance are becoming reality, and many different paradigms for administering this assistance have been developed. A promising paradigm is Assistance-As-Needed, which aims to provide physical assistance specific to the individual requirements of the operator. This requires that the needs of the operator be determined, which is challenging as they depend on both the task being performed, and the capability of the operator to perform it. Current solutions use performance-based methods which critique the operator from observations obtained during tasks, and then adapt assistance based on how they performed. This approach has shown success in applications such as robotic rehabilitation. However, empirical performance-based methods have inherent limitations, primarily due to the numerous observations required before the operator's assistance needs can be determined. The ideal Assistance-As-Needed paradigm should be able to determine the operator's assistance requirements without prior observations, and with respect to arbitrary tasks.

This thesis presents a novel Assistance-As-Needed paradigm using models to estimate the assistance needs of the human operator. An optimisation model is developed which utilises a publicly available musculoskeletal model representing the human upper limb to estimate their strength, which is compared to the strength required by the task being performed to gauge their assistance requirements. An advantage of this model-based

approach is it allows effects on the operator's assistance requirements due to task and physiological factors to be predicted. Furthermore, it avoids many of the limitations faced by empirical performance-based approaches since it does not require empirical observations. The model-based paradigm is demonstrated and evaluated in a number of simulated tasks involving the upper limb. Calculated upper limb strength is analysed with respect to factors such as the limb position, the direction of force at the hand, and muscular impairment. The calculated strength is shown to predict behaviours similar to those described in the literature. Experimental evaluation is performed by implementing the paradigm on a specially developed robotic exoskeleton to govern the assistance it provides a subject in a number of experimental tasks. The model-based Assistance-As-Needed paradigm is shown to successfully govern assistance towards specific muscles when needed in the tasks performed. Means of improving the paradigm, including methods for fitting the model to the subject, and the inclusion of additional physiological factors in the calculation of their assistance requirements is discussed.

Chapter 1

Introduction

There is much interest in the development of robots that interact and operate in physical contact with humans. These systems can provide assistance to their human operators as they both work collaboratively to perform physical tasks. For tasks which are physically intensive like those in industry, robots can assist workers and reduce the risk of injury. Likewise in health care, robots can assist care givers during the physically demanding task of patient handling. Another application is robotic rehabilitation where patients receiving treatment for conditions such as stroke are assisted by a robotic system as they perform physical therapy. Physically assistive robotic systems continue to be developed for an increasing variety of applications. The success of such technology relies on the robot providing assistance suited to the application, with some requiring assistance to be administered in a specific manner in order for the desired benefits to be achieved. Many different paradigms for providing a human with physical robotic assistance have been developed and continues to be an ongoing topic of research.

A promising paradigm is Assistance-As-Needed (AAN) which aims to provide a human with assistance specific to their requirements with respect to the task being performed. This paradigm has been shown to achieve better outcomes in certain applications when compared to alternative assistance paradigms. For a robot to assist its human operator according to their individual requirements necessitates that these assistance requirements first be determined. The assistance required is dependent on both the task being

performed and the capability of the operator to perform it. Determining an operator's capability is a challenge because human capability is highly complex and variable. A solution is to utilise empirical approaches which observe and critique the performance of the operator performing tasks. A measure of their assistance requirements is then derived from how well the tasks were executed. This is sometimes referred to as *performance-based* assistance and has shown success in providing assistance well suited to the needs of the operator. However empirical performance-based approaches have inherent disadvantages. Numerous observations of previous task performances are needed to gauge the operator's assistance requirements, before which either excessive or insufficient assistance can be provided. Performance-based AAN also requires the tasks to be well defined to be able to critique them based on some performance criterion.

This thesis presents a new AAN paradigm utilising models to estimate the assistance requirements of the human operator. It combines a task-requirement model with an operator-capability model to calculate how capable the operator is at performing desired tasks. An estimate of the assistance required by the operator can then be derived and subsequently used to govern the assistance provided by a robot during task execution. A benefit of this approach is that no observations are needed to estimate an operator's assistance requirements, avoiding the limitations associated with empirical AAN methods. A musculoskeletal model is used to represent the physical capabilities of the operator. An optimisation model is developed to calculate the strength of the operator taking into consideration limb pose, muscular impairment, and interaction forces during task execution. The operator's estimated strength is compared with the strength required to perform the task to gauge their assistance requirements.

1.1 Background and Motivation

Modern robotics have been utilised to assist humans ever since they were first put into service for General Motors in 1961 [Hägele *et al.*, 2008]. However only recently are robotic systems which physically interact with humans being realised, and their introduction into practice becoming reality. Traditional industrial robots, like those

shown in Figure 1.1a do not physically interact with humans, rather they assist by performing on our behalf repetitive, labour intensive tasks. Inherent safety risks require that they remain isolated from any direct human contact whilst in operation.

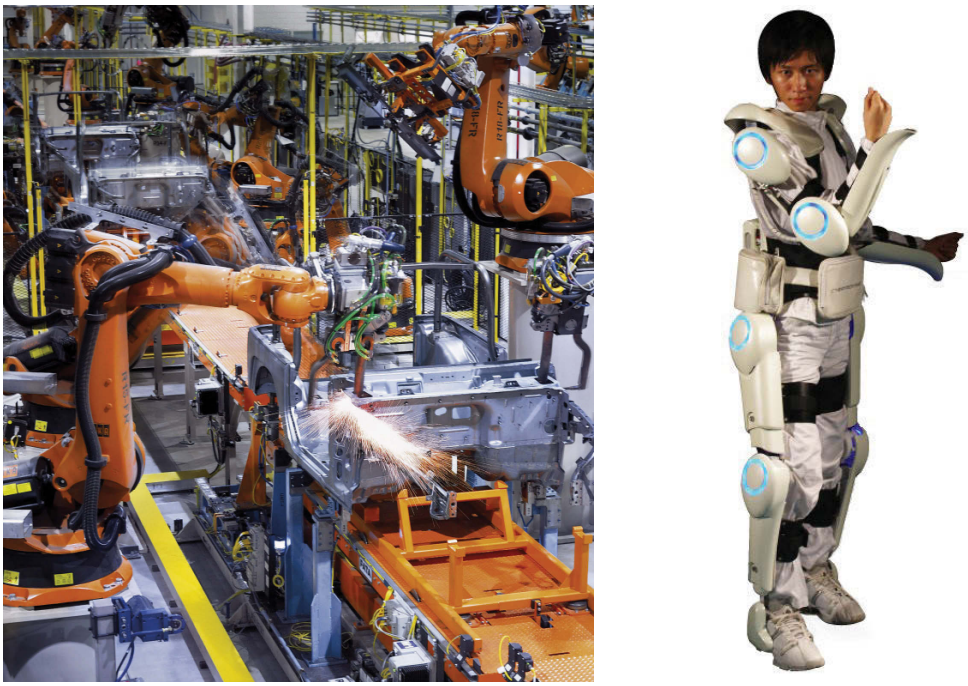

(a) **(b)**

Figure 1.1: Examples of robotic systems. (a) Traditional robot manipulators used in industry (`www.kuka.com`). (b) Hybrid assistive limb (HAL) full-body exoskeleton, developed by Cyberdyne Inc (`www.cyberdyne.jp`).

The desire to have robots and humans work together has resulted in the research field of physical human-robot interaction, with ensuring human safety being of primary concern [De Santis *et al.*, 2008]. New robotic methodologies such as low inertia [Hirzinger *et al.*, 2002; Zinn *et al.*, 2004], mechanically compliant [Bicchi and Tonietti, 2004; Pratt and Williamson, 1995], or actively compliant [Hirzinger *et al.*, 2001] robotic systems have resulted in practical solutions that satisfy the tradeoff between ensuring safety whilst maintaining performance. The result has been a paradigm shift, with robots emerging out from the isolated confinements of traditional industry applications to operate alongside and collaboratively with humans in industrial, nonindustrial and domestic domains.

Many manual tasks performed in industry are physically intensive and hence the risk of injuries such as Musculoskeletal Disorders (MSD) are high. MSD are conditions involving nerves, tendons, muscles, and the skeleton [U.S. Department of Health and Human Services, 1997] accounting for 130 million health care encounters and cost between $45 to $54 billion dollars annually in the United States [National Research Council *et al.*, 2001]. Causes include the repeated and prolonged performance of tasks, particularly those requiring large physical exertion, or a mismatch between the task's physical demand and the person's biological compatibility [Kumar, 2001]. With safe and practical solutions available, physically assistive robots such as intelligent assist devices (IAD) [Colgate *et al.*, 2003] and exoskeletons [Brown *et al.*, 2003; Dollar and Herr, 2008; Kawamoto *et al.*, 2003] like that shown in Figure 1.1b are being developed. Such technologies can mitigate the risks leading to MSD and other injuries, providing large personal and societal benefits.

Continuing research is also seeing physically assistive robots being developed for more exotic applications outside of traditional industry. The use of robotics in health care is gaining attention, largely driven by the realisation that populations around the world are ageing [United Nations. Dept. of Economic and Social Affairs. Population Division, 2002]. In Australia the population aged over 65 will increase from 13% in 2007 to an estimated 23% in 2056, with a decline in the working population [Australian Bureau of Statistics, 2009]. This difference in age distribution is illustrated in Figure 1.2. Pressure from an ageing population requiring increased health services, combined with a decreasing working population capable of providing it will have significant implications on existing health care systems [Swan, 2010]. Robotics has been identified as a technology capable of mitigating the health care burdens of an ageing population by assisting in a number of health care tasks benefiting both health providers and patients [Flandorfer, 2012; Meng and Lee, 2006; Sparrow and Sparrow, 2006]. For instance, occupations involving patient handling have the highest incidence of MSD for any occupational group due to their physical demands [Morse *et al.*, 2008]. Robotic systems are being developed to physically assist nurses during patient handling in anticipation of population ageing [Hu *et al.*, 2011a; Yamamoto *et al.*, 2004]. Another application

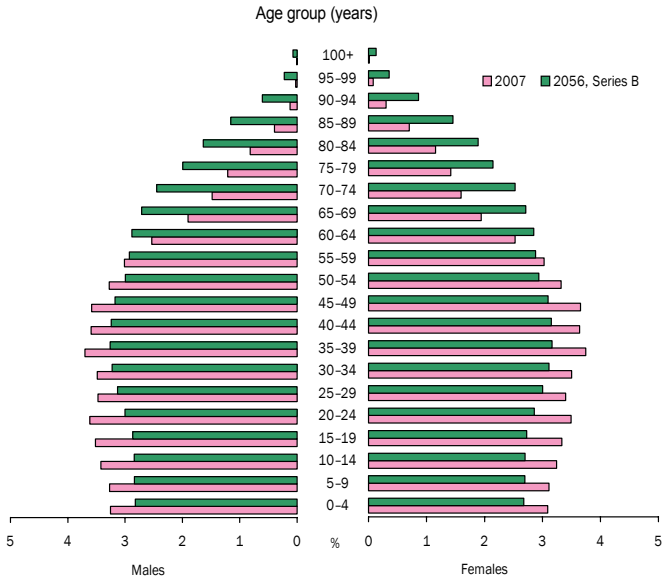

Figure 1.2: Age distribution forecast in Australia from 2007 to 2056. Graph reproduced from [Australian Bureau of Statistics, 2009].

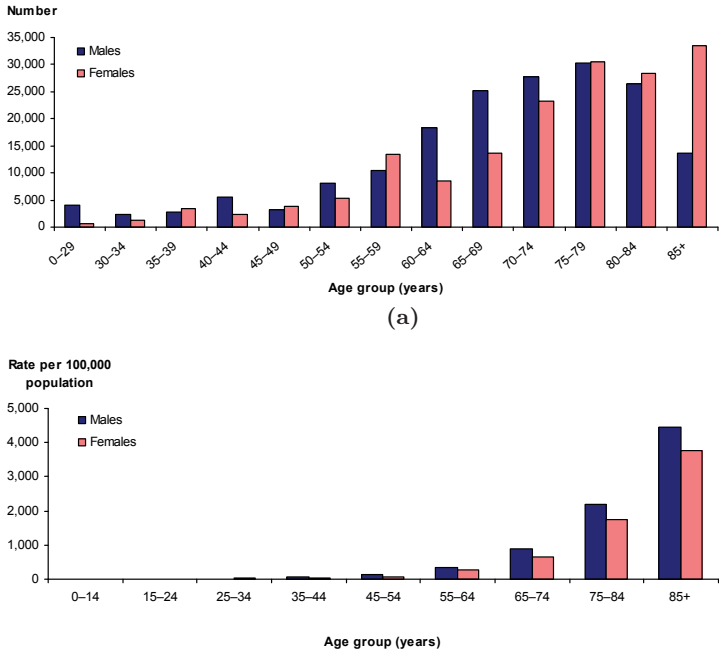

Figure 1.3: Stroke in Australia, by age and sex. (a) Prevalence in 2003. (b) Incidence in 1997. Graphs reproduced from [Senes, 2006].

is the rehabilitation and management of physically incapacitating disabilities such as stroke. Stroke is a leading cause of adult disability in the United States [Lloyd-Jones *et al.*, 2009] with direct medical cost of $28.3 billion annually [Heidenreich *et al.*, 2011]. With incidence increasing with age (shown in Figure 1.3) the prevalence in the US is forecast to increase by 24.9% between 2010 and 2030, and increase the direct annual costs by 238% [Heidenreich *et al.*, 2011]. Much cost results from long term management as 15%-30% of sufferers are left permanently disabled, with 20% still requiring institutional care three months after injury [Lloyd-Jones *et al.*, 2009]. Studies using robots during therapy for disabilities such as stroke have shown benefits when compared to little therapy [Takahashi *et al.*, 2008] or conventional non-robotic therapy [Coote *et al.*, 2008; Hesse *et al.*, 2005; Housman *et al.*, 2009; Lum *et al.*, 2002; Pohl *et al.*, 2007].

There is clear motivation to utilise physically assistive robots for industrial and health care applications. However for such technology to be beneficial it is essential that they operate in a manner suitable for the application. This can require assistance to be provided in a particular way, otherwise the desired benefits are not realised and outcomes may be worse than without using the technology all together. Consider a robot providing interaction forces to assist in lifting heavy objects. If the *wrong* forces are provided (e.g. forces that don't contribute towards a desired objective) then the technology may provide more hindrance than assistance. Alternatively, in specific applications unique benefits may be achieved by providing assistive forces in an ingenious manner. Kazerooni [1998] describes an exoskeleton-type robot assisting in a jackhammer task. Acting as a mechanical interface between the tool and operator, the robot can be programmed to reflect only the low-frequency forces to the operator to remove the high-frequency components which produce fatigue [Kazerooni, 1998]. This achieves different benefits compared to attenuating jackhammer forces without removing the high frequency component. Another example is robotic rehabilitation where it is essential that assistance be provided in such a way to promote recovery. Utilising a suitable assistance paradigm is instrumental to the rehabilitation of the patient [Cai *et al.*, 2006; Hogan and Krebs, 2004]. Inappropriate assistance paradigms can produce worse results when compared to traditional non-robotic therapy [Hidler *et al.*, 2009; Hornby *et al.*, 2008]. This demon-

strates how different techniques for providing robotic assistance can produce different benefits, or determine if any benefit is achieved at all.

The Assistance-As-Needed (AAN) paradigm is an example of providing physical assistance in a specific manner. Providing assistance specific to the needs of the operator can achieve certain benefits and be used to meet higher objectives relating to the application. For example in many applications an objective is to encourage the operator to contribute in the task being performed by providing the minimum amount of assistance the operator requires to successfully perform it. This AAN paradigm has achieved greater outcomes when compared to other assistance paradigms for specific applications. For example to achieve efficacious neurorehabilitation following a stroke it is essential that the patient actively participates during therapy [Hogan *et al.*, 2006]. AAN which promotes active participation by limiting assistance to the minimum the patient requires has been shown to be well suited for this application. The AAN paradigm is also applicable in other applications, for example Lynch *et al.* [2002] discusses a paradigm for materials handling. The robot enforces motion constraints only in specific directions the operator requires assistance due to little control or high risk of injury.

1.2 Research Question

Although the AAN paradigm has been shown to be well suited for specific applications, there are challenges in developing robotic systems which provide assistance based on the specific requirements of the operator. A measure of their assistance requirements is needed, and obtaining this measure is difficult. Firstly the assistance the operator requires depends on the task being performed. The more difficult a task is to accomplish, the more assistance required to perform it. Furthermore the task's requirements can vary, either inherently during its execution, or from external disturbances. A worker performing a materials handling task requires greater assistance the heavier the load being lifted. A stroke patient supporting their upper limb against gravity has a reduced range of motion because certain limb positions require more strength than they can exert. The strength requirements of this task, and hence the assistance requirements

of the patient change depending on their limb position. Such variations should be accounted for when providing assistance as needed.

Secondly, the needed assistance also depends on the capability of the operator to perform the task. This introduces challenges as the capability of a person in performing physical tasks varies amongst the population [Amell, 2004]. For applications in health care where the operator has an impairment, variation in physical capability is further exacerbated [Arva *et al.*, 2004; Bohannon and Andrews, 1987; Mercier and Bourbonnais, 2004]. Other factors, both physiological and task related affect the ability to accomplish physical tasks. Limb posture, motion, external forces, and fatigue are some examples. Overall the human body is a highly complex system and estimating the physical capability of an individual is a challenge.

A solution is to use empirical *performance-based* methods to determine the assistance an operator requires when performing tasks [Emken *et al.*, 2005; Krebs *et al.*, 2003; Wolbrecht *et al.*, 2007, 2008]. These approaches critique the operator as tasks are executed to derive a performance measure, which is subsequently used to adapt robotic assistance. The better the operator is judged to have performed, the less assistance it is deemed they require, and assistance is adjusted accordingly. A disadvantage of this approach is that numerous observations of tasks being executed are required. The robot is essentially required to learn the appropriate assistance to provide based on observation. This learning can take time, during which the assistance may be either insufficient or excessive in relation to the operator's true requirements. If a disturbance (e.g. an external force) is introduced, the system learns its effect on the assistance requirements of the operator based on changes in their task performance. Again this requires observations before it can adapt accordingly to the disturbance. If assisting in a number of different tasks, each task's requirements as well as the capability of the operator to perform each task is likely to be unique. This requires more observations for the more variations of tasks to be assisted. Furthermore it is required that the tasks are well defined so they can be critiqued and a measure of the operator's performance during the task's execution can be derived. In an industrial or rehabilitation context this is acceptable as applications commonly involve the repeated execution of a few, well

defined tasks. However is it desirable (or even inevitable) that in the future physically assistive robotic technology will be used outside of such structured environments to assist workers performing manual duties, or the incapacitated during activities of daily living. In this scenario the robot is required to assist in numerous variations of tasks, with operators requiring different levels of assistance for each.

The ideal Assistance-As-Needed system would be capable of determining the appropriate assistance the operator requires, specific for each task and for the individual operator. Furthermore it would not be limited to tasks for which observations of past performances are available. If a disturbance is measured or anticipated, it would be able to predict its effect on the assistance requirements of the operator and adjust accordingly. These features require the use of a model to be able to predict assistance requirements.

1.3 Scope

The work in this thesis investigates a model-based Assistance-As-Needed paradigm for physically assistive robots. The paradigm utilises two models as the basis for estimating the assistance requirements of a human operator for desired tasks. The first model represents the task being performed and is used to calculate the physical strength capabilities required in order for it to be performed. The second model represents the human operator and is used to estimate their individual physical strength capability with respect to the desired task. Results of the two models are combined to gauge the assistance required by the operator, and subsequently used to control a robotic system providing assistance.

A musculoskeletal model is used to represent the operator with their physical capability defined at the muscular level. An optimisation model is developed which applies this muscular capability towards the desired task. With a model that adequately represents the operator, effects from limb position, movement, impairment, task variation, and other factors can be calculated. The advantage of this approach is that factors affecting the operator's assistance requirements can be predicted, without the need for previous

observation or measurement of task performances. Furthermore since the capability of the operator is represented at the muscular level and is independent of the task being performed, their assistance requirements for arbitrary tasks can be estimated and is not limited to tasks for which previous observations are available.

The use of a model representing a system as complex as the human body raises many questions. This thesis investigates the feasibility of using a musculoskeletal model to estimate the capability of a human operator, and subsequently govern robotic assistance. The development of musculoskeletal models or their adaption to represent a human operator is outside the scope of this work, but is considered for future work. The scope is limited to assisting the upper limb only, however wider use of the approach presented may be applicable (e.g. for the lower limbs). Strength is used as the measure representing the operator's assistance need. It is understood that other factors, not just strength, are involved in the ability to accomplish tasks. Such factors are not incorporated in this present work, but their consideration in future work is discussed. The AAN paradigm has gained attention in the field of rehabilitation robotics and hence many references will be made to this specific application. However the model-based AAN paradigm this thesis presents is not limited to this, with potential benefits in many applications where robotic assistance based on the operator's physical capabilities is required.

1.4 Contributions

The following are the main contributions from the work presented in this thesis:

- Development and demonstration of a framework for model-based robotic Assistance-As-Needed consisting of two models to estimate the assistance requirements of a human operator with respect to desired tasks.
- An optimisation model is developed utilising a musculoskeletal model to estimate the physical strength capabilities of a human's upper limb at the hand. Application of this model to estimate the effects of limb pose, task variation, and physical

impairment on a subject's strength is presented. The calculated effects on strength were consistent with behaviours described in the literature and with anticipated results.

- A technique for analysing how physical impairment at the muscular level affects a subject's capability for performing physical tasks. This technique allows the magnitude of an impairment and its distribution across different muscles to be analysed in terms of its effect on a person's strength at their hand, and their assistance requirements for different tasks. It also allows analysis of the tasks most affected by different muscular impairments.
- Practical evaluation of the model-based Assistance-As-Needed paradigm utilising a musculoskeletal model. A robotic exoskeleton platform was specially developed to implement the paradigm. The robot provided assistance to a subject performing a number of experimental tasks as the model-based AAN paradigm attempted to adapt assistance to their specific physiological needs. Results showed that assistance was targeted towards the requirements of the subject, giving promise to the proposed paradigm and encouraging future research.
- Development of an experimental robotic exoskeleton platform specially designed for evaluation of the model-based AAN paradigm. The platform is capable of providing controllable assistance to the upper limb during physical tasks. Analysis demonstrated the suitability of using virtual loads to evaluate utilising the robot to assist in numerous tasks with variations. This platform is a valuable tool for research and continues to be used.

The following list are publications resulting from the research presented in this thesis:

- Carmichael, M.G., Liu, D., *Estimating Physical Assistance Need Using a Musculoskeletal Model*, IEEE Transactions on Biomedical Engineering, volume 60, pp.1912-1919, 2013.

- Carmichael, M.G., Liu, D., *Experimental Evaluation of a Model-based Assistance-As-Needed Paradigm using an Assistive Robot*, Engineering in Medicine and Biology Society, EMBC, 2013 Annual International Conference of the IEEE , pp.866-869, Jul. 3 2013-Jul. 7 2013.
- Carmichael, M.G., Liu, D., *Admittance Control Scheme for Implementing Model-based Assistance-As-Needed on a Robot*, Engineering in Medicine and Biology Society, EMBC, 2013 Annual International Conference of the IEEE , pp.870-873, Jul. 3 2013-Jul. 7 2013.
- Carmichael, M.G., Liu, D., *A Task Description Framework for Robotic Rehabilitation*, Engineering in Medicine and Biology Society, EMBC, 2012 Annual International Conference of the IEEE , pp.3086-3089, Aug. 28 2012-Sept. 1 2012.
- Carmichael, M.G., Liu, D., *Towards Using Musculoskeletal Models for Intelligent Control of Physically Assistive Robots*, Engineering in Medicine and Biology Society, EMBC, 2011 Annual International Conference of the IEEE , pp.8162-8165, Aug. 30 2011-Sept. 3 2011.
- Carmichael, M.G., Liu, D., Waldron, K.J., *Investigation of Reducing Fatigue and Musculoskeletal Disorder with Passive Actuators*, Intelligent Robots and Systems (IROS), 2010 IEEE/RSJ International Conference on , pp.2481-2486, 18-22 Oct. 2010.

1.5 Thesis Structure

Chapter 2 reviews work related to the model-based AAN paradigm this thesis presents. Existing approaches for controlling assistive robots and the assistance they provide are reviewed, with a focus on the Assistance-As-Needed paradigm. Current AAN methodologies are described including the challenges they face and their limitations. The methodologies used in musculoskeletal modelling are also reviewed.

Chapter 3 presents the framework for model-based AAN used for estimating the assistance requirements of a person performing physical tasks. A generalisation of the

AAN paradigm is used as the basis for the framework which uses models to calculate task requirements and human capabilities. Two case studies simulating upper limb tasks demonstrate the framework, and how it can be used to estimate the assistance requirements of a person with respect to physical tasks.

Chapter 4 develops an optimisation model to estimate the capability of a human to perform physical tasks. The optimisation utilises a musculoskeletal model to calculate the strength of a human's upper limb at the hand in directions the task requires. The model is used to estimate strength and how it is affected by limb pose, direction of external force during task execution, and muscular impairment. Evaluation of the estimated upper limb strength produced qualitative results consistent with the literature.

Chapter 5 implements the model-based AAN paradigm on a specially developed upper limb robotic exoskeleton. The robot assists a subject performing tasks with the model-based AAN paradigm governing the assistance the robot provides. Evaluation of the paradigm is made on its ability to target assistance towards the subject's muscles defined as impaired when they are required by the tasks performed.

Chapter 6 summarises the work presented in this thesis and its contributions. The outcomes of this work and topics for future work are discussed.

Chapter 2

Related Work

This chapter reviews work related to the model-based Assistance-As-Needed (AAN) paradigm that is presented in this thesis. Section 2.1 introduces examples of assistive robotic systems currently available or being developed for various applications. Focus is on systems which provide physical assistance, however other forms of assistive robot are also presented.

Section 2.2 provides a non-exhaustive review of control methodologies commonly utilised by robotic systems to provide physical assistance. Different control schemes and their suitability for use in applications where robot and human are in physical interaction are discussed. Assistance paradigms operating above these control schemes to govern their assistance are also reviewed, with a focus on the AAN paradigm.

Section 2.3 reviews the methodologies used in musculoskeletal modelling. The model-based AAN paradigm developed in this thesis makes use of musculoskeletal models to estimate the physical capabilities of the human operator, and hence a background is required. Applications using musculoskeletal models are also detailed.

2.1 Assistive Robotics

Robots provide assistance to humans in many different forms and for a wide range of applications. This thesis relates to robots that provide assistance in the AAN paradigm which inherently expects the operator to contribute (when possible) to the task being performed. Hence AAN is typically used for applications where the human and robot work collaboratively to perform physical tasks. This section presents examples of assistive robotic systems used in a number of different applications, with a focus on physically assistive systems relevant to the AAN paradigm. Some examples of assistive robots less relevant to AAN are also described.

2.1.1 Industry

Modern robotic systems were first designed for industry, so it is not surprising that the first examples of robots working in physical collaboration with humans were developed for industrial applications. A common motivation for robotics in industry is to reduce the risk of injury inherent in physically intensive tasks. A form of robot often used to meet this objective is the Intelligent Assist Device (IAD). IADs are single or multi-axis devices that assist their human operators by providing a variety of benefits such as strength augmentation and motion guidance [Colgate *et al.*, 2003]. The strength and endurance of the robot is exploited while the human operator provides the signals required for fine motion control. A common form of IAD is an overhead hoist mounted on a ceiling, wall, or gantry like that shown in Figure 2.1a. It uses an actuated cable to reduce the effective weight of lifted objects, controlled by the movements of the operator's hands detected using sensors. The operator is proximate to the load being lifted and controls the task via direct physical interaction with either the robot or the load itself. This gives the operator the advantage of immediate apprehension as tasks are performed, allowing easy correction of minor issues (e.g. obstructions such as cables during assembly) and provides haptic feedback [Bicchi *et al.*, 2008]. This is in contrast to teleoperation where the operator is distanced from the task and controls the robot by other means, such as a joystick or a master device.

Advancements in robotics are seeing more sophisticated systems such as robotic exoskeletons and human extenders being developed. Exoskeletons like that shown in Figure 2.1b can be considered as a less structured form of IAD, having a kinematic design matching that of its operator allowing it to follow their motions. Like IADs they can assist workers performing physical tasks. The Wearable Agri-Robot [Toyama and Yamamoto, 2009] is a full body exoskeleton designed for farming tasks required to be performed by hand. Development is motivated by increasing pressures expected to be placed on the agriculture industry due to an ageing population. The robot has 10 active joints (shoulders, elbows, hips, knees, ankles) actuated by motors and has a total weight of 30kg.

(a) **(b)**

Figure 2.1: Physically assistive robotic systems for industrial applications. (a) Intelligent Assist Device (IAD) [Colgate *et al.*, 2003]. (b) The Wearable Agri-Robot exoskeleton [Toyama and Yamamoto, 2009].

2.1.2 Assisted daily living

Robots can be used to assist during activities of daily living. Many robotic systems are being developed for applications in elderly care, largely due to the population ageing that is predicted around the world. Honda has developed assistive devices to assist with walking [Honda, 2009]. The Stride Management Assist (Figure 2.2a) is a wearable device designed for people who have weakened leg muscles but are still capable of walking. The

system weighs 2.8kg and provides assistance to the hips using two brushless DC motors. Sensors measuring hip angle are used to provide cooperative assistance which lengthens and regulates the wearer's walking stride making it easier to walk. Another device is the Bodyweight Support Assist (Figure 2.2b) designed to assist persons who have weakened leg muscles, or healthy persons during physically demanding tasks. Weighing 6.5kg, the system uses motors to help support a percentage of the wearer's body weight, reducing the load in the hips, knees and ankles during activities such as walking, climbing or descending stairs, or standing in semi-crouched positions. Both systems operate for approximately 2 hours powered by a rechargeable lithium ion battery.

(a) **(b)**

Figure 2.2: Walking assist devices from Honda (www.walkassist.honda.com). (a) Stride Management Assist device. (b) Bodyweight Support Assist device.

Wearable robots can assist persons with physical impairments to replace the functionality lost in their impaired limbs. The Independent Walk Assist (Figure 2.3a) is being developed by Toyota to support independent walking for people whose ability to walk has been impaired from leg paralysis or other causes. Mounted on the impaired limb it detects the wearer's intention using thigh position and foot load sensors. It then assists bending of the knee as the leg is brought forward to facilitate natural walking and provide reliable support when body weight is supported by the knee. The system weighs 3.5kg and is aimed for commercialisation from 2013 [Toyota, 2011].

Providing assistance to both the upper and lower body is the HAL-5 (Hybrid Assistive Limb) full body exoskeleton [Kawamoto *et al.*, 2003; Sankai, 2011] shown in Figure 2.3b. Sensors are used to measure joint angle, acceleration, and floor reaction force. It also uses bioelectrical sensors to measure the wearer's muscle activity from which their own joint torque is estimated, and subsequently used to control the assistive torque provided. This allows HAL to assist a healthy person in activities such as standing, walking, climbing up and down stairs, and lifting objects up to 70kg. Because the support is based on bioelectrical signals, interaction with it is more intuitive than with manual control inputs like a joystick. When used as an assistive device by someone with a physical impairment the bioelectrical signals alone are sometimes not enough since such signals can be affected by the impairment. For such applications HAL uses a hybrid approach using an autonomous control that observes the wearer to identify their intention. This autonomous control can make use of what bioelectric signals are available to provide the appropriate support to the user. The system runs for 2 hours and 40 minutes on battery and has a total weight of 23kg [Sankai, 2011].

(a) **(b)**

Figure 2.3: Exoskeletons for replacing lost functionality due to impairment. (a) Independent Walk Assist device from Toyota [Toyota, 2011]. (b) HAL-5 (Hybrid Assistive Limb) exoskeleton from Cyberdyne Inc (`www.cyberdyne.jp`).

The aforementioned examples of robots for assisted daily living all worked collaboratively with the wearer to augment their capabilities (or the capability remaining after impairment). Assistive robots can also provide the support required when the operator has lost all functionality due to severe impairment. Figure 2.4 shows a number of exoskeleton devices developed recently which allow paraplegics who have lost all functionality in their lower limbs to walk.

(a) (b) (c)

Figure 2.4: Lower limb exoskeletons for paraplegics. (a) ReWalk from Argo Medical Technologies (www.rewalk.com). (b) Ekso from Berkeley Bionics (www.eksobionics.com). (c) Rex from Rex Bionics (www.rexbionics.com)

The ReWalk exoskeleton from Argo Medical Technologies (Figure 2.4a) is a commercial device currently available in Europe. It provides battery powered support to the wearer's knees and hips to enable paraplegics to stand upright, walk and climbs stairs with the aid of crutches. An on-board computer uses motion sensors to detect subtle changes in the user's centre of gravity which it uses to control movement. Users achieve walking by repeated body shifting to produce sequences of steps. Another system is the Ekso (Figure 2.4b) from Berkeley Bionics which is a hydraulically actuated exoskeleton allowing paraplegics to stand and walk with the assistance of crutches or a walker. Using force and motion sensors it interprets the wearer's intentions to orchestrate the appropriate stride. Powered by lithium batteries it drives actuators at the knees and

hips allowing walking speeds up to 1.6 km/h. It is expected to be available for private use in 2014. Another system is the REX exoskeleton by Rex Bionics (Figure 2.4c). This system takes a different approach to assisting persons with impaired mobility. The robot supports the wearer's legs providing stable support whether the system is powered on or off. Commands are given to the robot from the user via control pad and joystick to perform motions such as standing, sitting, walking, turning, ascending and descending stairs. Since the system is fully stable the user does not require the use of crutches or a walker to stand. The REX can walk continuously for over two hours and weighs approximately 38kg. The REX has been commercially available since 2011.

2.1.3 Rehabilitation

Rehabilitation is gaining much interest in the field of robotics. An objective of rehabilitation robotics is to improve the efficiency and efficacy of patient recovery from conditions such as stroke, cerebral palsy, spinal cord injury or other incapacitating disabilities requiring lengthy physical rehabilitation post injury. Recently a number of robotic systems for providing therapy have become commercially available.

The InMotion Arm Robot (Figure 2.5) is a system based on the MIT Manus [Krebs *et al.*, 1998] designed to assist the upper limb of patients as they perform therapy for stroke, cerebral palsy and other neurological conditions. It assists the patient's shoulder and elbow during horizontal planar movements as therapy is performed. A visual interface instructs the patient to perform specific arm movements within the context of a video game. Assistance is provided to help the patient initiate and coordinate movements, during which the performance of the patient is assessed. This is used to adapt assistance accordingly [Krebs *et al.*, 2003] as well as provide clinicians with quantifiable feedback on the progress of the patient during therapy.

Commercially available from Hocoma are a range of robotic systems for the rehabilitation of both the upper and lower limbs. An example is the ArmeoPower, an upper limb exoskeleton for neurorehabilitation shown in Figure 2.6a. Based on the ARMin robot [Nef *et al.*, 2006], this system uses six active degrees of freedom to provide arm support

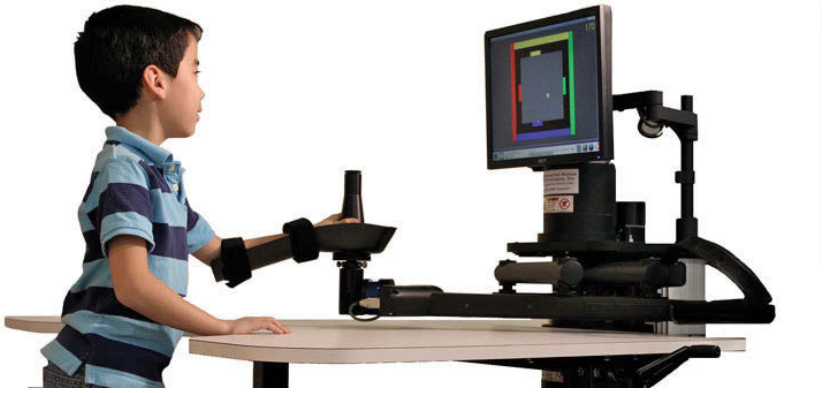

Figure 2.5: The InMotion Arm Robot by Interaction Motion Technologies (www.interactive-motion.com).

(a) **(b)**

Figure 2.6: Rehabilitation devices available from Hocoma (www.hocoma.com). (a) ArmeoPower upper limb rehabilitation robot. (b) LokomatPro lower limb rehabilitation robot.

in a large 3D workspace. Patients utilise their arm as they perform a range of games and motivational exercises designed to simulate regular activities of daily living. The system provides motivational feedback to the patient whilst it adjusts the assistance it provides based on the patient's needs and personal recovery. Monitoring of recovery is done by assessing the patient's ability to move using measures such as reaching distance, reaction time, velocity, precision, coordination, range of motion, strength and limb stiffness. Another system from Hocoma is the LocomatPro, a lower limb exoskeleton shown in Figure 2.6b. It is a treadmill-based system which administers functional locomotion therapy to the lower limbs of a patient using four actuators located at the knee and hip joints. An active body weight support system provides gravity compensation to the patient. Measuring gait and patient activity using force sensors in the robot's drive system, it adapts assistance using performance measures such as hip and knee stiffness, strength, and range of motion. The system enables a single therapist to administer the therapy, unlike manual training which is labour intensive, requires sufficient staff, and can only be performed in relatively short sessions.

2.1.4 Other examples of assistive robots

There are many other types of assistive robots that can operate with varying levels of physical interaction with the user. Robotic prosthetics like the Luke Arm from DEKA [Adee, 2008] shown in Figure 2.7a can return some of the functionality which was lost due to a missing limb. Other robotic devices can provide assistance by performing dedicated every day tasks in the home. Robotic feeders like the MySpoon shown in Figure 2.7b can help the elderly or disabled feed themselves, reducing the aid required by care givers. Robots can also assist health care givers during patient handling which is a physically intensive task. An example is the RIBA-II (Robot for Interactive Body Assistance) [Riken, 2011] shown in Figure 2.7c which is a mobile robot with two arms for lifting and carrying patients. Assistance provided by robots is not limited to physical assistance. Socially assistive robots can provide a number of benefits through non-physical social interaction. Shown in Figure 2.7d is the Paro robotic pet modelled off a baby harp seal. Used in animal assistance therapy, it is designed to elicit an emotional

response and calming effect in the patients of hospitals and nursing homes. Using tactile sensors it responds to petting with sounds and movements. It has been commercially available since 2004.

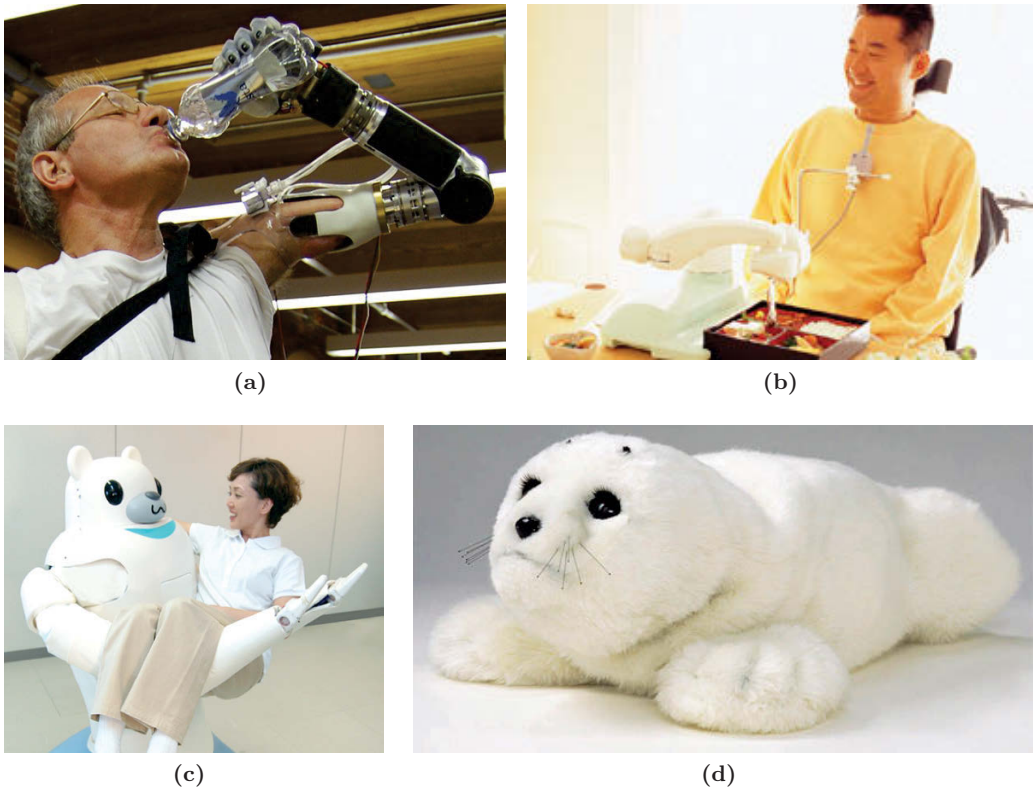

(a) **(b)** **(c)** **(d)**

Figure 2.7: Other examples of assistive robotic systems for various applications. (a) The Luke Arm from DEKA (www.dekaresearch.com). (b) MySpoon feeding robot from Secom (www.secom.co.jp). (c) RIBA-II patient handling robot from Riken (www.riken.jp). (d) Paro socially assistive robot (www.parorobots.com).

These robotic systems all provide some form of assistance to their human operator. Typically they do not involve the robot and human working collaboratively together to share the effort required in performing tasks, and hence they are not particularly relevant with respect to AAN. However they do demonstrate that there are numerous tasks in which robots can provide assistance in a wide range of applications and industries.

2.2 Control of Physically Assistive Robots

The control of robotic systems is a fundamental area of research in robotics. This section is a non-exhaustive review of the methodologies and techniques used for controlling physically assistive robots related to the work in this thesis. To avoid confusion the terms *Control Scheme* and *Assistance Paradigm* are defined here to make a clear distinction between the lower and higher levels of an assistive robot's control (represented in Figure 2.8) and are used consistently throughout this thesis.

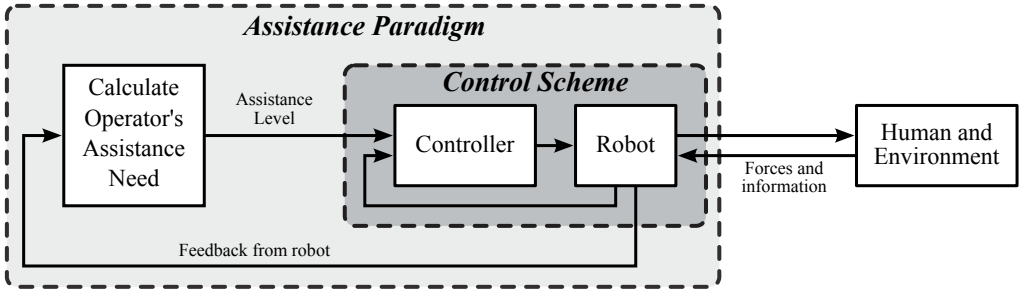

Figure 2.8: Distinction between the control scheme and the assistance paradigm of an assistive robot. At the lower level the *Control Scheme* controls the robot's active behaviour using feedback from the operator and the environment as tasks are performed. The *Assistance Paradigm* operates at a higher level above the control scheme to govern how assistance is administered to the operator.

Control Scheme: This is what would traditionally be referred to in the literature as the robot's control system. It is responsible for controlling the actuation of the robot's hardware, usually in the form of a feedback loop using information acquired from the robot's sensors (e.g. encoders). This actuation determines the robot's active behaviour, and consequently its interaction with the operator and the environment. It is from this interaction the physical assistance is provided. Some examples of robot control schemes include trajectory tracking, impedance control, and admittance control.

Assistance Paradigm: This refers to paradigms which operate above the robot's control scheme to govern how assistance (provided via the control scheme) is administered to the operator. Often assistance is not governed at all, leaving it purely dependent on the control scheme. For example a robot may use a control scheme to assist in lifting heavy objects by supporting a percentage of the object's weight. The simplest assistance

paradigm would be to set this percentage to some fixed value resulting in a constant level of assistance. Alternatively a more sophisticated paradigm might adjust the percentage of the load supported by the robot to achieve some higher level objective, for example to ensure active participation of the operator.

2.2.1 Control schemes in assistive robotics

Motion control schemes

Industrial robots are traditionally required to perform repeated motions with high positioning accuracy and repeatability [Hägele *et al.*, 2008] and hence motion-based control strategies are common. Traditional motion control consists of planning a trajectory as to perform the desired task whilst avoiding problems such as collisions [Kavraki and LaValle, 2008], and then controlling the robot as to carry out the planned motion [Chung *et al.*, 2008]. It typically requires a detailed description of the robotic system and its environment to be known [Siciliano and Villani, 1999] and hence is suitable for repetitive, structured, and well defined industrial tasks.

Applications where a robot interacts and provides physical assistance to its human operator are not suited to pre-planned motions as accurate task planning is required, and human collaboration is inherently difficult to define [De Santis *et al.*, 2008]. Motion control may be used to assist an operator who issues commands from an input device such as a joystick, however this distances the operator from the task and can require additional cognitive effort. Instead it is desirable to control the robot with direct physical interaction, placing the operator proximate to the task and to provide haptic feedback [Bicchi *et al.*, 2008]

Although motion control alone is not commonly used as a control scheme for physically assistive robots, motion control is often used within more sophisticated control schemes. For example in admittance control the robot is operated such that it moves in response to measured external forces. An outer control loop uses force measurements to produce a desired trajectory, and an inner motion control loop is then used to follow it. The

result is a type of indirect force control scheme.

Force control schemes

Force control schemes are used to control the forces resulting from the robot interacting with its environment (including its human operator). They are essential in achieving robust behaviour in poorly structured environments and for safe operation in the presence of humans [Villani and Schutter, 2008]. Controlling the forces portrayed by the robot during physical interactions allows means for ensuring safety of the operator, and hence force control schemes are commonly used in physically assistive robotic systems. Force control schemes can be categorised as being either *direct* or *indirect* [Siciliano and Villani, 1999].

Direct force control uses measurements from force sensors as feedback to create a closed force-feedback loop. An example is hybrid control [Raibert and Craig, 1981] where the force and position in orthogonal directions are controlled simultaneously. Contact forces are controlled using feedback of the measured force, whilst orthogonal directions are under position control. This scheme requires a detailed model of the environment which in most practical situations is not available [Siciliano and Villani, 1999]. A modified scheme is parallel force/position control, which can be used when a detailed environment model is not available. It combines force and position controls using a priority strategy such that the force control always prevails [Chiaverini and Sciavicco, 1993].

Indirect force control uses the motion of the robot to indirectly control interaction forces. Approaches include damping [Whitney, 1977], stiffness [Salisbury, 1980], impedance [Hogan, 1985], and admittance [Kazerooni *et al.*, 1986a,b] based schemes. A model of a dynamic system (typically spring-mass-damper) is used to relate robot forces to its motion. The robot is then controlled as to behave as this dynamic system in response to external interactions. Impedance control uses deviations in position measurements to calculate the reaction forces the desired dynamic system would produce. These forces are then actuated by the control scheme. Admittance control operates the

opposite way, reacting to measured external forces by generating appropriate motions. Later in this work an admittance control scheme is utilised for experimentation. Section 5.1.3 describes the admittance control and how it was implemented on the robotic system. For additional information on the current theory and practices of admittance control readers are directed towards the literature [Villani and Schutter, 2008].

The performance of force control schemes relies largely on the construction and actuation of the robot. Impedance control requires a robot with accurate position sensing and high bandwidth force servo capabilities. This implies that actuators should be almost ideal force sources and therefore have low inertia and friction, which puts specific demands on the robot's design [van der Kooij *et al.*, 2006]. Alternatively, admittance control requires accurate force sensing and high bandwidth, accurate positioning servo capabilities. This implies the use of high power actuators and a robot with stiff construction [van der Kooij *et al.*, 2006].

These schemes require the robot to be fitted with force/torque sensors. If interaction only occurs at the robot's end-effector then often a sensor is put into the wrist. Robots with several points of interaction (e.g. a full body exoskeleton) require force measurements at each interaction point [van der Kooij *et al.*, 2006]. Alternatively, high precision torque sensing can be incorporated into the robot's joints directly as done in the DLR-III robot [Hirzinger *et al.*, 2001].

2.2.2 Physical assistance paradigms

Physical assistance paradigms refer to the manner in which the assistance provided via a robot's control scheme is governed as to achieve some higher level objective relevant to the application. An example is the Assistance-As-Needed (AAN) paradigm, which is often used to adjust assistance to the specific requirements of the operator with the objective of maximising operator participation during tasks. This has been shown to be beneficial in applications such as rehabilitation.

The following are examples of different assistance paradigms. A taxonomy of such paradigms has yet to be established, so categorisation is made with best efforts to group

paradigms based on the mechanisms used to govern assistance. The AAN paradigm is detailed separately in Section 2.2.3

Force reflection

Force reflection paradigms aim to control the force that the operator experiences, typically such that they are a scaled down equivalent of the forces required by the task being performed. Other common names for this paradigm include force feedback, strength augmentation or amplification, and load sharing. The robot is operated using some form of control scheme (e.g. admittance or impedance control) which is arranged such that the load felt by the operator is some set percentage of the total task load. This provides the operator with haptic feedback of the task being performed while less effort is required from them to perform it. The strength and endurance of the robot is exploited to assist the operator; however the operator has total cognitive control over the system to decide how the task is performed. Because assistance is the result of reducing the forces required from the operator, this paradigm is often used in applications which require large physical effort, for example materials handling.

Force reflection was used in one of the first exoskeleton robots. The *Hardiman* robot (Figure 2.9a) developed in the 1960s by General Electric was an early and ambitious attempt at an assistive robot for materials handling. It consisted of a pair of geometrically superimposed robotic exoskeletons operating in a master-slave configuration. With the master exoskeleton worn by the operator it would provide them with force feedback as the slave exoskeleton performed the physically intensive task. The force feedback was scaled down such that the operator's strength and endurance would be amplified by a factor of 25:1 [Makinson, 1971]. Its success was limited and because of instability problems it was never tested with a human on board [Kazerooni, 2008; Makinson, 1971].

Greater success was achieved by Kazerooni in developing robots to assist manoeuvering large loads. These *human extenders* (Figure 2.9b) did not use a master-slave configuration but instead acted as a single intermediatory device between the load and operator. Load forces were transmitted through the robot with sensors used to measure

robot interaction forces between both the load and operator, which were used by the robot's control scheme to generate a motion trajectory. This admittance-type control scheme is configured such that the force felt by the operator is a scaled down representation of the force between the robot and the load. The amount of assistance provided is determined by how much this feedback force is scaled down [Kazerooni, 1998]. IADs in industry use a similar approach by supporting a fixed percentage of lifted loads, scaling down the apparent weight felt by the operator [Colgate *et al.*, 2003].

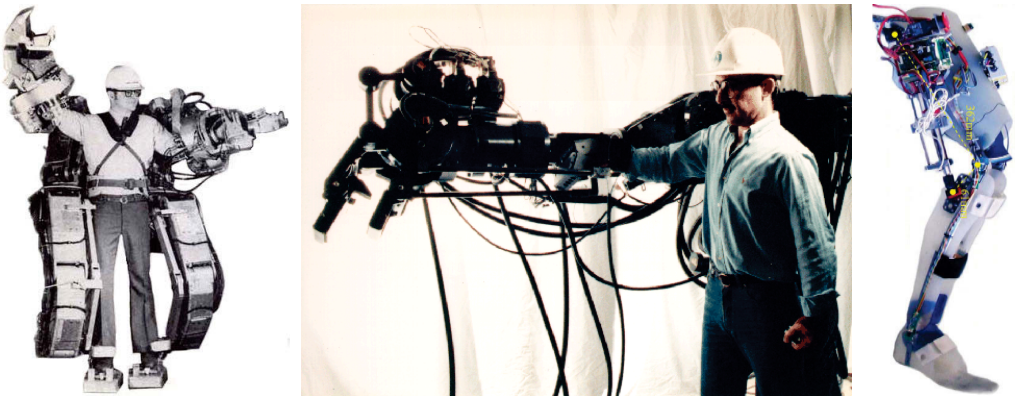

(a) **(b)** **(c)**

Figure 2.9: Physically assistive robotic systems that use force reflection paradigms. (a) Hardiman by General Electric [Makinson, 1971]. (b) Human extender [Kazerooni, 1998]. (c) EMG-controlled knee exoskeleton [Fleischer and Hommel, 2008].

Rather than using sensors to measure the interaction forces between the robot, operator, and the task being performed, robots such as the knee exoskeleton developed by Fleischer and Hommel (Figure 2.9c) use electromyography (EMG) signals of the operator's muscles to infer the muscular torque in the joints of the operator. This estimate of operator joint torque is multiplied by some gain and then used to control the assistive torque provided by the robot [Fleischer and Hommel, 2008]. Since the robot's torque is proportional to the torque in the operator's knee, only a portion of the task force is felt by the limb. This approach can be considered as another form of force reflection.

Guidance

In applications where a person is maneuvering a load, assistance can be provided not only by reducing the magnitude of the load felt by the operator, but also in the form of robotic guidance. Bicchi *et al.* [2008] describes an IAD designed by Fanuc which incorporated virtual walls used as a funnel shape to assist moving a payload without collision.

A novel approach named *Collaborative Robots* (Cobots) [Peshkin *et al.*, 2001] provides guidance by enforcing passive constraints on motion. The constraint directions are actively servo-controlled but no energy is transferred to the load. The system is passive and therefore is stable and safe. Energy required for motion must come from the operator working *hands-on* with the load, but guidance can assist the operator by slowing down the load and guarding against collisions.

Frequency/tremor suppression

Assistance can be provided by suppressing the frequency component of tasks. For example when using an assistive robot in a jackhammer task consisting of unwanted high frequency forces, these forces can be filtered so the operator feels only the scaled-down low-frequency components of the task [Kazerooni, 1998]. Assistance comes not only from a reduction of the load felt by the operator, but also how this force feedback is shaped. Frequency suppression is also implemented in surgical robots to filter out the tremor in the hands of a surgeon during precise hand motions before such motions are used to guide the path of surgical instruments under robotic control [Guthart and Salisbury, 2000; Taylor *et al.*, 2008].

Rocon *et al.* [2007] developed an exoskeleton to suppress tremor in the upper limb for persons with disability. Information from sensors measuring limb motion are processed to discriminate between voluntary limb movement and tremor. The exoskeleton then attempts to suppress the tremor using impedance or active compensation control schemes. Experiments showed success in suppressing a significant component of tremor in patients tested.

Precision/dexterity assistance

Applications such as surgery require precise, dexterous movements. Robots can be used to enhance these capabilities. The daVinci surgical system [Guthart and Salisbury, 2000] shown in Figure 2.10a uses the robot to position and manoeuver the surgical instruments. The robot is operated as a slave device, performing operations instructed by the surgeon at a master console. Dexterity is increased by the robot having a larger range of motion than the natural range of motion of the surgeon. Scaling of the motion between the master and slave allows the surgeon to manoeuver surgical instruments with greater precision than would typically be possible by hand. For example a 3:1 scaling allows a 3cm input from the surgeon at the master end to produce a 1cm output by the robotic slave, making delicate motions easier to perform [Guthart and Salisbury, 2000].

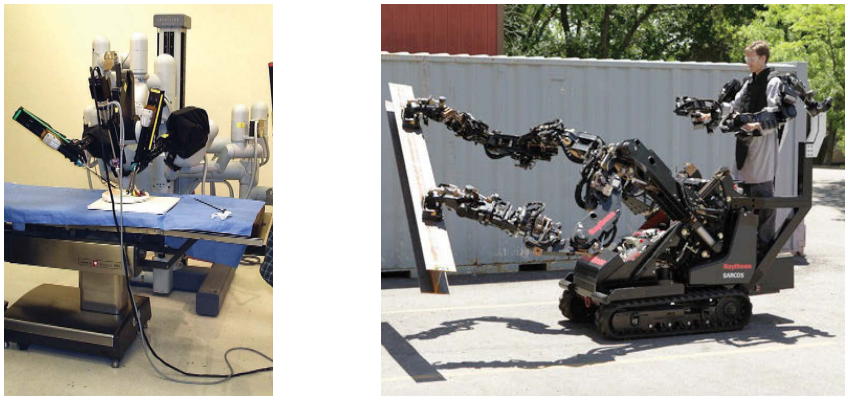

(a) **(b)**

Figure 2.10: Robots which scale up or down operator motions. (a) The daVinci surgical robot system. (b) The Big Arm materials handling system by Raytheon [Raytheon, 2012].

As well as improving precision by scaling down the movements of a human, robots can scale up human movement to increase their reach. The Big-Arm Teleoperation System by Raytheon shown in Figure 2.10b uses a master-slave configuration to allow a human operator to control either a single or a pair of robotic arms. These large arms have a reach of over 2 metres and allow large objects weighing up to 180kg to be manipulated with ease [Raytheon, 2012].

2.2.3 The Assistance-As-Needed (AAN) paradigm

As its name suggests, the Assistance-As-Needed (AAN) paradigm aims to provide the operator with assistance specific to their individual requirements. This level of assistance depends on both the requirements of the task being performed, and the capabilities of the operator to perform it. For example if the difficulty of a task is increased then the assistance provided by the robot should be increased accordingly. Likewise if the capability of the operator to perform the task increases, assistance should be reduced. If the operator does not require assistance, then no assistance should be provided.

The paradigm can be implemented in different ways to achieve objectives related to the application. For example in physically intensive industrial tasks the operator's *requirement* may be defined as the assistance required so that they can accomplish tasks whilst also being provided enough assistance such that the risk of injury is reduced to acceptable levels. In an application described by Lynch *et al.* [2002] robotic trolleys are used to guide heavy loads manoeuvered by workers with the objective of reducing the forces between the load and worker in the directions they require greater assistance due to higher risk of injury.

A common objective is to assist an operator as they perform tasks whilst encouraging them to contribute as much as they can. This is achieved by providing the minimum amount of assistance they require in order for the task to be successfully performed. Due to the nature of this paradigm and how it administers assistance, it has gained much attention in the area of rehabilitation robotics. Typical rehabilitation for conditions such as stroke involve patients undergoing physical therapy sessions with the aim of improving the functional ability of their impaired limbs. Robotic rehabilitation aims to improve the efficiency and efficacy of patient recovery, using robots in the role of physiotherapists to administer therapy. Therapy often involves the therapist (or robot in the case of robotic rehabilitation) providing assistance to the patient as they perform tasks using their impaired limb. These tasks contain motion and/or force components, and depending on the severity of the patient's impairment, are often unable to be performed without the aid of external assistance. Much research has been done on

developing new control strategies to improve rehabilitation efficacy [Marchal-Crespo and Reinkensmeyer, 2009]. Outcomes have shown that the quality of the recovery is largely dependent on how assistance during therapy is provided. For example using a robot to continuously manoeuver a limb as the patient remains passive has benefits such as preventing contracture [Liebesman and Cafarelli, 1994] and increasing joint integrity [Lynch *et al.*, 2005], but does not facilitate motor neuron recovery [Hogan *et al.*, 2006]. It has been shown that patient active participation in the performance of tasks during therapy is essential for facilitating neurorehabilitation [Hogan *et al.*, 2006]. Because the AAN paradigm inherently forces the patient to actively participate in the performance of tasks it is well suited for applications such as neurorehabilitation.

The primary challenge in AAN is determining the true assistance requirements of the operator. Estimating the assistance required to exactly fill the void between the difficulty of the task and the capabilities of the operator (if a void exists at all) is challenging, mainly due to the highly complex factors affecting a human's capability to perform tasks. The physical capability of an operator is specific to the individual, and varies amongst the population. Furthermore, in health care applications this variation is exacerbated by any physical impairments resulting from a patient's disability [Arva *et al.*, 2004; Bohannon and Andrews, 1987; Mercier and Bourbonnais, 2004]. Adding to the difficulty is that the task itself can vary, either inherently during its execution or due to external disturbances.

Empirical performance-based AAN

A solution to determining the assistance requirements of the operator is to use empirical methods. As the operator (assisted by the robot) performs a task, task related measurements obtained from the robot (e.g. movements or force interactions) are acquired. Using this information the performance of the operator is critiqued based on some predefined criterion. Based on how well the operator is deemed to have performed the assistance is adjusted. If the operator performs the task well then they are provided less assistance, and vice versa. This approach is sometimes referred to as providing *performance-based* assistance. Robots providing performance-based assistance

are prone to a phenomenon called *slacking* [Israel *et al.*, 2006; Wolbrecht *et al.*, 2008]. Slacking is thought to be a natural consequence of the human motor system adapting to novel dynamic environments where by the motor system attempts to minimise both task error and physical effort [Emken *et al.*, 2007; Secoli *et al.*, 2011]. To combat slacking, performance-based AAN solutions can incorporate a strategy that continually challenges the operator. A *forgetting factor* [Emken *et al.*, 2005] can be implemented which slowly reduces the assistance provided by the robot over time. A generalisation of a performance-based AAN control is shown in Figure 2.11 where the outer loop represents the operator's performance being critiqued and subsequently used to adapt the robot's assistance. Depending on the application, this outer loop may operate in real time to adapt assistance during use. Alternatively this outer loop may operate offline, using information from previous task *sessions* to calculate the appropriate assistance to provide in the next.

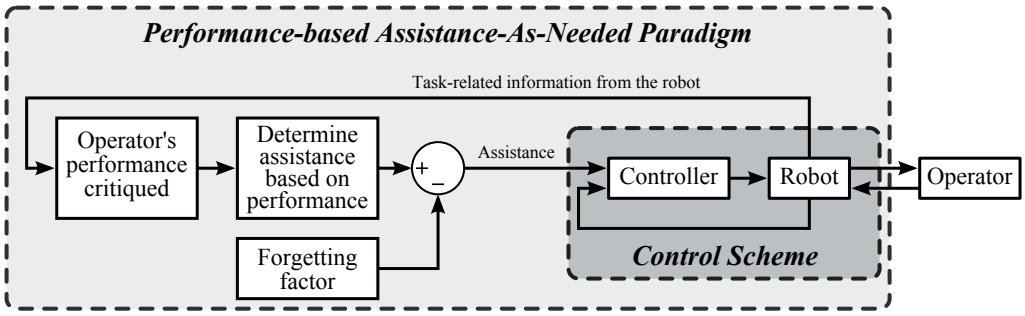

Figure 2.11: Generalisation of performance-based Assistance-As-Needed. The robot provides assistance to the operator via a control scheme, with feedback used to critique their performance against some predefined criterion. Based on how the operator is deemed to have performed the assistance is adjusted. A forgetting factor can be utilised to continually challenge the operator to combat slacking.

Krebs *et al.* [2003] implemented performance-based AAN using the MIT-MANUS robot to assist patients performing upper limb movements. Patients performed planar point-to-point movements cued by a computer game, with the desired task to move the hand from a start to end point. Tasks were critiqued using four performance measures [Krebs *et al.*, 2001] which included how well the movement fitted a minimum-jerk profile. This is based on experiments which show typical point-to-point hand movements fit the minimum-jerk profile [Flash and Hogan, 1985]. Other performance measures include

the ability to initiate, aim, and finalise hand movement [Krebs *et al.*, 2001]. Assistance is provided by the robot using an impedance control scheme to produce assistive forces along the desired minimum-jerk trajectory. The amount of assistance is adjusted by changing the stiffness of the impedance control, and the allotted time the patient has to make movements. In each game session the assistance parameters were adjusted based on the four performance measures derived in previous games. A separate algorithm which observed performance over time adapted assistance to continually challenge the patient [Krebs *et al.*, 2003].

Emken *et al.* [2005] treated the idea of providing the minimal amount of assistance needed as an optimisation problem. During therapy of the lower limb, the desired task was to allow the patient's foot to achieve a desired step height during the gait swing phase. Assistance was quantified as the peak upwards force exerted on the limb per step by the assistive robot. The control was formulated as a weighted optimisation problem minimising two terms, the kinematic step height error, and the assistive force provided. This was based on a model of the patient's leg dynamics, including how their nervous system adapts to perturbing forces. The result was a control law that uses the step height error to adjust assistive force, combined with a forgetting factor that decrements assistance when error is small [Emken *et al.*, 2005]. Assistance is updated on a step-by-step basis [Emken *et al.*, 2007].

Another example [Wolbrecht *et al.*, 2007, 2008] used the Pneu-WREX robot to assist stroke patients in upper limb motor training. An adaptive controller used a distributed spatial grid of radial basis functions to represent the level of assistance required by the patient to be able to support their arm as they attempt to track desired trajectories throughout the workspace. Error-based adaption of the radial basis function amplitudes is performed based on kinematic tracking errors to construct a representation of the assistive forces required by the patient throughout the workspace. This was combined with a forgetting factor that exponentially reduced the radial basis function amplitudes, resulting in a reduction of assistance when the kinematic error is small, and was essential to combat patient slacking. The result was a robot controller that adapted quickly in real time to the different assistive needs of the patient throughout the different areas of

the workspace [Wolbrecht *et al.*, 2007, 2008].

Limitations of empirical performance-based AAN

Performance-based methods have shown success in applications such as robotic neurorehabilitation [Emken *et al.*, 2005; Krebs *et al.*, 2003; Wolbrecht *et al.*, 2007]. However they have inherent limitations due to their empirical nature. These methods calculate the assistance to provide from observations acquired over time of the operator performing the task. These are used to critique the performance of the operator, and from this the robot effectively learns their assistance requirements. However since the robot has no indication of the operator's assistance needs before such observations are available, during this learning process it is likely that the assistance is either excessive or insufficient to the true requirements of the operator. Additionally, if the operator's assistance requirements are altered due to factors unbeknown to the system, it takes time for the robot to adapt accordingly since these must be learnt from subsequent observations. For example if an operator becomes fatigued, and a solely performance-based paradigm is employed, then only after their performance is observed to have noticeably reduced will the assistance be increased.

Learning through observation is also problematic if a number of different tasks are being assisted. Different tasks have different requirements, and the operator has different capabilities of performing each. Even if a robot learns the assistance required in a number of tasks, the assistance required in a new, previously unobserved task is still unknown. Ideally, the assistance required in each task would be known so that the robot can assist each task accordingly. This would require a performance-based paradigm to obtain numerous observations of each distinct task. If only a few, somewhat similar tasks are performed, then the variations between them could be ignored; however this limits the potential applications. For example in robotic rehabilitation, therapy commonly involves repeatedly performing a small number of well defined tasks. A common scenario is a patient manoeuvering their hand so as to follow a desired trajectory between targets that are defined in locations throughout the workspace [Krebs *et al.*, 2003; Wolbrecht *et al.*, 2007]. In reality, the movements between each of the targets would have unique

assistance requirements, however they may be considered similar enough so that all are critiqued and assisted as one task. Although this simplifies the paradigm, it has been shown that separating movements into smaller discrete tasks, critiquing and then assisting them independently allows assistance to be provided that is better suited to the requirements of the operator [Rosati *et al.*, 2008]. A caveat of defining a number of discrete tasks is the more tasks which are defined, the more observations required to determine the operator's assistance requirements for each. The work by Wolbrecht *et al.* [2007] manages this by using observations to construct a model of the assistance required as a continuous function across the workspace, rather than separating it into distinct, independently assisted tasks that would each require observations. This allows variation in the operator's assistance requirements due to variation in the task (in this example, different locations of the hand) to be managed by the model. However the model quickly becomes highly dimensional as more task variables are considered. For example other task variables may be the direction and magnitude of an external force (e.g. from interaction with the environment), the position of the elbow if independent of hand position, or the direction of hand movement which if considered can improve the assistance provided [Rosati *et al.*, 2008].

A range of different metrics have been used in performance-based AAN to critique the performance of the operator. Selection of this metric needs to be made based on its suitability for the application, however this then limits the types of tasks in which the robot can critique and subsequently provide assistance. For example in upper limb therapy, point-to-point hand movements are commonly critiqued based on a minimum-jerk profile [Krebs *et al.*, 2003]. Using this metric to evaluate task performance is suitable as long as only tasks for which minimum-jerk movements indicate good performance are being assisted. Another factor to be considered is this performance metric is an indirect measure of their actual assistance requirements. The evaluation of performance, and the adjustment of assistance, are often expressed in different units. For example, assistance can be controlled by adapting the robot's stiffness (in units of N/m) according to performance evaluated based on minimum-jerk movement movements [Krebs *et al.*, 2003]. Another example, assistive forces (in units of N) can be adapted according to

performance based on kinematic error (in units of m) [Emken *et al.*, 2005]. Even if the performance metric has a monotonic relationship with the level of assistance being provided (i.e. as assistance increases, the performance increases) it is unlikely this relationship will be linear. A non-linear relationship may rely heavily on the previously mentioned forgetting factor [Emken *et al.*, 2005] for the robot to reach an assistance equilibrium which is suitable for the operator and the task being performed.

In some applications the aforementioned limitations with empirical performance-based methods are less problematic. For example, in controlled environments where the tasks performed may be limited to a small number with little variation, and have well defined criteria of what constitutes good performance from the operator performing them. However it is desirable, or possibly inevitable that in the future assistive robotics will be used in less structured environments to assist human operators in a range of applications. An example would be to assist the disabled or the elderly as they perform household activities common in daily life. A large number of different tasks would be performed, with each having its own unique and widely varied assistance requirements, hence the limitations inherent in empirical performance-based AAN are problematic in such scenarios.

2.3 Musculoskeletal Modelling

Musculoskeletal models provide a means of simulating biological systems and allow the complex and non-linear relationships of the body including the skeletal structure, joints, tendons and muscles to be derived. The work presented in this thesis does not focus on the development of musculoskeletal models, or methods of improving their representation of biomechanical systems. It does utilise models and methodologies that are the result of a long history of musculoskeletal modelling research, and outcomes of this work depend on the musculoskeletal models utilised. It is hence beneficial to present a background on the musculoskeletal modelling methods and theory related to the work in this thesis.

The following section reviews some commonly used musculoskeletal modelling tech-

niques. It is not an exhaustive review as many methods and approaches for musculoskeletal modelling exist in the literature. Complexity ranges from relatively simple rigid representations of body segments combined with straight line representations of muscle-tendon paths [Maurel and Thalmann, 1999; Seireg and Arvikar, 1989] to complex finite-element representations [Bai *et al.*, 2008; Blemker *et al.*, 2005]. This review covers modelling methods common in many musculoskeletal models, including the upper limb musculoskeletal model utilised later in this thesis [Holzbaur *et al.*, 2005].

2.3.1 Musculotendon Unit (MTU) model

Actuation by muscles in the human body is modelled by musculo-tendon units (MTU). Each MTU represents a particular muscle or muscle group in the body, along with its tendons connecting it to the skeleton. Primary use of the MTU model is to calculate its force producing capabilities given its state (typically length and velocity). There exists many different MTU models in the literature [Schutte *et al.*, 1993; Thelen *et al.*, 2003; Zajac, 1989] with most models derived from the Hill muscle model which relates maximum muscle fibre tension to its contraction velocity [Hill, 1938].

An example MTU model is shown in Figure 2.12. This lumped-element model uses separate elements representing individual force-producing components in the MTU. An active contractile element is placed in parallel with a passive element to represent both the active and passive force producing capabilities of muscle fibre. These elements are in series with an elastic element representing the tendon attaching the muscle fibre at each end to the skeleton. Lengths of the muscle fibre and tendon are denoted as l^m and l^t respectively. The total length of the MTU from origin to insertion is denoted as l^M.

Many muscles in the human body are pennate, meaning the muscle fibers attach obliquely to the tendon. As a result pennate muscles contain more fibers and thus have higher strength capacity, but do not pull the tendons as far when contracted resulting in less range of motion [Martini, 2001]. With pennation angle represented as α the total MTU length l^M accounting for pennation is calculated using the geometric relationship

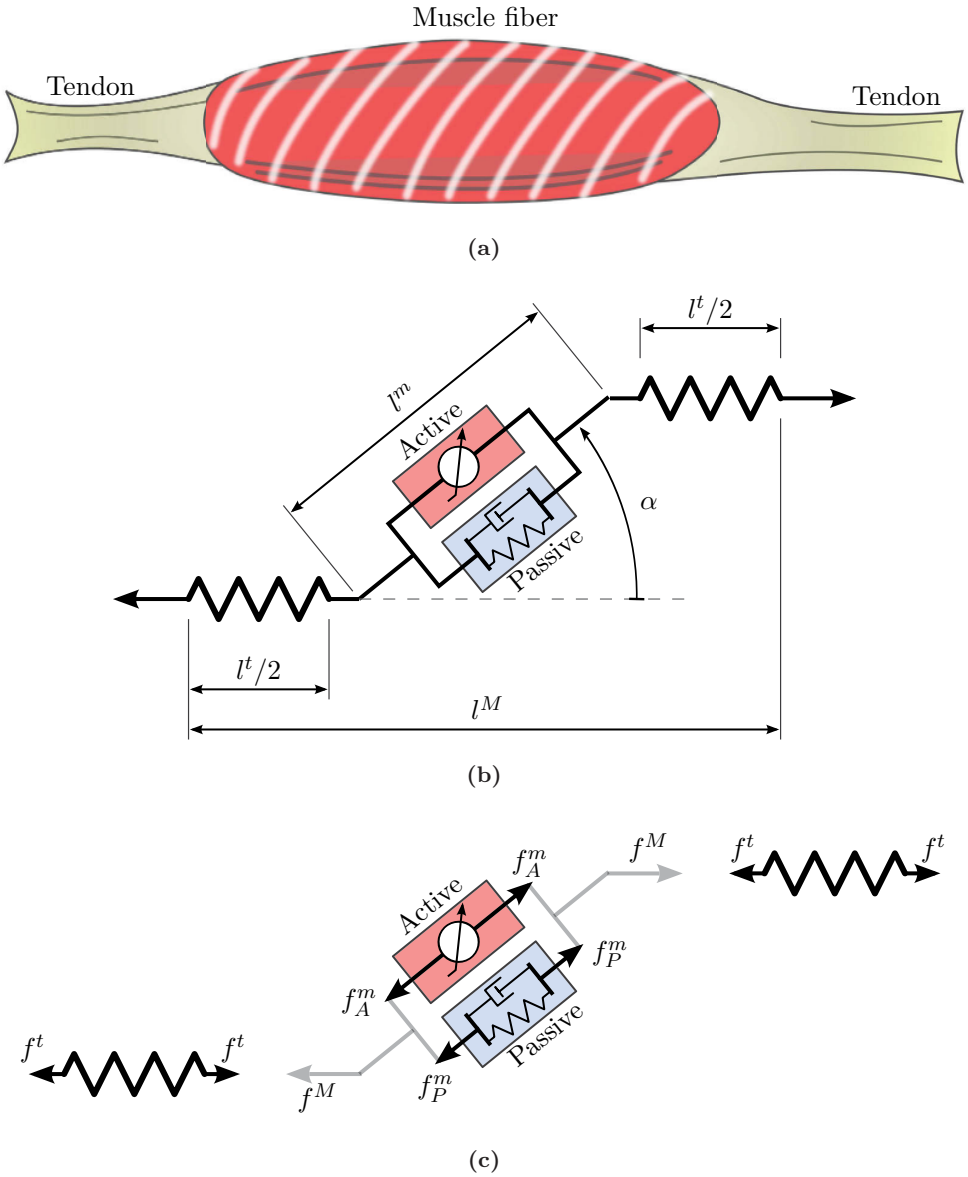

Figure 2.12: Typical Hill-type musculotendon unit (MTU) model. (a) Physiological representation of a muscle and its tendons. (b) Lumped-element model of MTU with its geometric dimensions shown. Parallel active and passive components represents the muscle fiber. Elastic elements in series represent tendons. (c) MTU model with the force relationships between muscle and tendons shown.

in Equation (2.1).

$$l^M = l^t + l^m \cos\alpha \tag{2.1}$$

The force-producing properties of muscle and tendon are complex biomechanical functions largely dependent on fibre/tendon length and velocity. Zajac [1989] used dimensionless curves (shown in Figure 2.13) to form a normalised MTU model preserving its force-length-velocity relationships. These normalised curves can then be scaled using MTU intrinsic parameters listed in Table 2.1 to fit the model to represent specific muscle groups. Functions $\tilde{f}_A^m(\cdot)$ and $\tilde{f}_P^m(\cdot)$ represent the curves relating the muscle fiber's normalised length to its normalised active and passive forces (Figure 2.13a), respectively. These curves are both functions of the muscle fiber normalised length $\tilde{l}^m$, calculated as $\tilde{l}^m = l^m / L_0^m$ where l^m is the fiber length and L_0^m is the fiber intrinsic optimal length at which its active force output is maximum. Similarly, function $\tilde{f}_V^m(\cdot)$ represents the curve relating muscle fiber normalised velocity to its normalised force (Figure 2.13b). This curve is a function of the muscle fiber normalised velocity $\tilde{\dot{l}}^m$, calculated as $\tilde{\dot{l}}^m = \dot{l}^m / V_0^m$ where $\dot{l}^m$ is the fiber velocity and V_0^m is the fiber intrinsic maximum contraction velocity.

These curves can then calculate muscle fiber active and passive forces using Equations (2.2) and (2.3), respectively. The curve outputs are scaled using parameter F_0^m representing the muscle fiber's intrinsic maximum isometric force (corresponding to its optimal length L_0^m). The active fiber force is also scaled using parameter a called the muscle's *activation*. This represents the level of active force production resulting from neural excitation. Activation ranges from 0 to 1 with $a = 0$ indicating a completely passive muscle, and $a = 1$ the muscle is at maximum active force output. The total muscle fiber force is the sum of its active and passive components. This net force is then transmitted via the tendons to the skeleton. After accounting for muscle pennation the total MTU force output f^M is calculated using Equation (2.4).

$$f_A^m = \tilde{f}_A^m(\tilde{l}^m) \cdot \tilde{f}_V^m(\tilde{\dot{l}}^m) \cdot F_0^m \cdot a \tag{2.2}$$

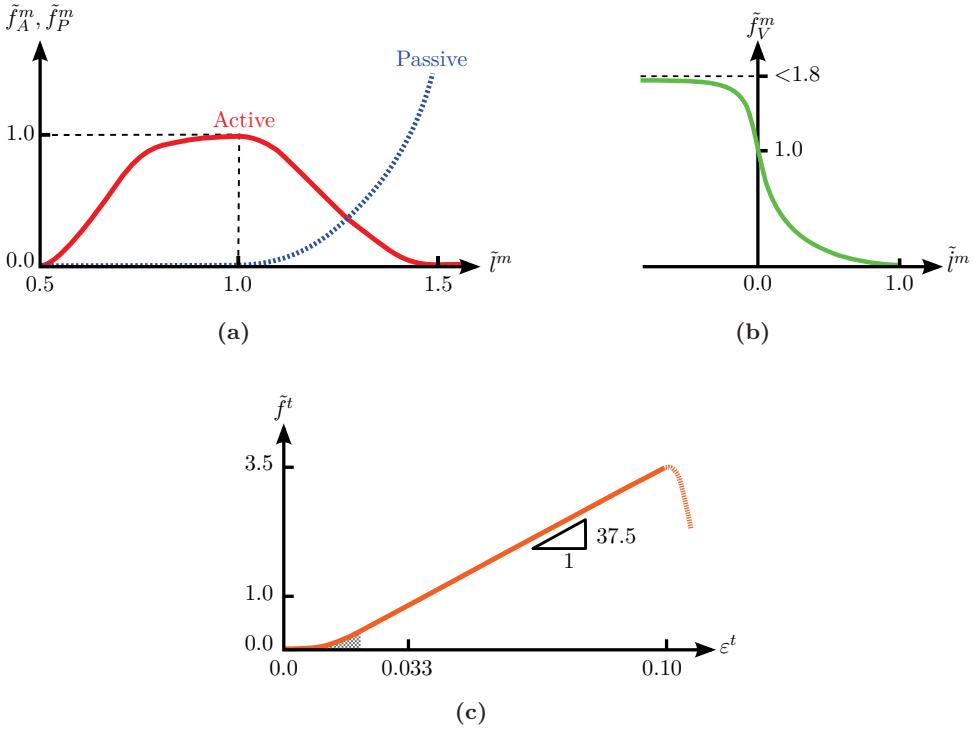

Figure 2.13: Normalised muscle force-length-velocity, and tendon force-strain curves. Recreated from [Zajac, 1989]. (a) Normalised muscle fibre force vs normalised length. (b) Normalised muscle fibre force vs normalised velocity. (c) Normalised tendon force vs tendon strain.

MTU scaling parameters		
Parameters	*Description*	*Units*
F_0^m	Muscle maximum isometric force	(N)
L_0^m	Muscle optimal length coinciding with F_0^m	(m)
V_0^m	Muscle maximum contractile velocity	(m/s)
α_0	Muscle pennation at optimal length	(rad)
L_s^t	Tendon slack length	(m)

Table 2.1: Intrinsic parameters used for scaling the normalised MTU model.

$$f_P^m = \tilde{f}_P^m(\tilde{l}^m) \cdot F_0^m \tag{2.3}$$

$$f^M = (f_A^m + f_P^m)\cos\alpha \tag{2.4}$$

Calculating MTU force requires the muscle fiber length to be determined as its state is independent to the total MTU length due to tendon elasticity. For example as the fiber is activated and its force increases, the length of the fiber shortens due to the tendon stretching even if the total MTU length remains constant. Fiber length can be found by equating MTU force output f^M to the tendon force f^t resulting from its strain. Function $\tilde{f}^t(\cdot)$ represents the curve relating tendon strain to its normalised force (Figure 2.13c). Tendon strain is represented as ε^t and calculated as $\varepsilon^t = [l^t - L_s^t]/L_s^t$ where l^t is its length and L_s^t is its intrinsic length when slack ($f^t = 0$). The tendon force is then calculated using Equation (2.5).

$$f^t = \tilde{f}^t(\varepsilon^t) \cdot F_0^m \tag{2.5}$$

The MTU force output given its total length, velocity, and activation requires the muscle fiber length to be found such that $f^M = f^t$. Once found, this force is the total MTU force output transmitted to the skeleton. A convenient simplification is to assume the tendon is rigid such that muscle fiber length is not independent and becomes geometrically related to the total MTU length [Sapio *et al.*, 2005]. This assumption is often made as tendons exhibit little stretch during use, around 3% when the muscle is producing peak isometric force [Zajac, 1989]. With this simplification the muscle fiber length can be calculated as a function of total MTU length using Equation (2.6) [Fleischer and Hommel, 2008] where α_0 is the pennation angle of the muscle fiber at its optimal length L_0^m.

$$l^m = \sqrt{(L_0^m \cdot \sin\alpha_0)^2 + (l^M - L_s^t)^2} \tag{2.6}$$

2.3.2 MTU length, velocity and moment-arms

A muscle and its tendons form a path starting at its origin and ending at its insertion sites where the tendons attach to the skeleton. The length and velocity of the MTU along this path is required to calculate MTU force output as discussed in the previous section. The MTU path is also required to calculate the moment-arms of muscles about the joints in the skeletal system, which produce joint torque from MTU force.

Early musculoskeletal models used a straight-line approach with MTUs represented as straight paths between origin and insertion sites [Maurel and Thalmann, 1999; Seireg and Arvikar, 1989]. This does not take into account effects such as muscles and tendons wrapping over bones or other parts of the body, and hence is not adequate from an anatomical and mechanical perspective [Raikova, 1992; Toshev and Raikova, 1985; van Zuylen *et al.*, 1988]. Another approach called the Centroid Line Approach [Jensen and Davy, 1975] derived MTU paths from cadaver specimens, measuring the centroid of the muscle cross section to define its path. The resulting path only corresponds to the pose that the cadaver was in when measured [Raikova, 1992].

A more generalised solution is to define MTU paths by sets of via points defined in the local reference frames of the bones. Total MTU length equals the sum of the straight line distances between via points [Delp and Loan, 1995]. This approach can be combined with wrapping the paths over virtual surfaces to represent muscles and tendons passing over bone or other bodily structures [Garner and Pandy, 2000].

The MTU lengths change as the skeletal pose is changed. A vector of generalised coordinate positions $\mathbf{q} = [q_1, q_2, \cdots, q_k]^T$ is used to define the pose of a musculoskeletal model consisting of k degrees of freedom. Using the appropriate method, a vector column of MTU lengths $\mathbf{l} = [l_1^M, l_2^M, \cdots, l_m^M]^T$ for a system with m muscles can be calculated as a function of $\mathbf{q}$ (2.7). The partial derivative of this relationship produces the Jacobian matrix $\mathbf{L}$ (2.8) which can be used to relate generalised coordinate velocities $\dot{\mathbf{q}} = [\dot{q}_1, \dot{q}_2, \cdots, \dot{q}_k]^T$ to MTU velocities $\dot{\mathbf{l}} = [\dot{l}_l^M, \dot{l}_2^M, \cdots, \dot{l}_m^M]^T$ as shown in Equation (2.9).

$$\mathbf{l}(\mathbf{q}) = [l_1^M, l_2^M, \cdots, l_m^M]^T \tag{2.7}$$

$$\mathbf{L}(\mathbf{q}) = \begin{bmatrix} \frac{\partial l_1^M}{\partial q_1} & \frac{\partial l_1^M}{\partial q_2} & \cdots & \frac{\partial l_1^M}{\partial q_k} \\ \frac{\partial l_2^M}{\partial q_1} & \frac{\partial l_2^M}{\partial q_2} & \cdots & \frac{\partial l_2^M}{\partial q_k} \\ \vdots & \vdots & \ddots & \vdots \\ \frac{\partial l_m^M}{\partial q_1} & \frac{\partial l_m^M}{\partial q_2} & \cdots & \frac{\partial l_m^M}{\partial q_k} \end{bmatrix} \tag{2.8}$$

$$\dot{\mathbf{l}} = \mathbf{L}\ \dot{\mathbf{q}} \tag{2.9}$$

Individual elements in the Jacobian $\mathbf{L}$ are partial derivatives of MTU length with respect to joint position, for single MTU and joint combinations. These elements equate to the moment-arms of the corresponding MTUs about the skeletal joints [Pandy, 1999].

2.3.3 Muscular joint torque produced by MTU forces

Forces produced by the MTUs result in torque produced about the skeletal joints. With the MTU forces represented as vector $\mathbf{f} = [f_1^M, f_2^M, \cdots, f_m^M]^T$ the muscular torque $\boldsymbol{\tau}^M = [\tau_1^M, \tau_2^M, \cdots, \tau_k^M]^T$ about the skeletal joints resulting from the MTU forces can be calculated using Equation (2.10). The negative sign is due to the convention of muscle length shortening when producing a positive force.

$$\boldsymbol{\tau}^M = [-\mathbf{L}]^T\ \mathbf{f} \tag{2.10}$$

2.3.4 Rigid body kinematics

Position and orientation of body segments are represented in terms of reference frames assigned to one or more bones in the model. Skeletal movement is provided by joints describing the transformations between frames as functions of generalised coordinates [Delp and Loan, 1995] previously defined as $\mathbf{q} = [q_1, q_2, \cdots, q_k]^T$. This approach can be used to model the movement of physiological joints as being ideal, operating about

fixed axes of rotation [Chéze *et al.*, 1996; Huang *et al.*, 1994; Lenarcic and Umek, 1994] and is generally sufficient for simple joints [Maurel *et al.*, 1996].

Movement not adequately represented by joints with a fixed rotation axis can be described as functions of generalised coordinates derived empirically from biomechanical investigation [Delp and Loan, 1995]. The axis of elbow rotation has been reported to translate as a function of elbow angle [Chao and Morrey, 1978]. Similarly the knee has been modelled as a planar joint consisting both translational and rotational movement [Schutte *et al.*, 1993; Yamaguchi and Zajac, 1989], or approximated by a 4-bar mechanism [Baydal-Bertomeu *et al.*, 2008].

Transformations defined as functions of generalised coordinates can also be used to simplify the representation of highly complex articulations such as the human shoulder, which is described as one of the most complicated articulations in the human body [Engin, 1980]. Including clavicle and scapular movement the shoulder can be modelled as having as many as 11 degrees of freedom [Maurel and Thalmann, 1999] making calculations such as inverse dynamics difficult to solve. The degrees of freedom can be reduced by defining multiple joint motions as functions of a reduced number of generalised coordinates. Lin *et al.* [2005] simplified the shoulder rhythm of an upper limb model by constraining scapula position and orientation as a function of humerus movement based on empirical data from Fung *et al.* [2001]. Movement of the scapula alters muscle moment-arms [Holzbaur *et al.*, 2005; Lin *et al.*, 2005] and hence not accounting for it is a source of model inaccuracy. Using prescribed motions to reduce the degrees of freedom in the model, while still allowing realistic scapula movement can provide a balance between model accuracy and complexity.

With the kinematics of the musculoskeletal system defined, the relationship between generalised coordinates $\mathbf{q}$ and the global position of a point within a body segment can be derived. Let column vector $\mathbf{x} = [x_1, x_2, x_3]^T$ represent the global cartesian position of a point defined locally in a body segment, for example $\mathbf{x}$ is at the centre of the hand. Using the kinematics defined within the musculoskeletal model, the relationship between the position of point $\mathbf{x}$ in global coordinates and the generalised coordinates $\mathbf{q}$ of the model can be calculated, represented by Equation (2.11). The partial derivative

of this relationship produces the kinematic Jacobian matrix $\mathbf{J}_v$ (2.12) which can be used to relate generalised coordinate velocities $\dot{\mathbf{q}}$ to the velocity of point $\mathbf{x}$ as shown in Equation (2.13).

$$\mathbf{x}(\mathbf{q}) = [x_1, x_2, x_3]^T \tag{2.11}$$

$$\mathbf{J}_v(\mathbf{q}) = \begin{bmatrix} \frac{\partial x_1}{\partial q_1} & \frac{\partial x_1}{\partial q_2} & \cdots & \frac{\partial x_1}{\partial q_k} \\ \frac{\partial x_2}{\partial q_1} & \frac{\partial x_2}{\partial q_2} & \cdots & \frac{\partial x_2}{\partial q_k} \\ \frac{\partial x_3}{\partial q_1} & \frac{\partial x_3}{\partial q_2} & \cdots & \frac{\partial x_3}{\partial q_k} \end{bmatrix} \tag{2.12}$$

$$\dot{\mathbf{x}} = \mathbf{J}_v \, \dot{\mathbf{q}} \tag{2.13}$$

With an external load applied to the musculoskeletal model at point $\mathbf{x}$, the Jacobian matrix $\mathbf{J}_v$ can calculate the resulting torque loads experienced on the skeletal joints. With the external force applied to point $\mathbf{x}$ defined in global coordinate as $\mathbf{F}^E = [F_1^E, F_2^E, F_3^E]^T$, the resulting joint loads represented as $\boldsymbol{\tau}^E$ is calculated using Equation (2.14).

$$\boldsymbol{\tau}^E = \left[\mathbf{J}_v\right]^T \mathbf{F}^E \tag{2.14}$$

If the external load contains a moment component then this can be included by using a wrench instead of a pure force, and utilising a kinematic Jacobian that includes the relationship between the generalised coordinate velocities and the angular velocities of the body segment.

2.3.5 Rigid body dynamics

The dynamics of the musculoskeletal system are tantamount to the canonical joint space formulation of a robotic system [Featherstone and Orin, 2008]. Each body segment is

treated as rigid and is assigned inertial properties equivalent to that of the respective body segment in a human. The joint space dynamics are represented by Equation (2.15) where $\mathbf{H}(\mathbf{q})$ is the joint space inertia matrix, $\mathbf{C}(\mathbf{q}, \dot{\mathbf{q}})$ represents centrifugal and Coriolis effects, and $\boldsymbol{\tau}^G(\mathbf{q})$ are the joint torques required to support the system against gravity. Vector $\boldsymbol{\tau}^M$ are the joint torques produced by MTU forces which are calculated using Equation (2.10). Vector $\boldsymbol{\tau}^E$ are joint torques from an external load applied to the musculoskeletal system, calculated using Equation (2.14).

$$\mathbf{H}(\mathbf{q})\ \ddot{\mathbf{q}} + \mathbf{C}(\mathbf{q}, \dot{\mathbf{q}}) + \boldsymbol{\tau}^G(\mathbf{q}) = \boldsymbol{\tau}^M + \boldsymbol{\tau}^E \tag{2.15}$$

2.3.6 Muscle activation dynamics

As previously mentioned, muscle activation is defined as a and represents the level of active force production in the muscle fibers of a MTU, ranging from 0 to 1. This activation is the result of neural excitation, which is defined as u and also ranges from 0 to 1. The conversion of neural excitation u into muscle activation a is not instantaneous and is often modelled as a first order system. It is assumed that the activation dynamics and the muscle's force-producing contraction dynamics are uncoupled [Zajac, 1989].

For naturally excited muscle, activation has a faster time constant compared with deactivation [Schutte *et al.*, 1993; Zajac, 1989]. With muscle activation having time constant of T_a when fully excited ($u = 1$) and T_d when fully unexcited ($u = 0$) the change in muscle activation $\dot{a}$ can be related to activation a and neural excitation u using Equation (2.16) [Thelen *et al.*, 2003].

$$\dot{a} = \frac{u - a}{T} \begin{cases} T = \left[\frac{u}{T_a} + \frac{(1-u)}{T_d}\right]^{-1} & \text{, for } u \geq a \\ T = T_d & \text{, for } u < a \end{cases} \tag{2.16}$$

2.3.7 Musculoskeletal model applications

Musculoskeletal models have been successfully applied in various applications to analyse a number of clinical issues. For example models of the human shoulder have been used to analyse shoulder stability, rotator cuff tears, shoulder arthroplasty and tendon transfers [Favre *et al.*, 2009]. Applications typically involve the simulation of the human body with most analyses categorised into two groups; *forward* and *inverse* analyses.

Inverse analyses

Inverse analyses use the recorded motions and external forces of a person performing activities of interest, and inversely solve the dynamic system to analyse the musculoskeletal system. A common example is to use the walking gait of subjects recorded using motion capture technology. An inverse kinematics solution creates a trajectory for the musculoskeletal model that best fits that recorded motion, then inverse dynamic calculations are performed to estimate the joint torques required to achieve this motion.

Further inverse analysis can calculate solutions for the forces, activation and neural excitation in individual muscles during the recorded activity. The human body has 244 kinematic degrees of freedom [Morecki *et al.*, 1984], and a conservative estimate of 630 muscles, meaning on average each degree of freedom is actuated by 2.6 muscles [Prilutsky and Zatsiorsky, 2002]. This highlights the redundancy of the human body which results in infinite solutions to computing muscle activations corresponding to the dynamic state of musculoskeletal models. This indeterminacy is commonly addressed using optimisation methods guided by a cost function related to some physiological metric. Examples of such cost functions include the minimisation of muscle stress [Collins, 1995; Crowninshield *et al.*, 1978; van der Helm, 1994] or the sum of muscle forces to the n-th power [Collins, 1995; Forster *et al.*, 2004; van der Helm, 1994], maximise endurance [Brand *et al.*, 1986; Nieminen *et al.*, 1995; Pedersen *et al.*, 1997], and minimise metabolic cost [Anderson and Pandy, 2001; Happee and der Helm, 1995]. The estimation of individual muscle forces has been successfully applied in a variety of clinical investigations, and is an ongoing topic of research in musculoskeletal modelling [Favre *et al.*, 2009].

Forward analyses

An alternate approach for analyses using musculoskeletal models are forward analyses, based on using the predicted motions resulting from neural excitation. Rather than using a reference trajectory to inversely calculate the kinematics and dynamics of the musculoskeletal system, forward dynamics is used with muscle excitation as the input from which the resulting motion of the musculoskeletal system is calculated. Comparing the calculated trajectory against an experimentally obtained reference trajectory, the muscle excitations can be optimised such that the forward dynamic motion result closely matches the experimental data [Thelen *et al.*, 2003]. An advantage of using forward dynamics is that it is less dependent on the kinematic and force measurements, and also inherently includes muscle dynamics in the solution [Erdemir *et al.*, 2007].

Forward analyses are not limited to using motion as the basis for calculating the solution. The difference between computed and measured joint torque can also be used as the optimisation criterion, as done in [Buchanan *et al.*, 2005] to simulate ankle joint torque during isokinetic and walking tasks. It is also not required that the optimisation criteria be obtained experimentally. Other criteria calculated from the motion resulting from the forward simulation can be used to find the solution. For example in a pedaling task the optimal muscle excitation and coordination was calculated using a forward analysis with maximum-speed used as the optimisation objective [Raasch *et al.*, 1997].

2.3.8 Musculoskeletal models in robotics

There are examples in the literature of musculoskeletal models used in the control of robotic systems. To date the author is unaware of any attempt to utilise a musculoskeletal model to estimate the assistance needs of a person for the purpose of providing robotic assistance within an AAN paradigm.

Khatib *et al.* [2004] utilised a full body musculoskeletal model as the basis for governing the motion of a humanoid robot. The purpose was to find solutions to the robot's kinematic redundancy with human-like motions. Using the musculoskeletal model, the

redundancy was resolved by controlling the robot to position itself such that the muscular effort in the musculoskeletal model is minimised, which resulted in human-like motions.

Fleischer and Hommel [2008] used a musculoskeletal model of the leg to calculate the relationship between muscle excitation and the resulting torque about the knee. Using measured EMG signals the resulting muscular torque was calculated using the musculoskeletal model. This estimated torque was used as a reference from which assistive torque provided by an exoskeleton was controlled. The system acts as a torque amplifier, using the estimated knee torque calculated from the musculoskeletal model based on EMG measurement. It does not use the musculoskeletal model to estimate a subject's capabilities and subsequently their assistance needs.

Research by Ueda *et al.* [2010] is to date the closest relating to the work in this thesis in terms of utilising a musculoskeletal model for controlling a robot. It aims to induce predictable muscle activation patterns in a subject's upper limb such that analysis of neurological impairment can be performed. Firstly the desired change in muscle activity is defined in terms of ratio change. A musculoskeletal model is then used to calculate the exoskeleton torques required to induce this change in muscle activation by applying interaction forces between the robot and the subject's upper limb. Experiments measuring the muscle activity demonstrated the feasibility of achieving expected changes in muscle activations. Motivation for this research is the idea that by using a robot to apply unique loads to subject's limbs to induce predictable changes in muscle activity, differences between anticipated and measured muscle activity may provide useful diagnostic information to assist in identifying impairments and plan tailored therapies for specific disorders.

2.4 Summary

Robots which operate collaboratively with humans to provide physical assistance have been developed for a variety of applications in industry and health care. However the success of such technology relies on that they provide assistance in a manner suitable

for the application. Numerous methods have been developed for controlling robots so as to provide assistance to the operator, as well as many paradigms to govern how this assistance is given. An example to governing physical assistance is the AAN paradigm which aims to provide the operator with the amount of assistance specific to their requirements to successfully perform the task. Currently, typical AAN paradigms use empirical performance-based approaches where the robot learns the assistance requirements of the operator by observing and critiquing their performance. Although this approach has shown success in applications such as robotic rehabilitation, empirical approaches have inherent limitations due to the need of observations of the operator performing tasks on which to derive an estimate of their assistance requirements. In this thesis a model-based AAN paradigm is developed. It uses a musculoskeletal model representing the operator to avoid the limitations associated with empirical AAN methods. Such models are used for simulating the biomechanics of the human body and have been successfully applied in various clinical and robotic applications.

Chapter 3

A Framework for Model-based Robotic AAN

The Assistance-As-Needed (AAN) paradigm aims to provide a human operator with assistance specific to their needs as they perform physical tasks. This means that assistance should be adjusted with respect to both the task being performed and the operator performing it. As the difficulty of the task changes (e.g. an object being carried becomes lighter) then assistance should be changed accordingly. Likewise if the operator's capability to perform the task changes (e.g. they become fatigued) then ideally assistance should also be adapted. Deriving an estimate of the operator's assistance requirements is the main challenge with the AAN paradigm. Current solutions typically use empirical approaches where the performance of the operator is critiqued, from which their assistance requirements are inferred. As detailed in Section 2.2.3, approaches that use an operator's performance to gauge assistance requirements have inherent limitations.

The ideal AAN implementation requires that the operator's assistance requirements for the task being performed be known, and subsequently be provided by the assistive robot during the task. It also requires that this can be achieved for any task. Since different tasks have different requirements, and since it is impossible for a robot to learn the operator's assistance requirements for every possible task, the ideal system would be able to predict their assistance requirements even without the need for empirical

observation. These ideals form the motivation behind the model-based paradigm developed in this thesis. If a model is available from which the assistance requirements of the operator can be calculated with respect to arbitrary tasks, then there is no need to observe task performance. Furthermore, the model may be used to predict how assistance should be adapted in response to factors relating to the task and the operator.

In this chapter a framework is presented to estimate the assistance requirements of a human with respect to physical tasks. A two-model framework is used, the first model calculating the requirements of the task being performed. The second model uses a musculoskeletal model to estimate the capability of the operator to perform the task. Results from these models are used to gauge the assistance requirements of the operator. After presenting this framework it is then demonstrated by applying it to two typical activities of daily living. Lastly, the peculiarities of estimating the assistance needs of a human using a musculoskeletal model to provide AAN are discussed. Alternative model-based approaches are compared, and the benefits of the musculoskeletal model based approach (in particular for applications such as rehabilitation) are discussed.

3.1 Framework

Consider the generalised scenario of a person performing a physical task whilst being assisted by a robot working in collaboration with them. An arbitrary physical task requires some amount of physical capability for it to be performed. In turn, the human has some amount of physical capability to be able to perform the task. If they have capability greater than or equal to what the task requires, then by this definition they are capable to perform it without the need for external assistance. Alternatively if the human's physical capability is less than the requirements of the task, then they are unable to perform it to the required sufficiency. There is a *gap* between the task's requirements and the human's capability, which is conceptually illustrated in Figure 3.1.

Assistance provided by a robot working collaboratively with the human is thought of as reducing the requirements of the task, or alternatively increasing the capabilities of its human operator. The effect is that the gap between task requirement and human

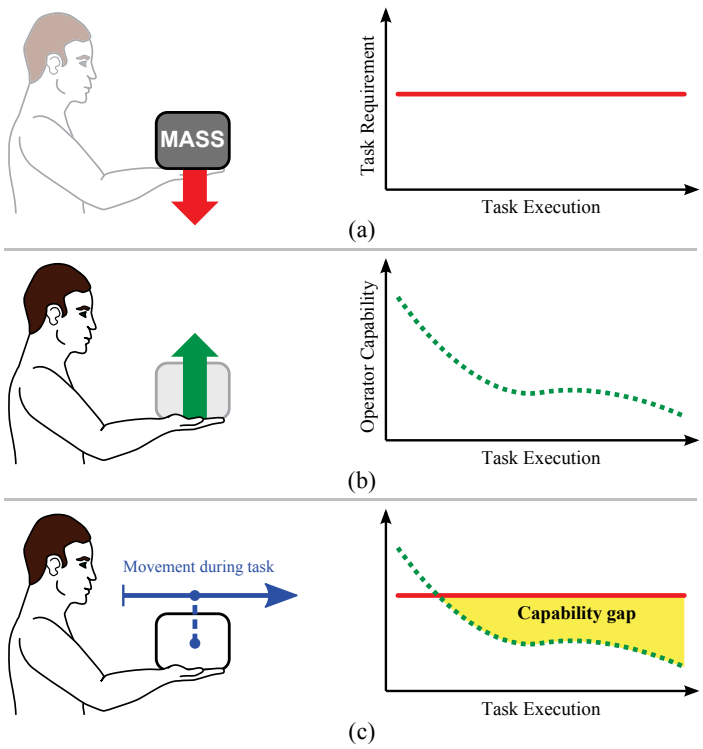

Figure 3.1: Generalisation of Assistance-As-Needed, represented as the gap between the requirements of a task and the capability of a human to perform it. (a) Requirements of a task. (b) Capability of a human to perform a task. (c) The gap between the task requirements and the human's capability as the task is executed.

capability is supplemented by the assistance provided by the robot. With the objective of providing AAN such that the human (assisted by the robot) is capable of meeting the requirements of the task, this gap then signifies the amount of assistance which should be provided by the AAN paradigm. By definition providing assistance less than this amount means the operator cannot perform the task as it is defined. Alternatively, providing assistance greater than this still allows the task to be performed, but provides more assistance than what the human requires. If the capability of the operator is greater than what the task requires (i.e. the gap is negative) then no assistance should be provided. It is on this basis that the framework for the model-based AAN paradigm is developed.

3.1.1 Structure

The framework developed for model-based AAN is shown in Figure 3.2. It is separated into two levels. At the lower level the robot is controlled by a control scheme as it provides assistance to its human operator via physical interaction with them and the environment. The control scheme remains generalised as various types may be utilised (see Section 2.2.1). Later in Chapter 5 an admittance-based control scheme will be implemented.

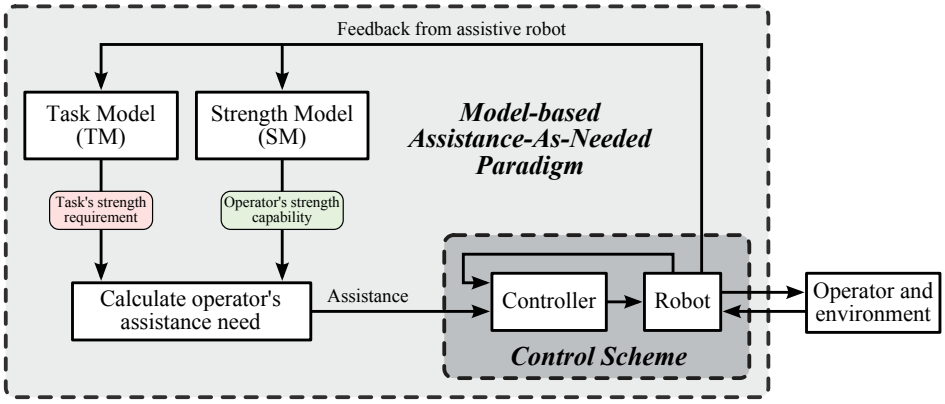

Figure 3.2: The model-based Assistance-As-Needed framework.

The higher level of the framework is responsible for determining the assistance requirements of the operator. Sensory information from the robot is used to obtain task and operator related information such as limb position, velocity, and force interaction between the robot, the operator and their environment. This information is used by two models to determine the required assistance. A Task Model (TM) calculates the strength the task requires from the operator for it to be performed. A Strength Model (SM) represents the operator and is used to calculate (with respect to the task being performed) how much physical strength capability they have to perform it. This estimation of operator strength will be derived using a musculoskeletal model, as is discussed later. Results from these two models are combined to determine the assistance requirements of the operator, which is then fed to the robot's control scheme. This forms an outer control loop operating at the higher level of the framework to govern how the lower level control scheme administers robotic assistance to the operator.

This framework is designed taking many factors into consideration. Strength is used to represent both the task's requirements and the operator's capability. Section 3.2 defines the term *strength* in the context of this thesis and the justification for using it as the measure on which assistance is based. The capability of an operator to perform tasks is affected by numerous complex factors. Calculating assistance requirement based on strength allows many factors (e.g. limb position, external forces, physical impairments) to be considered during this calculation. The result is a single measure that represents the operator's assistance requirement for the task being performed, whilst encapsulating numerous factors which affect the operator's strength. Because this calculation is performed in the high level of the framework, the result can be used with a wide range of control schemes to adapt parameters so as to adjust the assistance it provides. For example the result could adjust the stiffness of an impedance control scheme [Krebs *et al.*, 2003], or the gain in a force augmentation scheme [Kazerooni, 1990]. This allows existing control schemes to be easily incorporated into the framework, simplifying integration with currently available robotic systems.

Another reason for abstracting the assistance requirement calculation from the robot control scheme is the computational cost. A musculoskeletal model will be utilised to estimate the operator's strength capability. Analyses utilising musculoskeletal models (see Section 2.3.7) typically require computationally expensive numerical techniques such as inverse dynamics and optimisation methods. As the operator performs a task their assistance requirements continually change, and hence their strength capability needs to be continually calculated during task execution. It is anticipated that such calculations are unable to be performed at the same rate the robot control scheme operates at, which can be at rates of 1kHz or greater. However since the operator's assistance requirement is calculated at a higher level, it may be calculated at a slower rate with the result fed into the low level control scheme at this slower rate. Applications in which the operator's assistance requirements do not change quickly may allow this high level computation to be performed at relatively low rates. The minimum rate required for this calculation depends on the specific application. Aspects regarding real time calculations are later discussed in Section 6.2.4.

3.2 Strength as the Measure of Capability

In this thesis the capability of a subject to perform tasks, and consequently their assistance requirements, is determined based on their strength. The term strength is defined as the maximum force that a person can physically exert [Kumar, 2004]. Because this thesis focuses on tasks using the upper limb with interaction occurring at the hand, the term *strength* is used (unless stated otherwise) to represent the maximum magnitude of force that can be exerted by a subject at their hand. Occasionally, the term will be used explicitly referring to the maximum torque or force that can be exerted at the joints or in the muscles of the upper limb.

There are many factors that determine the requirements of different tasks. Physical tasks commonly involve interaction with the environment [Matsumoto *et al.*, 2011], and hence require the ability to express forces (i.e. strength). The tasks can also require a person to have the dexterity needed to control this interaction, for example to manipulate an object as required in an assembly task. From the perspective of the person performing the task, there are numerous factors that determine if they can meet a task's requirements. Whether they have the required strength is determined by a number of complex physiological factors. Tasks which require large physical effort or lengthy durations of force production are affected by factors such as fatigue. Tasks such as surgery require precise coordinated movements. These as well as other physical and cognitive factors affect the capability of a person to perform tasks. Representing all the factors relating to task requirements and human capabilities in a model is an immense challenge and outside the scope of this project. For practicality the model-based approach developed in this thesis uses the strength at the hand as the measure by which both the requirements of a task, and the capability of an operator to perform it, are represented and subsequently compared to determine the assistance requirements of the operator.

There are several rationales for using strength as the measure from which the assistance requirements of an operator are derived. Firstly, a model-based approach requires the task requirement and the operator capability to be combined in order to determine

the gap. It is not useful to use two incompatible metrics, for example using the positional accuracy as the measure of the task's requirement, then comparing this to the strength capability of the operator. The two metrics must be able to be related through some relationship to determine a gap representative of the operator's need for assistance. It is convenient to use the same two metrics so that a measure of the gap between them can be found directly. Strength (represented in Newtons) is a metric which both the task requirement and the operator capability can be represented and easily combined.

Secondly, strength is relatively easy to calculate using a model compared with other possible metrics. The forces required by a task where an object is manoeuvered can be calculated if the object's trajectory and inertial properties are known. Alternatively, if unknown the forces may be measured directly using sensors. The strength capability of the operator can also be derived, either from the literature [Kumar, 2004] or calculated from a model [Chaffin and Erig, 1991; Roman-Liu and Tokarski, 2005]. Other factors affecting the ability to perform tasks are not as easy to implement in a model; for example muscle synergies which are hypothesised for controlling limb coordination but are not well understood [Tresch and Jarc, 2009].

Lastly, strength is a major determinant of limb functionality [Canning *et al.*, 2004; Mercier and Bourbonnais, 2004]. In a disability such as stroke it is common for the limb functionality of patients to be diminished. Regimes for rehabilitation often fall into the categories of either *force* (i.e. strength) or *motion*, with debate as to which is the preferred approach [Hogan *et al.*, 2006]. Canning *et al.* [2004] showed that both limb strength and dexterity contribute to limb functionality, however it was determined that strength was the bigger factor [Canning *et al.*, 2004]. Furthermore, strength training has been shown to increase limb functionality after stroke [Morris *et al.*, 2004; Ouellette *et al.*, 2004; Patten *et al.*, 2006; Weiss *et al.*, 2000]. It is for these reasons described why strength is selected as the measure of capability.

3.3 Task Model (TM)

The Task Model (TM) is developed for calculating the strength required by the operator to perform tasks involving the upper limb. As discussed in Section 2.2.3 the AAN paradigm has gained attention in robotic rehabilitation. This therapy often involves patients performing tasks designed to mimic Activities of Daily Living (ADLs). The TM is developed with ADLs used to provide a realistic context for the type of tasks the AAN paradigm is commonly applied to. A study by Matsumoto *et al.* [2011] analysed the needs of people in every day life by logging the ADLs performed. The frequency of the ADLs recorded is shown in Figure 3.3. Lifting was the predominant activity, being included in 43% of recorded user-involved behaviours. Other upper limb tasks such as putting down, manipulating and carrying objects are also often performed in daily life [Matsumoto *et al.*, 2011]. Such upper limb activities include both movement of the limb and physical interaction with the environment. Based on this the TM is developed using these two components; *limb motion* and *external force*.

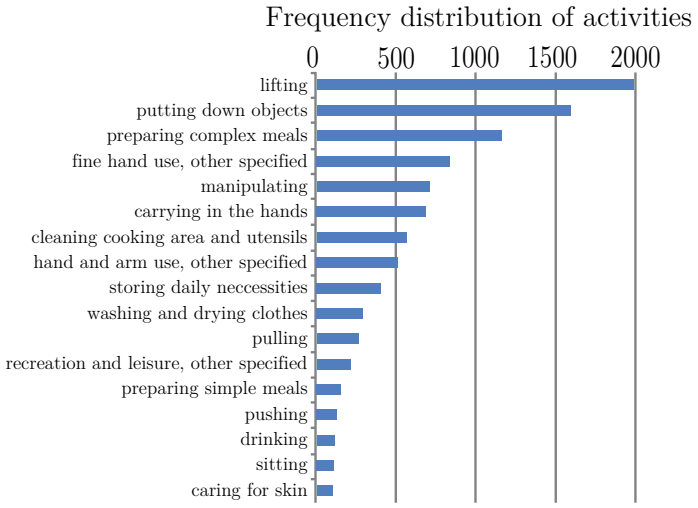

Figure 3.3: The frequency distribution of Activities of Daily Living (ADLs) performed in every day life. The results are reproduced from [Matsumoto *et al.*, 2011].

3.3.1 Limb motion

Motion defines the position, velocity, and acceleration of the limb as the task is carried out. It is assumed the task is performed by interacting with the environment at the operator's hand. The upper limb is kinematically redundant, meaning the hand can be placed in a desired position/orientation using infinite combinations of shoulder, elbow, and wrist joint angles. This means motion of the hand alone does not fully define the motion of the upper limb. This redundancy needs to be considered when calculating limb strength, since limb joint strength varies with position. A set of generalised coordinates representing the positions of the joints in the limb is used. This fully defines the limb motion with the additional benefit of allowing the same generalised coordinates to be used in the strength model developed later. The position of the joints in a limb with k degrees of freedom are defined as $\mathbf{q} = [q_1, q_2, \cdots, q_k]^T$.

The velocity and acceleration of the limb are defined by $\dot{\mathbf{q}} = [\dot{q}_1, \dot{q}_2, \cdots, \dot{q}_k]^T$ and $\ddot{\mathbf{q}} = [\ddot{q}_1, \ddot{q}_2, \cdots, \ddot{q}_k]^T$, respectively. However for slow motions the dynamic effects may be ignored. In a study by Rosen *et al.* [2005] the upper limb motions of 24 ADLs were recorded, and using inverse dynamics the joint loads due to gravity, inertial, and centrifugal/Coriolis effects were calculated. Results showed the overall shape of the joint load torques were dictated solely by the low frequency gravitational load in all ADLs, which was larger than the remaining dynamic loads combined. This suggests that for typical ADL tasks it is appropriate to ignore the dynamic loads and assume quasi-static conditions ($\ddot{\mathbf{q}} = \dot{\mathbf{q}} = 0$).

3.3.2 External force

The upper limb physically interacting with the environment results in external loads applied to the limb. It is assumed this interaction only occurs at the hand, and is represented by force $\mathbf{u} \cdot S_T$. Term $\mathbf{u} = [u_x, u_y, u_z]^T$ is a unit vector denoting the direction of the external force defined in the work space. Parameter S_T is the scalar magnitude of this external force. For simplicity it is assumed this load is a force acting through the centre of the hand, so moment loads about the hand are not considered.

3.3.3 Usage

An illustration of the TM is shown in Figure 3.4 with the limb motion $(\mathbf{q}, \dot{\mathbf{q}}, \ddot{\mathbf{q}})$ and the external force interaction at the hand $(\mathbf{u} \cdot S_T)$ defined. For the operator to perform the task as it is defined they are required to match the limb motion $(\mathbf{q}, \dot{\mathbf{q}}, \ddot{\mathbf{q}})$ whilst opposing an external force at the hand in direction $\mathbf{u}$ with magnitude S_T. If an external force of magnitude S_T in the direction of $\mathbf{u}$ cannot be opposed whilst the motion is carried out, then by definition the task is unable to be performed. Thus for a task defined by $\mathbf{q}$, $\dot{\mathbf{q}}$, $\ddot{\mathbf{q}}$, $\mathbf{u}$, and S_T, the task's strength *requirement* (at the hand in the direction of $\mathbf{u}$) to be capable of performing it is represented by the scalar magnitude S_T.

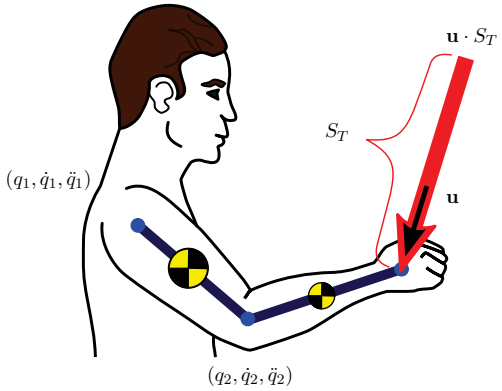

Figure 3.4: Example of the Task Model (TM). The external force $\mathbf{u} \cdot S_T$ represents the limb interaction with the environment.

Implementation of the TM depends on the application and the hardware available. Typically with assistive robotics it is possible to use the system's sensors to determine the position of the operator, particularly for wearable robots such as exoskeletons. From the motion of the robot, the operator's limb motion $(\mathbf{q}, \dot{\mathbf{q}}, \ddot{\mathbf{q}})$ may be derived. If the robot acts as a mechanical interface between the operator and task then forces between the operator, robot and task can be sensed (e.g. using force/torque sensors) to directly measure the external force required during task execution. From these measurements the direction $\mathbf{u}$ and magnitude S_T of the task's external force can be calculated. Alternatively the task's strength requirement S_T may be calculated from the TM as a function based on knowledge of the task being performed and the sensory information available, as generalised by Equation (3.1). Some examples of this are provided in the

following section. In simulations performed later in this thesis, the external force will be either explicitly defined based on the task, or derived as a function of the limb motion.

$$S_T = f\left(\mathbf{q}, \dot{\mathbf{q}}, \ddot{\mathbf{q}}, \mathbf{u}\right) \tag{3.1}$$

3.3.4 Examples

The generic TM can be implemented to accommodate variation in a specific task. Hence a single model can be used in tasks containing variable factors, rather than requiring to switch between several different models. The following examples demonstrate how the TM may be applied to some upper limb tasks.

The first example shown in Figure 3.5 involves a task requiring the operator to carry an object of known mass (m) in their hand. Assuming the object is moved by the operator in an unexceptional manner, dynamic forces between the object and the subject may be ignored. In this case the external force applied to the operator's hand has the magnitude equal to the weight of the object ($S_T = mg$, where $g = 9.81\text{m/s}$) and its direction ($\mathbf{u}$) is in the direction of gravity. The task's strength requirement S_T is constant and independent of limb motion.

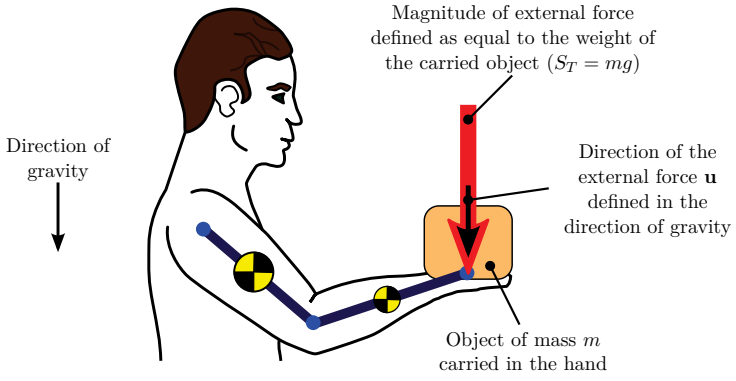

Figure 3.5: Example of applying the TM to a task where the operator is required to carry an object of known mass. The direction of the external force at the operator's hand ($\mathbf{u}$) is defined in the direction of gravity. The task requirement S_T is defined as equal to the weight of the object being carried.

The second example shown in Figure 3.6 involves the operator performing a sandblast-

ing task. A nozzle of mass m is held in their hand and blasts sand in the direction it is pointed, producing a reaction force of known magnitude F_R in the opposite direction. The operator is required to statically hold the nozzle as the blasting is performed. The external force applied to their hand is the sum of both the nozzle's weight force (mg) and its reaction force (F_R). The magnitude of the weight force is assumed constant and in the direction of gravity, similar to the previous example. The reaction force is assumed to have a constant magnitude, but its direction depends on the orientation of the nozzle. From an assistive robot worn by the operator the position of their limb ($\mathbf{q}$) can be derived, and from this the orientation of the nozzle is calculated. The net external force is then calculated by combining the nozzle's weight force in the direction of gravity with the reaction force in the direction opposite to where the nozzle is pointed.

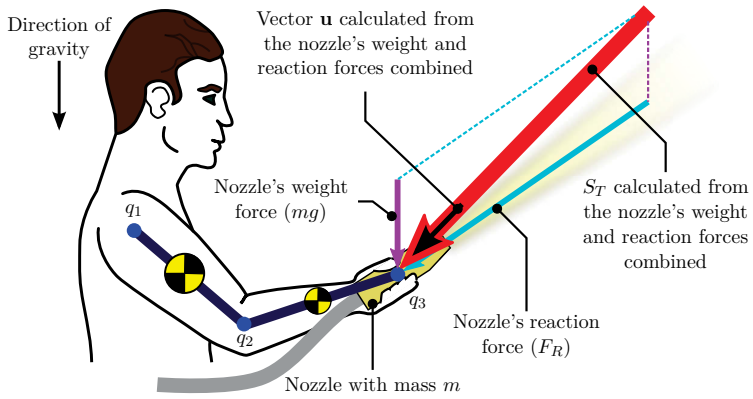

Figure 3.6: Example of applying the TM to a sandblasting task. The operator holds a nozzle of mass m with its weight force mg in the direction of gravity. The blasting produces a reaction force F_R in the opposite direction to where the nozzle is pointed. The external force applied to the operator at the hand is the combination of the nozzle's weight and its reaction force. To calculate this requires the orientation of the nozzle to be known. With the position of the operator's limb (represented in the figure by q_1, q_2, q_3) derived from the robot, the orientation of the nozzle and subsequently $\mathbf{u}$ and S_T can be calculated.

The third example shown in Figure 3.7 involves a stroke patient manoeuvering their hand as part of a rehabilitation exercise. As they move their hand from Point A to Point B, a spring (possibly a virtual spring) with known stiffness is connected between the hand and Point C which produces a disturbance force. The patient is required to oppose this force as they move their hand during the exercise. In this example, the external force applied to the hand depends on its location relative to Point C. The

robot, attached to the patient, is used to derive the position of their limb ($\mathbf{q}$), and from this the position of the hand relative to Point C is calculated. The direction of the spring force applied to the hand ($\mathbf{u}$) is calculated such that it points from the hand towards Point C. The magnitude of this force is calculated from the distance between the hand and Point C, multiplied by the stiffness of the spring.

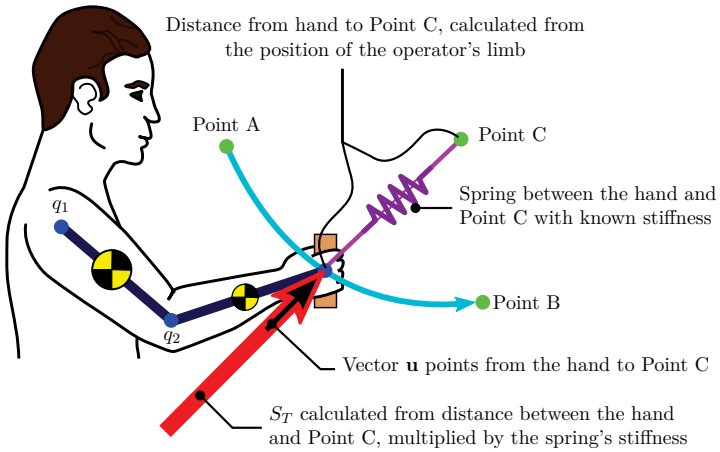

Figure 3.7: Example of applying the TM to a rehabilitation exercise. As the operator moves their hand from Point A to B, a spring with known stiffness attached between the hand and Point C produces a disturbance force. The magnitude and direction of this force is calculated from the position of the operator's limb which is derived from a robot attached to the operator. With the hand position known, the direction of the force at the hand ($\mathbf{u}$) is calculated such that it points from the hand to Point C. The magnitude of the force (S_T) is calculated from the distance between the hand and Point C multiplied by the spring's stiffness.

3.4 Strength Model (SM)

The Strength Model (SM) is developed to calculate the strength capability of the operator to perform the desired task. It complements the TM and hence shares some similarities. Like the TM, the SM uses limb motion and external force to define the task for which the model is being applied. Motion is again defined by the generalised coordinate positions, velocities, and accelerations ($\mathbf{q}, \dot{\mathbf{q}}, \ddot{\mathbf{q}}$) of the limb. The external force representing interaction with the environment during task execution is again applied to the hand with direction represented by unit vector $\mathbf{u}$. The magnitude of this

force is represented by scalar variable F^E (unlike the TM where magnitude S_T was set depending on the strength requirements of the task). An example is shown in Figure 3.8.

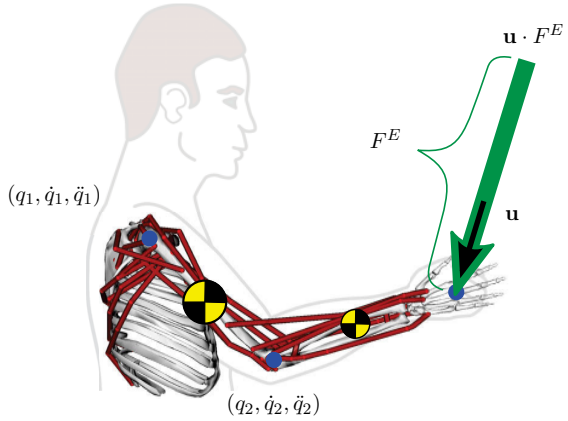

Figure 3.8: Example of the Strength Model (SM). The external force $\mathbf{u} \cdot F^E$ is the limb's interaction with the environment during the task.

The SM is used to calculate the strength of the operator, which corresponds to the maximum magnitude of external force (F^E) they can exert at the hand. The value of F^E is not explicitly set but rather is a variable with its maximum referred to as the *strength capability* of the operator, defined as $S_P = \max[F^E]$. Since the purpose of the SM is to calculate operator strength with respect to the task, this maximum magnitude of external force must be producible whilst the task is being performed as required. That is, this strength must be calculated taking into account effects dependent on $\mathbf{q}, \dot{\mathbf{q}}, \ddot{\mathbf{q}}$, and $\mathbf{u}$ since this is what constitutes the task. The limb motion dictates the dynamic and gravity loads that the limb needs to overcome whilst the external force is being opposed. The position of the limb and direction of the external force dictates how much load is placed on each of the joints in the limb from the external force. Additionally the maximum magnitude of external force the upper limb can oppose is limited by constraints imparted by the physiology of the operator. The problem of calculating operator strength capability S_P for a desired task (whilst obeying task and physiological constraints) is formalised in Equation (3.2). Once calculated the operator's strength capability (S_P) is used with the strength requirements of the task (S_T) to gauge the capability of the operator with respect to the task and estimate their assistance requirements.

$$\begin{aligned} \text{Calculate strength capability :} \quad & S_P = \max\left[F^E\right] \\ \text{For the task defined by :} \quad & \{\mathbf{q}, \dot{\mathbf{q}}, \ddot{\mathbf{q}}, \mathbf{u}\} \end{aligned} \tag{3.2}$$

The steps for calculating S_P are illustrated in Figure 3.9. A musculoskeletal model (MM) of the upper limb is used to represent the operator, and it is from this model their physical strength capability to be able to perform desired tasks is derived. This MM is used along with the limb motion defined by $\mathbf{q}, \dot{\mathbf{q}}, \ddot{\mathbf{q}}$ to calculate the load torques at each joint resulting from gravity and dynamic effects. For typical ADL movements the dynamic loads may be ignored as discussed in Section 3.3.1. Next, as discussed in Section 2.3.1 the force each muscle can produce depends on its length, velocity, and a number of intrinsic properties. The force capability of each muscle is calculated with respect to the task's limb motion. The torque that each muscle can produce about the joints in the limb, and subsequently how the joint torque contributes to the strength at the hand is calculated using kinematic relationships between the muscles, joints and hand. These relationships are also calculated from the MM. With the dynamic/graviational joint loads, force producing capability of the muscles, and the kinematic relationships calculated from the MM, the final step is to solve for the largest maximum magnitude of external force the operator can oppose at the hand in the direction of $\mathbf{u}$. This final process of finding S_P is an optimisation process which requires the use of numerical methods.

Calculating operator strength capability as defined in Equation (3.2) can be performed using different model-based approaches. The method utilising a musculoskeletal model which is developed in this work, and other model-based approaches are compared in Section 3.6.2, where their benefits and limitations are discussed.

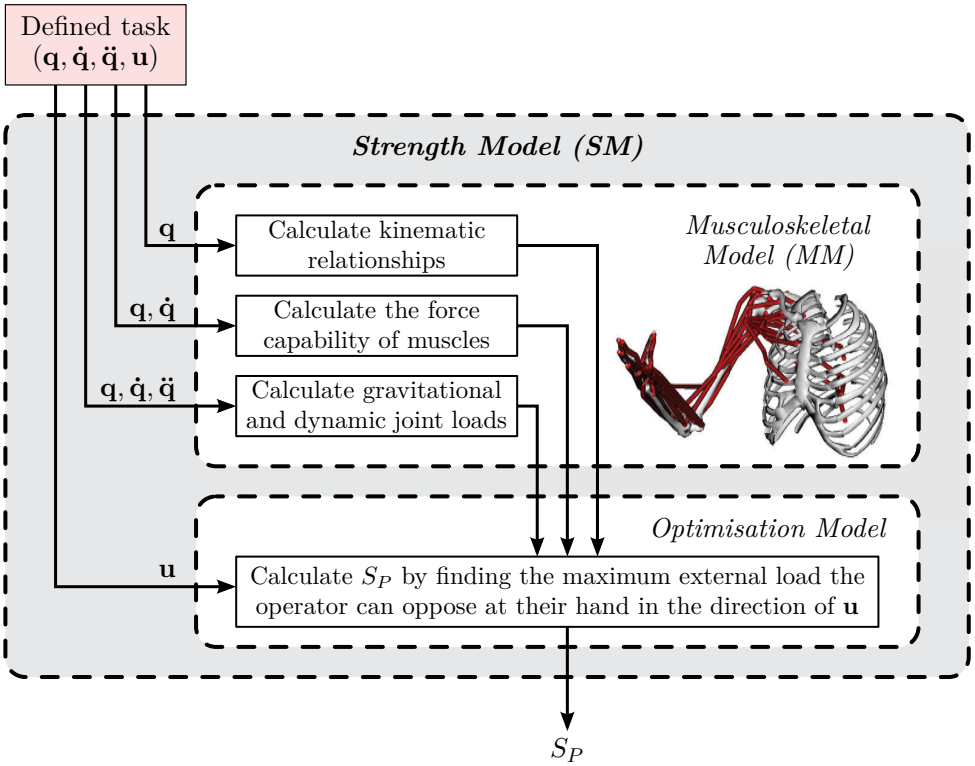

Figure 3.9: Overview of calculating operator strength capability (S_P) using the SM. The limb motion and direction of external force are defined by $\mathbf{q}, \dot{\mathbf{q}}, \ddot{\mathbf{q}}, \mathbf{u}$. The musculoskeletal model is used to calculate the dynamic and gravitational joint loads resulting from the task's motion. The force producing capability of each muscle in the limb is calculated. Kinematic relationships between the muscles, joints and the hand are used to allow the contribution of the muscle forces to the strength at the hand to be calculated. The calculated joint loads, muscle force capabilities and kinematic relationships are then used in an optimisation model to calculate the strength of the operator at the hand, in the direction of $\mathbf{u}$.

3.4.1 Upper limb musculoskeletal model (MM)

The model-based AAN framework requires a MM, but it is not specific to any particular model. Several upper limb models exist in the literature [Garner and Pandy, 2001; Holzbaur *et al.*, 2005; Maurel *et al.*, 1996]. The MM developed by Holzbaur *et al.* [2005] shown in Figure 3.10 is used in this thesis. It was chosen as it is publicly available, and has been shown to adequately represent upper limb characteristics such as individual joint strength [Holzbaur *et al.*, 2005], muscle moment-arms [Gatti *et al.*, 2007] and limb end-point stiffness [Hu *et al.*, 2011b]. It consists of 15 degrees of freedom and

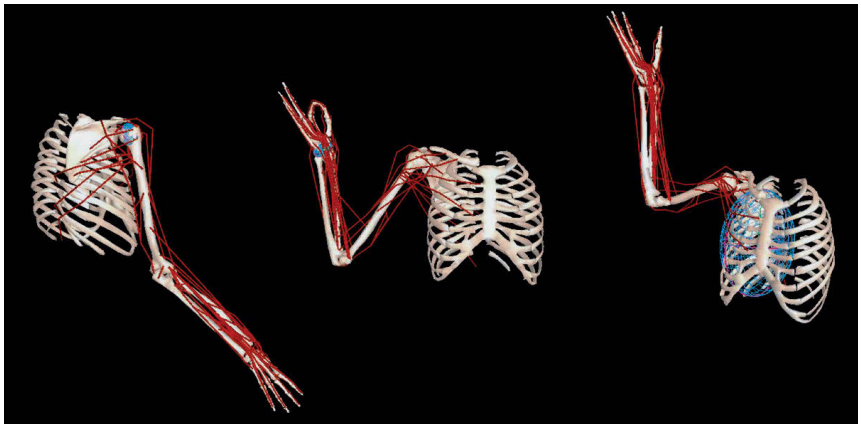

Figure 3.10: Upper limb musculoskeletal model, image from [Holzbaur *et al.*, 2005]

50 musculotendon units (MTU, see Section 2.3.1) to model the shoulder, elbow, wrist, finger and thumb. Shoulder movement has only three degrees of freedom, however clavicle/scapular movement is retained by using regression equations derived experimentally from de Groot and Brand [2001] to relate their movement to humerus elevation. For simplicity in this thesis the MM was reduced to the four degrees of freedom relating to the shoulder and elbow. The remaining joints (hand, finger, thumb) were not of interest and ignored by making them fixed. The MTUs which were made obsolete after reducing the degrees of freedom were also ignored to increase the speed of calculations involving the model. Details are provided in Appendix A.1.

This publicly available MM has no inertial properties assigned to the limb segments. These are required for gravitational and dynamic analyses to be performed. Limb segment inertial properties based on the average male were assigned to the model. Based on the average male height and weight (1.75m and 78kg, respectively [Gordon *et al.*, 1989]) the mass and centre of mass of upper limb body segments are calculated using anthropometric equations [Winter, 1990]. Principal moments of inertia from Chandler *et al.* [1975] are also assigned to the upper limb segments. Details of these mass and inertial properties are provided in Appendix A.2. The OpenSim software environment [Delp *et al.*, 2007] is used to obtain the dynamic and musculoskeletal parameters from the model for analysis.

3.4.2 Strength calculation assuming uncoupled joints

So far an explicit method for calculating S_P using the MM has not been presented. Development of the method for estimating operator strength, and the evaluation of the strength results is paramount to the efficacy of the proposed AAN paradigm. Chapter 4 will focus on this since it requires extensive investigation. The focus of the current chapter is to introduce the framework for model-based AAN. However, to be able to demonstrate this framework a method of calculating S_P is needed, and therefore a simplified method will be briefly utilised this chapter. This method makes the assumption that each joint in the limb is independent, ignoring joint coupling that exists by muscles which produce torque about multiple joints. Although the assumption of uncoupled joints is not consistent with physiology, it greatly simplifies the calculation of S_P which allows the focus of this chapter to remain on the application of TM and SM within the model-based AAN framework. Furthermore, demonstrating the limitations of this uncoupled method provides the motivation for the more sophisticated method that does consider joint coupling, which is developed and evaluated in Chapter 4.

The uncoupled approach towards calculating S_P is similar to a method used by Ambrose and Diftler [1998] to calculate the strength of a robotic manipulator at its end-effector based on the torque capabilities at its joints. Each joint is considered an independent actuator, and its contribution towards producing force in the desired direction at the end-effector is calculated. With the maximum of this force calculated for each joint, the joint capable of the least force is considered the weakest, with its corresponding force considered as the strength of the entire robot. Here instead of a robot with actuators producing torque at the joints, the strength of the upper limb with joint torque produced by muscles is calculated. Unlike Ambrose and Diftler who did not account for gravity or dynamic loads, it is included when the uncoupled operator strength is calculated. The detailed derivation of this uncoupled method is presented in Appendix B.

3.5 Framework Applied to Example Tasks

In this section the TM and SM are applied to example tasks to demonstrate the model-based AAN framework and how it can be used to calculate the assistance requirements of an operator. As discussed in Section 3.3, the AAN paradigm has gained popularity in robotic rehabilitation in which therapy often involves patients performing tasks which mimic activities of daily living (ADL). Therefore typical ADLs which utilise the upper limb are used to provide a realistic context for the kind of tasks this framework may be utilised for in the future. During experiment a subject performs two different ADL tasks. Consultation was made with the Human Research Ethics Committee (HREC) at the University of Technology, Sydney.

Upper limb ADLs commonly involve the lifting and manipulating of objects, with approximately 90% of objects lifted weighing 300g or less [Matsumoto *et al.*, 2011]. Examples of heavier objects often lifted include a kettle filled with water (1kg) and a vacuum cleaner (3.8kg) [Matsumoto *et al.*, 2011]. Considering this the two tasks are designed around the lifting and manipulation of a 600ml water bottle.

3.5.1 Case study 1: drinking task

In this task the subject's hand is stretched outwards to pick up a water bottle (Figure 3.11a), which is then brought to the subject's mouth so as to drink the water (Figure 3.11b), then returned to the point where it was picked up. This task was designed to incorporate elements common in several ADLs (lifting, picking up, putting down, carrying, drinking [Matsumoto *et al.*, 2011]). It is also similar to tasks performed by patients during robotic rehabilitation [Wolbrecht *et al.*, 2008].

Hand movements were made between the mouth (target M) and 10 other targets located in front of the subject. Each target was reached for twice, resulting in a total of 20 motions to and from the targets. Five targets (A,B,C,D,E) were located on a table surface approximately 25cm below the origin of the subject's shoulder joint. Another five targets (F,G,H,I,J) were positioned at identical locations except raised to approximately

(a) (b)

Figure 3.11: Subject performing the drinking task. (a) Hand stretched outwards to pick up bottle. (b) Hand brought to the subject's mouth so as to drink from the bottle. Motion was recorded using Xsens MVN Biomech motion capture system.

3cm above the subject's shoulder (28cm above the previous five targets). Dimensioned positioning of the target locations is shown in Figure 3.12. Each of the targets were positioned such that the subject's arm was at full reach when lifting/placing the water bottle. Targets A, B, C, D and E are each spaced at 15° intervals about the shoulder, with the middle target C directly in front of the shoulder. Similarly, targets F, G, H, I and J are spaced at 15° intervals with target H in front of the shoulder.

No instruction was given to the subject regarding the path or the speed of their hand during movements. Only the start and end locations where the bottle was moved to were defined. Motion in between the targets was left to the subject to perform as they felt comfortable. The drinking task was performed with the subject carrying a water bottle that was filled with water to weigh 600g.

TM applied to drinking task

As the subject performed the task their motion was recorded using the Xsens MVN Biomech motion capture system. The recorded motion was processed to extract marker

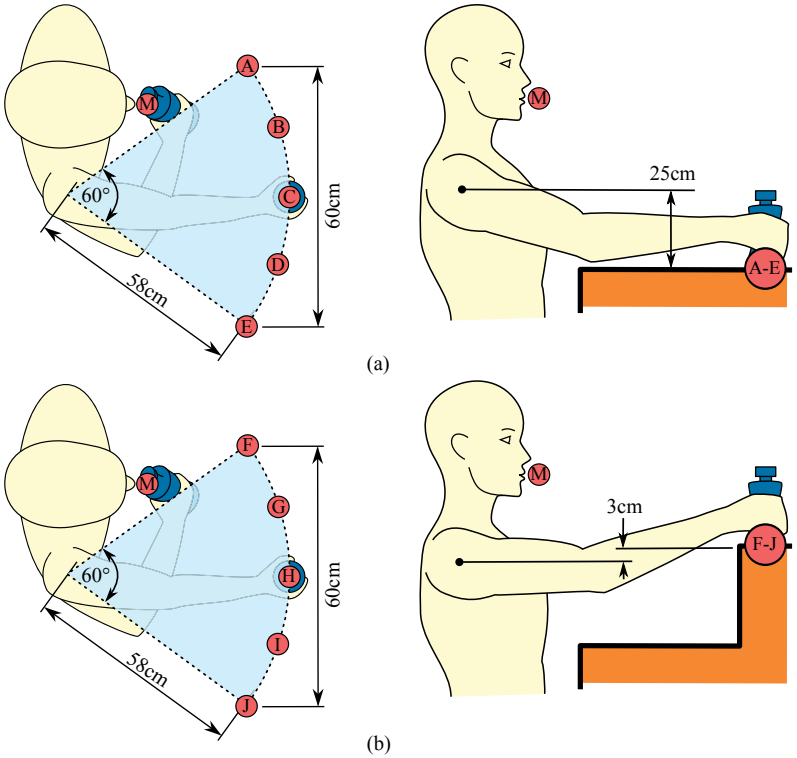

Figure 3.12: Locations of the targets in the drinking task. (a) Targets A, B, C, D, and E are located at table height, approximately 25cm below shoulder height of the subject. (b) Targets F, G, H, I and J are approximately 3cm above subjects shoulder height.

points local to the limb segments. The motion of the upper limb MM is fitted to match the recorded motion using inverse kinematics based on least-squares optimisation using the OpenSim software package [Delp *et al.*, 2007]. After being fitted to the recorded motion the MM generalised coordinate positions ($\mathbf{q}$), velocities ($\dot{\mathbf{q}}$), and accelerations ($\ddot{\mathbf{q}}$) during the motion are available. An example of a motion recorded between two targets is show in Figure 3.13.

The TM external force represents the hand's interaction with the environment, which in this task is the 600g water bottle carried by the subject. This force was not measured during the drinking task, instead it is defined with $\mathbf{u}$ in the direction of gravity, and magnitude equivalent to the weight of the carried bottle ($S_T = 6\text{N}$). Dynamically generated interaction forces between the bottle and the hand were ignored. The suitability of ignoring these effects is discussed in Section 3.6.3.

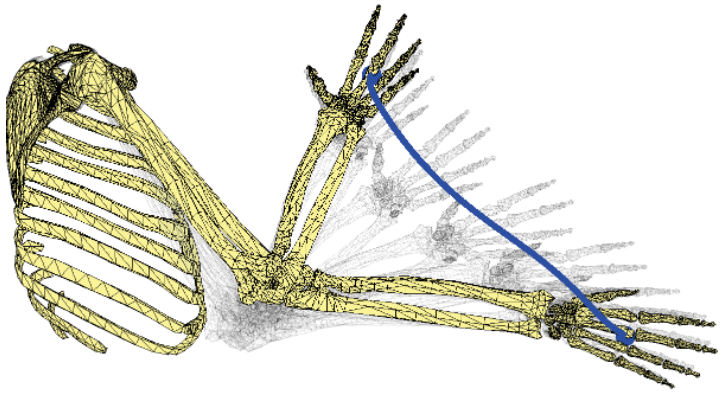

Figure 3.13: Example of the upper limb motion captured during the drinking task.

SM applied to drinking task

The SM calculates operator strength capability at a single instant in time. To calculate strength during the entire task the SM is repeatedly applied to each successive time instant of the recorded motion. For each time instant, the recorded limb motion $(\mathbf{q}, \dot{\mathbf{q}}, \ddot{\mathbf{q}})$ and the direction of the external force $(\mathbf{u})$ are utilised, along with the upper limb MM to calculate the operator strength capability S_P (in this chapter using the uncoupled method detailed in Appendix B). This process is applied to the drinking task as the hand is moved between the subject's mouth (target M) and the remaining targets. The hand is moved starting at target M, towards one of the targets, then back to target M at the mouth. For each target this motion is repeated twice whilst carrying the 600g water bottle.

Results

Because the task's strength requirement was constant during the task ($S_T = 6N$) the attention is on the operator's strength capability calculated using the SM. For each of the movements between the mouth (target M) and the remaining targets (A,B,C,D,E,F,G,H,I,J) the calculated operator strength S_P is shown in Figure 3.14. The time taken for the subject to complete each movement was relatively consistent, taking on average 1.74 seconds to move the bottle from mouth to target (and vice versa).

Due to small variations in the time taken for the subject to complete each movement, the time axes in the plots are normalised so the strength results corresponding to each movement's start and end positions are aligned.

The results indicate that the subject's strength capability varies as the task is performed. Across all the movements it is observed that this strength reduces as the hand is extended away from the mouth towards a target, and then increases again as it is brought back to the mouth. The task was defined with external force being in the direction of gravity, hence this strength represents the ability of the subject to provide forces at the hand in the upwards direction. This relationship showing that strength decreases as the hand is extended is what is expected, both intuitively based on human experience regarding how strength changes with limb position, and from an understanding of biomechanics. As the hand is extended the bottle's weight force produces larger moment loads about the shoulder and elbow, requiring more torque from the subject to hold it against gravity. Other factors such as changing muscle moment-arms about the joints are also contributing to this relationship but are less intuitive.

Variations in the speed at which each motion was performed results in the S_P curves having slightly different shapes, however a similar profile was observed. Strength capability with the hand stationary at targets A-J were all similar, however the strength was marginally larger for target positions at table height (A,B,C,D,E) compared with those above shoulder height (F,G,H,I,J).

At all times during the task the strength capability remained well above $S_T = 6$N. This is not surprising since the MM used is based on an average, healthy male who is expected to be more than capable of supporting the weight of a 600g bottle during this drinking task. If a robot was assisting via an AAN paradigm then zero assistance would be provided by the robot since the operator is capable of performing this task (indicated by $S_P > S_T$). If the task difficulty was increased such that its strength requirements were greater, then assistance may be required by the subject. Figure 3.15a shows the calculated operator strength for one of the movements compared with the drinking task's strength requirement ($S_T = 6$N), and a second strength requirement if task difficulty was increased ($S_T = 150$N). For the task with increased strength requirement it is seen

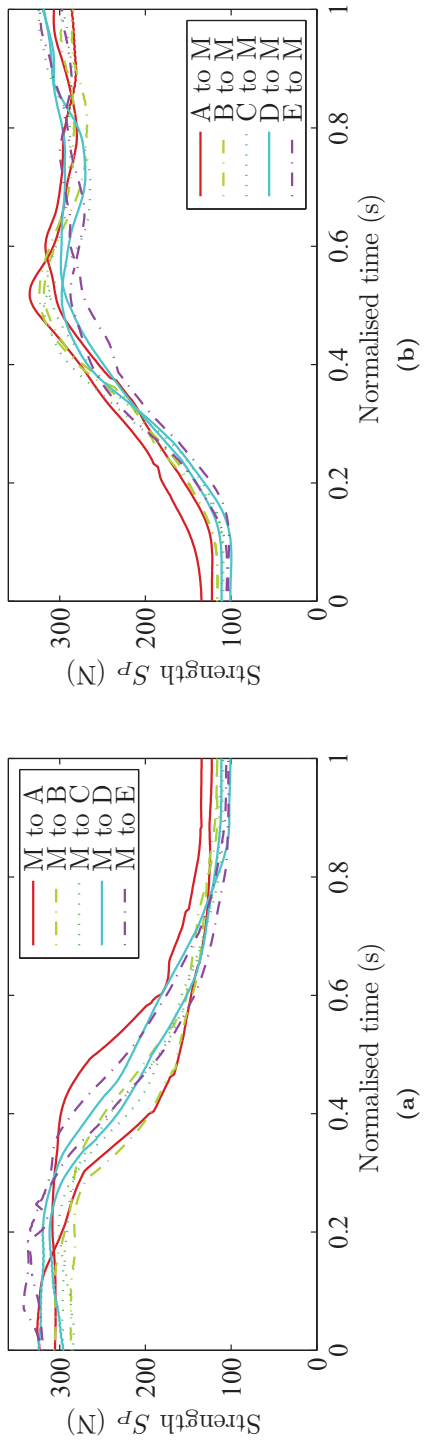

Figure 3.14: The subject's calculated strength capability (S_P) for the drinking task. (a) Hand movement from mouth to targets A,B,C,D,E. (b) Hand movement from targets A,B,C,D,E to mouth. (c) Hand movement from mouth to targets F,G,H,I,J. (d) Hand movement from targets F,G,H,I,J to mouth. Movements made towards identical targets are shown in matching colours in each subplot.

that for a portion of the task the subject's estimated strength is actually reduced below what is required by the task. This gap is plotted in Figure 3.15b.

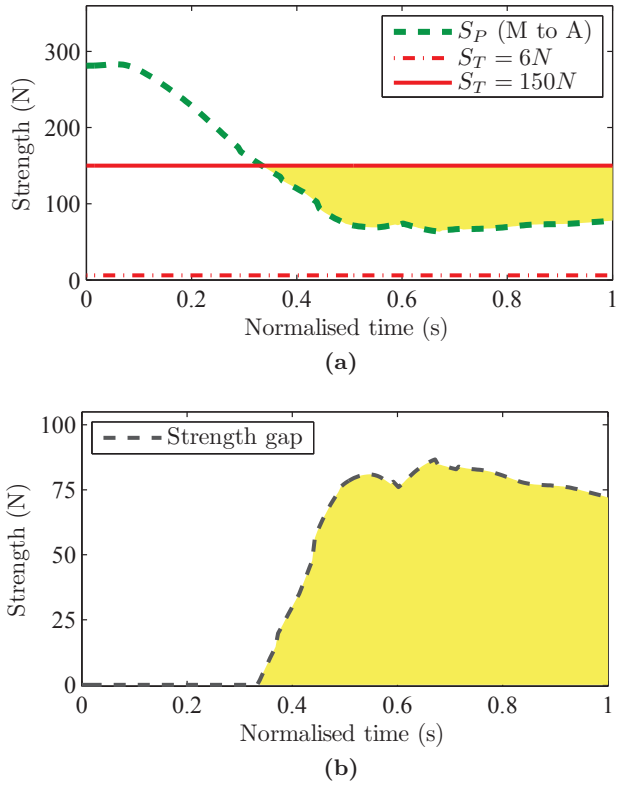

Figure 3.15: Gap between the task's strength requirement and the subject's calculated strength during the drinking task movement. (a) Comparison between the calculated subject strength during drinking task (S_P), the task strength requirement ($S_T = 6N$), and the requirement if the task difficulty was increased ($S_T = 150N$). (b) The gap between the difficult task requirement ($S_T = 150N$) and the calculated subject strength capability.

3.5.2 Case study 2: sliding task

The second task involves the subject sliding an object in a defined path on a table surface. This task was designed to incorporate elements common in several ADLs (manipulating, pulling, pushing [Matsumoto *et al.*, 2011]). It is also similar to tasks required to be performed by patients during robotic rehabilitation [Krebs *et al.*, 2003].

Targets are located on a table surface in front of the subject approximately 25cm

below shoulder height, illustrated in Figure 3.16. A 600g water bottle is held in the subject's hand as it is slid across the table surface. The bottle is slid in a circle passing through targets A, B, C and D in a clockwise motion. Again the subject is not instructed on the speed of the hand motion or the path between the targets.

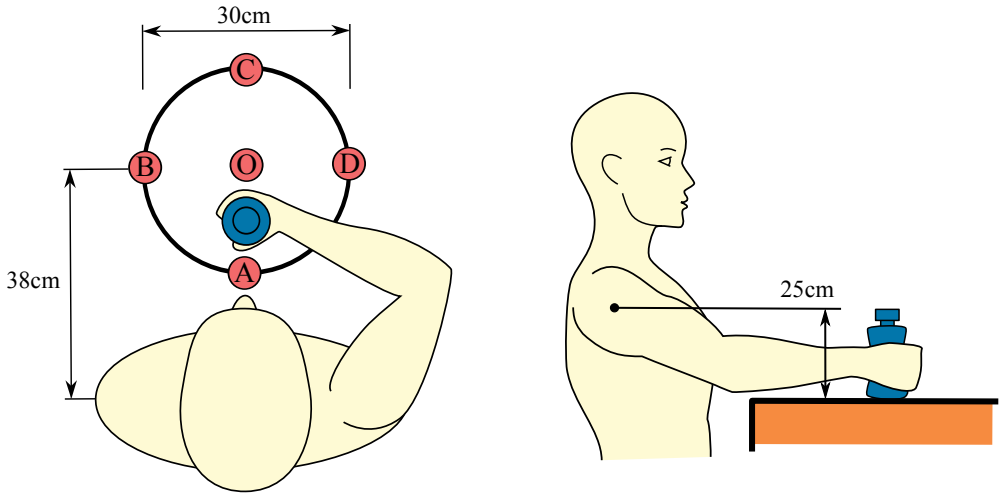

Figure 3.16: Locations of the targets in the table sliding task. Targets A, B, C, and D are located at table height approximately 25cm below shoulder height of the subject.

TM applied to sliding task

The upper limb motion $\mathbf{q}$, $\dot{\mathbf{q}}$, and $\ddot{\mathbf{q}}$ is obtained using the same motion capture system and processing method used in the previous drinking task (Section 3.5.1). A plot of the captured hand motion and target locations is shown in Figure 3.17a. This task involves a person sliding an object across a table surface, therefore the external force applied to the subject's hand is in the direction opposing its movement. It is confined to a horizontal plane parallel with the table to represent friction across this surface. A larger force would exist if the subject applied force out of the plane, e.g. pressing the bottle downwards to increase friction. We assume that this is not the case as typical human motion will endeavour to minimise the forces required. Figure 3.17b shows the clockwise hand motion, with the external force direction $\mathbf{u}$ represented by black arrows

pointing in the opposite direction of the motion. The magnitude of the external sliding force was not measured during the task. Instead it is explicitly defined based on typical forces required to slide objects. A force of $S_T = 2.5$N is used as this is approximately the force required to pull a 700g bowl across a table surface [Yeong *et al.*, 2009].

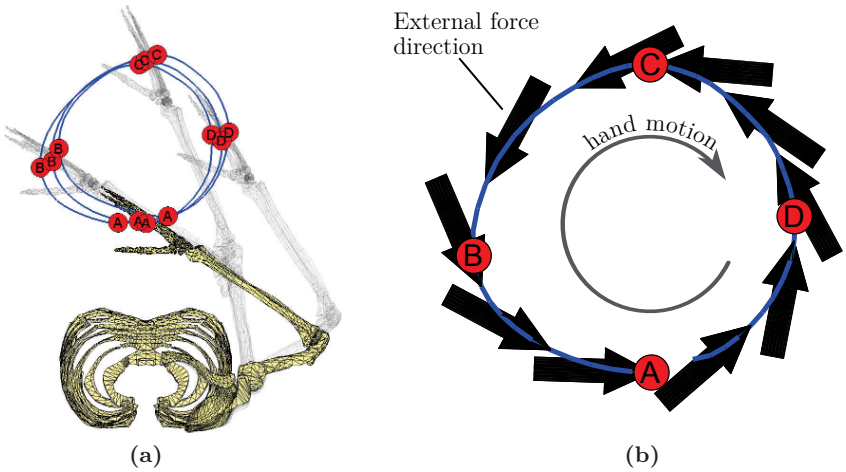

Figure 3.17: The upper limb motion captured during the sliding task. (a) Hand movement and target positions plotted based on motion capture data. (b) Direction of external force vector **u** shown at intervals during one circular movement. Hand moves in a clockwise direction with the external force vector opposing the movement to simulate the friction force of an object being slid on the table surface.

SM applied to sliding task

At each time instant during the sliding task with limb motion and external force direction defined by $\mathbf{q}$, $\dot{\mathbf{q}}$, $\ddot{\mathbf{q}}$, and $\mathbf{u}$ the SM is used to calculate the subject's strength capability S_P. The results for the three circular motions are shown in Figure 3.18. The time axis in between when the hand is at the target locations is normalised such that they align in the plot for easy visualisation.

Results

The strength plots show a similar pattern as the hand is slid on the table in a circular motion. Two peaks of strength occur when the hand is located before target B and

target D. At these two positions the limb and the direction of the external force are such that the external force is directed parallel with the forearm resulting in push/pull type actions. For these two actions the moment-arm between the external force at the hand and the shoulder/elbow joints is less, requiring less strength at each joint as a result. Alternatively, when the external force is almost perpendicular to the forearm, the moment-arm of the external force is greater, and the calculated strength is much less as a result. This behaviour agrees with data in the literature showing push/pull strength being greater than strength in medial/lateral directions [McCormick, 1970]. However the peak strength result of $S_P \approx 1200$N is greater than expected. A potential reason is that joint coupling from muscles producing torque about multiple joints is not considered in this strength estimation.

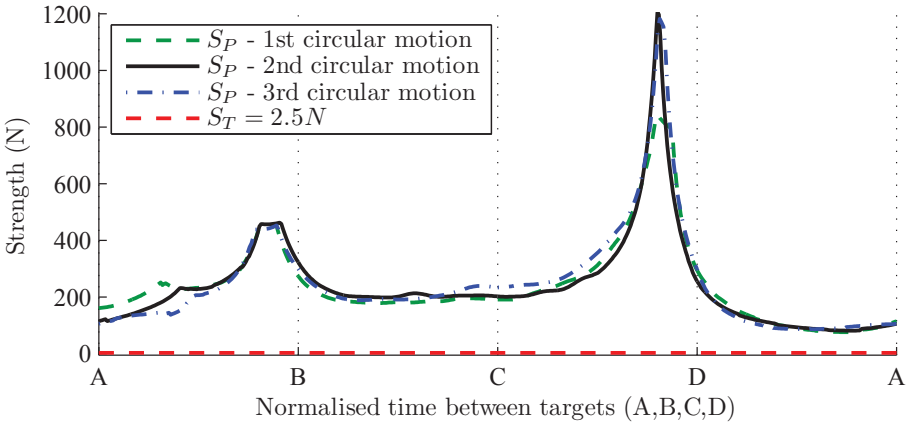

Figure 3.18: The subject's calculated strength capability (S_P) during the sliding task. Hand passes through locations A, B, C, D three times in a circular motion. The three motions are overlayed in the plot. The time in between when the hand is at the target locations is normalised such that they align in the plot for easy visualisation.

At all times S_P remains greater than $S_T = 2.5N$ which is again expected as the subject should be capable of performing this sliding task. A robot providing assistance via an AAN paradigm would hence provide zero assistance. As was done in the analysis of the drinking task, the task difficulty is increased such that the operator requires assistance. Figure 3.19a shows the calculated operator strength for one of the circular movements compared with the task's strength requirement ($S_T = 2.5N$), and a second strength requirement if task difficulty was increased ($S_T = 300N$). For the task with

increased strength requirement it is seen that in two locations during the task the subject's strength is below what the task requires. This gap is shown in Figure 3.19b. The two locations where the subject's strength is above what the task requires correspond to when the subject is performing push and pull type actions. Locations when the operator's strength capability is below the task's requirement correspond to forces in the medial and lateral directions, which as discussed are expected to have less strength [McCormick, 1970].

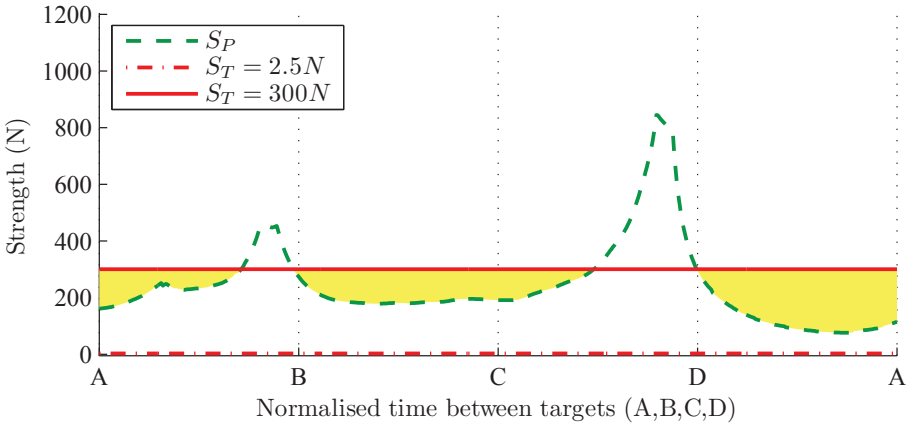

(a)

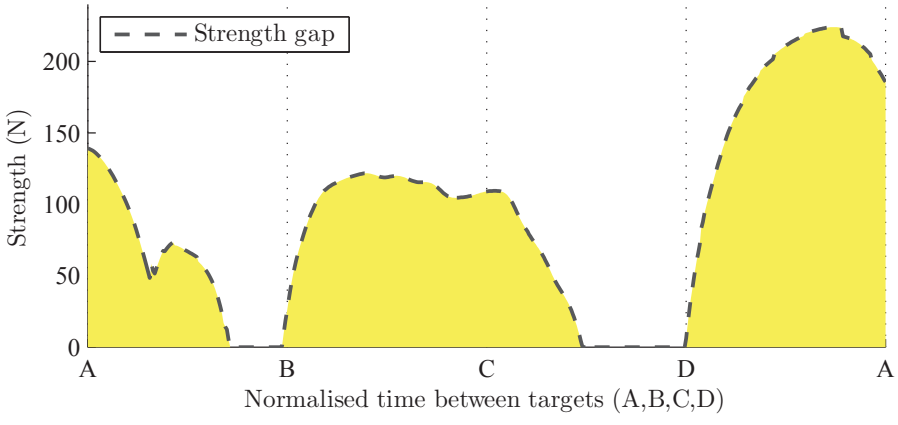

(b)

Figure 3.19: Gap between the task's strength requirement and the subject's calculated strength during the sliding task. (a) Comparison between the calculated subject strength during sliding task (S_P), the task strength requirement ($S_T = 2.5N$), and the requirement if the task difficulty was increased ($S_T = 300N$). (b) The gap between the task requirement with increased difficulty ($S_T = 300N$) and the calculated subject strength capability.

3.6 Discussion

3.6.1 Realism of the SM results

The realism of the strength capability results obtained using the SM directly depends on the ability of the musculoskeletal model to represent the operator's physical capabilities. The MM used has already been shown to adequately replicate certain biomechanical characteristics of the human upper limb [Gatti *et al.*, 2007; Holzbaur *et al.*, 2005; Hu *et al.*, 2011b]. However to accurately represent the capabilities of a specific individual it is likely that fitting the model to the operator will be required. The accuracy and limitations of using the MM to represent an individual operator is mentioned throughout this thesis, and is discussed in detail in Section 6.2.

The realism of the SM results also depends on the method used to derive the operator's strength capability from the MM. The demonstration of the AAN framework performed in this chapter used a method of calculating strength which assumed independent, uncoupled joints. Biarticular muscles which produce coupling between joints are prominent in the upper limb [Koeslag and Koeslag, 1993] and effects from this coupling are expected to influence the limb's strength capability. Strength results will be different if this coupling is taken into account, and hence a method using the SM to calculate strength capability taking into account joint coupling is required. The development and evaluation of such a SM is the focus of Chapter 4.

3.6.2 Alternatives to muscle-based strength

The model-based AAN paradigm relies on the SM to adequately estimate the operator's strength. There are different approaches in which the strength can be derived. This subsection presents a few different approaches that utilise definitions of operator strength in different spaces; task space, joint space, and muscle space. The limitations and benefits of each are discussed.

Strength defined in the task space

Since S_P represents operator strength in the task space, it is intuitive to develop a method for deriving its solution also in the task space. The simplest approach is to directly use measurements of strength taken in task space. In the literature there exist anthropometric surveys of human upper limb strengths measured at the hand [Amell *et al.*, 2000; Das and Forde, 1999; Das and Wang, 2004; McCormick, 1970; Roman-Liu and Tokarski, 2005]. These sources provide strength information for various limb positions, with strength at the hand measured in a distinct number of task space directions (e.g. push, pull, up, down, etc). These measurements provide insight, not only quantitatively regarding mean values of strength, but also qualitatively on how factors such as force direction and limb position affect strength.

To calculate operator strength for arbitrary tasks (i.e. any $\mathbf{q}$ and $\mathbf{u}$) a generalised representation of strength is required. Strength measurements in the literature only provide task space strength for a limited number of distinct limb positions and force directions. With a large set of measurements available it is possible to estimate strength within a range of $\mathbf{q}$ and $\mathbf{u}$ by interpolating between the closest matching measurements available, or to develop a predictive model using regression techniques. For example Roman-Liu and Tokarski [2005] derived models of upper limb strength as functions of seven coordinates defining limb position. These models predict strength at the hand in pushing and lifting directions only. To develop a similar model capable of predicting strength in any task space direction requires strength to be measured in numerous task space directions, and repeated at numerous limb positions to allow regression to be preformed. This is an enormous number of measurements required and to date the author is unaware of such a data set being available.

Strength defined in the joint space

Using upper limb strengths defined at the joint level allows generalised analytical solutions to be developed for calculating operator strength capability in task space. There exists in the literature numerous studies of human limb strength measured at the joint

level [Amell, 2004; Chaffin and Andersson, 1999; Hagberg *et al.*, 1995; Hartsell *et al.*, 1995; Lannersten *et al.*, 1993; Marley and Thomson, 2000; Mayer *et al.*, 1994; Pentland *et al.*, 1993; Tsunoda *et al.*, 1993; VanSwearingen, 1983; Walmsley and Dias, 1995; Weir *et al.*, 1992]. A kinematic model representing the upper limb allows the relationship between force at the hand and strength required at the limb's joints to be determined as a function of force direction and limb position. Chaffin and Erig [1991] developed a model of strength at the hand. With limb joint positions and external forces at the hands defined, a kinematic model of the body was used to calculate the joint loads resulting from the external forces at the hands and the weight of the body segments themselves. These joint loads were then compared to joint strength data available from anthropometric studies to determine the capabilities of the human to produce the strength required [Chaffin and Erig, 1991].

In the literature joint strength is often presented simply as the maximum measured isometric torque in a given position. In reality it varies with both joint position and velocity [Kumar, 2004]. Strength measurements of joint torque versus position (e.g. [Pinter *et al.*, 2010; Winters and Kleweno, 1993]) may be used to account for changing joint position, and strength measurements at different isokinetic velocities (e.g. [Hartsell *et al.*, 1995; Mayer *et al.*, 1994]) may be used to account for velocity. This allows operator strength capability to be calculated as a function of $\mathbf{q}$, $\dot{\mathbf{q}}$ and $\mathbf{u}$, but there are still limitations. Strength measurements of joints with multiple degrees of freedom are limited to single degree of freedom articulations. Measurements are typically performed for a number of standard articulations, for example shoulder strength is commonly categorised into abduction/adduction, flexion/extention, and medial/lateral rotation [Amell, 2004]. For articulations in between those for which strength data is available, strength must be estimated from the nearest available measurement, or other methods such as fitting a model and using interpolation must be used.

Furthermore, since joint strength is the result of muscle forces acting about each joint, and biarticular muscles produce torque about multiple joints, there exists coupling between these joints which affect their ability to produce torque and subsequently contribute to strength at the hand. For example the biceps brachii spans the shoul-

der, elbow and forearm, and due to its biarticular nature the strength of pronation and supination in the forearm can be significantly impacted by its torque contribution about other articulations [Amell, 2004]. Effects of such coupling may not be reflected in the joint strength data available, particularly if efforts were made to isolate the particular joint of interest during strength measurement.

Strength defined in the muscle space

The strength capability of the operator in the task space depends on the strength of the individual muscles in the body. These individual muscles produce torque at the joints of the limb, which provide the limb with the strength to oppose external force at the hand. An approach to calculating operator strength capability is to use operator strength defined at the muscular level, and calculate how this muscular strength can be applied towards a desired task. A musculoskeletal model (MM) representing the operator allows the strength capability of their individual muscles to be calculated. As detailed in Section 2.3.1 a muscle and the tendons connecting it to the skeleton can be modelled by a musculotendon unit (MTU) model. The MTU models of the operator's muscles can estimate the strength each can produce. The MM can calculate how these forces then contribute to the strength at each joint, and subsequently how this joint strength relates to the operator's strength at the hand.

Since the strength capability is derived from a model of strength at the muscular level, this approach can estimate an operator's strength capability for arbitrary tasks defined by $\mathbf{q}$, $\dot{\mathbf{q}}$ and $\mathbf{u}$. Using strength based at the muscular level also provides several additional benefits. The MM encapsulates the relationships between limb pose/velocity with muscle length/velocity and moment-arms, and hence effects of limb position and velocity are inherently accounted for when calculating strength. Secondly because a model representing the physiology of the operator is used, the role of physiological factors in affecting strength can be investigated. For applications which have an emphasis on operator physiology this has distinct advantages, for example in robotic rehabilitation to analyse the effects of physical impairment as discussed in Section 3.6.4.

3.6.3 Quasi-static simplification

When applying the framework, joint loads on the upper limb due to the limb's dynamics were included when calculating the operator's strength capability. However the calculation of the task's strength requirements made some quasi-static simplifications. An external force applied to the hand represented the reaction forces from the water bottle as it was carried or slid by the subject. This was simplified by only considering the bottle's weight or friction force, ignoring reaction forces from the bottle's dynamics. The suitability of ignoring such effects is analysed here.

The inertial forces from an object being carried can be estimated from the acceleration at the hand. The recorded hand motion is used to calculate the acceleration of a coordinate frame located at the subject's hand with origin located 8.5cm distal of the wrist, which was where the water bottle's centre of mass was approximately located. The linear and angular accelerations of the hand during the drinking task are shown in Figure 3.20 and Figure 3.21, respectively. Linear acceleration is seen to remain close to zero during the task, and was commonly an order of magnitude less than gravity (9.81 m/s^2) during the movements recorded. This indicates that for the object carried, the reaction force is largely dominated by its weight force due to gravity in comparison to its inertial load.

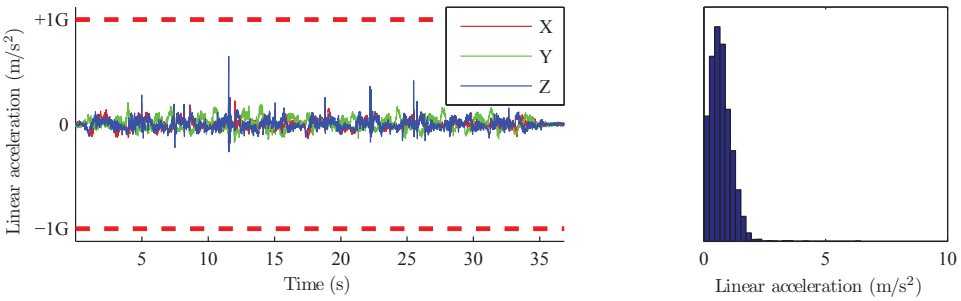

Figure 3.20: Linear acceleration (m/s^2) of the hand measured during the drinking task. (a) Acceleration in the different task space directions (X,Y,Z) during the task. Red dotted lines indicate gravity ($\pm 9.81 m/s^2$). (b) Histogram of the acceleration during the task. This histogram shows the distribution of the linear acceleration with its X-Y-Z components combined by calculating their Euclidean norm, hence results are positive.

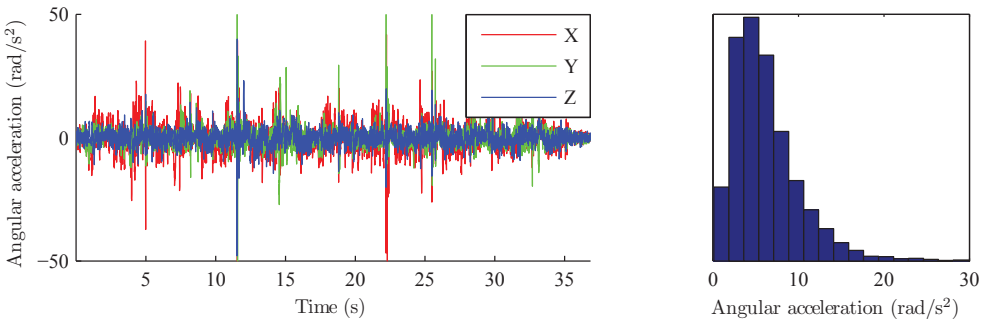

Figure 3.21: Angular acceleration (rad/s^2) of the hand measured during the drinking task. (a) Acceleration in the different task space directions (X,Y,Z) during the task. (b) Histogram of the acceleration during the task. This histogram shows the distribution of the angular acceleration with its X-Y-Z components combined by calculating their Euclidean norm, hence results are positive.

The angular acceleration of the object carried in the hand cannot be compared directly to gravity to gauge if it is appropriate to ignore. However, with the object's mass moment of inertia estimated, the interaction torque at the hand corresponding to the measured angular acceleration can be estimated. The bottle's inertial properties are approximated as a solid cylinder of equivalent size and weight. Because the result depends on the location of the axis about which the mass moment of inertia is calculated, three different axes are used for comparison. The first two axes pass through the bottle's centre of mass, one along the axial direction and the other in the radial direction. The third axis is in the radial direction, but located at the very end of the bottle. This last axis is positioned so as to produce a relatively large mass moment of inertia, and hence to result in a larger estimate of the inertial loads for the purpose of being conservative. The mass moments of inertia about these three axes are 0.000357 kg.m^2/rad^2, 0.001459 kg.m^2/rad^2, and 0.005299 kg.m^2/rad^2 (calculations are detailed in Appendix C). From the angular acceleration histogram (Figure 3.21b) it is seen there is negligible acceleration over 20 rad/s^2. Multiplying this angular acceleration with the three mass moments of inertia calculated results in torque loads of 0.007 N·m, 0.029 N·m, and 0.106 N·m. To place these calculated loads into context they are compared to the torque required about the shoulder to hold the 0.6kg bottle in the hand at full reach. The human arm is approximately 0.6m long from the shoulder to the hand. With the

arm at full reach, the moment produced by the bottle's weight about the shoulder is approximately $0.6 \times 0.6 \times 9.81 = 3.53$ N·m. This is over 30 times greater than the inertial torque load calculated using the largest mass moment of inertia. Considering that this mass moment of inertia was calculated conservatively suggests that the reaction forces from the object carried at the hand are largely dominated by its weight force.

Based on these results it appears appropriate to ignore the inertial loads of an object held in the hand for the ADL tasks that were simulated. This agrees with the literature describing that the majority of loads on the upper limb during ADLs are due to gravity [Rosen *et al.*, 2005]. This further suggests that the gravity component alone may be used during ADL-like tasks to determine the loads on the limb when calculating the assistance requirements of the operator.

3.6.4 Consideration of physical impairment

The AAN robotic paradigm has gained attention in rehabilitation applications to provide assistance suited to the needs of patients during therapy. Since patients are impaired this produces an additional challenge to provide assistance only as required. Effects on strength due to disability vary with great diversity, with impairments highly individual to a patient's specific injury or illness [Arva *et al.*, 2004].

The significance of this variability is gauged by analysing upper limb impairment from stroke. Stroke is chosen as it is a leading cause of long term disability [Lloyd-Jones *et al.*, 2009] and is often the target of robotic rehabilitation applications. Several studies have quantified the loss of strength due to stroke in the muscle groups of the upper limb by comparing strength in paretic versus non-paretic limbs [Bertrand *et al.*, 2007; Bohannon and Andrews, 1987; Dewald and Beer, 2001; Mercier and Bourbonnais, 2004]. Mercier and Bourbonnais [2004] studied 13 chronic hemiparetic stroke subjects. They measured paretic and non-paretic limb strength for certain muscle groups and grip strength. Limb functionality was also measured using various tests like the Box and Block Test, the Finger-to-Nose Test, the Fugl-Meyer Test and the TEMPA [Mercier and Bourbonnais, 2004]. Results showed large intra-subject imbalances between muscle

groups, and high variability in the weakness distribution pattern among the patients was noted. These results defied conventional teaching of weakness following stroke, which assumed a gradient distribution of weakness that effected proximal limb segments more than distal ones [Mercier and Bourbonnais, 2004].

Another study by Bohannon and Andrews [1987] compared the paretic and non-paretic strength of 69 hemiparetic stroke patients in 7 muscle groups. These were wrist extensors, elbow flexors and extensors, and shoulder internal rotators, external rotators, extensors and abductors. The mean and standard deviation of these strength measurements are shown in Figure 3.22a. Strength variation in paretic and non-paretic groups can be gauged from the coefficient of variation (CV) calculated by dividing the mean strength by its standard deviation. A larger CV indicates that strength varies more about the mean measurement, compared with smaller CV. The CV results shown in Figure 3.22b indicate that upper limb strength affected by stroke has more variation

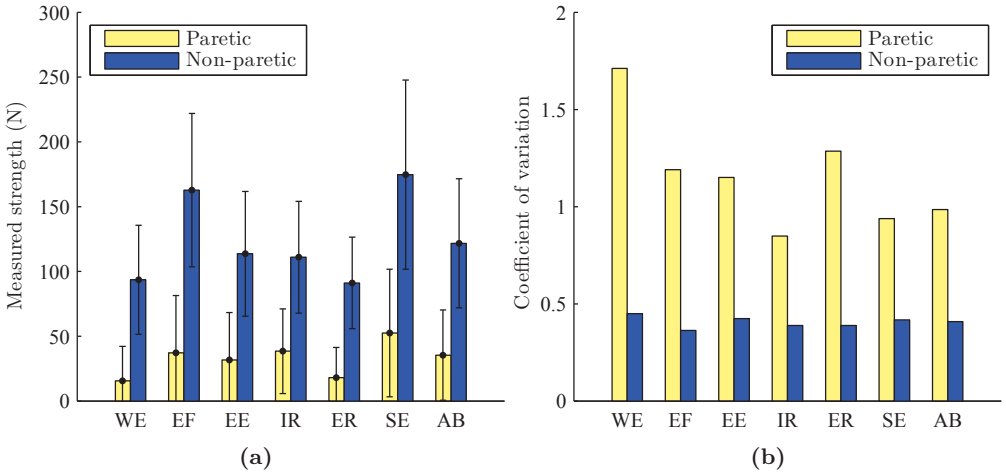

Figure 3.22: Comparison of the strength measured in the paretic versus the non-paretic upper limbs of stroke patients with hemiparesis, obtained from the literature [Bohannon and Andrews, 1987]. Upper limb muscle groups measured are; Wrist Extension (WE), Elbow Flexion (EF), Elbow Extension (EE), Shoulder Internal Rotation (IR), Shoulder External Rotation (ER), Shoulder Extension (SE), Shoulder Abduction (AB). (a) Strength measured for select muscle groups for paretic and non-paretic upper limbs. Error bars indicate standard deviation of the measurements. (b) Strength Coefficient of Variation (CV) for muscle groups in paretic and non-paretic limbs.

than unaffected strength (assuming the non-paretic limb is an adequate representation of unaffected limb strength). The additional variation in strength caused by a physical impairment makes it additionally challenging to determine the operator's physical capabilities, and subsequently their assistance requirements.

An advantage of the model-based AAN paradigm is that the estimation of the operator's assistance requirements are derived from a MM. This model is based on the physiology that underlies the operator's ability to produce the strength required to perform physical tasks. Using a model which is physiologically relevant allows prediction of the effects different physiological factors (e.g. impairment due to stroke) have on the operator's ability to perform tasks. Weakness in the upper limb may be simulated by reducing the force producing capabilities of individual muscles in the MM. For example, van Drongelen *et al.* [2006] modified a MM to mimic muscular impairment representing lesion and muscle paresis for analyses of the upper limb. The ability to predict the relationship between physical impairment and how it affects the assistance requirements of a human subject has the potential for significant benefits, particularly in applications that have a large emphasis on physiology. Since AAN has gained attention in robotic applications such as rehabilitation, this advantage is a primary motivation for choosing to utilise a MM as the basis for estimating operator capability.

3.7 Summary

In this chapter a model-based framework was presented for calculating the assistance requirements of a human operator such that robotic assistance may be provided using the AAN paradigm. It consisted of two models, the first being the Task Model (TM) used to represent the requirements of the task being performed, defined by the upper limb motion and external force applied to the hand. The magnitude of external force (S_T) required to perform the task is used as a measure of the task's strength requirement. The second was the Strength Model (SM) used to calculate the strength of the operator with respect to the desired task. Results from these two models can be used to determine the gap between task requirement and operator strength capability, and gauge the

operator's assistance requirements. Utilising the model-based framework allows these requirements to be calculated without the need of observations, and hence many of the limitations inherent with empirical performance-based methods are avoided.

A drinking task that mimicked the subject drinking, and a sliding task mimicking the subject sliding an object across a table top were simulated to demonstrate this framework. These two tasks were created based on activities of daily living since these type of tasks are typical of those performed by patients during rehabilitation, and the AAN paradigm is gaining interest for use in such applications. Analysis of the dynamic loads at the hand for the tasks simulated indicated the appropriateness of ignoring dynamic loads on the upper limb for typical ADL-like tasks. This conclusion agrees with the findings of others in the literature [Rosen *et al.*, 2005].

The benefits of using a musculoskeletal model (MM) representing the physiology of the operator in applications where the operator has a physical impairment was discussed. Using stroke as an example, the variability of impairments and consequently the resulting assistance needs of patients was shown using data from the literature. The need for the ability to examine the role physiology plays in the capability of performing tasks, particularly in health care applications was highlighted. Since health care applications such as rehabilitation are primary applications of AAN, this provides large motivation for developing a SM using a MM in an analysis operating at the muscular level.

Although the proposed framework has the potential to provide significant benefits over other AAN methods (i.e. empirical performance-based AAN) it relies on the ability of the MM to be able to provide an adequate estimation of the operator's strength. This chapter made use of an approach towards calculating operator strength which ignored joint coupling effects. The necessity of a method to calculate strength which does not ignore such effects was discussed. The development and evaluation of such a method to calculate strength is the focus of Chapter 4.

Chapter 4

Musculoskeletal Model-based Strength Estimation

In Chapter 3 the framework for a model-based AAN paradigm was presented and demonstrated on simulated tasks. At the core of this framework is the Strength Model (SM) used to estimate the strength of the operator with respect to desired tasks. To demonstrate the framework a method of calculating upper limb strength capability using a musculoskeletal model (MM) was developed. This method was based on a simplified case where coupling between the joints in the limb was ignored by calculating the strength at each joint independently. Coupling has significant effects on strength as approximately 65% of the muscles in the upper limb are biarticular, spanning two or more joints [Koeslag and Koeslag, 1993; Williams *et al.*, 1989].

In this chapter an optimisation model for calculating operator strength at the hand is developed. Using a MM it takes into account the physiology of the operator, including factors affecting strength such as the joint coupling which results from biarticular muscles. Section 4.1 formulates the optimisation model using parameters from the MM to find the maximum force at the hand the operator can oppose. This model takes into account constraints imparted by the MM physiology, gravitational and dynamic loads, and task constraints. In Section 4.2 the SM incorporating the developed optimisation model is evaluated in its ability to estimate upper limb strength and how

this strength is affected by factors including limb position, direction of external force, and physical impairment of the operator. Results are compared with the literature for validation. In Section 4.3 the model-based AAN framework, utilising the optimisation model developed in this chapter, is analysed within two case studies. The first applies the framework to a drinking task, and the second to a sliding task. In both studies, physical impairment derived from the literature which is consistent with stroke impairment is simulated in the upper limb. The purpose of these studies are to gain insight into the potential benefits a model-based AAN paradigm utilising a MM can provide, in particular how it allows the analysis of the role the operator's physiology plays on their ability to perform tasks. Lastly in Section 4.4, factors affecting the efficacy of using the developed optimisation model within the model-based AAN framework are discussed.

4.1 Optimisation Model

4.1.1 Considerations

The Strength Model (SM) presented in Section 3.4 is used in the model-based AAN framework to calculate the strength capability of the operator at their hand. The strength is calculated with respect to a specific direction at the hand and with the limb having a specific motion. This limb motion (represented by $\mathbf{q}$, $\dot{\mathbf{q}}$, $\ddot{\mathbf{q}}$) and the direction at the hand (represented by $\mathbf{u}$) are defined according to the task which the operator is performing. Figure 4.1 shows an example of the SM. An external force of magnitude F^E is applied to the hand in direction $\mathbf{u}$. The strength capability (S_P) of the operator corresponds to the maximum magnitude of this external force (F^E) that they can oppose whilst performing the task, i.e. $S_P = \max[F^E]$.

To calculate the operator's strength capability, an optimisation model within the SM is used (see Figure 3.9). This optimisation uses parameters from a musculoskeletal model (MM) representing the operator's upper limb to calculate the strength at the hand. This section formulates the optimisation model for calculating the operator's strength capability S_P utilising the parameters obtained from a MM. Before this optimisation

model is derived, there are several considerations made.

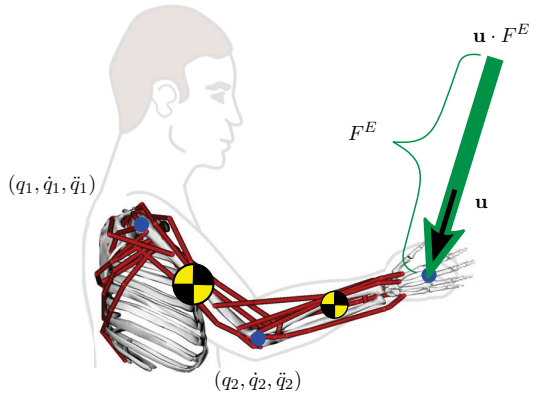

Figure 4.1: Example of the Strength Model (SM). The external force $\mathbf{u} \cdot F^E$ is the limb's interaction with the environment during the task.

Joint torque coupling due to biarticular muscles

In Chapter 3 the strength at the hand was calculated based on the strength in the joint space of the MM. Joints were analysed individually to determine the maximum magnitude of the external load that can be applied at the hand which each joint could oppose, based on its available joint strength. Because joints were analysed independently, factors such as joint coupling due to biarticular muscles were not accounted for.

To account for inter-joint coupling, the process of finding the strength at the hand is performed in the muscle space. Muscle activation determines the active force output of an individual muscle. For a given muscle's activation, the resulting torque produced in each joint the muscle spans is calculated, and subsequently related to the strength at the hand. An optimisation routine can search this muscle activation space to find the maximum external force the limb can oppose at the hand, in the direction of $\mathbf{u}$. Because muscle activation ranges from 0 to 1 the search space is bounded.

Muscular impairment

It is beneficial to incorporate means for examining the effects physical impairments have on strength. A physical impairment can be simulated by limiting the force producing

capability of individual muscles. A method used by van Drongelen *et al.* [2006] limited the force production of muscles in a MM to mimic muscular impairment from lesions and muscle paresis. Another method used by Steenbrink *et al.* [2009] disabled the forces in select muscles of the shoulder to simulate the effects of rotator cuff tears when investigating glenohumeral stability.

Muscle activation, a, is typically defined as ranging from $0 \leq a \leq 1$. An upper bound parameter s is introduced to define the maximum each muscle can be activated during the optimisation, effectively limiting the muscle's force output. Activation upper bounds are defined by vector $\mathbf{s} = [s_1, s_2, \cdots, s_m]^T$ with each element corresponding to a single muscle in the MM. Hence the muscle activation vector $\mathbf{a} = [a_1, a_2, \cdots, a_m]^T$ is bounded to $0 \leq \mathbf{a} \leq \mathbf{s}$, with each element in $\mathbf{s}$ ranging $0 \leq s \leq 1$. A muscle with its activation upper bound set to $s = 1$ has full activation range ($0 \leq a \leq 1$) and hence its force producing capability is not limited during the optimisation. Its force however is still limited by the musculotendon unit (MTU) model, see Section 2.3.1. A muscle with $s = 0$ is unable to be activated at all and hence is unable to produce any active force. This allows vector $\mathbf{s}$ to be used to simulate physical impairment, with control over the severity of strength loss and its distribution across the muscle space. This constraint is formally defined in Equation (4.1).

$$0 \leq \mathbf{a} \leq \mathbf{s} \tag{4.1}$$

Strength limit

Using a MM to relate muscle activation to the strength at the hand takes many factors into account. These include the effects of muscle length and velocity on the ability to produce muscle force, the moment-arms of muscle force about joints, inter-joint coupling from biarticular muscles, the joint loads due to gravity and limb dynamics, and the direction of the external force applied to the hand. Even so, there are other factors that affect and limit strength in the human body which are not considered. Examples are fatigue, comfort, pain, and joint stability. The optimisation model may produce a

large estimation of strength due to limiting factors such as these not being considered. For example, if the external force applied to the hand is in a direction passing almost directly through the axes of rotation of the limb's joints, the torque load that results at each of these joints is relatively small. Since mathematically it requires little strength to oppose this load, the optimisation would calculate that a large magnitude of this external force can be opposed by the operator. In reality other factors would limit the magnitude of the force which the operator could oppose.

To prevent returning a large result for the operator's strength, the limit $S_P^{\max}$ is defined as an upper limit in the optimisation model. Appropriate values for this limit may be set based on physiological or occupational health and safety limits in the literature. For example, from a table of the weight of objects which are acceptable for individuals to lift using both hands, a maximum of around 60kg can be obtained [Gallagher *et al.*, 2004]. Based on this an approximate strength limit of $S_P^{\max} = 300N$ per upper limb may be defined. If it is undesirable to limit the result of the optimisation, this limit can be defined as $S_P^{\max} = \infty$. This constraint is formally defined in Equation (4.2).

$$F^E \leq S_P^{\max} \tag{4.2}$$

4.1.2 Dynamic equation

The objective function is required to calculate F^E as a function of the search space input $\mathbf{a}$ to find its maximum value $S_P = \max[F^E]$. The relationship between F^E and $\mathbf{a}$ is governed by the dynamic equation of the musculoskeletal system, which is detailed in Section 2.3.5 and repeated here in Equation (4.3).

$$\mathbf{H\ddot{q}} + \mathbf{C} + \boldsymbol{\tau}^G = \boldsymbol{\tau}^M + \boldsymbol{\tau}^E \tag{4.3}$$

Before deriving the optimisation model, this dynamic equation is rearranged for convenience.

Joint torque due to the external force

External joint loads $\boldsymbol{\tau}^E$ are the result of the external force $\mathbf{u} \cdot F^E$ applied to the hand. This torque is calculated using Equation (2.14) as $\boldsymbol{\tau}^E = [\mathbf{J}_v]^T \ \mathbf{u} \cdot F^E$ (see Section 2.3.4). The kinematic Jacobian matrix $\mathbf{J}_v$ (2.12) is a function of the limb position, which is assumed to be constant during the process of calculating the strength of the operator. Likewise the direction of the external force is also assumed to be constant. For convenience the Jacobian matrix $\mathbf{J}_v$ and the external force direction vector $\mathbf{u}$ are combined to form vector $\mathbf{r}$ (4.4) and is assumed constant during the optimisation. Each element in $\mathbf{r}$ is the moment-arm of the external force $\mathbf{u} \cdot F^E$ acting about the axis of rotation of one of the k joints in the limb.

$$\mathbf{r} = \begin{bmatrix} r_1 \\ r_2 \\ \vdots \\ r_k \end{bmatrix} = [\mathbf{J}_v]^T \mathbf{u} \tag{4.4}$$

$$\boldsymbol{\tau}^E = \mathbf{r} \cdot F^E \tag{4.5}$$

Joint torque due to the dynamic and gravity loads

The limb motion which the operator is required to perform results in loads which must be considered when calculating operator strength. Limb velocity and acceleration $(\dot{\mathbf{q}}, \ddot{\mathbf{q}})$ determine the dynamic joint loads, and limb position $(\mathbf{q})$ determines the joint loads due to gravity. The motion of the limb is assumed constant during the calculation of the operator's strength capability. For convenience these dynamic and gravitational loads are combined into vector $\boldsymbol{\tau}^B$ (4.6) and are assumed constant during the optimisation.

$$\boldsymbol{\tau}^B = \mathbf{H}\ddot{\mathbf{q}} + \mathbf{C} + \boldsymbol{\tau}^G \tag{4.6}$$

Joint torque due to the muscle forces

The muscular torque $\boldsymbol{\tau}^M$ is the joint torque resulting from MTU forces acting about the joints in the MM. The MTU force output is a complex relationship (see Section 2.3.1), with its force being dependent on a number of intrinsic parameters (Table 2.1) and extrinsic parameters such as length, velocity, and activation. With the position and velocity of the limb defined $(\mathbf{q}, \dot{\mathbf{q}})$ the length and velocity of each MTU is calculated (see Section 2.3.2). The force output of each MTU in the model can then be calculated as a function of its activation, as represented by Equation (4.7).

$$f_i^M = f_i^M(a_i) \tag{4.7}$$

To derive an optimisation objective function in terms of muscle activation $\mathbf{a}$, the forces produced by each MTU, and subsequently the muscular joint torque, is separated into components dependent and independent of muscle activation. The independent component is calculated as the MTU force output with activation set to zero ($\mathbf{a} = 0$). This component is referred to as the passive force component, and is represented by vector $\mathbf{f}^P$ as shown in Equation (4.8).

$$\mathbf{f}^P = \begin{bmatrix} f_1^M(0) \\ f_2^M(0) \\ \vdots \\ f_m^M(0) \end{bmatrix} \tag{4.8}$$

As activation increases, so does the MTU force output until its maximum at $a = 1$ is reached. The MTU force component dependent on activation is linearised in this range and conveniently represented by the linear expression shown in Equation (4.9). The matrix $\mathbf{K}_A$ (4.10) is an activation-to-force gain matrix that produces the vector of

active MTU forces $\mathbf{f}^A$ from the vector of muscle activations $\mathbf{a}$.

$$\mathbf{f}^A = \begin{bmatrix} f_1^M(a_1) - f_1^M(0) \\ f_2^M(a_2) - f_2^M(0) \\ \vdots \\ f_m^M(a_m) - f_m^M(0) \end{bmatrix} = \mathbf{K}_A \mathbf{a} \tag{4.9}$$

$$\mathbf{K}_A = \begin{bmatrix} \left[f_1^M(1) - f_1^M(0)\right] & 0 & \cdots & 0 \\ 0 & \left[f_2^M(1) - f_2^M(0)\right] & \cdots & 0 \\ \vdots & \vdots & \ddots & 0 \\ 0 & 0 & 0 & \left[f_m^M(1) - f_m^M(0)\right] \end{bmatrix} \tag{4.10}$$

This linearisation assumes that MTU force changes linearly with activation, and that the independent passive force component remains constant. As detailed in Section 2.3.1 a muscle's passive force changes with length, and hence for the assumption to be correct the tendon must not stretch, otherwise the muscle fibers shorten which affects their passive force. The assumption of a stiff tendon is commonly employed in musculoskeletal analyses [Sapio *et al.*, 2005] because tendon stretch is typically small, around 3% when the corresponding muscle is producing peak isometric force [Zajac, 1989]. Furthermore, the linearised force-activation relationship respects the bounds of the MTU force output when compared to the relationship before the linearisation. Therefore this linearisation is acceptable in the context of calculating operator strength capability.

The MTU forces (both active and passive) produce torque about the joints in the MM. The Jacobian matrix $\mathbf{L}$ (2.8) relates MTU velocity to generalised joint velocity, and through the principal of virtual work can calculate the joint torque resulting from the MTU forces (see Section 2.3.3). Each element in the Jacobian is the moment-arm of each MTU about each joint axis of rotation [Pandy, 1999] and is used to calculate the passive torque $\boldsymbol{\tau}^P$ (4.11) and the active torque $\boldsymbol{\tau}^A$ (4.12) resulting from both passive

and active MTU force contributions.

$$\boldsymbol{\tau}^P = [-\mathbf{L}]^T \ \mathbf{f}^P \tag{4.11}$$

$$\begin{aligned} \boldsymbol{\tau}^A &= [-\mathbf{L}]^T \ \mathbf{f}^A \\ &= [-\mathbf{L}]^T \ \mathbf{K}_A \ \mathbf{a} \\ &= \ \mathbf{K}_\tau \ \mathbf{a} \end{aligned} \tag{4.12}$$

Matrix $\mathbf{K}_\tau$ is an activation-to-torque gain matrix created by combining the Jacobian matrix $\mathbf{L}$ and the activation-to-force gain matrix $\mathbf{K}_A$ as shown in Equation (4.13). The total muscular torque is the sum of both the active and the passive MTU torque contributions (4.14).

$$\begin{aligned} \mathbf{K}_\tau &= -[\mathbf{K}_A \ \mathbf{L}]^T \\ &\triangleq [-\mathbf{L}]^T \ \mathbf{K}_A \end{aligned} \tag{4.13}$$

$$\begin{aligned} \boldsymbol{\tau}^M &= \boldsymbol{\tau}^P + \boldsymbol{\tau}^A \\ &= [-\mathbf{L}]^T \ \mathbf{f}^P + \mathbf{K}_\tau \ \mathbf{a} \end{aligned} \tag{4.14}$$

4.1.3 Objective function

The objective of the optimisation model is to find $S_P = \max[F^E]$ using muscle activation as the design variables. An objective function is derived that expresses F^E as a function of the muscle activation vector $\mathbf{a}$, from which the solution to $S_P = \max[F^E]$ can be calculated. Equations (4.5), (4.6) and (4.14) are substituted into Equation (4.3) to produce the reformulated dynamic Equation (4.15). This equation describes the dynamics of the musculoskeletal system in the joint space, with each row of the expression

corresponding to one of the k joints in the MM.

$$\underbrace{\boldsymbol{\tau}^B}_{\text{dynamics + gravity}} = \overbrace{\mathbf{K}_\tau\ \mathbf{a}}^{\text{active torque}} + \underbrace{\boldsymbol{\tau}^P}_{\text{passive torque}} + \overbrace{\mathbf{r}\cdot F^E}^{\text{external load}} \tag{4.15}$$

In each joint of the musculoskeletal system, the torque resulting from the external force is dependent on the scalar term F^E. The moment-arm vector $\mathbf{r}$ determines the contribution of this term to the load at each joint. To derive a single expression containing the term F^E, a single row of Equation (4.15) can be extracted to produce Equation (4.16). The row that is extracted is referred to as row i, and consists of the corresponding i-th elements in vectors $\boldsymbol{\tau}^B$, $\mathbf{K}_\tau\mathbf{a}$, $\boldsymbol{\tau}^P$ and $\mathbf{r}$. The i-th element of the matrix multiplication $\mathbf{K}_\tau\mathbf{a}$ is represented as $[\mathbf{K}_{\tau i}]\mathbf{a}$, where $\mathbf{K}_{\tau i}$ is the i-th row of matrix $\mathbf{K}_\tau$ (4.17).

$$\tau_i^B = [\mathbf{K}_{\tau i}]\mathbf{a} + \tau_i^P + r_i\cdot F^E \tag{4.16}$$

$$\mathbf{K}_{\tau i} = \Big[\mathbf{K}_{\tau[i,1]}, \mathbf{K}_{\tau[i,2]}, \cdots, \mathbf{K}_{\tau[i,m]}\Big] \tag{4.17}$$

Equation (4.16) is rearranged into Equation (4.18) to describe F^E as a function of the muscle activation vector $\mathbf{a}$. This requires the expression to be divided by r_i which can result in numerical problems when r_i is close to zero. This is avoided by selecting the row in Equation (4.15) which is extracted to form Equation (4.16) by the row with the largest magnitude in the vector $\mathbf{r}$. The selection of this row is formally defined by Equation (4.19).

$$F^E = \left[\frac{\tau_i^B - \tau_i^P}{r_i}\right] - \left[\frac{\mathbf{K}_{\tau i}}{r_i}\right]\mathbf{a} \tag{4.18}$$

$$i = \underset{i\in\mathbb{N}_1 | i\leq k}{\operatorname{argmax}}\Big[|r_i|\Big] \tag{4.19}$$

Equation (4.18) expresses F^E as a function of two terms. The first term, $\left[\frac{\tau_i^B - \tau_i^P}{r_i}\right]$ is independent of the muscle activation vector $\mathbf{a}$. This term contains values that depend on task-related parameters such as the limb motion or the direction of the external force at the hand. As the operator performs a task, these parameters vary over time and hence this term will change every time the optimisation model is used to calculate the operator's strength capability. However at each individual instant during the task in which the optimisation is performed, this term is assumed constant. Its value τ_i^B is taken from the dynamic and gravitational torque vector $\boldsymbol{\tau}^B$ (4.6) and as discussed it remains constant during the strength optimisation. Likewise, the value r_i is taken from the moment-arm vector $\mathbf{r}$ (4.4) and also remains constant during the optimisation. The value τ_i^P is taken from the passive joint torque vector $\boldsymbol{\tau}^P$ (4.11). This vector is calculated from the passive MTU force vector $\mathbf{f}^P$ using the Jacobian matrix $\mathbf{L}$ (2.8). Both of these are functions of the limb's position (see Sections 2.3.1 and 2.3.2) and hence also remain constant during the optimisation.

The second term, $\left[\frac{\mathbf{K}_{\tau i}}{r_i}\right]\mathbf{a}$ is linearly dependent on muscle activation and hence is not constant during the optimisation. The solution to $S_P = \max[F^E]$ is found by maximising Equation (4.18). This requires its second term to be minimised due to the minus sign. The resulting objective function is shown in Equation (4.20). The constant term in this objective function may be disregarded during the minimisation of $\left[\frac{\mathbf{K}_{\tau i}}{r_i}\mathbf{a}\right]$, but must be considered afterwards to obtain the correct result for S_P.

$$S_P = \max\left[F^E\right]$$

$$S_P = \max\left[\left[\frac{\tau_i^B - \tau_i^P}{r_i}\right] - \left[\frac{\mathbf{K}_{\tau i}}{r_i}\right]\mathbf{a}\right]$$

$$S_P = \left[\frac{\tau_i^B - \tau_i^P}{r_i}\right] - \min\left[\frac{\mathbf{K}_{\tau i}}{r_i}\mathbf{a}\right] \tag{4.20}$$

4.1.4 Optimisation constraints

The objective function (4.20) used to find $S_P = \max[F^E]$ is derived from a single row of the dynamic equation of motion (4.15). Results obtained by using this objective function by itself only consider a single joint in the musculoskeletal system, and do not consider the remaining joints. All of the joints in the system need to be considered to account for inter-joint effects such as coupling from biarticular muscles and to ensure consistency in the dynamic system. Constraints need to be included to ensure that the dynamic Equation (4.15) is satisfied.

An equality constraint is created in the form $\mathbf{Aa}=\mathbf{b}$, where $\mathbf{A}$ is a constant matrix of size $k \times m$, $\mathbf{b}$ is a constant vector of size $k \times 1$, and $\mathbf{a}$ is the $m \times 1$ vector of muscle activations which are also the design variables in the optimisation objective function. This constraint is created from the dynamic Equation (4.15), thereby ensuring it is satisfied during the calculation of S_P. The steps of rearranging the dynamic equation to produce the equality constraint in the form $\mathbf{Aa}=\mathbf{b}$ are provided in Appendix D.2. After rearranging, expressions for $\mathbf{A}$ (4.21) and $\mathbf{b}$ (4.22) are produced.

$$\mathbf{A} = \mathbf{K}_\tau - \frac{\mathbf{r}}{r_i}\,\mathbf{K}_{\tau i} \tag{4.21}$$

$$\mathbf{b} = \boldsymbol{\tau}^B - \boldsymbol{\tau}^P + \mathbf{r} \cdot \left[\frac{\tau_i^P - \tau_i^B}{r_i}\right] \tag{4.22}$$

The equation $\mathbf{Aa} = \mathbf{b}$ creates k constraints, with each row corresponding to each of the k joints in the musculoskeletal system. Constraints are required because the objective function (4.20) calculates S_P by considering only a single joint in the system. However to ensure that the remaining $k-1$ joints are consistent with the objective function's result requires only $k-1$ constraints. Substituting (4.21) and (4.22) into $\mathbf{Aa} = \mathbf{b}$ and expanding, it is found that one of the rows in the equality constraint equation reduces to $0 \cdot \mathbf{a} = 0$. This row corresponds to the same joint which the objective function (4.20) considers when calculating S_P. This redundant constraint is not required and theoretically does not affect the optimisation result. However in practice, rounding

errors when calculating $\mathbf{A}$ or $\mathbf{b}$ may result in one side of this redundant constraint to be marginally non-zero. This may result in the optimisation failing to calculate a solution due to overly stringent constraints which cannot be met. To avoid this, the rows of both $\mathbf{A}$ and $\mathbf{b}$ corresponding to this redundant constraint can be explicitly set to zero, or removed completely before optimisation.

4.1.5 Summary of the optimisation model

The aim of the optimisation is to find the combination of muscle activations $\mathbf{a}$ which maximises the magnitude of external force the operator can oppose at the hand. The search space is bounded with activation ranging between $0 \leq \mathbf{a} \leq \mathbf{s}$, with $\mathbf{s}$ acting as an upper bound to analyse the effects of physical impairment at the muscular level. Bound $S_P^{\max}$ is set for the strength output to limit the S_P result. This is required in cases where the strength result can be large. In summary, the optimisation for calculating the strength S_P of the human operator with respect to a task is the following:

$$
\begin{array}{lll}
\text{Maximise:} & F^E & (4.18) \\
\text{Subject to:} & \mathbf{H\ddot{q}} + \mathbf{C} + \boldsymbol{\tau}^G = \boldsymbol{\tau}^M + [\mathbf{J}_v]^T \mathbf{u} \cdot F^E & (4.3) \\
& 0 \leq \mathbf{a} \leq \mathbf{s} & (4.1) \\
& F^E \leq S_P^{\max} & (4.2)
\end{array}
\tag{4.23}
$$

The procedure for performing this optimisation is illustrated in Figure 4.2. This process can be summarised step by step as the following:

1. The upper limb motion and direction of external force at the hand are defined based on the task the operator is performing ($\mathbf{q}, \dot{\mathbf{q}}, \ddot{\mathbf{q}}, \mathbf{u}$).
2. Using the MM, derive the following parameters: $\mathbf{r}$, $\mathbf{K}_\tau$, $\boldsymbol{\tau}^B$, $\boldsymbol{\tau}^P$.
3. Calculate the constraint terms $\mathbf{A}$ (4.21) and $\mathbf{b}$ (4.22).
4. Solve optimisation objective function (4.20) using numerical methods (e.g. linear programming) with the following constraints:

$$\mathbf{Aa} = \mathbf{b} \qquad 0 \leq \mathbf{a} \leq \mathbf{s} \qquad F^E \leq S_P^{\max}$$

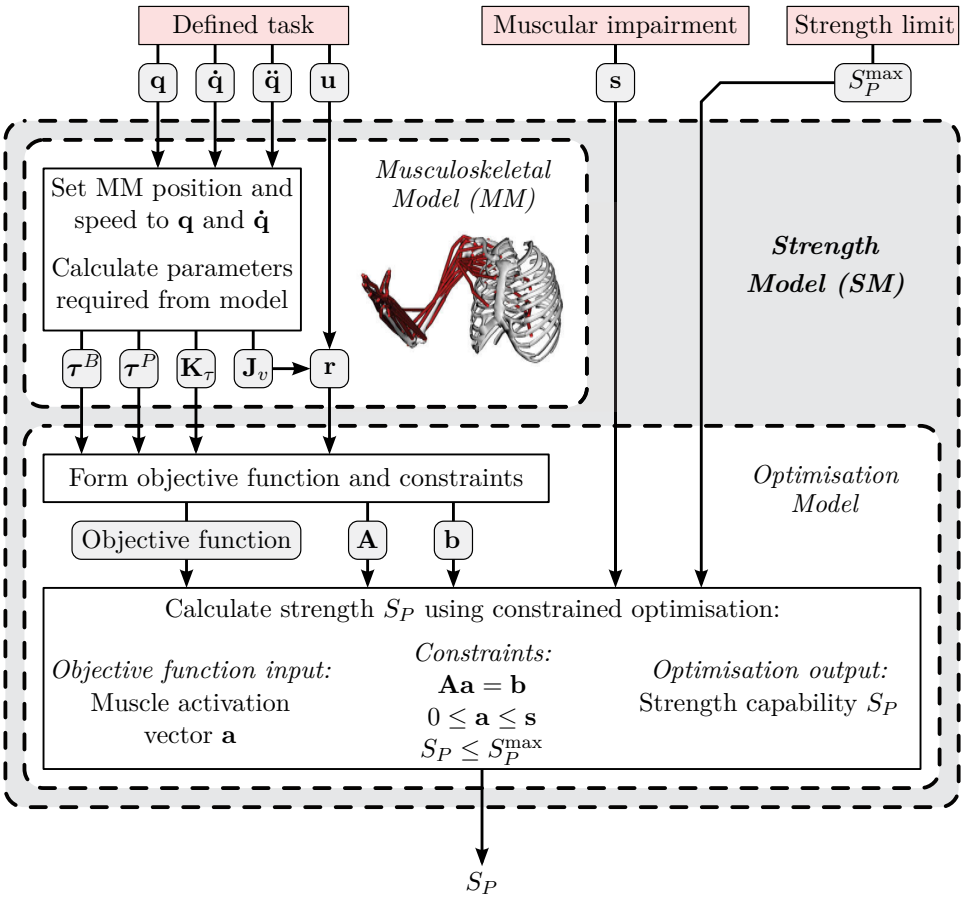

Figure 4.2: Procedure for calculating the operator's strength capability (S_P) using the optimisation model within the SM framework.

4.2 Evaluation

In this section the SM utilising the optimisation model developed in Section 4.1 is evaluated. Strength of the upper limb at the hand is calculated, and how this strength is affected by factors including limb position, the direction of external force, and physical impairment is analysed. A number of tasks involving the upper limb are simulated, and results compared with strength measurements available from the literature. The same MM of the upper limb used previously (detailed in Section 3.4.1) is utilised.

Before evaluation it is necessary to consider what are the indications that suggest the SM has the ability to estimate an operator's strength capability. Obtaining accurate quantitative estimates of an operator's strength capability is only a part of what is required from the SM. It is also required to portray *how* strength is affected by factors related to the task being performed, and the physical capacity (or incapacity in applications such as rehabilitation) of the operator. It is understood that using a MM to estimate strength which exactly matches some empirically obtained data set is not the objective. Firstly, strength itself varies from person to person, so no quantitative strength result will be representative of the entire human population. As an example, elbow flexion strength between the 5th and 95th percentile male population can range from 42 N.m to 111 N.m [Amell, 2004]. This highlights how much strength varies in the healthy population. In unhealthy populations, such as stroke patients, variation in strength is further exacerbated due to their impairment [Arva *et al.*, 2004]. Parameters within a MM can be fitted to a data set so they become a better representation of an individual [Buchanan *et al.*, 2005; Fleischer and Hommel, 2008; Manal and Buchanan, 2004; Nam and Uhm, 2011]. A process of fitting the model to match an available data set is often performed in the creation of the model itself [Garner and Pandy, 2001; Holzbaur *et al.*, 2005]. Using strength data available from the literature, it is possible to fit the MM to produce strength estimates which match well to a particular data set. However this is not the objective of this evaluation. Instead, evaluation of the strength estimation results will be performed with no effort made to fit or adjust the MM's parameters as to better fit the data. Hence it is expected that the quantitative strength

results will not equal those published, just as strength amongst the human population is so widely varied. Instead, the evaluation focuses on the ability of the SM to capture the *behaviour* of the strength. In other words, how this strength is affected by factors relating to the task being performed and the physical capability of the operator. The SM is evaluated based on how this agrees with behaviour described in the literature, and anticipated behaviours based on an understanding of biomechanics.

4.2.1 Strength vs force direction

Upper limb strength at the hand varies depending on the direction being considered [McCormick, 1970]. It is important that this behaviour be portrayed by the SM when used in the AAN paradigm. The direction of external forces applied to the hand can vary as tasks are performed. Hence the strength capability of the operator to oppose such external forces, and consequently the assistance required by the operator varies. A model-based AAN paradigm is required to estimate how changes in force direction affect an operator's assistance requirements.

Method

The SM is used to calculate upper limb strength at the hand in a number of different directions for a specific pose. Results are compared to equivalent strength measurements in the literature. Evaluation is based on how well the strength results match in terms of both magnitude and distribution across the different directions.

Whole-limb strength measurements made at the hand are required for comparison with the SM results. It is common for measurements to isolate individual joints in an attempt to mitigate factors affecting strength such as limb posture [Amell, 2004]. However for evaluation it is exactly such effects we wish the SM to portray. In ergonomic strength studies, the joints are not isolated during the measurement of strength at the hand for specific activities (e.g. pushing, pulling, lifting, etc). However often in such studies the subject's pose is not specified, or only minimal pose variables are set (e.g. arm reach length [Kumar and Garand, 1992]) leaving much of the body pose

undefined. The position of the limb is required such that the MM can be positioned accordingly. Furthermore since the MM is of the upper limb, effects on strength due to remaining body segments (i.e. torso, lower limbs, etc) should be minimised as much as possible. For these reasons the strength measurements by McCormick [1970] are used for comparison. These measurements are of the whole-limb strength at the hand, measured in six orthogonal directions and five upper limb positions. The strength of 55 healthy male subjects were measured with the mean and 5th percentile results published. Subjects were seated during the study making this data set ideal for comparison with the upper limb MM as effects due to other body segments were minimised.

Upper limb strength is compared against measurements in McCormick [1970] for the limb position and directions shown in Figure 4.3. The MM generalised coordinates $\mathbf{q}$ are defined such that the upper limb MM is in the equivalent pose which has the humerus in 30° extension and forearm horizontal. The external force direction $\mathbf{u}$ is set equivalent to each of the six force directions (*Push, Pull, Up, Down, In, Out*). Strength capability S_P is calculated using the SM for each direction. Static conditions ($\dot{\mathbf{q}} = \ddot{\mathbf{q}} = 0$) are assumed, and no impairment is simulated ($\mathbf{s} = 1$).

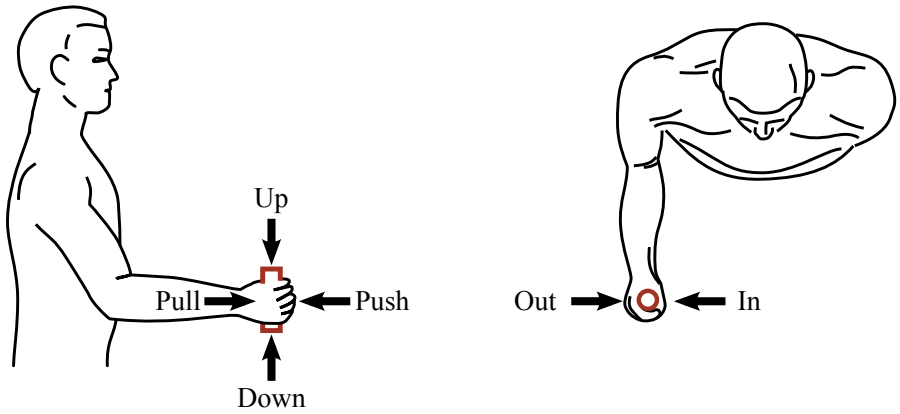

Figure 4.3: The six different directions for which the strength at the hand is calculated using the SM, and compared to strength measurements obtained from the literature [McCormick, 1970]. Arrows indicate the direction of external force applied to the hand ($\mathbf{u}$).

Results

The strength capability results calculated by the SM for each direction are shown in Figure 4.4, along with the corresponding strength measurements from McCormick [1970]. Results are displayed in descending order for convenience. A consistent difference between the SM results and the strength data from the literature across all six directions is observed. This is not surprising as no attempt was made to adjust the MM to fit the data, and upper limb strength varies amongst the population. Both results show a similar distribution of strength across the six directions. For both, strength is largest in the *Pull* direction, followed by the *Push* and then *Up* directions. Both data sets also had strength weakest in the *Out* direction. The SM estimated the strength for the *In* direction as being greater than for the *Down* direction. In the literature it was the reverse, however the difference in strength between these two directions within each of the data sets was relatively small.

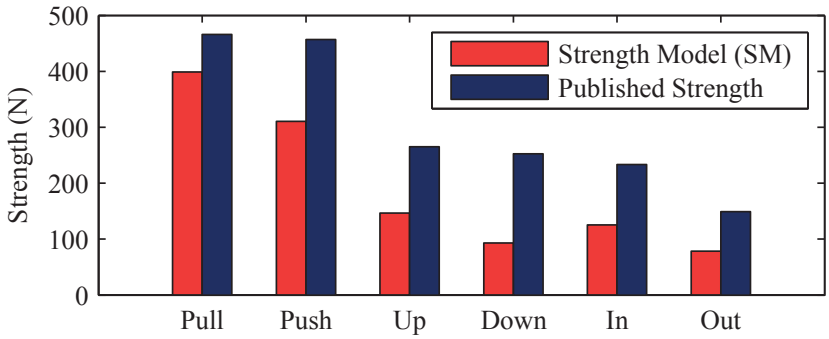

Figure 4.4: Strength at the hand in six orthogonal directions. Strength measurements from McCormick [1970] are compared with results obtained using the optimisation method within the SM.

4.2.2 Strength vs limb position

The position of the upper limb plays a large role in determining strength at the hand. The force producing capability of muscles are affected by their length, which is determined by the limb position. These forces produce torque at the joints depending on the moment-arms of the muscles about each joint, which are also determined by the limb's

position. Position of the limb also determines the load due to gravity, and which joints require the greatest strength to oppose an external force applied to the hand. The effect of upper limb position on strength has been measured in numerous studies [Amell, 2004; Caldwell, 1959; Kumar and Garand, 1992; McCormick, 1970]. This analysis evaluates the ability of the SM to predict the relationship between strength and limb position by comparing estimated strength capability against matching strength measurements from the literature.

Method

The strength data from McCormick [1970] is again used to compare against the strength capability estimated from the SM. Strength is calculated at the hand in five different upper limb positions shown in Figure 4.5. At each position, strength in the six directions *Push, Pull, Up, Down, In, Out* (shown in Figure 4.3) is calculated. Strength results calculated by the SM are compared to the equivalent strength measurements in the literature [McCormick, 1970].

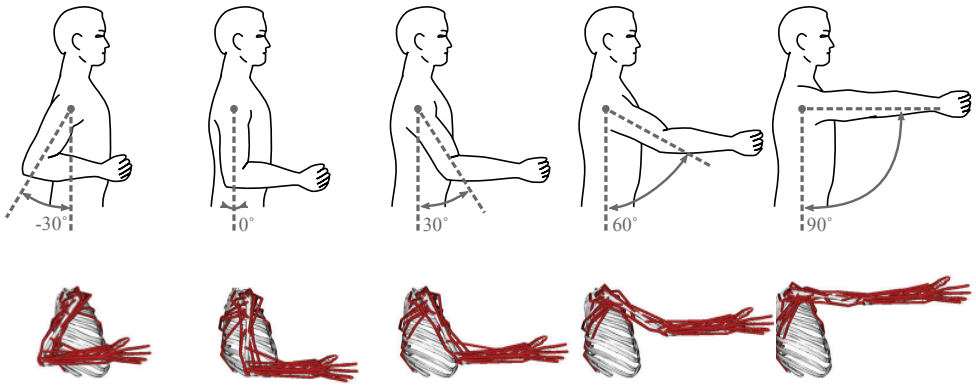

Figure 4.5: The five upper limb positions for which the strength at the hand is calculated using the SM, and compared to strength measurements obtained from the literature [McCormick, 1970]. The five poses have the humerus in −30°, 0°, 30°, 60°, and 90° extension, while the forearm remains horizontal.

The correlation between the results from the SM and the literature is analysed using the Pearson product-moment correlation coefficient (ρ). This value quantifies the linear relationship between the two data sets in the range of $-1 \leq \rho \leq 1$. A value of $\rho = 1$

denotes that the two data sets have a strong linear correlation. Alternatively a value of $\rho = -1$ indicates a negative linear relationship, and $\rho = 0$ indicates no linear correlation. Correlation between the calculated strength and strength from the literature is analysed for subsets within the strength results. For each of the five limb poses ($-30°$, $0°$, $30°$, $60°$, and $90°$) the correlation coefficient ρ is calculated for the subset of strength data relating to each individual pose. Similarly, for each of the six force directions (*Push, Pull, Up, Down, In, Out*) the correlation is calculated for the subset of strength data relating to each individual direction.

Equation (4.24) is used to calculate ρ for a specific strength data subset, where n is the size of the subset. When calculating ρ with respect to a single limb pose, $n = 6$ since this subset consists of strength results from both the SM and from the literature in each of the six orthogonal force directions at that pose. Alternatively with respect to a single force direction, $n = 5$ since this subset consists of strength results for each of the five limb poses. For each subset, S_{Pi} and S_{Li} are the i-th strength results from the SM and the literature, respectively. $\bar{S}_P$ and $\bar{S}_L$ are the average strengths from the SM and the literature for the subset.

$$\rho = \frac{\sum_{i=1}^{n}\left[(S_{Pi} - \bar{S}_P)(S_{Li} - \bar{S}_L)\right]}{\sqrt{\sum_{i=1}^{n}\left[(S_{Pi} - \bar{S}_P)^2\right]\ \sum_{i=1}^{n}\left[(S_{Li} - \bar{S}_L)^2\right]}} \tag{4.24}$$

Results

Both the SM results and the measurements from the literature are plotted in Figure 4.6 as a function of the limb position. As the arm is fully extended the SM estimates that strength in the *Push* (Figure 4.6a) and *Pull* (Figure 4.6b) directions increases. This strength increases rapidly when the arm is fully extended (towards $90°$ extension). The literature results also show an increase in strength as the arm is extended but not to the same extent. It is reasoned that the rapid increase in strength calculated by the SM is due to the limb being close to a kinematically singular position. With the arm fully extended, the external forces in both the *Push* and *Pull* directions pass almost

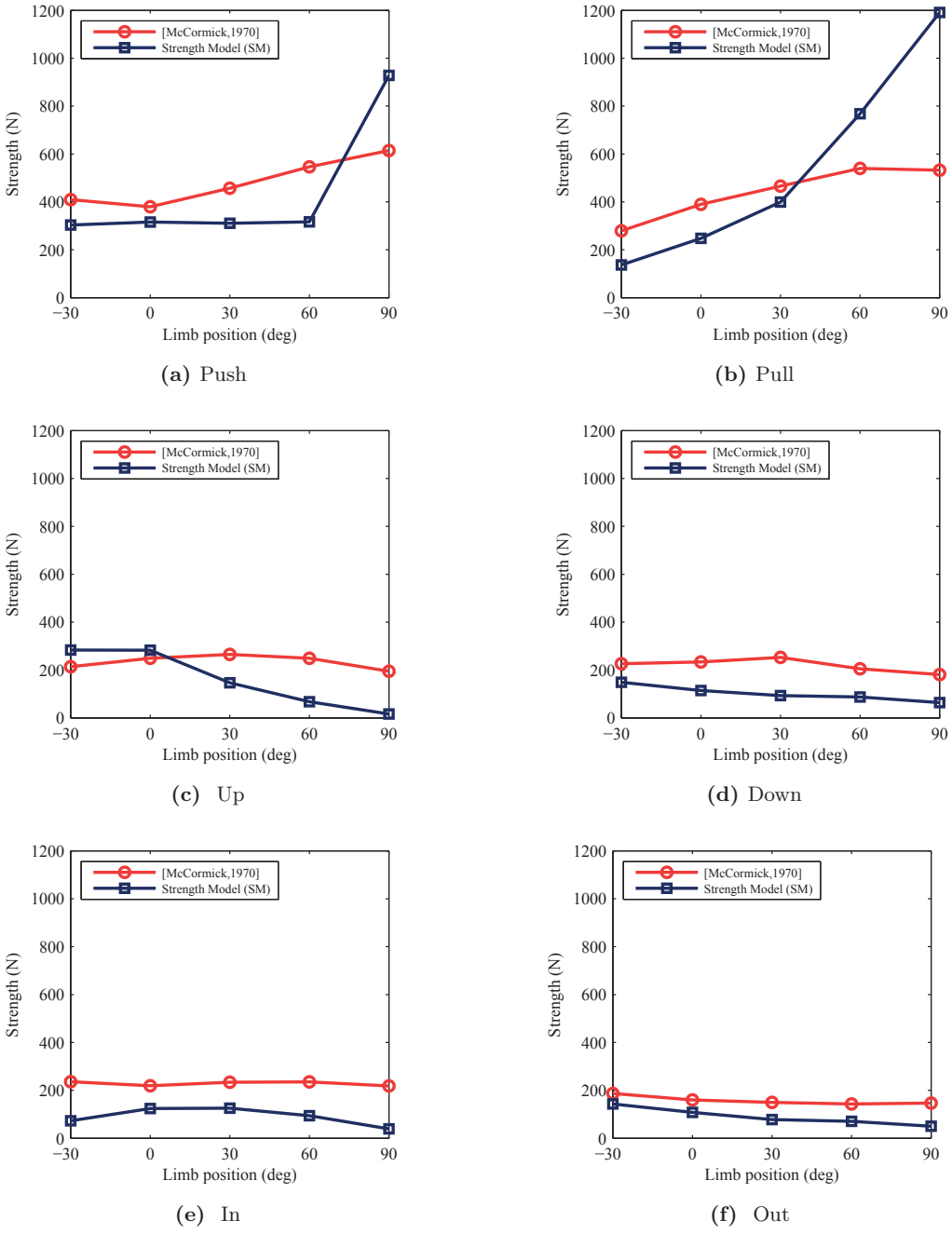

(a) Push **(b)** Pull

(c) Up **(d)** Down

(e) In **(f)** Out

Figure 4.6: Upper limb strength capability S_P versus limb position, calculated with the SM and compared to strength measurements from the literature [McCormick, 1970]. Each plot corresponds to one of the six external force directions; (a) *Push*. (b) *Pull*. (c) *Up*. (d) *Down*. (e) *In*. (f) *Out*.

directly through both the elbow and shoulder joints. This situation was discussed in Section 4.1.1. The $S_P^{\max}$ constraint may be set to limit excessively large strength results in situations such as this, however in this analysis it was not utilised ($S_P^{\max} = \infty$).

In the *Up* (Figure 4.6c), *Down* (Figure 4.6d), *In* (Figure 4.6e) and *Out* (Figure 4.6f) directions the results calculated by the SM and from the literature show similar strength behaviours as the hand is extended forward. With humerus extension in the 30° to 90° range the results show similar trends. In the −30° extension position the SM results tend to show a different trend to that in the literature. This is reflected by the correlation value calculated with respect to this limb position which equated to $\rho = 0.525$. This is far less compared with the other four limb positions ($\rho = 0.779, 0.958, 0.835, 0.952$).

When considering a specific direction at the hand (*Push*, *Pull*, *Up*, *Down*, *In*, or *Out*) the correlation across the different limb positions were ρ = 0.768, 0.845, 0.230, 0.529, 0.203, and 0.938 respectively. These values are smaller than those calculated for a specific limb position, particularly in *Up* and *In* directions. This suggests that the strength model is better at estimating how strength varies across different directions at the hand for a specific limb position, compared to estimating how strength varies across different limb positions for a specific direction at the hand. However it is noted that only a single motion of the upper limb is analysed, and both the calculated strength and the strength obtained from the literature for specific directions at the hand show relatively small variance compared to its mean value across this motion, which may contribute to poorer correlation values being calculated.

The correlation of the strength data for all poses and force directions was $\rho = 0.826$. All of the strength results calculated by the SM, the corresponding strength data from the literature, and their correlations ρ are shown in Table 4.1.

		External force direction						
		Push	*Pull*	*Up*	*Down*	*In*	*Out*	
Upper limb position	$-30°$	303.02 [409.18]	136.11 [278.96]	283.34 [213.85]	149.06 [226.20]	73.16 [236.30]	142.87 [186.91]	$\rho=0.525$
	$0°$	315.61 [379.72]	247.79 [389.82]	282.75 [249.50]	114.75 [233.78]	124.30 [219.19]	107.76 [159.69]	$\rho=0.779$
	$30°$	310.51 [456.89]	398.86 [465.87]	146.64 [264.93]	93.20 [252.58]	125.49 [233.50]	78.25 [149.30]	$\rho=0.958$
	$60°$	316.70 [546.42]	767.78 [539.68]	67.95 [248.93]	87.27 [205.15]	93.67 [235.46]	70.63 [143.41]	$\rho=0.835$
	$90°$	928.37 [614.61]	1191.06 [532.66]	16.59 [194.76]	64.39 [181.29]	39.50 [218.34]	49.81 [146.49]	$\rho=0.952$
		$\rho=0.768$	$\rho=0.845$	$\rho=0.230$	$\rho=0.529$	$\rho=0.203$	$\rho=0.938$	

Table 4.1: Upper limb strength at the hand in five different limb positions and in six different directions; comparison between the strength calculated by the SM, and strength data obtained from the literature. Strength units are in Newtons (N). Values not in brackets (e.g. 123.45) are results calculated by the SM. Values in brackets (e.g. [123.45]) are from the literature [McCormick, 1970]. Correlation ρ is calculated for each limb position, and each force direction subsets.

4.2.3 Strength vs muscle impairment

This analysis evaluates the ability of the SM to depict the effect physical impairment has on the strength capability of an operator. In applications such as rehabilitation, physical impairment can reduce the capability of a subject to perform physical tasks. The extent of this reduction of capability, and how it manifests itself depends largely on the impairment of the individual [Arva *et al.*, 2004]. The ability to estimate how a specific impairment affects a subject's capability to perform tasks, and hence affects their assistance requirements is useful in AAN applications.

Method

The relationship between a physical impairment and its effect on upper limb strength is observed by simulating impairments at the muscular level. Three different impairment types are simulated, localised into three distinct muscle groups; *biceps*, *triceps*, and *deltoid*. Impairment is simulated by limiting the activation of the muscles in each of these groups. This is done by setting the corresponding elements in vector $\mathbf{s}$ to $s = 0.01$, limiting the muscle's active force output to replicate the effects of an impairment during the optimisation. Table 4.2 details which MTUs in the MM have their activations limited for each of the three impairments.

Impairment	**MTUs impaired in MM** ($s = 0.01$)
No impairment	None
Impaired biceps	BIClong, BICshort
Impaired triceps	TRIlong, TRIlat, TRImed
Impaired deltoid	DELT1

Table 4.2: Names of the MTU models in the upper limb MM which have their activation limited to simulate impairment. The MTUs listed have their corresponding elements in the $\mathbf{s}$ vector set to $s = 0.01$. MTU names correspond to the muscles in the upper limb MM [Holzbaur *et al.*, 2005]. MTUs which are not listed in an impairment have do not have their activation limited ($s = 1$).

There is no comprehensive data available in the literature detailing the relationship between impairments at the muscular level and the effects of such impairments on upper limb strength at the hand. The ideal approach to obtaining this information would be to measure the hand strength of subjects before and after controlled impairments are introduced into specific muscle groups. Of course this is not feasible due to many factors, most notably ethical and safety concerns. Instead, the effect of localised muscle impairments on hand strength are anticipated based on an understanding of biomechanics. These expected behaviours are then compared to the SM results.

To visualise the effect of impairment on the strength capability, the SM is used repeatedly to calculate strength as the direction vector $\mathbf{u}$ is swept 360° about the hand in the vertical plane. At each direction, the operator's strength capability S_P is calculated. Results are plotted in a polar plot with its origin located at the hand. For each direction

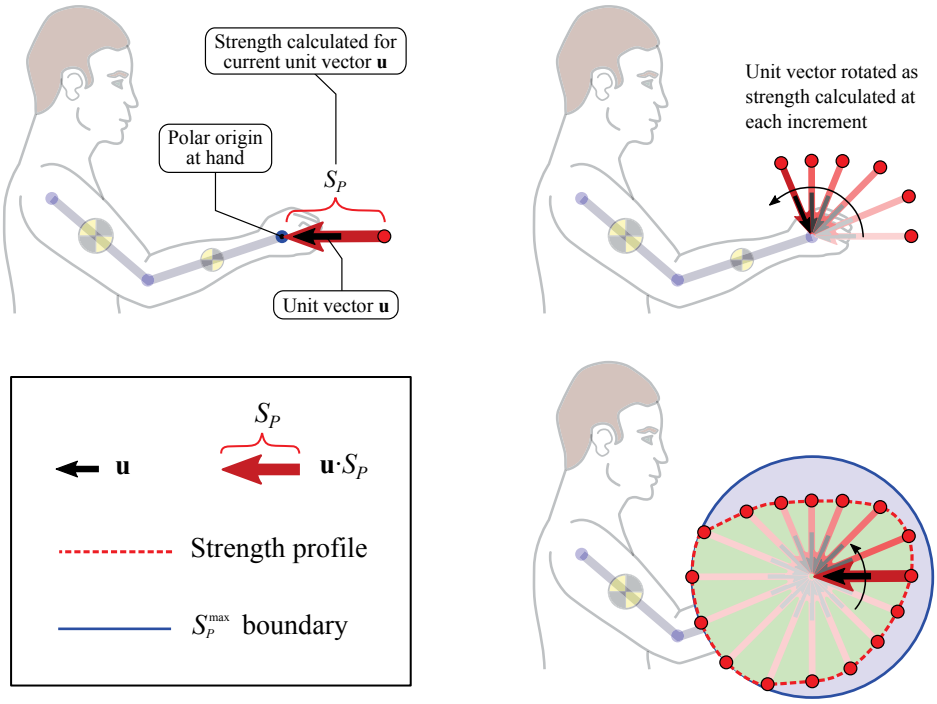

Figure 4.7: Visualisation of the SM results using a polar plot. With the limb motion defined by $\mathbf{q}, \dot{\mathbf{q}}, \ddot{\mathbf{q}}$, operator strength is calculated using the SM. The direction of external load $\mathbf{u}$ is rotated 360° as strength S_P is calculated at fixed intervals. Strength results are plotted as a polar plot with origin at the hand, as shown above. The result is a strength profile polar plot.

that S_P is calculated, the strength result is plotted as a point. Distance from the point to the polar origin represents the magnitude of the S_P result, while the direction from the point to the origin indicates the direction of $\mathbf{u}$ for which S_P was calculated. The resulting polar plot produces a strength profile as demonstrated in Figure 4.7. The outer circle of the plot indicates the $S_P^{\max}$ boundary, which was set to 300N in this analysis.

Strength is calculated with the hand positioned at chest height in front of the body. The polar plots are calculated with and without each of the three impairments present. The impaired strength plots can then be compared with each other and with the strength plot calculated with no impairment. This allows both the magnitude and directions in which the different impairments affect strength at the hand to be easily visualised, and a qualitative comparison between the different impairments made.

Results

Results are shown in Figure 4.8. In each subplot the strength profile without any impairment applied is shown. Subplots 4.8b, 4.8c and 4.8d are overlaid with the strength profiles resulting from impaired biceps, triceps, and deltoid, respectively. It is seen that each of the impairments produces a decrease of strength capability (compared with no impairment) in some direction. The direction of this strength decrease depends on which muscle group is impaired. Impairing the biceps (Figure 4.8b) resulted in a loss of strength in the upwards direction, and towards the torso. Impaired deltoids (Figure 4.8d) resulted in a loss of strength also in the upwards direction, but away from the torso. Impaired triceps (Figure 4.8c) reduced strength downwards and away from the body.

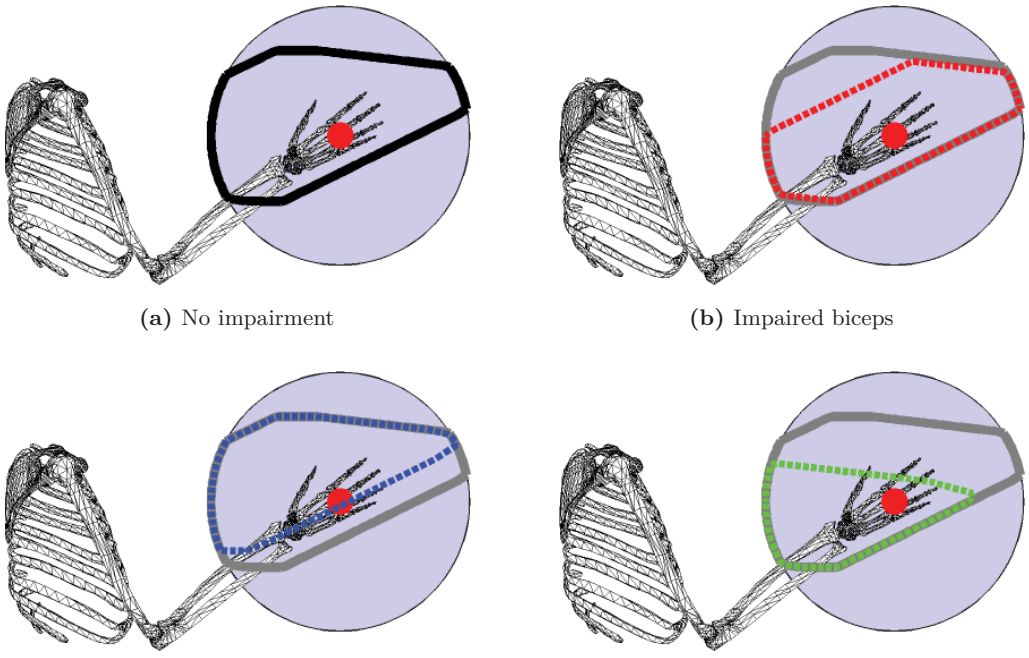

(a) No impairment

(b) Impaired biceps

(c) Impaired triceps

(d) Impaired deltoid

Figure 4.8: The effect of muscular impairment on strength at the hand. Plot (a) shows the strength calculated with no impairment applied. The remaining plots are overlaid with the strength results calculated with impairment localised in the following muscle groups; (b) Biceps. (c) Triceps. (d) Deltoid.

From an understanding of biomechanics these effects on strength is what could be

expected for this upper limb pose and the types of impairments introduced. In the upper limb position simulated, the biceps and anterior deltoid are both used in lifting motions. It is therefore expected that their impairment would result in weakness in the upwards direction. Alternatively, the triceps is largely responsible for downwards movements, and therefore impairment would result in downward weakness, as predicted by the SM.

4.3 Assistance Estimation Considering Impairment

Chapter 3 demonstrated the model-based AAN framework applied to example tasks utilising the upper limb. It was shown how the framework estimated the strength capability of the subject, how this capability varied during the task, and how it could be used to estimate their assistance requirements. Since the optimisation model developed in Section 4.1 operates in the muscle space of a MM representing the subject, it is possible to investigate the role physiology plays with respect to the capability of performing tasks.

In this section the framework is applied within two case studies which analyse the effects physical impairment have on the ability to perform simulated tasks. Muscle impairment profiles based on data from stroke patients are applied to the MM as the strength capability of a person is estimated. Observing how their strength capability varies with different applied impairments allows the relationship between muscle impairment and a person's assistance requirements to be analysed. Ideally, these results would be compared with empirical data which describe how impairments at the muscular level affect someone's ability to express forces at the hand and perform tasks. Validation of the model-based AAN could then be made using a statistical analysis of its efficacy in estimating this relationship. This would require a large controlled study involving numerous patients with differing impairments to be performed. Each patient's impairment would need to be quantified at the muscular level. Their assistance requirements with respect to numerous different tasks would then need to be determined through a series of experiments. It is not known if such a study has been performed in the past,

and at the current stage of this research implementing a study of such magnitude is not feasible. In the literature there have been studies quantifying impairment due to stroke at the physiological level. Using this information, averaged muscle impairment profiles which are consistent with that of stroke are created. Creating impairment profiles for specific patients is discussed later in Section 6.2.3.

The averaged stroke impairment profiles are used in the two case studies to observe the effects such impairments have on the strength at the hand, and consequently the assistance needs of a person. The results provide insight into the possible effects such impairments may have on a person's ability to perform tasks. It also demonstrates how incorporating a MM into an AAN paradigm has the potential to provide significant benefits, such as the capability of analysing physiological factors with respect to an individual's assistance requirements.

4.3.1 Impairment due to stroke

Impairment profiles are created based on a study in which the strengths of 69 stroke patients were recorded [Bohannon and Andrews, 1987]. The patients had hemiplegia, meaning the weakness due to their stroke was predominantly located in one side of their body. Strengths in both paretic and non-paretic upper limbs were recorded for seven limb articulations; wrist extension, elbow flexion, elbow extension, shoulder internal rotation, shoulder external rotation, shoulder extension, and shoulder abduction. The mean and standard deviation of the measured paretic and non-paretic strengths are shown in Figure 4.9a. The amount of strength remaining after a stroke (referred to as the residual strength) is calculated by normalising the mean paretic strength by the mean non-paretic strength for each articulation. The normalised standard deviation (σ) of the residual strength is calculated by dividing the paretic strength standard deviation by the non-paretic strength mean. The normalised residual strengths and normalised σ for each articulation are shown in Figure 4.9b. These normalised residual strengths provide a basis on which the different upper limb impairment profiles consistent with stroke are derived. Figure 4.9b suggests that the mean residual strength after a stroke is

in the range of approximately 17% to 35% across the different upper limb articulations. Residual strength σ is around 30%, indicating that the residual strength has large variation about the mean. Bohannon and Andrews [1987] noted that many patients were unable to produce any strength in one or more articulations.

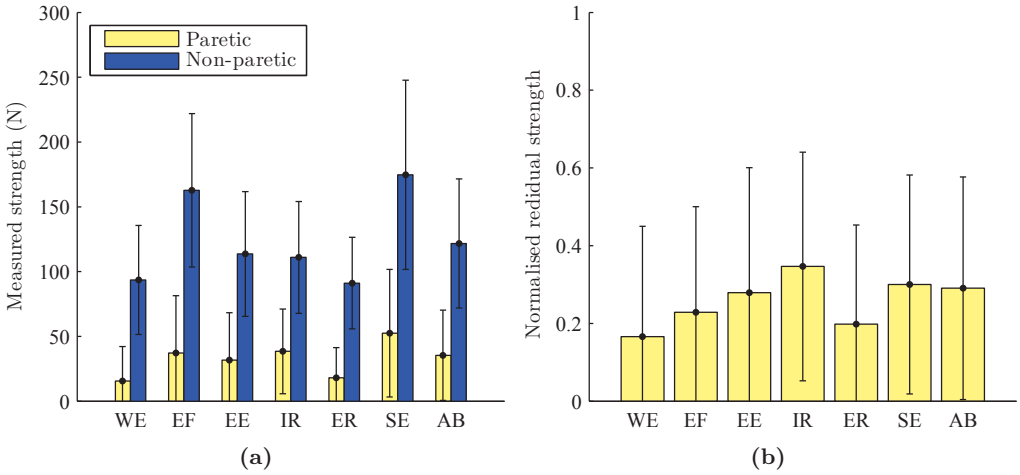

Figure 4.9: Measured strength comparison between the paretic and non-paretic upper limbs of stroke patients with hemiparesis, obtained from the literature [Bohannon and Andrews, 1987]. Strength is grouped by muscle group based on the following upper limb articulations; Wrist Extension (WE), Elbow Flexion (EF), Elbow Extension (EE), Shoulder Internal Rotation (IR), Shoulder External Rotation (ER), Shoulder Extension (SE), Shoulder Abduction (AB). (a) Strength measured for select muscle groups for paretic and non-paretic upper limbs. Error bars indicate standard deviation of the measurements. (b) Paretic strength measurements normalised by the non-paretic strength measurements. The bars are the mean paretic strength normalised by the mean non-paretic strength. The error bars is the paretic standard deviation normalised by the mean non-paretic strength.

Impairment profiles are created by defining several $\mathbf{s}$ vectors which limit muscle activation during the calculation of strength capability. Limiting muscle activation replicates impairment by reducing the amount of active force a muscle can produce. Each element in the $\mathbf{s}$ vector ranges from 0 to 1, with $s=0$ fully impairing a MTU, and $s=1$ producing no impairment at all. The normalised residual strengths also range from 0 to 1, and are used to set the level of impairment in the $\mathbf{s}$ vector. Five different impairment profiles are created. The first profile $\mathbf{s}_0$ represents no impairment ($\mathbf{s}_0=1$) and is used to provide a benchmark representing a healthy subject not impeded by stroke. Four other profiles are created from combinations of the *mean* and σ of the normalised residual strengths

shown in Figure 4.9b. In order from the least impaired to the most impaired these are; $\mathbf{s}_1 = (mean+\sigma)$, $\mathbf{s}_2 = (mean+\sigma/2)$, $\mathbf{s}_3 = (mean)$, and $\mathbf{s}_4 = (mean-\sigma/2)$. These five levels of impairment for the seven upper limb articulations in Bohannon and Andrews [1987] are shown in Figure 4.10.

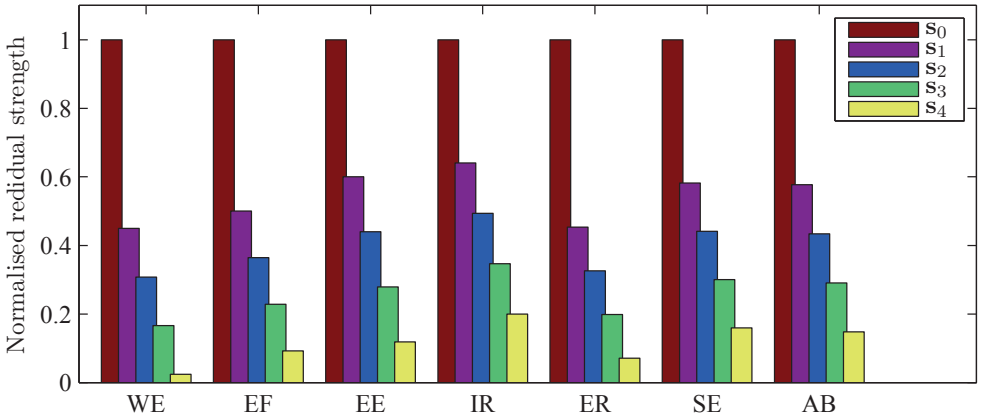

Figure 4.10: Strength impairment profiles with various impairment severity, derived from the literature [Bohannon and Andrews, 1987]. Impairments are sorted by muscle group based on the following upper limb articulations; Wrist Extension (WE), Elbow Flexion (EF), Elbow Extension (EE), Shoulder Internal Rotation (IR), Shoulder External Rotation (ER), Shoulder Extension (SE), Shoulder Abduction (AB).

To derive the vector $\mathbf{s}$ for an impairment, each MTU in the model is associated with one of the seven upper limb articulations. Its level of impairment is then set using the values from Figure 4.10 depending on the articulation it was assigned, and the severity of the impairment profile ($\mathbf{s}_0$, $\mathbf{s}_1$, $\mathbf{s}_2$, $\mathbf{s}_3$ or $\mathbf{s}_4$). Each MTU is assigned to an articulation by determining which articulation it contributes to the most by examining the MM's activation-to-torque gain matrix $\mathbf{K}_\tau$ (4.13). Each element in matrix $\mathbf{K}_\tau$ represents the active torque produced about a joint in the MM by a fully activated muscle. Each column corresponds to an individual muscle, and each row to a specific joint. Taking the column from $\mathbf{K}_\tau$ corresponding to the MTU in question, the row containing the element with the largest magnitude corresponds to the joint which produces the most torque as a result of the MTU's activation. This joint and the sign of the torque produced about it are then used to relate the MTU to one of the seven articulations. Since the data from Bohannon and Andrews [1987] does not provide strength measurements for

shoulder adduction and shoulder flexion, muscles which produce these articulations are impaired as if they produced shoulder abduction and shoulder extension, respectively. Appendix A.3 lists the impairment vectors $\mathbf{s}_0$, $\mathbf{s}_1$, $\mathbf{s}_2$, $\mathbf{s}_3$ and $\mathbf{s}_4$ for all MTUs in the MM.

4.3.2 Case study 1: drinking task

The drinking task detailed in Section 3.5.1 is simulated in this case study. The task involves a subject carrying a water bottle as it is moved from their mouth and placed on a table surface in front of them. The motion of the subject's upper limb was recorded using a motion capture system (Xsens MVN Biomech) and used to derive the generalised coordinates $(\mathbf{q}, \dot{\mathbf{q}}, \ddot{\mathbf{q}})$ for the MM. The bottle carried in the hand had mass of 0.6kg. In the AAN framework the carried bottle is represented by external force $\mathbf{u} \cdot S_T$ at the hand, with direction vector $\mathbf{u}$ pointed in the direction of gravity and $S_T = 6N$. Figure 4.11 shows the recorded upper limb motion as the hand is extended from the subjects mouth and the bottle placed on the table surface in front of them. At each time instant of the recorded motion the SM is used to calculate operator strength capability S_P. This process is performed five times, each with a unique impairment profile ($\mathbf{s}_0$, $\mathbf{s}_1$, $\mathbf{s}_2$, $\mathbf{s}_3$, $\mathbf{s}_4$) to simulate the effects of stroke.

Figure 4.12a shows the calculated strength capability S_P for the task for each impairment profile. As expected the strength at the hand decreases as the hand is extended away from the subject's torso. It is observed that the impairment profiles affect the calculated strength capability of the operator. As the severity of the impairment is

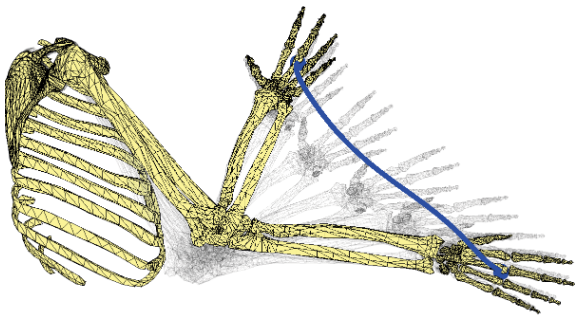

Figure 4.11: Upper limb motion recorded during the drinking task.

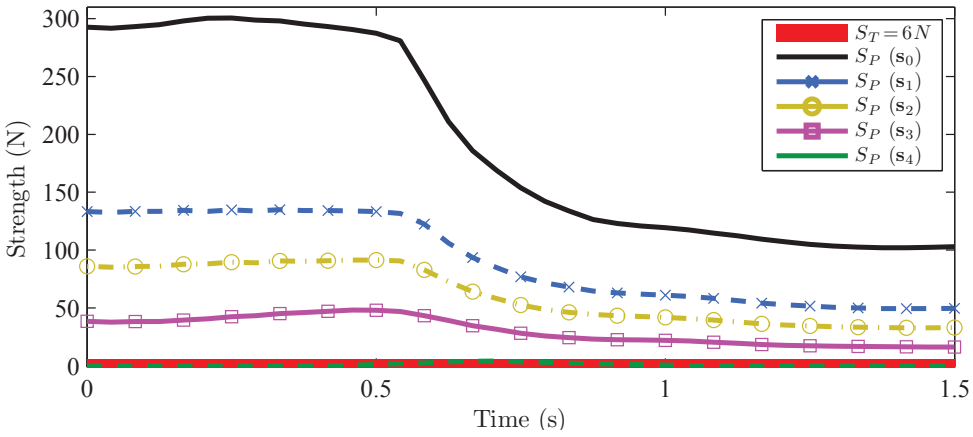

(a)

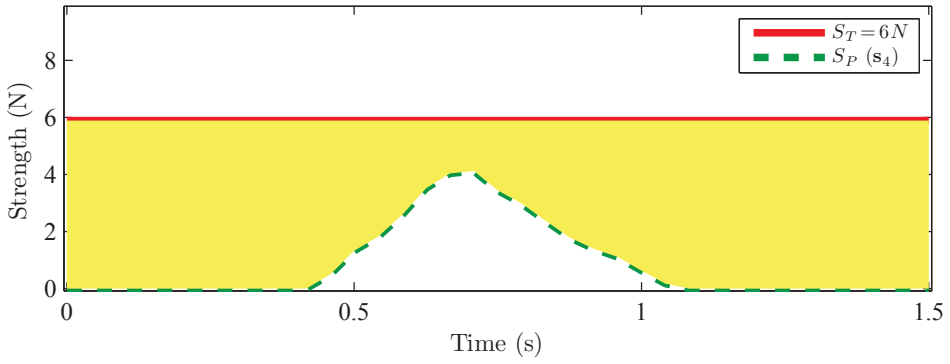

(b)

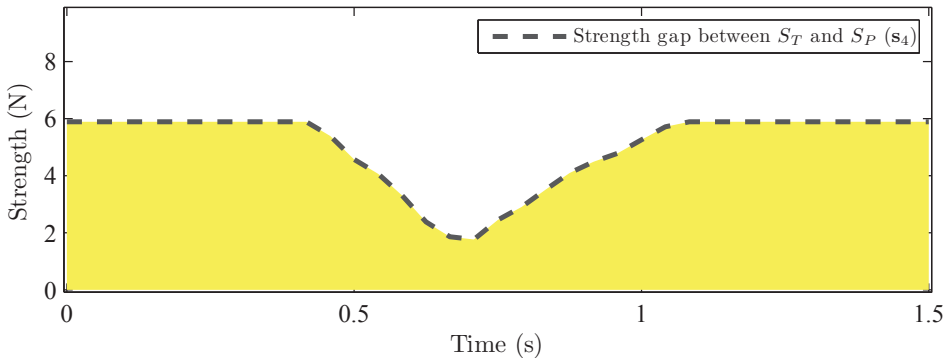

(c)

Figure 4.12: Results for the drinking task. (a) Calculated strength capability at the hand during the task. Each curve represents the operator with different severity of impairment ($\mathbf{s}_0$, $\mathbf{s}_1$, $\mathbf{s}_2$, $\mathbf{s}_3$, $\mathbf{s}_4$). (b) Enlarged view showing the calculated strength capability with impairment profile $\mathbf{s}_4$ applied. (c) Gap between the drinking task strength requirement S_T and the estimated strength capability S_P of the subject with impairment profile $\mathbf{s}_4$.

increased, the calculated strength at the hand reduces. Hence the gap between the operator's strength capability S_P and the task's strength requirement $S_T = 6N$ reduces as well. For the four least severe impairments ($\mathbf{s}_0$, $\mathbf{s}_1$, $\mathbf{s}_2$, $\mathbf{s}_3$) the operator's capability remains greater than what is required by the task (i.e. $S_P > S_T$). For the most severe impairment ($\mathbf{s}_4$) the subject is estimated as having less strength than the task requires ($S_P < S_T$). This strength is small compared to the others, making it difficult to visualise in the plot. An enlarged view the strength with impairment profile $\mathbf{s}_4$ is shown in Figure 4.12b. It is seen that the gap between S_P and S_T is not constant, but varies during the task. Interestingly the results suggest that less assistance is required in the middle of the movement, compared to the start and end positions.

4.3.3 Case study 2: sliding task

The second case study simulates the sliding task detailed in Section 3.5.2 in which the subject slides a water bottle in a circular motion on a horizontal table surface in front of them. Again the motion was recorded using a motion capture system from which the MM generalised coordinates are derived. A single circular motion shown in Figure 4.13a is used. A horizontal friction force of magnitude $S_T = 2.5N$ (based on Yeong *et al.* [2009]) is applied to the hand representing the friction force resulting from sliding the bottle. The unit vector $\mathbf{u}$ defining the direction of this external force is pointed such that it is parallel with the table surface and in the opposite direction of hand movement, as shown in Figure 4.13b. At each time instant of the recorded motion the SM is used to calculate operator strength capability S_P. Similar to the previous analysis this process is repeated for each unique impairment profile ($\mathbf{s}_0$, $\mathbf{s}_1$, $\mathbf{s}_2$, $\mathbf{s}_3$, $\mathbf{s}_4$).

Figure 4.14a shows the calculated strength capability S_P for the task for each impairment profile. The estimated strength capability varies during the task, showing a similar shape to that estimated for the same task in Chapter 3 (see Figure 3.18). Interestingly there is a visible difference between the calculated strengths using the optimisation model developed in Section 4.1 versus the method used in Chapter 3. The maximum strength which was noted as being unrealistically large ($\approx 1200N$) is reduced

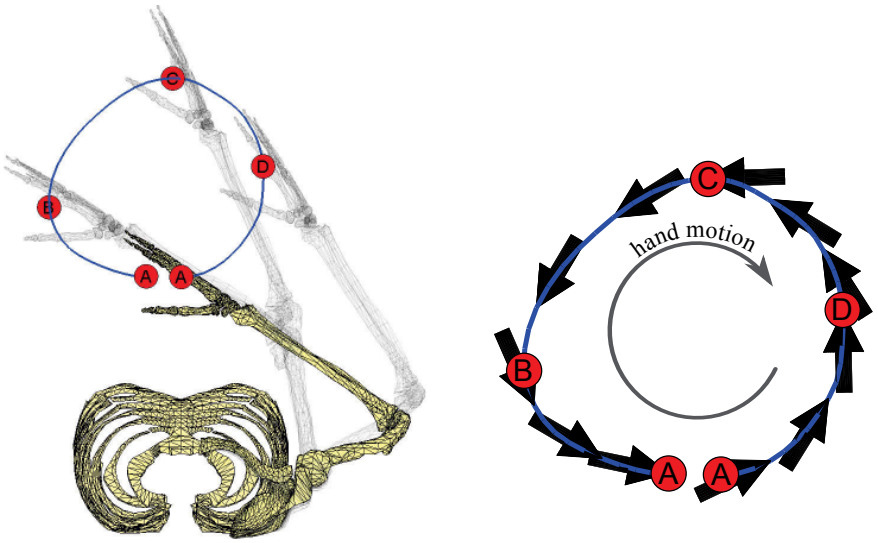

(a) (b)

Figure 4.13: Upper limb motion recorded during the sliding task. (a) The hand movement and target positions based on motion capture data. (b) The direction of the external force vector **u** is shown at intervals during one circular movement. The hand moves in a clockwise direction with the external force vector opposing the movement to simulate the friction force of an object being slid on a table surface.

to around $700N$. This strength corresponds to when the subject is sliding the bottle towards their torso in a pulling motion, and is a much more realistic value for the maximum strength that a typical person would be capable of performing in this type of action. Differences in the results are attributed to one method accounting for effects due to joint coupling, while the other method does not. This highlights the necessity of developing the optimisation model which estimates strength taking such effects into account.

It is observed that the impairment profiles affect the calculated strength capability of the operator. Similar to the analysis of the drinking task, as severity of impairment is increased the strength at the hand reduces. For the least severe impairments ($\mathbf{s}_0$, $\mathbf{s}_1$, $\mathbf{s}_2$, $\mathbf{s}_3$) the operator's capability remains greater than what is required by the task (i.e. $S_P > S_T$). For the most severe impairment ($\mathbf{s}_4$) the subject is estimated as having less strength than what the task requires ($S_P < S_T$) during certain portions of the movement. An enlarged view of the strength with impairment profile $\mathbf{s}_4$ is shown in

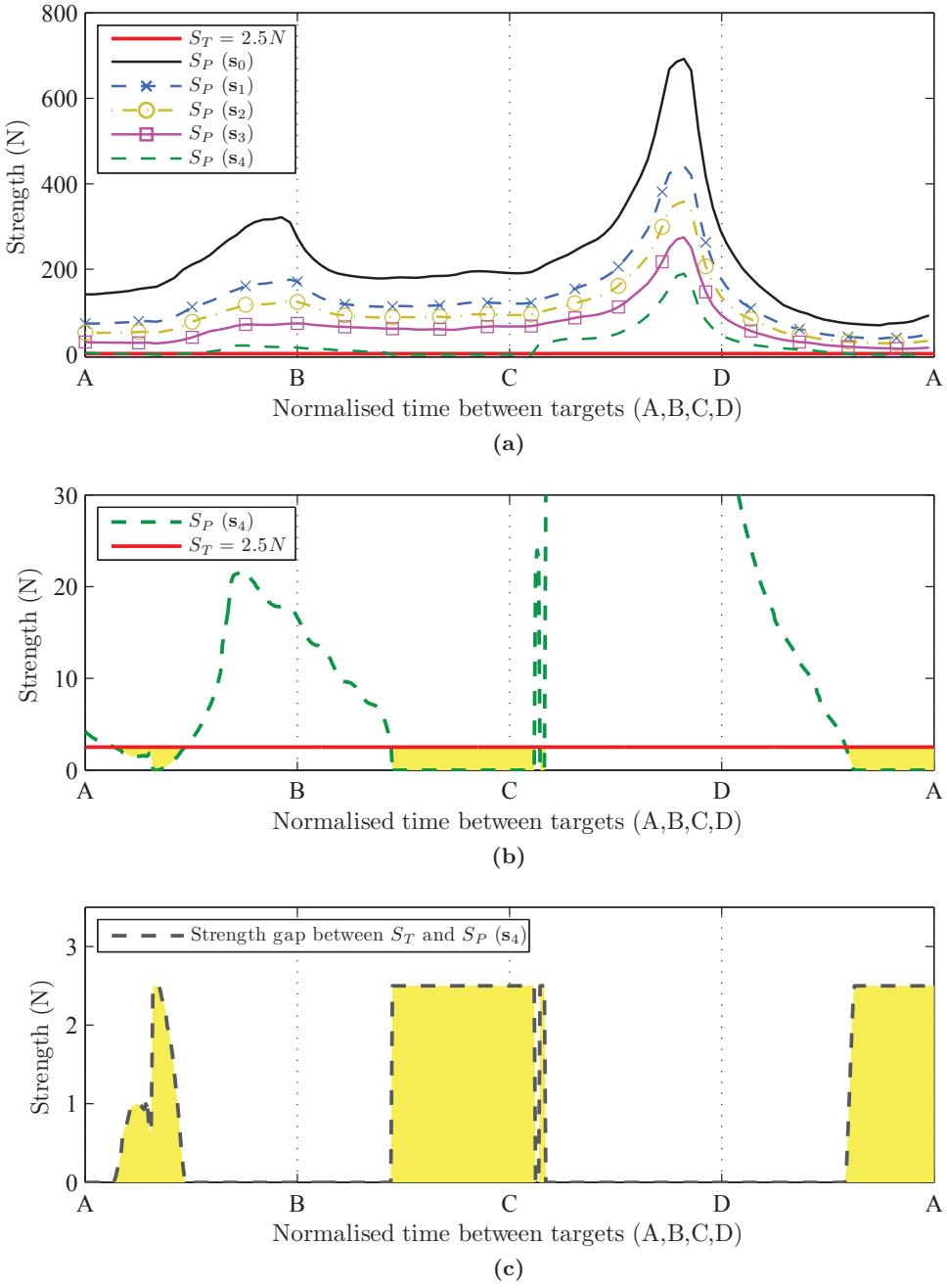

Figure 4.14: Results for the sliding task. (a) Calculated strength capability at the hand during the task. Each curve represents the operator with different severity of impairment ($\mathbf{s}_0$, $\mathbf{s}_1$, $\mathbf{s}_2$, $\mathbf{s}_3$, $\mathbf{s}_4$). (b) Enlarged view showing of the calculated strength capability with impairment profile $\mathbf{s}_4$ applied. (c) Gap between the drinking task strength requirement S_T and the estimated strength capability S_P of the subject with impairment profile $\mathbf{s}_4$.

Figure 4.14b. It is seen that the gap between S_P and S_T varies during the task. At two distinct times during the task the subject's strength is estimated as being greater than the friction force required to slide the bottle. These times are approximately when the hand is passing the B and D targets. Due to the direction of the friction force at these times, the task represents actions similar to that of pushing and pulling. As the sliding task is performed, and the hand motion changes such that the task transitions into medial and lateral hand movements, the estimated strength of the operator decreases. This behaviour is expected and matches with the literature [McCormick, 1970]. During these segments of the task the estimated strength drops below the strength requirements of the task. The gap between S_T and S_P is plotted separately in Figure 4.14c.

4.4 Discussion

4.4.1 Representation of physical impairment

A key benefit of the MM-based AAN approach is the ability to investigate the role physiology plays in physical capabilities, and hence the assistance requirements of a person. This chapter examined the effects of physical impairment on operator strength at their hand by setting limits on the degree to which certain muscles could be activated, reducing their active force output capability. This is a convenient approach as implementing it only requires the upper bounds of the muscle activation search space in the optimisation to be set according to the impairment being simulated. Other methods which reduce the force producing capabilities of muscles in a MM have been used to mimic the effects of physical impairment [van Drongelen *et al.*, 2006]. It is understood that there are many other factors that can contribute to an injury limiting the capability of a person to perform physical tasks. For example abnormal muscle synergies following a stroke can reduce the ability to coordinate limb movement [Hogan *et al.*, 2006]. Mechanical injuries such as tears in the muscle or tendon may not be adequately represented by limiting muscle activation since this only limits the active force producing components in the MTU.

Injuries which manifest themselves through muscular weakness can be the result of very different mechanisms of injury. Neuromuscular disease can cause muscular weakness either directly or indirectly. Direct neuromuscular disease directly affects the muscle pathology such as in the muscular dystrophy group of diseases. Indirect causes can be due to a loss or reduction in the ability to activate or control motor neurons that produce muscle activation. This can be caused by diseases such as stroke, multiple sclerosis, or cerebral palsy. Regardless of the cause of the weakness, we make the assumption that weakness in the muscle domain can be mapped by assigning each muscle a value representing its weakness in relation to baseline active force output.

4.4.2 Effect of joint coupling on strength estimation

A motivation for the optimisation model developed in this chapter is the necessity to consider effects from biarticular muscles spanning multiple joints when calculating operator strength capability. This is in contrast to the simplified method used in Chapter 3 which calculated strength assuming the joints in the limb were independent and uncoupled. Muscles which span multiple joints place additional constraints which need to be satisfied when the operator's strength is calculated. Without such constraints it is possible that a larger solution for the strength would be calculated, and hence may result in the assistance requirements of an operator being underestimated compared to if this coupling is taken into account.

This is observed by comparing the strength results obtained from these two methods of calculating strength. The first is the optimisation model developed in this chapter, Section 4.1 which accounts for joint coupling. The second is the strength calculation that was utilised in Chapter 3 which assumed independent joints. These two methods are used to recreate the same strength polar plots created in Section 4.2.3. This allows the difference between the strength results to be visually observed.

The calculated strength results from both the methods are shown in the same polar plot in Figure 4.15. Both results show a similar shape, with many of the polar points aligning in the plots. In two distinct regions of the plot, differences between the strength

results are observed (filled in yellow). This difference is attributed to one method taking into account joint coupling, while the other does not. As expected, in these regions the method assuming uncoupled joints produced larger strength results compared with the method that accounted for joint coupling. The largest difference in these results is approximately 15% of the coupled strength. This demonstrates that the simplification of assuming independent joints, although convenient and computationally efficient, comes with the cost of less confidence in the strength result.

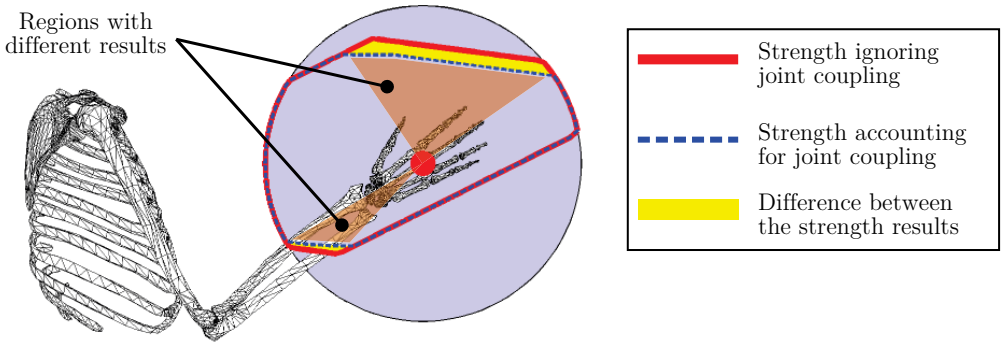

Figure 4.15: Differences in the strength results calculated with and without considering joint coupling. In the two regions highlighted, differences between the strength results are observed.

4.4.3 Redundancy

There are many different methods for utilising musculoskeletal models (see Section 2.3.7). A common objective is to find a solution to the muscle forces or activation patterns required for a specific task or motion to be performed. A challenge with such analyses is that there are an infinite number of solutions for the muscle utilisation that can perform a specific task. This is due to the human body having significant redundancy [Prilutsky and Zatsiorsky, 2002]. Optimisation methods are typically employed to find a solution, utilising a cost function based on some form of physiological rationale [Erdemir *et al.*, 2007]. For example a solution may be found that minimises the total muscle stress. Although such methods have been applied successfully in a number of clinical investigations, there currently exists no proven solution to solving this redundancy problem and continues to be a topic of ongoing research.

The model-based AAN paradigm that is presented in this thesis is different in the sense that it is not being used to estimate the physiological state of the operator during the task. Instead, the MM is used to gauge the maximum potential of the operator in terms of strength. The advantage is that, given the constraints imparted by the task being performed and the physiology of the musculoskeletal system, there exists a single solution to the maximum strength which the operator is able to achieve. Hence this approach which is based on determining the maximum strength of the operator is a convenient method of utilising the MM within the framework of a robotic control system, whilst avoiding the problems associated with solving the redundancy in the muscle space.

4.4.4 Ignored activation dynamics

The activation of a muscle behaves similar to a first order dynamic system (see Section 2.3.6). Therefore, given the activation of a muscle at a specific instant in time, the range of activation possible at the next time instant is limited by that muscle's activation dynamics. Taking these dynamics into account affects the strength calculation in two ways. Firstly, it adds constraints into the optimisation which would often limit the strength result to a lower value. Secondly it means that the strength cannot be calculated at each time instant independently, but rather is dependent on the previous activation state of the subject.

At this early stage of research the activation dynamics of the operator's muscles are ignored. This removes the requirement of the actual activation state of the operator to be calculated, avoiding the redundancy problems previously discussed. It also allows the strength capability of the upper limb to be calculated at each time instant during a task, independent of the previous states of the operator or the task. No constraints are considered when calculating operator capability with respect to previous states.

4.5 Summary

In this chapter an optimisation model for calculating the strength capability of a human operator was formulated and evaluated. The optimisation model uses parameters from a MM representing the operator to calculate the maximum strength at the hand, in a specific direction and for a specific limb motion. Unlike the method used in Chapter 3 to calculate strength, this optimisation model operates at the muscular level, taking into account effects such as joint coupling resulting from biarticular muscles. A comparison of the results obtained with and without considering such effects showed differences in strength estimation, justifying the need for its development.

The ability of the developed optimisation model to calculate strength was evaluated by estimating upper limb strength with respect to limb position, force direction, and physical impairment. The calculated relationship between upper limb strength with both force direction and limb position agreed well with strength results from the literature. These results are promising since no effort was made to adjust the MM as to better match with the results. The calculated relationship between strength at the hand and impairments in the biceps, triceps and deltoid muscle groups produced qualitative behaviours consistent with expectations based on an understanding of biomechanics.

Lastly, the optimisation model was applied to two upper limb tasks. The model-based AAN framework was used to calculate the relationship between the operator's physiology and their assistance requirements for the two tasks. Impairment profiles used for analysis were derived from a study of stroke patients. The effects of different impairment severity on the operator's assistance requirements were observed.

Chapter 5

Experimental Validation of Model-based AAN

In Chapter 4 an optimisation model for calculating the strength capability of an operator was developed and tested. It was applied in a number of simulated tasks using a musculoskeletal model (MM) of the upper limb [Holzbaur *et al.*, 2005]. The strength of an operator at their hand, and how this strength is affected by factors such as limb position, direction of force at the hand, and impairment at the muscular level was calculated. The results were shown to be consistent with data from the literature. The model-based Assistance-As-Needed (AAN) framework was also applied in two case studies in which upper limb tasks were simulated. It was demonstrated how the framework can be used to estimate the changing assistance requirements of an operator during tasks, and how these requirements vary due to physical impairment. It remains to be shown how the model-based paradigm for providing robotic AAN performs in a real world scenario.

In this chapter the model-based AAN framework is implemented on an experimental robotic system for evaluation. A specially developed exoskeleton is used to assist a subject performing a number of physical tasks involving the upper limb. Tasks which require the use of different muscle groups in the limb are performed. To evaluate the paradigm, the subject is assumed as having various physical impairments localised to specific muscles, reducing their ability to perform tasks. The assistance provided by

the robot to the subject in each task is controlled by the model-based AAN paradigm, taking into account the impaired muscles and the task being performed. The paradigm is evaluated on how effectively it provides assistance targeted towards the impaired muscles, only when tasks are performed which require them to be utilised. Measurements of the force interaction between the subject and the robot, and the subject's muscle activity are used in the analysis.

This chapter is organised as follows. Section 5.1 details the robotic exoskeleton platform which was specially developed to evaluate the model-based AAN paradigm. This includes details regarding the hardware, its physical interaction with the subject, and how it is operated to provide the subject with a controllable level of assistance. Section 5.2 introduces the experimental method, including the tasks which the subject performs, and the muscular impairment profiles that are applied. Also detailed is the method by which the AAN paradigm calculates the assistance to provide the subject in each of the tasks, and how their muscle activity is measured and processed. Section 5.3 presents the experimental results which are used for analysing the efficacy of the AAN paradigm. Section 5.4 summarises the experimental results and the evaluation of the model-based AAN paradigm.

5.1 Exoskeleton Platform

5.1.1 Physical interaction with the operator

The assistive robot used for experimentation is the exoskeleton shown in Figure 5.1. It is a specially developed robotic exoskeleton with three degrees of freedom (two at the shoulder, one at the elbow) mounted on a grounded platform. The exoskeleton acts as a mechanical interface between the operator and the task being performed, similar to the concept of a human extender [Kazerooni, 1990]. The robot interacts with the environment to provide the forces required to perform desired tasks. An admittance control scheme operates the robot such that a scaled down version of the force required to perform the task is felt by the operator. The amount of assistance to be provided to

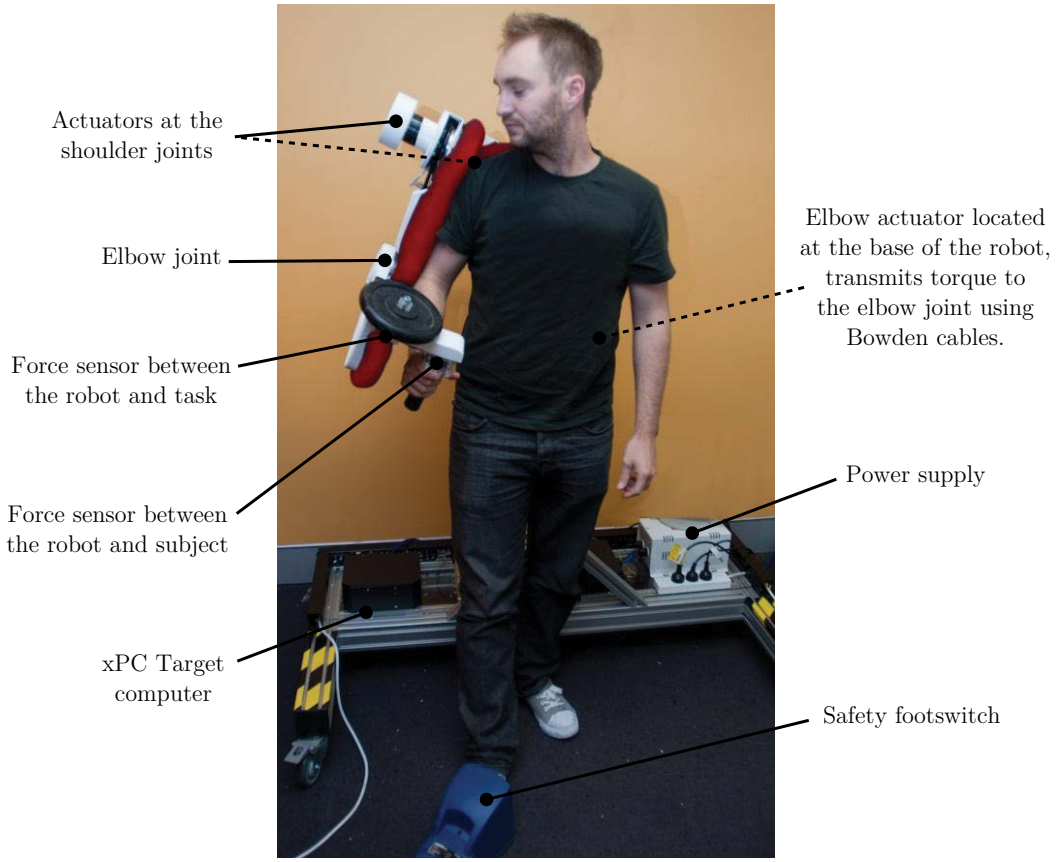

Figure 5.1: The exoskeleton platform developed to evaluate the model-based AAN paradigm. Dotted labels indicate components obscured by the robot or the subject.

the operator is set by how much this force is scaled down.

This exoskeleton platform is classified as an *external-force* system [Pons, 2008]. It couples with the operator's hand to transfer a portion of the task load externally to the ground. There is no other physical interaction between the operator and the robot apart from at the hand. This is in contrast to an *internal-force* exoskeleton which attaches to the limb of the operator at multiple locations and provides assistive forces between the body segments where it attaches. Both types are illustrated in Figure 5.2. An external-force exoskeleton was developed as it is well suited for the model-based AAN framework. The framework determines the operator's assistance requirements based on their strength at the hand, and it is at their hand that the exoskeleton provides assis-

tance. Additionally, coupling with the operator at the hand requires a less demanding kinematic design, and it reduces the risk of potentially unsafe interaction forces between the robot and the operator in comparison to internal-force exoskeletons [Pons, 2008].

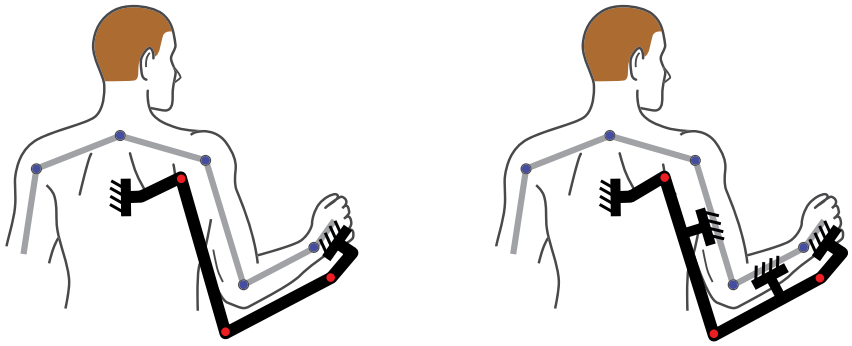

External-force exoskeleton Internal-force exoskeleton

Figure 5.2: Difference between external-force and internal-force exoskeleton systems. External-force exoskeletons, like the platform specially developed to analyse the model-based AAN paradigm, couple with the operator only at their hand. Assistance is provided by transferring a portion of the task's load to the ground. Internal-force exoskeletons attach to the operator at multiple locations on their body.

5.1.2 Exoskeleton hardware

Each joint is actuated using high torque brushless DC motors and a planetary gear reduction with ratio 91:1. This combination of a high torque motor with a low reduction gearbox was chosen to reduce the inertia reflected at the joints and increase its back-driveability. This increases the intrinsic safety of the robot with regard to physical human-robot interaction. Safety is also considered in the link design by using large, hollow, thin-walled members to produce rigid yet lightweight links. The shoulder actuators are located on the links, and couple to each of the joints directly via their gearbox. The elbow actuator and its gearbox are located at the base of the robot, with a Bowden cable transmission used for remote actuation. This removes the mass of the elbow actuator and gearbox from the links of the exoskeleton, which increases operator safety.

The operator controls the exoskeleton directly through physical interaction with the robot via a handle. A 6-axis load cell at the base of the handle measures interaction

forces between the robot and the hand of the operator. A second 6-axis load cell at the end-effector measures the interaction between the robot and the task being performed, for example the reaction forces when lifting a mass. The exoskeleton control scheme is executed in MATLAB's xPC Target environment. The xPC Target computer is a Diamond Systems *Poseidon* single board computer with integrated data acquisition capabilities. Additional details regarding the hardware of the exoskeleton are provided in Appendix E.

5.1.3 Control scheme

The exoskeleton is operated using an admittance control scheme (see Section 2.2.1). Measured forces applied to the robot at the end-effector are used to control the end-effector motion in cartesian space. The system behaves as an admittance by using the measured forces to produce a velocity response. Force interaction between the robot and operator (represented as $\mathbf{F}_H$) and the external task force (represented as $\mathbf{F}_E$) are combined into a single net force at the end-effector, represented by vector $\mathbf{F}_{EE}$. This is multiplied by an admittance gain (b) to produce a reference velocity ($\dot{\mathbf{x}}$), where vector $\mathbf{x}$ is the position of the robot's end-effector in cartesian space. Reference joint velocities are calculated using Equation (5.1) where $\mathbf{J}$ is the kinematic Jacobian of the robot. Reference joint velocity $\dot{\boldsymbol{\theta}}_r$ is integrated over time to produce a reference position trajectory $\boldsymbol{\theta}_r$, then both are fed to the robot's motion control scheme.

$$\dot{\boldsymbol{\theta}}_r = \left[\mathbf{J}^{-1}\right] \dot{\mathbf{x}} \tag{5.1}$$

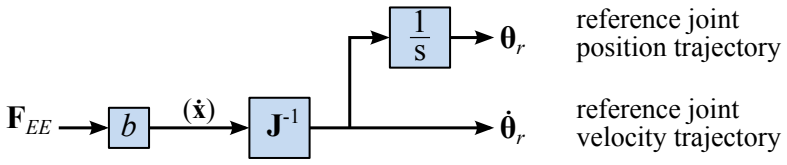

Figure 5.3: Robot motion trajectory created using an admittance control scheme.

The motion is controlled using a simple form of computed-torque control [Chung *et al.*,

2008] shown in Figure 5.4. To track the reference position and velocity trajectories in joint space a PD controller was used as a more sophisticated controller was not required. The errors between the measured joint position and velocity ($\boldsymbol{\theta}$ and $\dot{\boldsymbol{\theta}}$) and their reference trajectories ($\boldsymbol{\theta}_r$ and $\dot{\boldsymbol{\theta}}_r$) are multiplied by gains K_P and K_D respectively, and combined to form the PD controller's output. The output is multiplied by mass matrix $\mathbf{M}$ of the robot dynamic system to compute the desired torque to be actuated at the joints. The robot's gravity load is compensated, fed forward from a model of the system. It is common to compensate for Coriolis and centrifugal non-linearities, however this is not included as operation of the exoskeleton is relatively slow speed and these effects are assumed to be negligible. The desired joint torque is actuated using motor controllers operating in current control mode to produce the motor current corresponding to the desired torque.

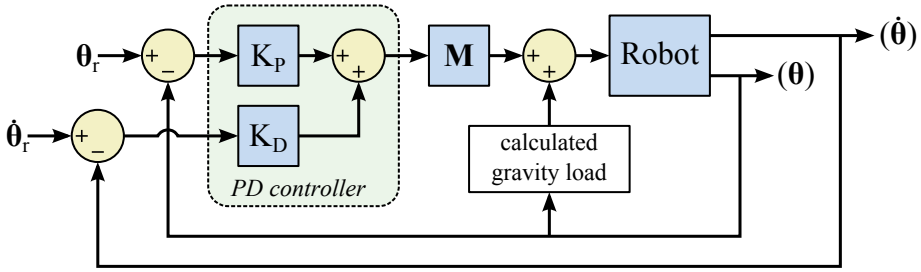

Figure 5.4: PD controller used to track the motion trajectory created from the admittance control scheme.

The robot's end-effector (and consequently the operator's hand) moves in response to both the operator force $\mathbf{F}_H$ and the external task force $\mathbf{F}_E$ via the admittance control scheme. For the operator to statically oppose the external force they are required to exert an equal and opposite force such that the net force is zero ($\mathbf{F}_{EE} = 0$) and subsequently no end-effector motion occurs. Assistance is provided by scaling down the external force before it is fed into the admittance control as shown in Figure 5.5. Parameter A, ranging between $0 \leq A \leq 1$, represents the amount of assistance to be provided to the operator. $A = 0$ means zero assistance is provided, and $A = 1$ means that the robot is providing all of the force required to perform the task. The external force is scaled down by the gain $1 - A$ such that when $A = 0$ a gain of 1 is applied

to $\mathbf{F}_E$. In this case, to statically oppose the external force the operator is required to exert an opposing force of equal magnitude. As parameter A is increased the external force is scaled down linearly, until $A = 1$ at which point it is scaled down equivalent to $\mathbf{F}_E = 0$. By scaling down the measured external load force before it is fed into the admittance controller, less force is required from the operator to oppose its effects on the resulting robot motion. The assistance level ($0 \leq A \leq 1$) is calculated and set by the model-based AAN paradigm operating above the admittance control scheme. The calculation of A is detailed in Section 5.2.3.

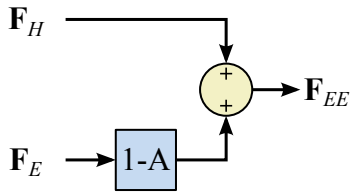

Figure 5.5: The combination of force measurements before they are fed to the admittance control scheme. The measured forces between the robot and the operator ($\mathbf{F}_H$), and the robot and the task being performed ($\mathbf{F}_E$), are combined before being fed into the admittance control scheme to control the robot. Assistance is provided to the operator by scaling down the external task force by a gain of $1 - A$ before it is fed into the admittance control scheme. The parameter A, in the range of $0 \leq A \leq 1$, is used to set the level of assistance.

In the experiment detailed next, instead of feeding the measured force between the robot and task into the admittance control, a simulated force created in software will be used to create a virtual load. This is explained in Section 5.2.6.

5.2 Experiment

For ethical and practical reasons the experiment was performed with a healthy, unimpaired subject. This places limitations on the experimental approaches which can be taken. The subject has greater strength compared with a physically impaired person whom would be a typical recipient of robotic AAN in applications such as rehabilitation. This means that to physically challenge the subject requires tasks involving larger forces. Such large forces have the risk of causing physical injury, particularly with prolonged or repeated exposure. Also, since the strength of the subject is greater than the robotic

exoskeleton itself, experiments involving such large loads have a risk of damaging the robot. Furthermore, in Chapter 4 the model-based framework was already evaluated by comparing the calculated strength of the operator against empirical upper limb strength measurements of healthy subjects from the literature. Repeating a similar analysis does not provide much additional insight into the model-based paradigm. For these reasons the experimental evaluation does not involve tasks which require the subject to operate at and beyond their physical strength capability.

Experimental evaluation is performed by analysing the paradigm's ability to provide robotic assistance targeted towards the requirements of the subject based on different muscular impairments. Different tasks require the use of different muscles, hence a subject inflicted with a muscular impairment requires assistance based not only on the severity of the impairment, but also on which muscles are impaired and if these muscles are required for the task being performed. A robot providing AAN to compensate for an impairment localised to specific muscle groups should ideally provide assistance only in tasks which the impaired muscles limit the subject from performing. Alternatively, for tasks not utilising the impaired muscles, the assistance should be minimal since the remaining non-impaired muscles would be capable of performing it. It is on this basis that the ability of the model-based AAN paradigm to provide assistance specific to the requirements of the subject is evaluated.

The experiment involves a healthy subject performing a series of physical tasks utilising their upper limb. Although the subject is not physically impaired, they are assigned profiles which define impairments localised to specific muscle groups in the upper limb. These impairment profiles give the subject a *virtual* assistance requirement. Tasks are then performed with the robot providing assistance governed by the AAN paradigm. The performance of the paradigm to govern the assistance such that it is targeted towards the *impaired* muscles, but only when they are required by the task being performed, is evaluated by measuring the subject's muscle activity using electromyography (EMG).

5.2.1 Tasks

The tasks require the subject to hold their upper limb in the position shown in Figure 5.6. While in this position, an external force equivalent to 5kg ($49N$) is applied to the hand. This magnitude of force was chosen as it was found to produce a noticeable change in the measured EMG whilst not being so large that the subject was physically strained. The 5kg load is applied to the hand in six different orthogonal directions, with each direction constituting a unique task. As a result, each task requires the use of different muscles in the limb to oppose this force depending on its direction. These six tasks are labelled T_1 to T_6 and are shown in Figure 5.7. Moment loads at the subject's hand are minimal since the torque measured at the handle would cause the robot to move, and a requirement of the task is that the subject hold their arm in a static position.

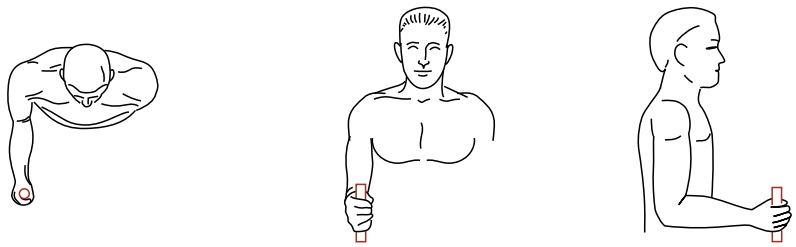

Figure 5.6: The subject's upper limb position during the experiment.

To orchestrate these tasks requires a 5kg load to be applied to the end-effector of the robot in the appropriate direction. When the load is in the direction of gravity (as is task T_3 shown in Figure 5.7) this could be achieved by attaching a 5kg mass to the robot. The other five directions however require the use of some apparatus to direct the external force in the direction required. A solution is to use a virtual force defined in software with the magnitude and direction that is required. This force is fed into the admittance control scheme of the robot as if it were an external force measured by the robot's sensors. The robot behaves as if an external load was applied, requiring the subject to provide an opposing force at their hand in order to hold their arm in a static position. This allows tasks with external forces in any direction and with any magnitude to be experimentally analysed without the need for complex apparatus. The use of virtual loads was validated in a separate experiment detailed in Section 5.2.6.

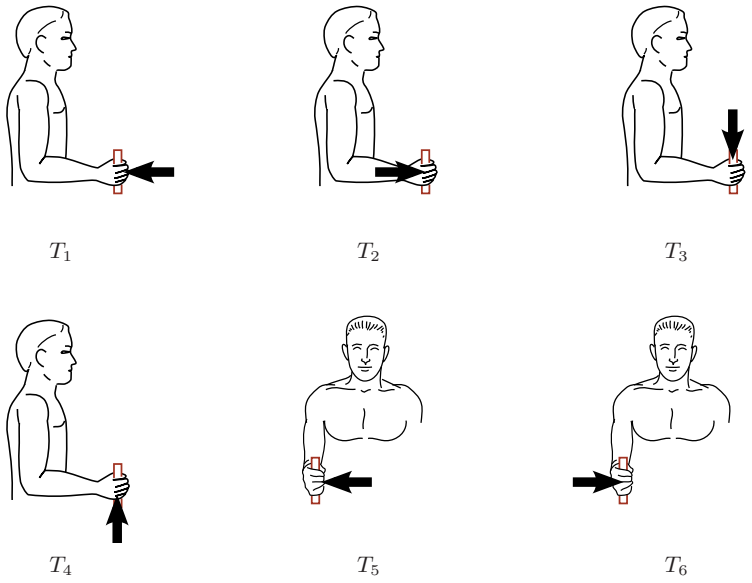

Figure 5.7: The six tasks (T_1, T_2, T_3, T_4, T_5, and T_6) performed by the subject in the experiment. All tasks have the upper limb in the position shown in Figure 5.6. Black arrows indicate the direction of the 5kg external force applied to the subject's hand, corresponding to unit vector **u** used in the process of calculating the operator's strength capability.

5.2.2 Impairment profiles

Various impairment profiles are defined with impairment localised to the following upper limb muscle groups; biceps, triceps, anterior deltoid, lateral deltoid, posterior deltoid, pectoralis major, infraspinatus, and latissimus dorsi. These muscle groups are shown in Figure 5.8. Impairments are implemented using the **s** vector to limit muscle activation during the strength capability optimisation (see Section 4.1). For each of the eight muscle groups a unique impairment profile ($\mathbf{s}_1$, $\mathbf{s}_2$, $\mathbf{s}_3$, $\mathbf{s}_4$, $\mathbf{s}_5$, $\mathbf{s}_6$, $\mathbf{s}_7$, $\mathbf{s}_8$) is defined by setting the vector elements corresponding to the impaired muscles to the arbitrary value of $s = 0.01$. The names of the impaired MTU models in the upper limb MM [Holzbaur *et al.*, 2005] for each impairment profile are listed in Table 5.1. Profile $\mathbf{s}_0$ has no muscles impaired ($\mathbf{s}_0 = 1$) and is used to obtain a benchmark strength estimate of the subject without any impairment.

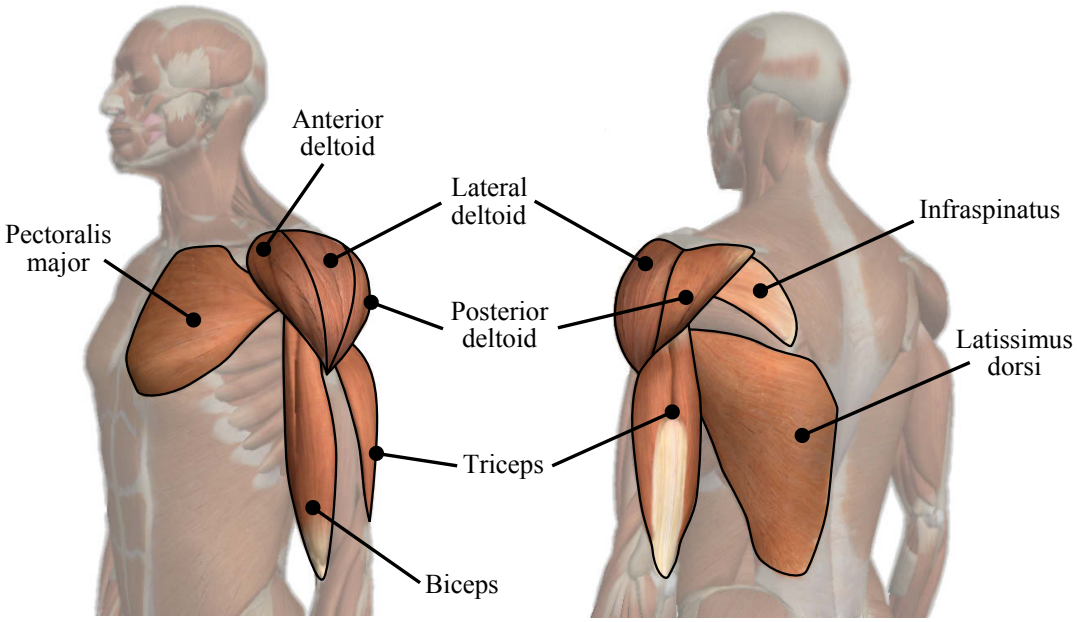

Figure 5.8: Muscles of interest during the experiment.

Impairment profile	Muscle group	Corresponding MTU names in the upper limb model
$\mathbf{s}_0$	None	—
$\mathbf{s}_1$	Biceps	BIClong, BICshort
$\mathbf{s}_2$	Triceps	TRIlong, TRIlat, TRImed
$\mathbf{s}_3$	Anterior deltoid	DELT1
$\mathbf{s}_4$	Lateral deltoid	DELT2
$\mathbf{s}_5$	Posterior deltoid	DELT3
$\mathbf{s}_6$	Pectoralis major	PECM1, PECM2, PECM3
$\mathbf{s}_7$	Infraspinatus	INFSP
$\mathbf{s}_8$	Latissimus dorsi	LAT1, LAT2 ,LAT3

Table 5.1: MTU impairment profiles used during the experiment. Eight profiles are defined with impairment localised to specific muscle groups by setting the corresponding elements in the vector $\mathbf{s}$ to $s = 0.01$. This replicates impairment by limiting muscle activation. The MTU names in the upper limb MM [Holzbaur *et al.*, 2005] corresponding to the impaired muscle are listed for each impairment. Remaining non-impaired muscles are set $s = 1$. Profile $\mathbf{s_0}$ represents the subject without any impairment.

5.2.3 Assistance calculation

The model-based AAN paradigm calculates the assistance requirements of the subject and subsequently controls the level of assistance the exoskeleton provides. Firstly, the subject's strength capability S_P for each task (T_1 to T_6) is calculated with each impairment profile ($\mathbf{s}_0$ to $\mathbf{s}_8$) applied. This is calculated by the Strength Model (SM) (see Section 3.4) utilising the optimisation model developed in Section 4.1. The upper limb MM [Holzbaur *et al.*, 2005] (detailed in Section 3.4.1) is used to represent the subject. The generalised coordinates of the model ($\mathbf{q}$) are defined such that its position matches that of the subject performing the tasks (shown in Figure 5.6). The direction of the external force at the subject's hand ($\mathbf{u}$) is defined corresponding to the task the subject is performing (shown in Figure 5.7). Quasi-static conditions are assumed in each task ($\dot{\mathbf{q}} = \ddot{\mathbf{q}} = 0$) and only the one upper limb position is considered.

From the strength capability S_P calculated for each task and with each impairment profile applied, the assistance parameter A is derived with the aim of providing robotic assistance suited to the requirements of the subject. Notation for S_P and A, calculated with respect to task T_i and impairment $\mathbf{s}_j$, is as follows:

$$S_P^{[i,j]} = \begin{array}{l}\text{Subject strength capability } S_P \\ \text{calculated for task } T_i \text{ and impairment } \mathbf{s}_j\end{array}$$

$$A^{[i,j]} = \begin{array}{l}\text{Assistance parameter } A \\ \text{calculated for task } T_i \text{ and impairment } \mathbf{s}_j\end{array}$$

For example, the subject's strength capability and assistance parameter calculated for task T_5 with impairment profile $\mathbf{s}_3$ applied is represented as $S_P^{[5,3]}$ and $A^{[5,3]}$ respectively. The results of the strength capability S_P calculated for each task and with each impairment profile applied are shown in Table 5.2.

Two different methods for deriving parameter A from the calculated strength capability of the subject have been conceived. They are described as follows.

	Impairment profile								
Task	$\mathbf{s}_0$	$\mathbf{s}_1$	$\mathbf{s}_2$	$\mathbf{s}_3$	$\mathbf{s}_4$	$\mathbf{s}_5$	$\mathbf{s}_6$	$\mathbf{s}_7$	$\mathbf{s}_8$
T_1	355.05	289.66	320.42	178.25	270.15	355.05	235.16	275.23	355.05
T_2	280.05	280.05	214.34	280.05	280.05	238.41	280.05	213.07	208.87
T_3	246.89	134.07	246.89	147.23	209.83	246.89	190.18	200.81	246.89
T_4	98.57	98.57	19.63	98.57	98.57	98.57	98.57	98.57	98.57
T_5	123.58	114.68	117.20	102.64	123.16	123.58	90.48	123.58	101.95
T_6	99.79	99.79	99.00	99.09	87.42	97.34	99.05	25.93	99.79

Table 5.2: The subject's strength capability S_P, calculated for each task, and for each impairment profile. Units are in Newtons.

Assistance calculated from strength gap

This method calculates A directly from the gap between the task's strength requirement and the operator's strength capability. Each task requires the operator to oppose a $49N$ external force at the hand; hence the task strength requirement is $S_T = 49N$. For each task with an impairment profile applied the subject's strength capability S_P is calculated. By comparing S_T and S_P the percentage of the task load which the subject is unable to oppose is estimated, and parameter A is set such that this portion of the load is supported by the robot. If the result is negative (i.e. $S_P > S_T$) then it is set to $A = 0$ since no assistance is required. This calculation is shown in Equation (5.2).

$$A^{[i,j]} = \max \left[\frac{S_T - S_P^{[i,j]}}{S_T} \ , \ 0 \right] \tag{5.2}$$

This method is suited for applications where the strength of the operator is often less than the requirements of the tasks. For example in robotic rehabilitation, a patient due to their injury may be unable to perform the therapy without assistance. In the experiment performed this chapter the subject is not impaired, and hence is capable of performing each task unassisted. There is no gap between S_T and S_P, and for this reason a different method for calculating A is used.

Assistance calculated from strength loss due to impairment

This method derives the assistance parameter A based on the calculated effect each impairment has on the subject's capability to perform each task. The strength at the hand with an impairment profile applied is compared to the strength when no impairment ($\mathbf{s}_0$) is present. The amount of strength lost due to the impairment is normalised by the strength calculated with no impairment, and used to set the percentage of the external task load the robot supports. This method is used to calculate A for each task and with each impairment profile applied using Equation (5.3). The results are shown in Table 5.3.

$$A^{[i,j]} = \frac{S_P^{[i,0]} - S_P^{[i,j]}}{S_P^{[i,0]}} \tag{5.3}$$

It is hypothesised that this method for calculating the assistance required due to muscular impairment will be less sensitive to errors in strength estimation, compared to the first method of directly using the gap between S_T and S_P. If the MM is not an accurate representation of the subject's physical capabilities, then error in the strength estimation will skew the calculated assistance requirements of the subject. However it is plausible that even if the MM is poor at representing the magnitude of the subject's physical strength, the relative strength loss at the hand due to a relative strength loss in a muscle group may still be similar in both the MM and the subject. This hypothesis

	Impairment profile								
Task	$\mathbf{s}_0$	$\mathbf{s}_1$	$\mathbf{s}_2$	$\mathbf{s}_3$	$\mathbf{s}_4$	$\mathbf{s}_5$	$\mathbf{s}_6$	$\mathbf{s}_7$	$\mathbf{s}_8$
T_1	0.00	0.18	0.10	0.50	0.24	0.00	0.34	0.22	0.00
T_2	0.00	0.00	0.23	0.00	0.00	0.15	0.00	0.24	0.25
T_3	0.00	0.46	0.00	0.40	0.15	0.00	0.23	0.19	0.00
T_4	0.00	0.00	0.80	0.00	0.00	0.00	0.00	0.00	0.00
T_5	0.00	0.07	0.05	0.17	0.00	0.00	0.27	0.00	0.18
T_6	0.00	0.00	0.01	0.01	0.12	0.02	0.01	0.74	0.00

Table 5.3: Results for the assistance parameter A that is calculated for each task, and for each impairment profile. Results are calculated using Equation (5.3). Assistance is in the range $0 \leq A \leq 1$, where $A = 0$ is the robot providing zero assistance, and $A = 1$ is the robot providing 100% assistance by fully supporting the external task load.

is based on the previous analyses in Chapter 4 showing that the MM was capable of calculating the qualitative behaviour between strength and factors such as limb position and force direction, even through no effort was made to adjust the MM to better fit the data. For these reasons this approach is expected to be more robust in the presence of strength estimation errors.

5.2.4 Experimental procedure

Before each experiment the robot's assistance level is set using parameter A depending on the task being performed and the impairment profile applied. The values for A were precalculated using the method described, and are shown in Table 5.3.

Next the subject grips the exoskeleton handle and initiates the task by holding a trigger. Once their upper limb is moved into the desired position, a virtual force representing the external task force of $S_T = 49N$ is applied to their hand. After this force has been statically opposed with their upper limb kept stationary for more than 2 seconds, the subject releases the trigger to end the task. EMG and force measurements made during this time are saved for post analysis. This procedure is repeated for each of the six tasks, and with each of the nine impairment profiles applied.

5.2.5 EMG acquisition

The subject is fitted with surface EMG electrodes measuring the muscle activity of the eight upper limb muscle groups listed in Table 5.4. Each measured muscle corresponds to one of the muscle groups impaired in impairment profiles $\mathbf{s}_1$ to $\mathbf{s}_8$. Measurements are made using the Bagnoli surface-EMG system from Delsys sampled at 10kHz. Additional technical details regarding EMG acquisition are provided in Appendix F. Electrode placement is shown in Figure 5.9 and is based on the literature [Konrad, 2005].

During the experiments the raw EMG signals are acquired. These signals undergo a series of post-processing steps before a measurement indicative of the muscle's activation is obtained. Notch filtering is applied to eliminate any noise resulting from the mains

Muscle number (m)	**Muscle group name**
1	Biceps
2	Triceps
3	Anterior deltoid
4	Lateral deltoid
5	Posterior deltoid
6	Pectoralis major
7	Infraspinatus
8	Latissimus dorsi

Table 5.4: Muscle groups measured using EMG and their associated numbering

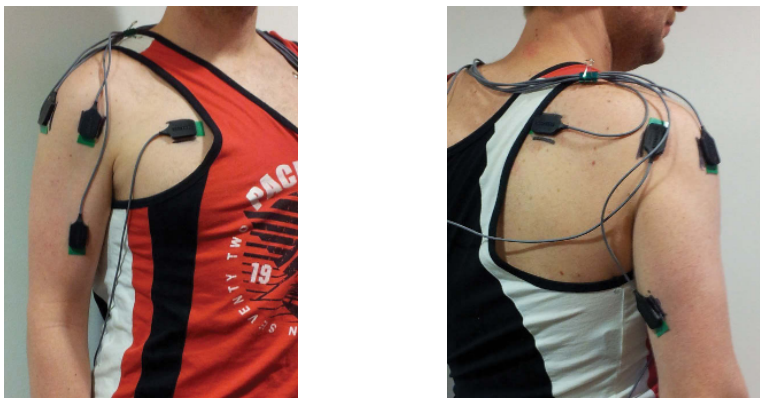

Figure 5.9: Example of surface EMG electrode placement.

power supply. Next a high-pass filter is used to remove DC bias and any low-frequency artifacts that might be present. The signal is then rectified such that all of its values are positive. Lastly, the signal is passed through a low-pass filter to smooth the signal and produce a linear envelope. Zero-phase low-pass filtering is performed by processing the signal in both forward and reverse directions to achieve zero phase distortion. This creates additional attenuation of the signal which is counteracted by doubling the signal before low-pass filtering is applied. These processing steps are illustrated in Figure 5.10, and an example EMG signal at each stage of processing is shown in Figure 5.11. The noticeable low-frequency artifact seen in Figures 5.11a and 5.11b is added deliberately to highlight the effect of the high-pass filter. During the experiments low-frequency artifacts like this were not observed.

The measured EMG signals are voltages resulting from the muscles being neurologically activated, however these signals by themselves do not provide a quantitative

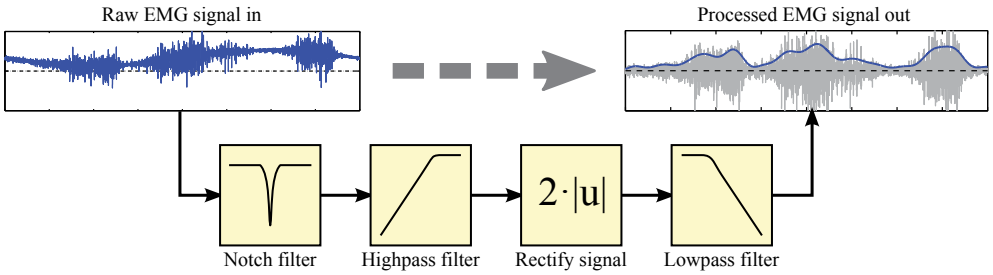

Figure 5.10: EMG signal processing sequence.

measure of the muscle's activation or the force the muscle is producing. Furthermore, signals are affected by factors such as skin impedance and electrode placement relative to the muscle. To obtain a measurement which has some relevance in terms of how much each muscle is being used requires the signals to be normalised. Once the electrodes have been attached and before the tasks are performed, the subject performs a series of Maximum Voluntary Contractions (MVC). This involves the subject performing static exercises which maximise the activation of their upper limb muscles. Different exercises are performed specific to each muscle group to achieve maximum excitation. EMG measurements made during the MVCs undergo the same processing previously detailed to produce a linear envelope. The largest MVC measurement for each muscle is used to normalise subsequent EMG measurements made during experimental tasks. Once normalised, the EMG then represents the amount the muscle is utilised in the task, with a value of 0 representing totally unused, and 1 representing the muscle being used at full capacity (e.g. during MVC). The presence of crosstalk, which is the unwanted measurement of neighbouring muscles, was also analysed prior to the experiments. This was done using the *muscle function testing* method [De Luca, 1997] and was determined to not be significant in the EMG measurements.

For each experimental task performed the EMG for the eight muscles measured are acquired, filtered, and normalised. Each signal is then averaged during the time the subject was statically performing the task to produce a single value representing the mean muscle usage. EMG results are represented as $E_m^{[i,j]}$ where m is the muscle for which the EMG is measured (see Table 5.4), i is the task being performed, and j is the impairment profile applied to the subject during the task.

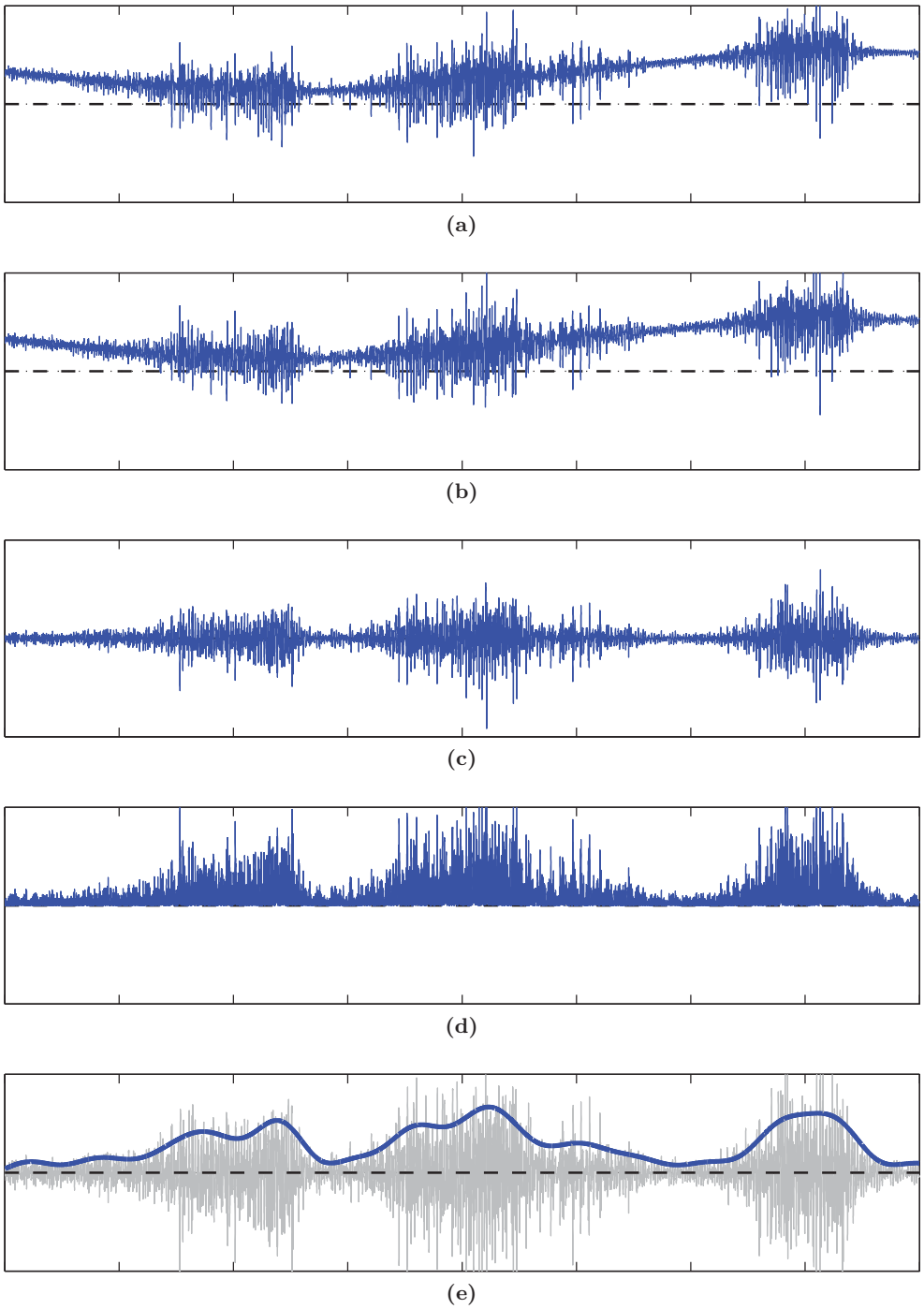

Figure 5.11: An example EMG signal at each stage of the filtering process. Shown is an eight second measurement sampled at 10kHz. Filtering process is as follows: (a) Unfiltered EMG signal. (b) Signal after notch filtering. (c) Signal after high-pass filter. (d) Signal after being doubled and rectified. (e) Signal after zero-phase low-pass filter (overlaid with previous EMG signal in grey).

5.2.6 Virtual load forces

The tasks require an external force applied to the robot's end-effector which the subject (assisted by the robot) is required to oppose. Rather than applying a physical external force onto the robot using some mechanical apparatus, a convenient alternative is to use a virtual external force defined in software. This virtual force can mimic the external force $\mathbf{F}_E$ that would be measured by the force sensor. The admittance controller uses this force, just like it would with a real measured external force, to produce a resulting robot motion. This greatly simplifies the process of experimentally performing tasks which cannot be performed by simply attaching a mass to the robot's end-effector. For example tasks with horizontal forces would require an apparatus to produce forces in the desired directions.

To validate the use of virtual loads implemented in software, an analysis is performed to test if outcomes using virtual loads are consistent with those if a genuine external load is used. The subject carries an object at shoulder height at a number of distances in front of their chest, as shown in Figure 5.12. As the hand is extended away from the chest it becomes more difficult to hold against gravity. The effort required by the subject is measured by the EMG activity of the biceps, triceps, anterior deltoid, lateral deltoid, and posterior deltoid muscles.

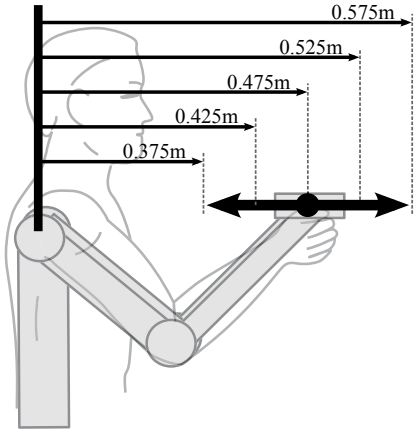

Figure 5.12: Hand positions during the experiment to analyse the suitability of using virtual forces to mimic physical loads.

This experiment is performed with the three variations shown in Figure 5.13, and are described as follows:

1. The mass is held entirely by the subject in free space. The robot is not used at all, apart from being positioned such that its end-effector provides a visual guide for the subject to position their hand.

2. The mass is attached to the robot's end-effector and held in position by the subject. Assistance is set to $A = 0$ such that the operator is required to fully support the object against gravity via the robot's admittance control. A display showing the actual and desired end-effector positions was used to guide the subject.

3. No mass is attached to the robot, instead a virtual force defined in software mimicking the weight force of the mass is fed into the admittance control. Assistance was set to $A = 0$ and a display showing end-effector position guided the subject.

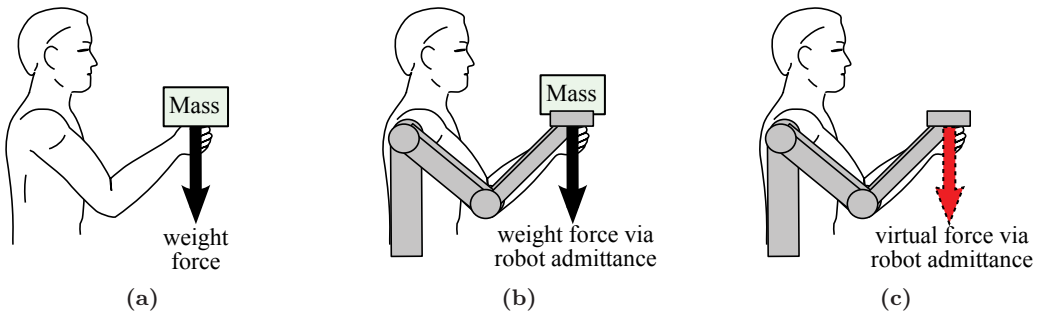

Figure 5.13: The three experiment variations implemented during the experiment to analyse the suitability of using virtual forces to mimic physical loads. (a) A real load is held, and supported against gravity by the subject without the robot utilised at all. (b) A real load is attached to the robot, and supported against gravity by the subject through the robot's admittance control. (c) A virtual load is applied to the robot, and supported by the subject through the robot's admittance control.

These three experiment variations were repeated with external loads (either mass or an equivalent virtual force) of 0kg, 2.5kg and 5kg. Each combination of load variation and load magnitude was repeated three times with the EMG results in all three averaged together. This was performed in an alternating fashion so as to mitigate artifacts in the EMG measurement which may develop over time. Figure 5.14 summarises the results with each subplot corresponding to a single muscle with one of the load magnitudes applied. In each plot, measured EMG versus the hand position for each of the three experiment variations is shown. The triceps, lateral deltoid and posterior deltoid muscles all show little change in activity during the task. The biceps and anterior deltoid muscles show noticeable change in activity, hence the analysis will focus on these two muscles with their measured EMG shown in detail in Figure 5.15.

For the biceps (Figure 5.15a) and the anterior deltoid (Figure 5.15b) their measured EMG activity increases as the magnitude of the external load is increased. As expected, it also increases as the hand is extended outwards away from the subject's chest. The results show that the curves for each of the three variations are relatively consistent. Differences between the curves can be partly attributed towards the fact that the robot is not completely back-drivable, with its friction assisting the subject in holding the load against gravity. Comparing the EMG at different load magnitudes the results show similar muscle utilisation for the three task variations. This indicates that the subject performing this task is required to exert similar amounts of muscle effort to perform it, irrespective of whether the load is real or the result of a virtual force defined in software. From this it is assumed to be appropriate to use a virtual external force to evaluate the model-based AAN paradigm.

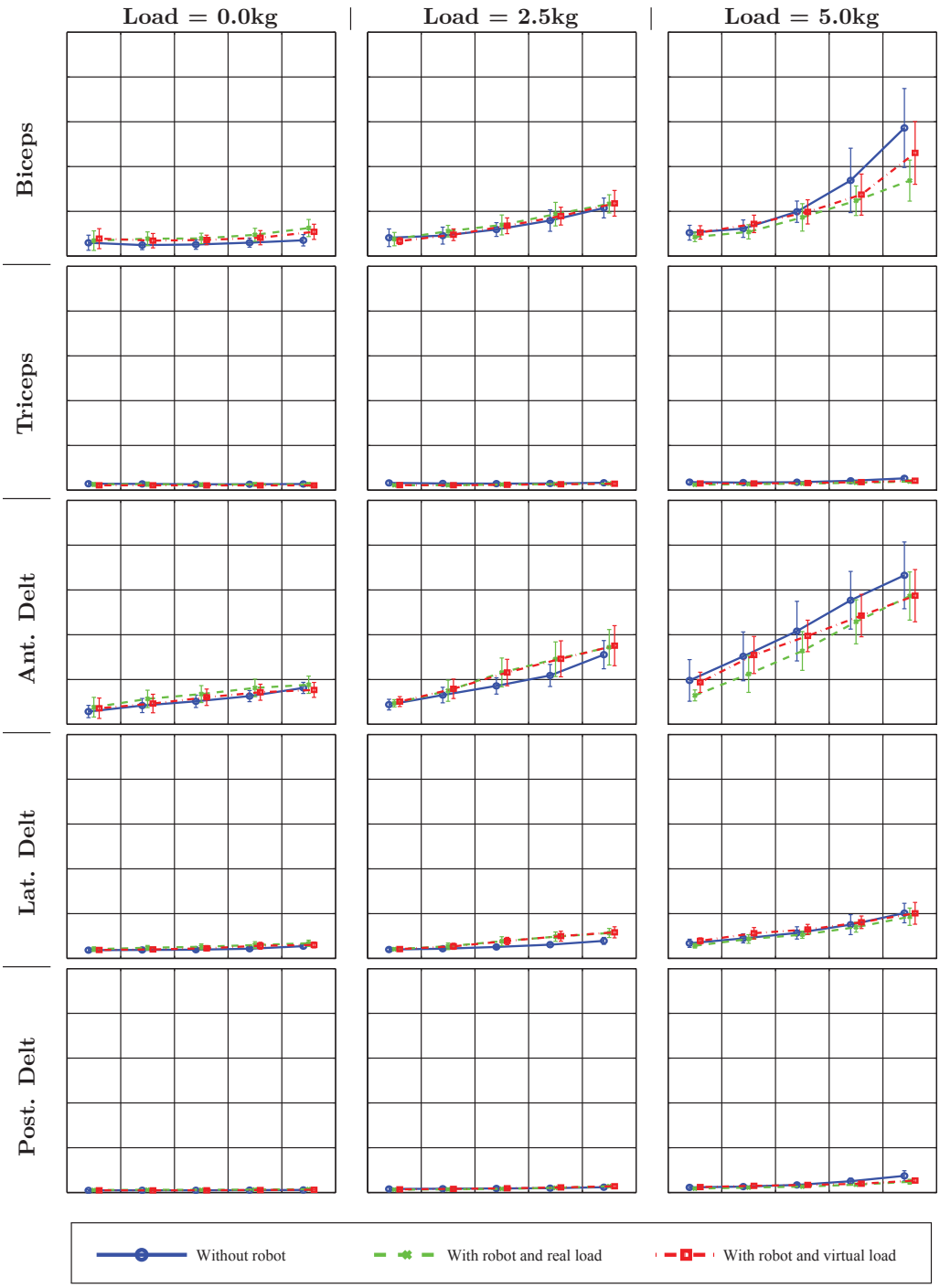

Figure 5.14: The experiment validating the use of virtual external loads; results for all muscles. Each subplot shows the measure EMG for a single muscle (biceps, triceps, anterior deltoid, lateral deltoid, or posterior deltoid) and for a magnitude of external load (0kg, 2.5kg, or 5.0kg). The horizontal axes in each plot corresponds to the position that the hand is in during measurement. The vertical axes are the measured normalised EMG ranging from 0 to 1.

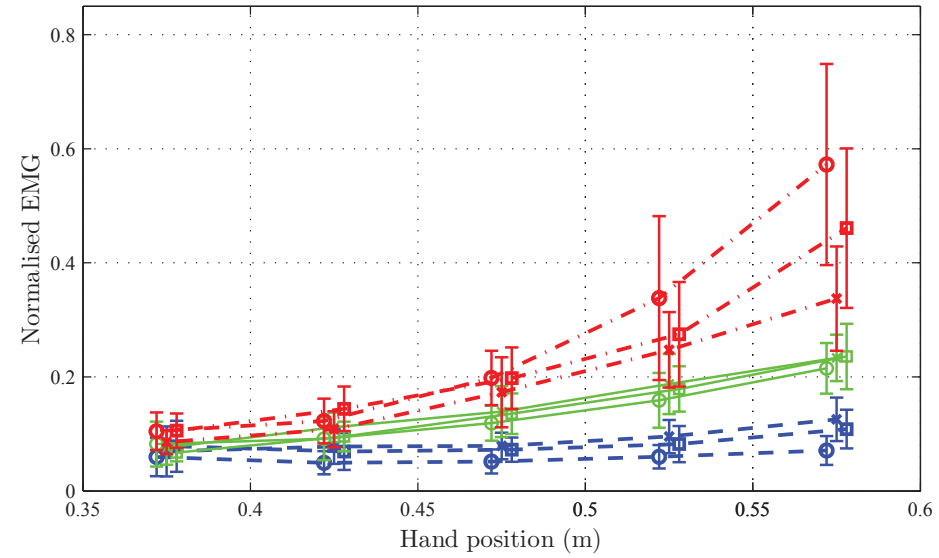

(a) Biceps

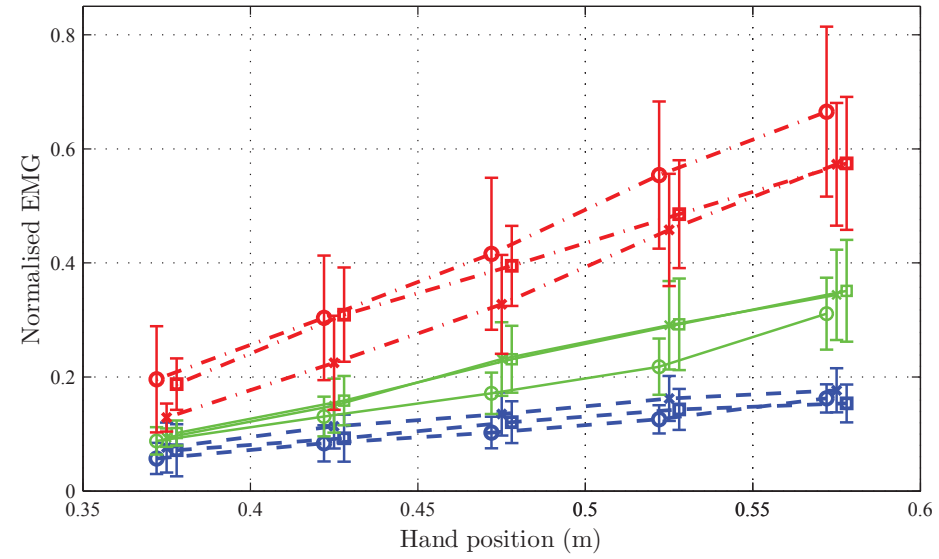

(b) Anterior Deltoid

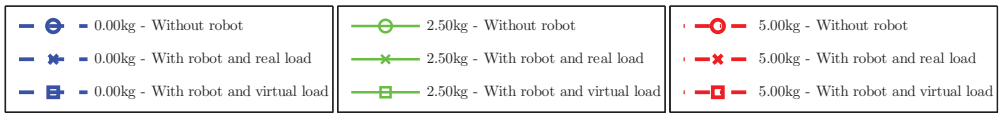

Figure 5.15: The experiment validating the use of virtual external loads; results for biceps and anterior deltoid muscles. The plots show the measured EMG of a single muscle versus the hand position of the subject. Each curve corresponds to a magnitude of the load (0kg, 2.5kg, or 5kg) implemented with one of the variations shown in Figure 5.13. (a) Results for the biceps muscle. (b) Results for the anterior deltoid muscle.

5.3 Experimental Results

5.3.1 Muscle activity for different tasks

Before evaluating the AAN paradigm it is worthwhile to visually observe the EMG results obtained for the different tasks and at different levels of assistance. This provides insight into the relationship between the tasks performed, the muscle usage in the tasks, and the assistance provided. Tasks performed with no impairment (i.e. $\mathbf{s}_0$) received no assistance ($A = 0$). For comparison tasks were also performed with the assistance explicitly set to $A = 0.5$ and $A = 1$ (rather than determined by the model-based AAN paradigm). The mean EMG measurements for each task at these three set levels of assistance are shown in Figure 5.16.

Because the robot is an external-force exoskeleton providing assistance at the hand it is expected that assistance is received by all muscles in the limb. It is observed that as assistance is increased, the EMG for all muscles decreases. Muscles which had the largest EMG when $A = 0$ showed the largest decrease, however even muscles with comparatively small EMG levels are seen to reduce their measured activity in response to increased assistance. This supports the notion that external-force exoskeletons have inherent limitations in targeting assistance to individual muscle groups.

The EMG measurements made when no assistance is provided ($A = 0$) indicate which muscles are utilised the most for each task. Comparing which muscles produced the largest EMG in each task it is seen that, as expected, different tasks utilise certain muscles more than others. This supports the notion that impairments localised in specific muscle groups are likely to have a greater effect on certain tasks depending if they require the use of the muscles which are impaired. This strengthens the reasoning behind why an AAN paradigm capable of estimating assistance need at the muscular level is beneficial, particulary in applications which assist subjects with physical impairment such as in robotic rehabilitation.

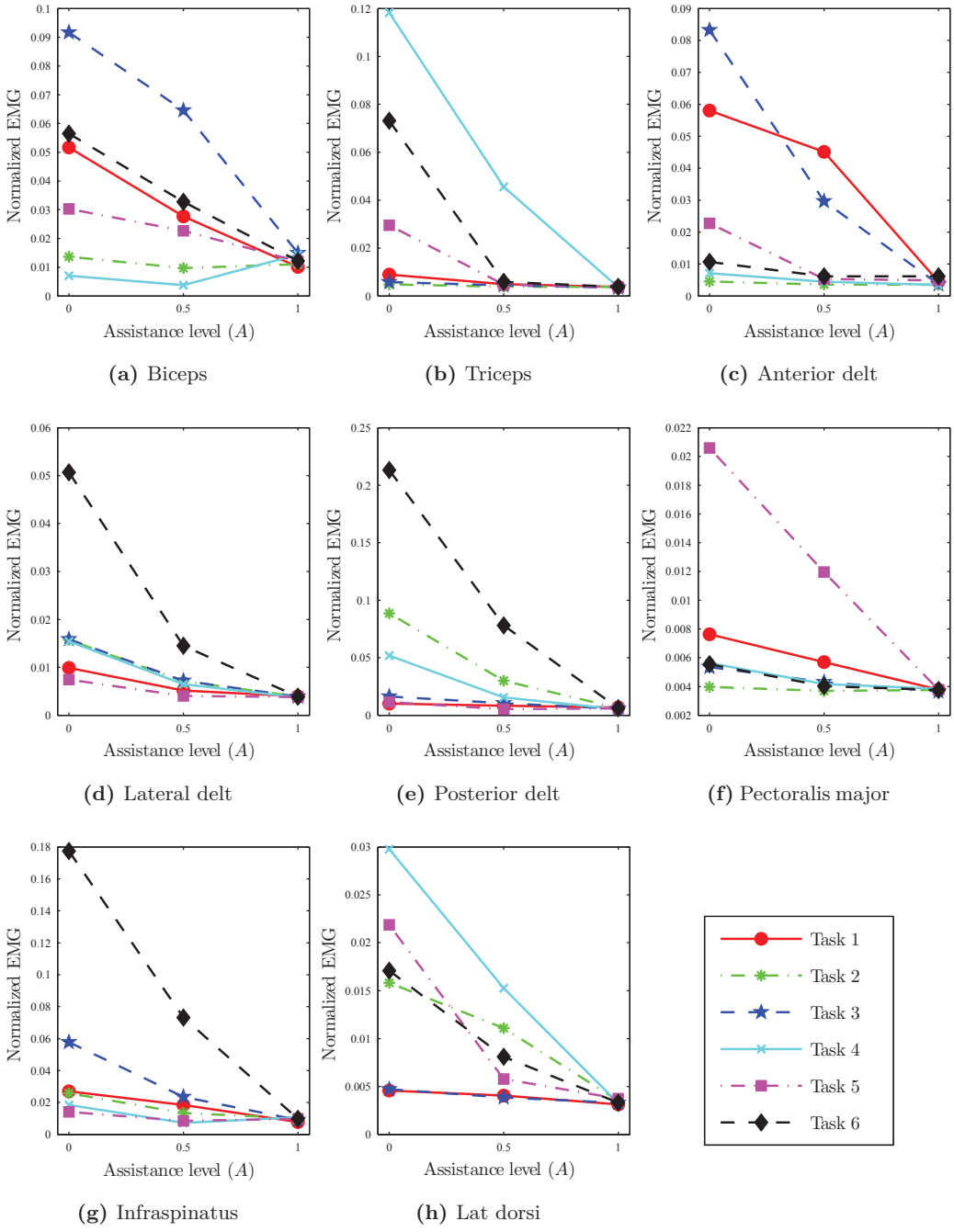

(a) Biceps **(b)** Triceps **(c)** Anterior delt

(d) Lateral delt **(e)** Posterior delt **(f)** Pectoralis major

(g) Infraspinatus **(h)** Lat dorsi

Figure 5.16: Measured EMG for each task at different levels of robotic assistance. The plots show the EMG measured at three different levels of assistance ($A = 0$, $A = 0.5$, $A = 1$) during each of the six tasks (T_1 to T_6) for a single muscle. (a) Biceps. (b) Triceps. (c) Anterior deltoid. (d) Lateral deltoid. (e) Posterior deltoid. (f) Pectoralis major. (g) Infraspinatus. (h) Latissimus dorsi.

5.3.2 Assistance at the hand

For all of the experiments the force measured between the subject's hand and the robot ($\mathbf{F}_H$) was recorded. This measurement represents the amount of force the subject was required to apply at the handle of the exoskeleton to oppose the virtual task load and keep their hand stationary. Comparing the magnitude of this force with the magnitude of the task load S_T gives a measurement of the actual assistance the subject received at their hand. For task T_i with impairment $\mathbf{s}_j$ applied, the mean magnitude of force $\mathbf{F}_H$ measured during the task is represented as $F_H^{[i,j]}$. Assistance at the hand ranging from 0 to 1 is then calculated using Equation (5.4), where $S_T = 49N$.

$$A_H^{[i,j]} = 1 - \left(\frac{F_H^{[i,j]}}{S_T} \right) \tag{5.4}$$

A_H is plotted against the desired level of assistance A in Figure 5.17 for each of the experimental tasks performed. As expected a linear relationship is observed. When zero assistance is desired ($A = 0$) the force at the subject's hand closely matches the magnitude of the virtual task force, meaning almost zero assistance is being provided. As assistance is increased the measured hand force decreases linearly until full assistance

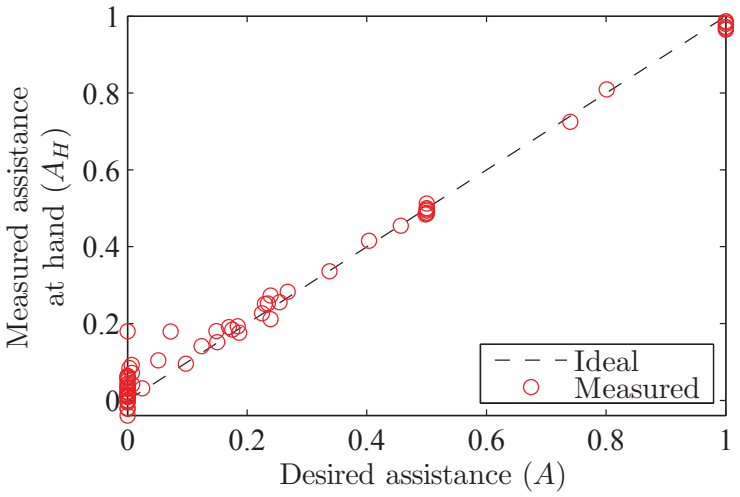

Figure 5.17: The assistance measured at the subject's hand versus the desired assistance to be provided. The correlation coefficient between the measured and desired assistance is $\rho = 0.995$.

is provided ($A = 1$) and negligible hand force is measured. The measured assistance at the hand matches well with the desired assistance with a correlation coefficient of $\rho = 0.995$. This shows that the robot was capable of providing the level of assistance desired.

5.3.3 Assistance at the muscles

Calculating how much EMG measurements decrease as a result of the robot providing assistance, compared to the EMG measured when no assistance was provided allows the assistance received at the muscular level to be quantified. If $\mathbf{E}^{[i,j]} = [E_1^{[i,j]}, E_2^{[i,j]}, \cdots, E_8^{[i,j]}]^T$ is the vector of EMG measurements for task T_i and impairment $\mathbf{s}_j$, the assistance at the muscular level is estimated by the normalised change in the EMG vector. This is calculated using Equation (5.5), where $\|\mathbf{E}^{[i,j]}\|$ is the norm of the vector $\mathbf{E}^{[i,j]}$.

$$A_E^{[i,j]} = \frac{\|\mathbf{E}^{[i,0]}\| - \|\mathbf{E}^{[i,j]}\|}{\|\mathbf{E}^{[i,0]}\|} \tag{5.5}$$

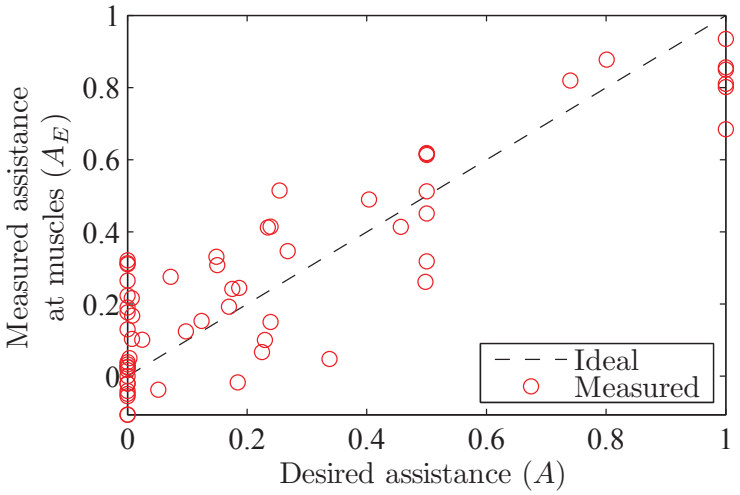

Figure 5.18: The assistance at the subject's muscles calculated by the change in EMG, versus the desired assistance to be provided. The correlation coefficient between measured and desired assistance is $\rho = 0.887$.

The desired assistance A for all the experiments is plotted against the calculated muscular assistance A_E in Figure 5.18. A linear relationship similar to that shown in Figure 5.17 is observed, however there is more variation about the ideal result. This can be attributed to the noise and other measurement artifacts inherent in EMG measurements. Regardless, the desired assistance matches relatively well with the measured assistance based on EMG, with a correlation coefficient of $\rho = 0.887$.

5.3.4 Assistance targeted for impaired muscles

The objective of the AAN paradigm in this experiment was to provide targeted assistance for impaired muscles when the task being performed requires them. It is difficult to quantify exactly how much different tasks rely on the physical capabilities of specific muscles. It is logical that the more a muscle is utilised in a task (compared to other tasks), the more that particular task relies on that muscle. Based on this, the measured EMG is used to infer how much each task relies on each of the muscles. Consider a single muscle m. How much this muscle is required in task T_i is inferred by its EMG measured in the task with no assistance provided (i.e. $E_m^{[i,0]}$). The task with the largest EMG measurement for muscle m is considered to require the most assistance if that same muscle was impaired. Alternatively, the task with the smallest EMG for muscle m is considered to require the least assistance if that muscle was impaired.

The AAN paradigm is evaluated as follows: Firstly an impairment profile ($\mathbf{s}_j$) is selected. Next, one of the muscle groups (m) for which EMG was measured is selected. Then for all tasks (T_i, where $i = \{1, 2, 3, 4, 5, 6\}$) the assistance provided by the AAN paradigm for impairment $\mathbf{s}_j$ ($A^{[i,j]}$) is correlated with the measured EMG of muscle m with no assistance provided ($E_m^{[i,0]}$). The correlation result is represented as $C^{[m,j]}$ and is formalised in Equation (5.6).

This correlation calculation is repeated for all combinations of impairment profile $\mathbf{s}_j$ (excluding $\mathbf{s}_0$) and EMG muscle m. The result forms the 8×8 matrix shown graphically in Figure 5.19. The elements in the diagonal of the matrix $C^{[m,j]}$ are the correlation results when the muscle which is impaired (and hence the assistance should be targeted

towards), and the EMG indicating how much a muscle is required, are for the same muscle (i.e. $m = j$). Because the paradigm should ideally provide greater assistance for tasks in which the impaired muscles produce larger EMG measurements, the diagonal should ideally show strong correlation results.

$$C^{[m,j]} = \text{corr}\left(\begin{bmatrix} E_m^{[1,0]} \\ E_m^{[2,0]} \\ E_m^{[3,0]} \\ E_m^{[4,0]} \\ E_m^{[5,0]} \\ E_m^{[6,0]} \end{bmatrix}, \begin{bmatrix} A^{[1,j]} \\ A^{[2,j]} \\ A^{[3,j]} \\ A^{[4,j]} \\ A^{[5,j]} \\ A^{[6,j]} \end{bmatrix} \right) \tag{5.6}$$

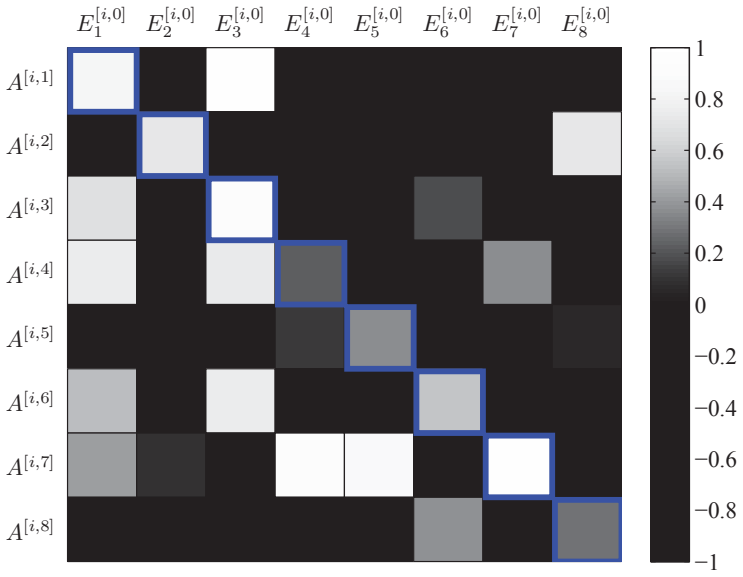

Figure 5.19: Correlation between the assistance provided for a specific impaired muscle ($A^{[i,j]}$), and the EMG measured for each muscle without assistance ($E_m^{[i,0]}$), for each of the experimental tasks performed ($i = \{1, 2, 3, 4, 5, 6\}$). The elements in the diagonal of the matrix correspond to the correlation between the assistance provided for a specific impaired muscle, and the EMG measured without assistance for that same specific muscle (i.e. $m = j$). The results range from -1 to 1. Negative results are black as to make the positive correlation results easier to visualise. The results in the diagonal show reasonably strong correlation results, indicating that assistance was targeted towards the impaired muscles when tasks which required them were performed.

Observing the diagonal in Figure 5.19 (highlighted in blue) shows a reasonably strong correlation. The results for muscles m_1, m_2, m_3, m_6, and m_7 all show correlation greater than 0.5. Muscles m_4, m_5, and m_8 show less correlation, but are still above zero and are noticeably larger than many of the other off-diagonal correlation results. Figure 5.20 shows the EMG measurements and the assistance provided in each task which were correlated to produce these diagonal results. These are plotted side by side for each muscle. Indeed for muscles m_1, m_2, m_3 and m_7 there is noticeable similarity between the measured EMG and the assistance provided. For muscles m_4, m_5, m_6 and m_8 there was less similarity which is reflected by the correlation coefficients calculated.

The off-diagonal results in Figure 5.19 with strong correlation represent cases where the AAN paradigm inadvertently assisted non-impaired muscles when tasks which required them were performed. Some of this may be attributed to the fact that when external-force exoskeletons provide assistance to the hand, all muscles receive assistance and hence some amount of cross-assistance is to be expected. Averaging the 56 off-diagonal correlation results produces a mean correlation of -0.143, while the 8 diagonal correlation results produce a mean of 0.574. These results suggests the model-based AAN paradigm was reasonably successful in providing assistance targeted for when it was needed, based on the impairments assigned in specific muscle groups.

There are several factors anticipated as contributing towards lowering the correlation results that were obtained. One factor is the large redundancy in the musculoskeletal system. Multiple muscles work together when performing tasks, each with different amounts of contribution towards the task. When assistance is provided the relative contributions of the muscles is likely to change, hence when providing assistance targeted towards a specific muscle this may cause the actual assistance it receives to not be as expected. Another factor is the stability of the shoulder. The glenohumeral joint is the most commonly dislocated major joint of the human body, with its stability primarily ensured by proper coordination of muscular forces [Favre *et al.*, 2009]. Several studies have identified muscles including the lateral deltoid, posterior deltoid, pectoralis major and latissimus dorsi as prominently contributing to shoulder stability, or instability [Ackland and Pandy, 2009; Steenbrink *et al.*, 2009; Yanagawa *et al.*, 2003]. These same

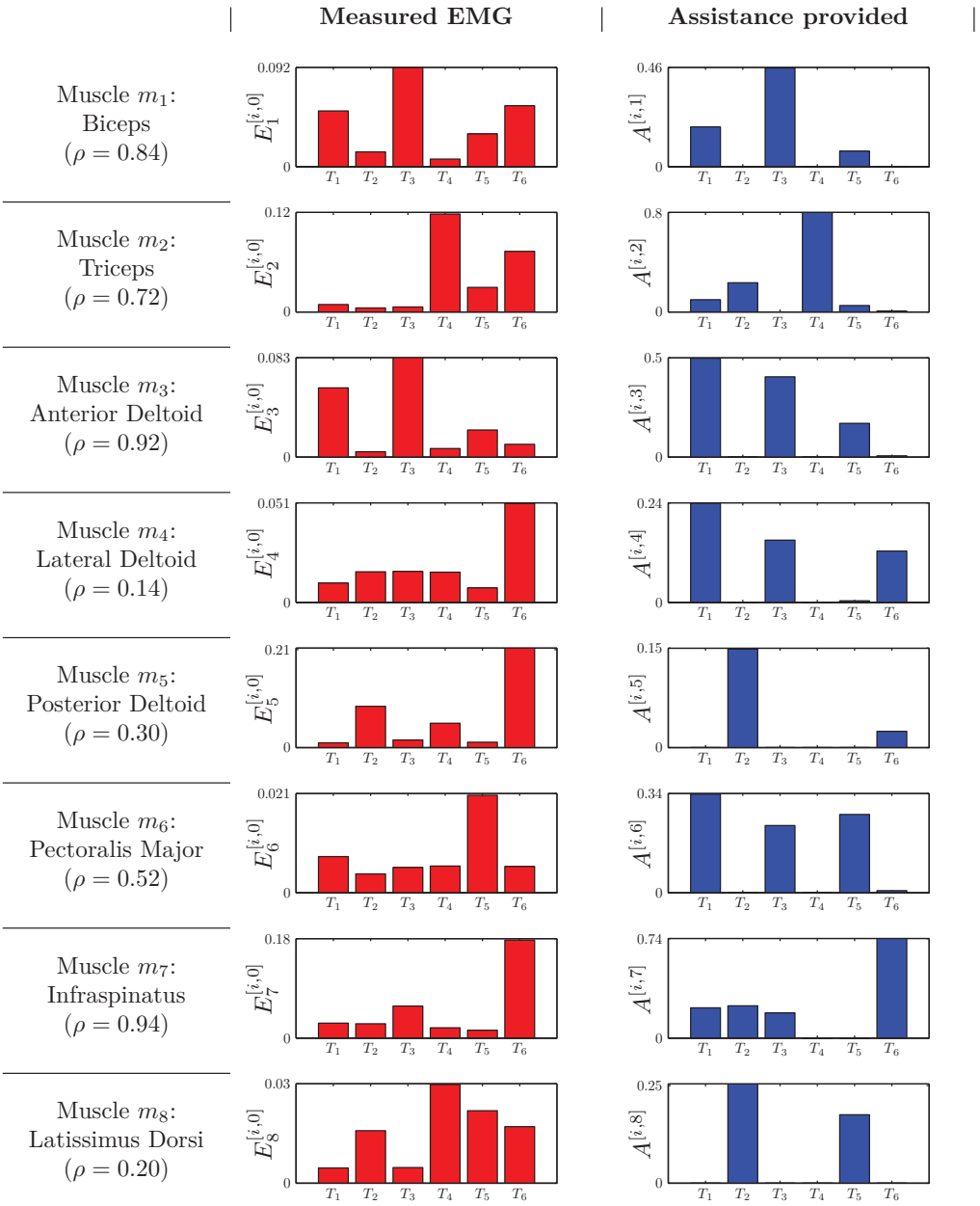

Figure 5.20: Comparison between the assistance provided by the AAN paradigm ($A^{[i,j]}$) with muscle m impaired, and EMG for that same muscle measured with no assistance provided ($E_m^{[i,j]}$). Each plot show the results obtained in each experimental task (T_1 to T_6). Plots are provided with respect to each individual muscle impaired.

muscles produced the lowest correlation results. It is speculated that not considering joint stability when estimating the upper limb strength may be a contributing factor to why these muscles did not achieve as good results as other muscles. Even so, overall the results showed the model-based AAN paradigm was capable of predicting the tasks which would be the most affected by particular muscular impairments, and then providing assistance accordingly.

5.4 Summary

In this chapter the model-based AAN paradigm was implemented on a robotic exoskeleton platform for experimental evaluation. The robot assisted a healthy subject as they performed a number of tasks involving their upper limb. Although the subject did not have any physical impairments, for the purpose of evaluation a number of various impairment profiles defined at the muscular level were assigned to the subject. The amount of assistance the subject received was determined by the AAN paradigm, based on the task being performed and the muscular impairment applied.

Evaluation was based on the ability of the paradigm to provide assistance targeted towards tasks which rely on the muscles defined as impaired. Using EMG measurements of the subject's muscle activity during the tasks, the reliance of each task on different muscle groups was inferred. This was then correlated to the assistance provided by the AAN paradigm when these same muscles are defined as impaired. The results showed that the paradigm was relatively successful in providing assistance targeted towards tasks requiring the use of impaired muscles. Assistance targeted to individual impaired muscles resulted in positive correlation with respect to all muscles. Most had a correlation greater than 0.5, the largest being 0.94 (infraspinatus) and the lowest being 0.14 (lateral deltoid). The average correlation with respect to all the muscles was 0.574. This was significantly greater than the average when assistance was miss-targeted towards non-impaired muscles, which was -0.143. From the results it is speculated that accounting for shoulder stability will improve the ability of the paradigm to target assistance towards specific upper limb muscles.

Chapter 6

Conclusion

This thesis presented a musculoskeletal model-based Assistance-As-Needed (AAN) paradigm for governing the assistance provided by physically assistive robots. This paradigm allows the assistance requirements of an operator performing upper limb tasks to be predicted without the need for observations, unlike empirical performance-based methods currently used. The integration of a musculoskeletal model (MM) representing the operator allows the influence of physiological factors such as muscular impairments to be analysed with respect to the tasks the operator is performing. This capability is of particular benefit in applications with an emphasis on operator physiology, such as robotic rehabilitation. The paradigm is developed based on a generalisation of AAN, with strength at the hand used as the measure by which the operator's assistance requirements are derived. Models were developed and utilised within the framework to calculate the assistance requirements of an operator performing physical tasks. To estimate the strength of the operator at the hand, an optimisation model was developed to calculate the strength using a publicly available MM of the upper limb. Evaluation of this novel model-based AAN paradigm was performed in both simulation and by implementation on a specially developed robotic exoskeleton, and its ability to provide assistance specific to the requirements of the operator demonstrated.

6.1 Summary of Contributions

6.1.1 A novel model-based AAN framework

A framework for a model-based AAN paradigm is developed to calculate the assistance requirements of an operator performing upper limb tasks. Providing the assistance required by an operator is generalised into the problem of supplementing the gap between the requirements of the task being performed, and the capability of the operator to perform it. The framework is then developed with models used to calculate the operator's assistance requirements based on their strength at the hand. A Task Model (TM) is developed which calculates the strength requirements of the task being performed. A Strength Model (SM) is developed which calculates the strength capability of the operator using a musculoskeletal model representing their upper limb. Using these models the assistance requirements of the operator is gauged, and then subsequently utilised as the basis for governing the assistance provided by a robot. This novel framework allows the changing assistance requirements of an operator to be calculated with respect to the task being performed, without needing empirical observations as is the case when using performance-based AAN methods.

6.1.2 Optimisation model for calculating strength

An optimisation model was developed which utilises parameters from an upper limb MM representing an operator to calculate their strength at the hand. Unlike simpler methods of calculating strength based at the joint level of a model, this method operates at the muscular level and accounts for joint coupling resulting from biarticular muscles. Comparison between the strength calculated with and without considering the effects of joint coupling showed that ignoring such effects influences the strength result. The strength estimation was evaluated by calculating upper limb strength at the hand using a publicly available MM. Strength was calculated and analysed with respect to factors which affect strength including limb position, the direction of force at the hand, and muscular impairment. Outcomes were compared with data obtained from the literature.

Analysis showed that the strength optimisation was capable of calculating upper limb strength behaviours similar to those described in the literature, even through no attempt to fit the MM to match the data was made.

6.1.3 Analysis of physical impairment

A technique for analysing the effects that physical impairment at the muscular level have on the capability to perform physical tasks was developed. The method developed uses a vector to enforce upper bounds on the muscle activations in a MM during strength calculation, limiting their force producing capabilities to mimic impairment. Observing how strength varies in response to different impairment profiles allows the effects of impairments to be analysed. Insight may be gained into how the strength at the hand is affected by the severity of impairment, and by the distribution of the impairment across the muscle space. It also allows insight into which tasks are more affected by specific muscular impairments.

6.1.4 Practical validation on a robotic system

The model-based AAN paradigm has been implemented and demonstrated on a real robotic platform. The paradigm governed the assistance provided by the robot to a subject as various experimental tasks were performed. The subject was assigned virtual impairments isolated to specific muscle groups in the upper limb. The assistance was provided to the subject during numerous tasks, with the paradigm taking into account the impairment they were assigned. Assistance provided to the subject was quantified by their interaction forces at the hand, and their muscle activity measured using EMG. Changes in the measured EMG were correlated to the muscles which were defined as impaired, and hence requiring greater assistance. The results have demonstrated that the model-based AAN paradigm provided assistance specifically targeted to when the subject required it, based on the impairment profile assigned.

6.1.5 Development of a robotic exoskeleton

A robotic upper limb exoskeleton was specially developed for implementing the presented AAN paradigm. It uses an admittance control scheme to assist the operator by supporting a controllable percentage of an external load at the hand. Analysis of a subject's muscle activity as they are assisted by the exoskeleton shows that it is capable of providing a controllable level of assistance. The use of virtual external loads implemented in software to mimic physical external loads is shown to be acceptable for the experimental tasks that are performed, and permits the use of virtual loads to simulate a wide variety of task scenarios. This platform is a valuable tool for research and continues to be used.

6.2 Discussion and Limitations

Using models as the basis for implementing an AAN paradigm can overcome many of the limitations inherent in empirical performance-based paradigms. However, as well as providing a number of benefits, a model-based approach also introduces its own limitations which need to be considered. This section discusses the model-based AAN paradigm and its limitations.

6.2.1 Reliance on the musculoskeletal model

An obvious limitation is that the efficacy of the model-based paradigm relies ultimately on the models being capable of estimating the true assistance requirements of the operator. This is challenging as the human body is a complex system with many factors affecting a person's capability to perform tasks. Musculoskeletal models have been shown to adequately represent the human body and have been successfully applied in numerous clinical applications [Favre *et al.*, 2009]. The particular model used in this thesis has been shown to represent upper limb characteristics such as individual joint strength [Holzbaur *et al.*, 2005], muscle moment-arms [Gatti *et al.*, 2007] and limb stiffness [Hu *et al.*, 2011b] to an adequate accuracy. However as mentioned throughout this

thesis there is significant variation amongst the human population. For a MM to be an accurate representation of an individual it is expected that parameters within the model will need to be adjusted to fit the model to the subject.

Sophisticated models contain numerous parameters which can be utilised for fitting. For example the model used in this work [Holzbaur *et al.*, 2005] contains 50 MTU models, each containing five intrinsic parameters (see Table 2.1) which can be used to scale the models to represent specific muscles and tendons. This alone provides 250 potential parameters for fitting the model. Additionally, modifications can be made to the shapes of the MTU force-length-velocity curves, the MTU paths on the skeleton, the skeletal kinematics, limb inertial properties, and more. Fitting of complex models may be simplified by exploiting common human characteristics, e.g. estimating muscle volume and cross-sectional area from an individual's total muscle volume [Holzbaur *et al.*, 2007b]. Although many factors affect limb strength, a strong correlation between strength and muscle volume suggests a model may be fitted through a reduced set of parameters [Holzbaur *et al.*, 2007a]. For example, adapting the MTU intrinsic maximum isometric force (F_0^m) alone may allow a generic upper limb model to represent a subject's strength at the hand to an accuracy that is adequate for the application.

Methods of adapting models to fit empirically obtained data have been described in the literature. Garner and Pandy [2003] optimised MTU parameters including peak isometric force, optimal muscle-fiber length, and tendon slack lengths for 26 muscle groups of the upper limb. Using a two-phase, nested optimisation procedure and knowledge of muscle volume and the minimum and maximum physiological lengths of the MTUs, parameters were estimated based on comparing the calculated maximum joint torque with the measured torque from subjects [Garner and Pandy, 2003]. Buchanan *et al.* [2005] fitted a lower extremity model using a forward-inverse optimisation method to adapt numerous parameters by minimising the error between recorded and model-predicted movements. These parameters were related to the muscle activation dynamics, muscle optimal lengths, and tendon slack lengths [Buchanan *et al.*, 2005]. Special attention may be given to parameters for which the model's strength is highly sensitive. For example MTU force has been shown to be sensitive to tendon slack length [Fleischer and

Hommel, 2008; Nam and Uhm, 2011]. Fleischer and Hommel [2008] optimised tendon slack lengths for three extensor and three flexor muscles spanning the knee based on measured EMG and joint torque. Nam and Uhm [2011] also optimised tendon slack lengths for five knee extensor muscles using measured knee torque assuming full activation. Manal and Buchanan [2004] developed a numerical method for calculating tendon slack length for a single muscle, based on multiple muscle length measurements.

In this thesis a generic upper limb MM was able to estimate strength at the hand with its qualitative behaviour consistent with empirical data from the literature. This was encouraging as no effort was made to adjust the model as to better fit the data. Fitting the MM to specific subjects is anticipated to improve the efficacy of the model-based AAN paradigm, and hence MM fitting in the context of this AAN paradigm is highlighted for future work and is discussed further in Section 6.3.3. Musculoskeletal modelling continues to be an ongoing area of research, and it is anticipated that as models continue to be developed their accuracy in representing individuals or the human body in general will continue to improve.

6.2.2 Factors other than strength affecting tasks

This work used strength as the metric by which both the task's requirements and the operator's capability are measured. Reasons for using strength were discussed in Section 3.2. The human body is a complex system with many factors other than strength affecting how much assistance an individual requires when performing tasks. For example following a stroke the coordination capabilities of a patient can be impaired [Hogan *et al.*, 2006]. Assistance regimes for robotic rehabilitation have been developed which use motion assistance (rather than force, i.e. strength) as the mechanism by which therapy is based [Hogan *et al.*, 2006]. Depending on the application other factors such as fatigue, joint stability, ergonomic and cognitive factors may also prominently contribute in determining the assistance requirements of an individual. The inclusion of some of these factors into the presented AAN paradigm is an idea for future work, and is discussed further in Section 6.3.2.

6.2.3 Definition of the subject's impairment

A major advantage of the model-based AAN paradigm is, because it incorporates a musculoskeletal model representing the subject, the effect of physiological factors such as impairments on their assistance requirements with respect to tasks can be analysed. Impairments were defined in the muscle space of the subject by setting constraints on the amount each muscle can be neurally activated. Observing the effects such constraints have on the estimated strength of the subject provides insight into how such impairments affect their need for assistance. This requires that a quantitative description of the subject's physical impairment at the muscular level be available. The benefits and technical limitations of fitting musculoskeletal models to individual patients (including their impairment) and then using the model to perform optimal treatment has been discussed in the literature [Fregly *et al.*, 2012]. Standardised assessment methods such as the *Fugl-Meyer Assessment* used by physiotherapists to evaluate motor and sensory impairment following a stroke already exist and are commonly used. It is speculated that a standardised assessment method may allow clinicians to quantify the strength of subjects (or lack of) at the muscular level, however the feasibility and accuracy of estimating impairment at the muscular level has yet to be determined.

It is noted that a model of the physiological mechanism which is responsible for the impairment is not required, if the effects of the impairment can be adequately represented as a loss of strength at the muscular level. Specific types of impairment or other physiological factors may not be appropriately simulated by limiting muscle activation as was done in this work, however other approaches may be suitable. For example the effects due to tendon transfer surgery may be simulated by changing the location of the tendon insertion locations [Magermans *et al.*, 2004]. Spasticity may be simulated by incorporating a model of the stretch reflex response to simulate the velocity-dependent effects of the impairment [Koo and Mak, 2006]. The AAN paradigm that was presented permits a wide range of impairments to be simulated due to it containing a model of the musculoskeletal system.

6.2.4 Real time computation

A motivation for designing the model-based AAN framework in a two-level hierarchy was so the computationally expensive calculation of operator strength can be abstracted from the assistive robot's high rate control scheme. Regardless, in the practical implementation it was found that the framework was still unable to be run in real time, since the strength estimation required too much time to compute. Experimental evaluation with the robotic exoskeleton resorted to precalculating the operator's assistance requirements before the tasks were performed. This was acceptable as the subject's limb position and the direction in which strength is calculated was known before hand and remained constant during each task.

The optimisation for calculating strength is a simple linear problem and by itself is quick to compute. An investigation of the calculations involved found that the majority of computational time required was in the calculation of the muscle Jacobian matrix $\mathbf{L}$. Currently all musculoskeletal related calculations are performed using libraries from OpenSim v2.0. Newer versions have since been developed boasting speed improvements in calculations such as muscle moment-arms and dynamics. Implementing the framework with these newer libraries may provide the speed improvements required to run the framework in real time. If not, other means may be employed to quicken the online computation. For example polynomial models representing MTU lengths and moment-arms as functions of generalised coordinates may be created offline using regression techniques [Menegaldo *et al.*, 2004] then used to quickly derive the parameters required for optimisation in real time.

6.3 Future Work

6.3.1 Trials with impaired subjects

The experimental evaluation of the model-based paradigm performed in Chapter 5 involved assisting a healthy subject based on virtual impairments defined in their upper limb. The paradigm was successful in governing the assistance provided by the robot

such that it was targeted towards the tasks which required the subject to utilise muscles defined as impaired. These results are promising and encourage further evaluation of the paradigm and its ability to estimate the assistance requirements of different individuals. Further evaluation of the paradigm's efficacy in predicting the effects of physical impairment requires empirical data from real impaired participants. Future work involving trials with participants that have real impairments is intended to broaden the evaluation of the model-based paradigm.

6.3.2 Strength estimation improvement

Efficacy of the AAN paradigm may be improved by considering factors in the estimation of operator strength capability which currently are not considered. An example of one such factor is shoulder joint stability. Studies considering shoulder stability using musculoskeletal models has been described in the literature [Magermans *et al.*, 2004; Steenbrink *et al.*, 2009; van Drongelen *et al.*, 2006]. A stability constraint can be created and included along with the existing constraints during the strength optimisation. It is anticipated that adding this constraint may, in certain cases, reduce the strength estimation result, similar to the way the additional constraints from biarticular muscles was shown to reduce the strength estimated compared to when they were not considered. Implementation of this constraint within the strength capability estimation, and analysis of its effect on the results are planned for future research.

6.3.3 Fitting the MM to individual subjects

The model-based AAN paradigm achieved encouraging results, particularly considering a generic model of the upper limb was used. It is anticipated that fitting the MM to the subject will improve the paradigm's efficacy. As discussed, several methods for fitting models using numerous different techniques have been detailed in the literature. In the work presented, estimated strength at the hand is used to calculate the subject's assistance requirements. Using strength measurements to fit models typically involves adapting the model such that its maximum producible torque about each joint matches

the measured joint strength of a subject. Fitting the MM to the subject based on joint strength is likely to improve the accuracy of the estimated strength at the hand, particularly if the model was a poor representation of the subject to begin with. However within the context of this work which uses strength at the hand, it is logical to also use strength measured at the hand to fit the model to the subject.

A proposed procedure for this is as follows. Firstly the subject's strength at the hand is measured for a specific limb position, measured in numerous directions in the workspace. This is then repeated for a sufficiently large number of different limb positions throughout the work space. Using the MM to be fitted, strength at the hand is estimated using the approach presented in this thesis. Estimated and measured strengths are then compared for equivalent arm positions and directions at the hand. A non-linear optimisation procedure recursively adapts select parameters within the MM to minimise the error between the measured and estimated strength at the hand.

This proposed approach to fitting the model has several potential benefits within the context of the work in this thesis. Firstly since the same form of strength (i.e at the hand, as opposed to about the joints) is used to fit the model as is later used in the AAN paradigm, strength estimates made after fitting may be more accurate to the empirical data, particularly near the limb positions and force directions for which strength measurements were used for fitting. Secondly, factors that affect strength at the joints are inherently included in the strength measured at the subject's hand. This includes factors such as the limb's pose, and joint coupling due to biarticular muscles. These same effects are also included when using the MM to estimate strength at the hand when fitting is performed. However when fitting based on joint strength, such effects may not be consistent in both the empirically measured and MM estimated strengths. For example elbow strength can significantly vary with shoulder flexion [Winters and Kleweno, 1993], hence if both the subject and the MM were not in identical limb positions when elbow strength was measured and estimated, then the fitting would be skewed.

It is not known how many measurements would be required to adequately fit the model. If it is a large number then the effort in obtaining them may be comparable to

an empirical approach where the subject's assistance needs are estimated by measuring their performance during numerous tasks. Even so, the model-based method is more powerful as it has the capability of predicting assistance need for tasks which the model was not fitted with. Future work is needed to investigate this method of fitting the MM to individuals, and the resulting effect it has on the efficacy of the model-based AAN paradigm.

6.3.4 Hybrid model-empirical AAN paradigm

In the literature exists examples of robotic systems utilising empirical performance-based methods to implement the AAN paradigm [Emken *et al.*, 2005; Kim *et al.*, 2010; Krebs *et al.*, 2003; Wolbrecht *et al.*, 2007]. These systems critique the operator during tasks to create a performance measure, which is then used to adapt the assistance the robot provides. For example the Active Leg Exoskeleton (ALEX) assists the lower limbs of a subject as they walk on a treadmill [Kim *et al.*, 2010]. As the subject walks their foot trajectory is compared to a predefined *healthy* trajectory. Assistance is provided by supplying a compliant force to the leg which encourages the foot towards the desired footpath. The error between the actual and desired trajectories is used to control the magnitude of assistive force the robot provides.

Using a subject's performance to control assistance is convenient in that for many tasks a suitable performance metric indicative of their assistance needs can be calculated. A limitation is that numerous observations are required before an estimate of these needs can be derived. Furthermore assistance can only be estimated for the specific tasks observed. The model-based AAN paradigm presented in this thesis overcomes many of these limitations. However since their assistance requirements are derived from a model, it is essential that the model be capable of adequately estimating the capabilities of the operator. As was discussed, methods of improving this estimation by fitting the model to the individual and making it a better representation of their physical capabilities can be performed. This requires that empirical measurements of the operator are available which the model can be fitted to.

These two approaches (empirical and model-based) have opposing advantages and limitations. An idea deserving further research is the combination of the model-based AAN with current empirical methods. Using the model-based AAN paradigm, an assistive robot may provide assistance to an operator. Simultaneously, as tasks are performed the performance of the operator is observed. Quantitative data representing the capabilities of the operator are recorded, for example the forces expressed at the hand measured by a force/torque sensor. As measurements are accumulated over time, the musculoskeletal model may be repeatedly fitted to match the operator's observed performance. Ideally the model would converge over time to become an accurate representation of the operator's physiological capabilities, improving the accuracy of the subsequent calculations made utilising the model.

This proposed hybrid approach introduces a number of new challenges. Methods for adapting the musculoskeletal model based on the operator's observed performance need to be researched. In the example of the ALEX robot, this would require the subject's error in following the desired foot trajectory to be mapped to its physiological causation, and then adapting the musculoskeletal model to represent this. This also requires the ability to identify the error due to actual impairment, as opposed to voluntary error by the subject. Similar methods for the reverse procedure, using the musculoskeletal model to estimate the assistance required to follow the foot trajectory, also need to be created.

Despite the challenges, this hybrid approach provides a number of significant benefits. In the ALEX example, the musculoskeletal model would be fitted to the subject during the walking exercise. However once an adequately accurate musculoskeletal model is available it could also be used to estimate assistance need in different types of tasks, for example as the subject transitions between sitting and standing, or during running. Additionally, since representation of the operator's capability is physiologically relevant, the model may be used as a tool by physiotherapists to observe the severity of a patient's impairment, how this impairment is distributed across their muscles, track impairment over time and plan therapy accordingly. Such information would also provide motivation for a patient during rehabilitation.

Appendix

A Upper Limb Musculoskeletal Model

The musculoskeletal model used in this thesis to estimate human strength is the publicly available model of the upper limb created by Holzbaur *et al.* [2005]. This model consists of 15 degrees of freedom and 50 MTU models.

A.1 Reduction to four degrees of freedom

To reduce computational complexity the upper limb model was reduced to the 4 joints of the shoulder and elbow. Remaining joints were effectively disabled by ignoring them in any calculations. Table A.1 lists the generalised coordinates in the model, and if they were or were not utilised during analysis.

MTUs which do not produce torque about these 4 joints were also ignored in any calculation. This reduced the effective number of MTUs from 50 down to 37. This greatly reduced the computational time required for calculations, in particular the calculation of the muscle Jacobian $\mathbf{L}$. Table A.2 lists the MTUs that did not span the shoulder and elbow joints, and hence were not utilised. Alternatively, listed in Table A.3 are the MTUs that did span the shoulder and elbow, and hence were utilised.

Coordinate name	Utilised in model?
elv_angle	Yes
shoulder_elv	Yes
shoulder_rot	Yes
elbow_flexion	Yes
pro_sup	No
deviation	No
flexion	No
cmc_flexion	No
cmc_abduction	No
mp_flexion	No
ip_flexion	No
2mcp_flexion	No
2mcp_abduction	No
2pm_flexion	No
2md_flexion	No

Table A.1: List of the generalised coordinates in the upper limb musculoskeletal model [Holzbaur *et al.*, 2005]. Details regarding which coordinates were utilised during analysis, and which were ignored are listed.

MTU number	Label	Name
19	SUP	Supinator
31	PQ	Pronator quadratus
34	FDSM	Flexor digitorum superficialis
35	FDSI	Flexor digitorum superficialis
36	FDPL	Flexor digitorum profundus
37	FDPR	Flexor digitorum profundus
38	FDPM	Flexor digitorum profundus
39	FDPI	Flexor digitorum profundus
45	EIP	Extensor indicis propius
46	EPL	Extensor pollicis longus
47	EPB	Extensor pollicis brevis
48	FPL	Flexor pollicis longus
49	APL	Abductor pollicis longus

Table A.2: List of MTUs that are *not* utilised in the upper limb musculoskeletal model [Holzbaur *et al.*, 2005].

MTU number	Label	Name
0	DELT1	Anterior deltoid
1	DELT2	Lateral deltoid
2	DELT3	Posterior deltoid
3	SUPSP	Supraspinatus
4	INFSP	Infraspinatus
5	SUBSC	Subscapularis
6	TMIN	Teres minor
7	TMAJ	Teres major
8	PECM1	Pectoralis major clavicle
9	PECM2	Pectoralis major sternum
10	PECM3	Pectoralis major ribs
11	LAT1	Latissimus dorsi Tvert
12	LAT2	Latissimus dorsi Lvert
13	LAT3	Latissimus dorsi Iliac
14	CORB	Coracobrachialis
15	TRIlong	Triceps brachii long
16	TRIlat	Triceps brachii lat
17	TRImed	Triceps brachii med
18	ANC	Anconeus
20	BIClong	Biceps long
21	BICshort	Biceps short
22	BRA	Brachialis
23	BRD	Brachioradialis
24	ECRL	Extensor carpi radialis long
25	ECRB	Extensor carpi radialis brev
26	ECU	Extensor carpi ulnaris
27	FCR	Flexor carpi radialis
28	FCU	Flexor carpi ulnaris
29	PL	Palmaris longus
30	PT	Pronator teres
32	FDSL	Flexor digitorum superficialis
33	FDSR	Flexor digitorum superficialis
40	EDCL	Extensor digitorum communis
41	EDCR	Extensor digitorum communis
42	EDCM	Extensor digitorum communis
43	EDCI	Extensor digitorum communis
44	EDM	Extensor digiti minimi

Table A.3: List of MTUs that are utilised in the upper limb musculoskeletal model [Holzbaur *et al.*, 2005].

A.2 Upper limb mass and inertia properties

The upper limb musculoskeletal model [Holzbaur *et al.*, 2005] used in this thesis is not provided with mass or inertial properties assigned. However performing dynamic analyses requires inertial properties to be known. Such properties are obtained from the literature. The body segment mass and centre of mass are calculated using anthropometric equations from Winter [1990] for the average male height and weight (1.75m and 78kg [Gordon *et al.*, 1989]). Principal moments of inertia (Ixx, Iyy, Izz) are taken from Chandler *et al.* [1975].

Mass and inertial properties are assigned to the following upper limb body segments; *upper arm*, *forearm*, and *hand*. In the MM by Holzbaur *et al.* [2005] these segments correspond to the bodies labelled as; *humerus*, *radius*, and *capitate*, respectively. The musculoskeletal modelling software suite OpenSim [Delp *et al.*, 2007] requires every body in the musculoskeletal system to have assigned non-zero inertial properties to perform dynamic analyses. Therefore remaining bodies are assigned negligible mass and inertial values (1×10^{-8}).

	Upper arm	**Forearm**	**Hand**
Body label in MM	*Humerus*	*Radius*	*Capitate*
Centre of Mass (m)	[0,-0.142,0]	[0,-0.110,0]	[0,-0.0940,0]
Segment Mass (kg)	2.184	1.248	0.468
Ixx (kg-m^2)	0.01330	0.00669	0.000615
Iyy (kg-m^2)	0.00220	0.00088	0.000215
Izz (kg-m^2)	0.01327	0.00645	0.000754

Table A.4: Mass and inertial properties assigned to the upper limb musculoskeletal model.

A.3 Upper limb impairment consistent with stroke

		Impairment profiles				
MTU	**ART**	$\mathbf{s}_0$	$\mathbf{s}_1$	$\mathbf{s}_2$	$\mathbf{s}_3$	$\mathbf{s}_4$
DELT1	SE	1	0.582	0.441	0.300	0.159
DELT2	AB	1	0.577	0.434	0.291	0.148
DELT3	SE	1	0.582	0.441	0.300	0.159
SUPSP	AB	1	0.577	0.434	0.291	0.148
INFSP	ER	1	0.453	0.326	0.198	0.071
SUBSC	IR	1	0.641	0.494	0.347	0.199
TMIN	ER	1	0.453	0.326	0.198	0.071
TMAJ	SE	1	0.582	0.441	0.300	0.159
PECM1	AB	1	0.577	0.434	0.291	0.148
PECM2	AB	1	0.577	0.434	0.291	0.148
PECM3	AB	1	0.577	0.434	0.291	0.148
LAT1	SE	1	0.582	0.441	0.300	0.159
LAT2	SE	1	0.582	0.441	0.300	0.159
LAT3	SE	1	0.582	0.441	0.300	0.159
CORB	AB	1	0.577	0.434	0.291	0.148
TRIlong	SE	1	0.582	0.441	0.300	0.159
TRIlat	EE	1	0.601	0.440	0.279	0.119
TRImed	EE	1	0.601	0.440	0.279	0.119
ANC	EE	1	0.601	0.440	0.279	0.119
BIClong	EF	1	0.500	0.364	0.228	0.092
BICshort	EF	1	0.500	0.364	0.228	0.092
BRA	EF	1	0.500	0.364	0.228	0.092
BRD	EF	1	0.500	0.364	0.228	0.092
ECRL	EF	1	0.500	0.364	0.228	0.092
ECRB	EE	1	0.601	0.440	0.279	0.119
ECU	EE	1	0.601	0.440	0.279	0.119
FCR	EF	1	0.500	0.364	0.228	0.092
FCU	EF	1	0.500	0.364	0.228	0.092
PL	EF	1	0.500	0.364	0.228	0.092
PT	EF	1	0.500	0.364	0.228	0.092
FDSL	EF	1	0.500	0.364	0.228	0.092
FDSR	EF	1	0.500	0.364	0.228	0.092
EDCL	WE	1	0.450	0.308	0.166	0.024
EDCR	WE	1	0.450	0.308	0.166	0.024
EDCM	WE	1	0.450	0.308	0.166	0.024
EDCI	WE	1	0.450	0.308	0.166	0.024
EDM	EE	1	0.601	0.440	0.279	0.119

Table A.5: MTU impairment profiles based on the study of stroke patients [Bohannon and Andrews, 1987]. Each MTU corresponds to a muscle in the upper limb model [Holzbaur *et al.*, 2005]. For each MTU, its major articulation (ART) is determined as either; elbow flexion (EF), elbow extension (EE), shoulder internal rotation (IR), shoulder external rotation (ER), shoulder extension (SE), shoulder abduction (AB). Four different impairment profiles, each with different impairment severity are created. Each profile defines values in the $\mathbf{s}$ vector to replicate impairment by limiting muscle activation. Note: MTUs in the MM which do not span the shoulder or elbow are not listed, as these joints (i.e. wrist, fingers) were not of interest.

B Strength Capability Calculation with Uncoupled Joint Simplification

The following is the method used in Chapter 3 to calculate the strength at the hand of the human operator using a musculoskeletal model. It is simpler than the method developed and evaluated later in Chapter 4 since it analyses the joints in the model independently when calculating limb strength. As a result, effects such as joint coupling from biarticular muscles are not considered.

As described in Section 3.4, the strength at the hand is calculated in a direction defined by the unit vector $\mathbf{u}$, and with the limb having a motion defined by the generalised coordinates $\mathbf{q}$, their velocity $\dot{\mathbf{q}}$, and acceleration $\ddot{\mathbf{q}}$. With this defined, the strength is calculated as the maximum magnitude of external force which the limb can oppose at the hand. To calculate this the dynamic equation of the musculoskeletal system is used, which was introduced in Section 2.3.5 and is repeated here for convenience:

$$\mathbf{H}\ddot{\mathbf{q}} + \mathbf{C} + \boldsymbol{\tau}^G = \boldsymbol{\tau}^M + \boldsymbol{\tau}^E$$

The external torque $\boldsymbol{\tau}^E$ results from the external force $\mathbf{u} \cdot F^E$ applied to the hand of the upper limb. This is expressed as $\boldsymbol{\tau}^E = [\mathbf{J}_v]^T \mathbf{u} \cdot F^E$ as was detailed in Section 2.3.4. The muscular torque $\boldsymbol{\tau}^M$ is the result of muscle forces acting about the joints in the limb. This is expressed as $\boldsymbol{\tau}^M = [-\mathbf{L}]^T \mathbf{f}$, where $\mathbf{f}$ is the column vector of MTU forces as was detailed in Section 2.3.3. The result is the following dynamic equation:

$$\mathbf{H}\ddot{\mathbf{q}} + \mathbf{C} + \boldsymbol{\tau}^G = [-\mathbf{L}]^T \mathbf{f} + [\mathbf{J}_v]^T \mathbf{u} \cdot F^E$$

For convenience this equation is rearranged by combining the dynamic and gravitational loads into vector $\boldsymbol{\tau}^B = \mathbf{H}\ddot{\mathbf{q}} + \mathbf{C} + \boldsymbol{\tau}^G$, and combining the terms $[\mathbf{J}_v]^T$ and $\mathbf{u}$ into $\mathbf{r} = [\mathbf{J}_v]^T \mathbf{u}$. The result is the following dynamic equation:

$$\boldsymbol{\tau}^B = [-\mathbf{L}]^T\mathbf{f} + \mathbf{r} \cdot F^E$$

This method of calculating strength considers joints as being independent. Each row in this dynamic equation corresponds to a single joint in the musculoskeletal system. To analyse a single joint, a single row of this equation is analysed individually. If the i-th joint is being considered, then the i-th row of this dynamic equation is extracted to produce the following expression:

$$\tau_i^B = [-\mathbf{L}_i]^T\mathbf{f} + r_i \cdot F^E$$

The term τ_i^B is the i-th element in vector $\boldsymbol{\tau}^B$. The term r_i is the i-th element in vector $\mathbf{r}$. The term $\mathbf{L}_i$ is a vector, created by taking the i-th column of the Jacobian matrix $\mathbf{L}$.

From this equation, the strength of the operator (with respect to the i-th joint) can be found by calculating the maximum magnitude of the external force (F^E) which can be opposed. The equation is rearranged into the following form:

$$F^E = \frac{\tau_i^B}{r_i} + \frac{[\mathbf{L}_i]^T}{r_i}\mathbf{f}$$

The strength of the operator is calculated by determining the MTU forces which maximise F^E. The elements in the vector $\mathbf{f}$ are the forces that each MTU is producing, which subsequently produces torque at the joints and contributes to opposing the external force at the hand. The calculation of the forces produced by the MTU models was detailed in Section 2.3.1. The force produced by the j-th MTU in a musculoskeletal system consisting of m MTU models is represented here as f_j^M. This force is a function of the muscle's activation, which is represented as a_j. Activation ranges from $0 \leq a \leq 1$, where $a = 0$ represents the muscle being totally inactivated, and $a = 1$ represents the muscle being fully utilised to produce active force output. Using this representation, the MTU force vector $\mathbf{f}$ is rewritten as follows:

$$\mathbf{f} = [\ f_1^M(a_1),\ f_2^M(a_2),\ \cdots\ ,\ f_m^M(a_m)\ ]^T$$

The forces produced by the MTU models contribute either positively or negatively to opposing the external force. The MTU forces in the $\mathbf{f}$ vector are always positive, so whether or not a specific MTU contributes positively to opposing the external force is determined by if $\frac{\mathbf{L}_{ji}}{r_i} > 0$. The term $\mathbf{L}_{ji}$ is the element in the i-th column and in the j-th row of the Jacobian matrix $\mathbf{L}$. MTU models which are determined to have a positive contribution should be fully utilised (i.e. $a = 1$) to oppose the external force at the hand. Alternatively, the remaining MTU models should be utilised as little as possible (i.e. $a = 0$). Still considering the i-th joint independently, the strength of the operator is found using the following equation.

$$\max[F^E]_i = \frac{\tau_i^B}{r_i} + \sum_{j=1}^{m} \left[\ \frac{\mathbf{L}_{ji}}{r_i} \cdot f_j^M(a_j)\ \right] \begin{cases} a_j = 1, & \text{for } \frac{\mathbf{L}_{ji}}{r_i} > 0 \\ a_j = 0, & \text{for } \frac{\mathbf{L}_{ji}}{r_i} \leq 0 \end{cases}$$

The result of $\max[F^E]_i$ is the calculated strength at the hand, only considering the i-th joint alone. When this is recalculated for the remaining $k-1$ joints the result will be different. With this strength repeatedly calculated with respect to each of the k joints in the limb, the effective strength of the whole limb (considering all of the joints) is limited by the weakest joint. Therefore the operator strength capability S_P is taken as the minimum of the strength values calculated using this equation for all the joints in the upper limb. This is represented as follows:

$$S_P = \min_{i \in \mathbb{N}_1 | i \leq k} \left[\max[F^E]_i \right]$$

This is the method used in Chapter 3 to calculate the strength S_P at the hand of a human with respect to the desired task.

C Water Bottle Inertial Properties

In Section 3.6.3 the inertial loads of a bottle carried in the hand is analysed. The bottle used was filled with water to weigh 0.6kg, had a height of 16cm and a diameter of 6.9cm. Treating it as a cylindrical homogeneous solid object, its mass moment of inertia is calculated for the three axes (z, x, w) shown in the figure below. Axes x and y have equal mass moment of inertia.

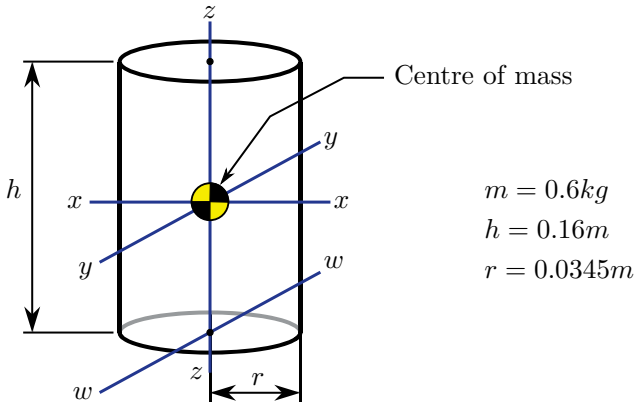

$$I_z = \frac{mr^2}{2} = \frac{0.6 \times 0.0345^2}{2} = 0.000357 \quad \left(\frac{\text{kg} \cdot \text{m}^2}{\text{rad}^2}\right)$$

$$I_x = I_y = \frac{m(3r^2 + h^2)}{12} = \frac{0.6(3 \times 0.0345^2 + 0.16^2)}{12} = 0.001459 \quad \left(\frac{\text{kg} \cdot \text{m}^2}{\text{rad}^2}\right)$$

$$I_w = \frac{m(3r^2 + 4h^2)}{12} = \frac{0.6(3 \times 0.0345^2 + 4 \times 0.16^2)}{12} = 0.005299 \quad \left(\frac{\text{kg} \cdot \text{m}^2}{\text{rad}^2}\right)$$

D Strength Capability Calculation Considering Joint Coupling

The following is the detailed derivation of the objective function and the constraints used in the optimisation model for calculating operator strength presented in Section 4.1.

D.1 Optimisation objective function

The objective function is derived from the MM dynamic Equation (2.15):

$$\mathbf{H\ddot{q}} + \mathbf{C} + \boldsymbol{\tau}^G = \boldsymbol{\tau}^M + \boldsymbol{\tau}^E$$

Substitute in Equations (4.5), (4.6), and (4.14):

$$\boldsymbol{\tau}^B = \mathbf{K}_\tau \mathbf{a} + \boldsymbol{\tau}^P + \mathbf{r} \cdot F^E$$

Extract a single row (the i-th row) depending on Equation (4.19):

$$\tau_i^B = [\mathbf{K}_{\tau i}]\mathbf{a} + \tau_i^P + r_i \cdot F^E$$

$$\text{where,} \quad \mathbf{K}_{\tau i} = \left[\mathbf{K}_{\tau[i,1]}, \mathbf{K}_{\tau[i,2]}, \cdots, \mathbf{K}_{\tau[i,m]}\right]$$

Rearrange into a solution for F^E:

$$F^E = \left[\frac{\tau_i^B - \tau_i^P}{r_i}\right] - \left[\frac{\mathbf{K}_{\tau i}}{r_i}\right]\mathbf{a}$$

Formulate function for finding $S_P = \max[F^E]$:

$$S_P = \max\left[F^E\right] = \max\left[\left[\frac{\tau_i^B - \tau_i^P}{r_i}\right] - \left[\frac{\mathbf{K}_{\tau i}}{r_i}\right]\mathbf{a}\right]$$

Take the constant $\left[\frac{\tau_i^B - \tau_i^P}{r_i}\right]$ term out from the maximisation:

$$S_P = \left[\frac{\tau_i^B - \tau_i^P}{r_i}\right] + \max\left[-\left[\frac{\mathbf{K}_{\tau i}}{r_i}\right]\mathbf{a}\right]$$

Complete the objective function by turning into a minimisation problem:

$$\boxed{S_P = \left[\frac{\tau_i^B - \tau_i^P}{r_i}\right] - \min\left[\frac{\mathbf{K}_{\tau i}}{r_i}\ \mathbf{a}\right]}$$

D.2 Optimisation constraints

The constraints are derived from the MM dynamical Equation (2.15):

$$\mathbf{H\ddot{q}} + \mathbf{C} + \boldsymbol{\tau}^G = \boldsymbol{\tau}^M + \boldsymbol{\tau}^E$$

Substitute in Equations (4.5), (4.6), (4.11) and (4.12):

$$\boldsymbol{\tau}^B = \boldsymbol{\tau}^P + \boldsymbol{\tau}^A + \mathbf{r}\cdot F^E$$

Rearrange and divide each side by the scalar term F^E to produce a proportional relationship:

$$\mathbf{r}\cdot F^E = \boldsymbol{\tau}^B - \boldsymbol{\tau}^A - \boldsymbol{\tau}^P$$
$$\mathbf{r} \propto [\boldsymbol{\tau}^B - \boldsymbol{\tau}^A - \boldsymbol{\tau}^P]$$

Divide each side by their elements in corresponding rows. This normalises each side of the equation, allowing it to be equated. The i-th row, depending on Equation (4.19), is used to normalise to avoid numerical problems when r_i is close to zero:

$$\frac{\mathbf{r}}{r_i} = \frac{\boldsymbol{\tau}^B - \boldsymbol{\tau}^A - \boldsymbol{\tau}^P}{\tau_i^B - \tau_i^A - \tau_i^P}$$

Substitute in the expression for $\boldsymbol{\tau}^A$ in terms of $\mathbf{a}$. The i-th element in $\boldsymbol{\tau}^A$ is expressed by the i-th row of matrix $\mathbf{K}_\tau$.

$$\frac{\mathbf{r}}{r_i} = \frac{\boldsymbol{\tau}^B - \boldsymbol{\tau}^P - \mathbf{K}_\tau \mathbf{a}}{\tau_i^B - \tau_i^P - \mathbf{K}_{\tau i}\mathbf{a}}$$

Then rearrange into the form $\mathbf{Aa} = \mathbf{b}$:

$$\frac{\mathbf{r}}{r_i}\left[\tau_i^B - \tau_i^P - \mathbf{K}_{\tau i}\mathbf{a}\right] = \boldsymbol{\tau}^B - \boldsymbol{\tau}^P - \mathbf{K}_\tau \mathbf{a}$$

$$\frac{\mathbf{r}}{r_i}[\tau_i^B - \tau_i^P] - \frac{\mathbf{r}}{r_i}[\mathbf{K}_{\tau i}\mathbf{a}] = \boldsymbol{\tau}^B - \boldsymbol{\tau}^P - \mathbf{K}_\tau \mathbf{a}$$

$$\mathbf{K}_\tau \mathbf{a} - \frac{\mathbf{r}}{r_i}[\mathbf{K}_{\tau i}\mathbf{a}] = \boldsymbol{\tau}^B - \boldsymbol{\tau}^P - \frac{\mathbf{r}}{r_i}[\tau_i^B - \tau_i^P]$$

$$\left[\mathbf{K}_\tau - \frac{\mathbf{r}}{r_i}\mathbf{K}_{\tau i}\right]\mathbf{a} = \boldsymbol{\tau}^B - \boldsymbol{\tau}^P + \mathbf{r}\left[\frac{\tau_i^P - \tau_i^B}{r_i}\right]$$

From this, expressions for $\mathbf{A}$ and $\mathbf{b}$ are taken:

$$\mathbf{Aa} = \mathbf{b}, \text{ where: } \mathbf{A} = \mathbf{K}_\tau - \frac{\mathbf{r}}{r_i}\mathbf{K}_{\tau i}$$

$$\mathbf{b} = \boldsymbol{\tau}^B - \boldsymbol{\tau}^P + \mathbf{r}\left[\frac{\tau_i^P - \tau_i^B}{r_i}\right]$$

E Robotic Exoskeleton Platform

The following are details of the hardware contained in the robotic exoskeleton that was used for experimentation in Chapter 5.

E.1 Actuation

Actuation is performed using three brushless DC motors (Maxon EC-90). High voltage motors (42V) are used as they have a higher torque to weight ratio compared to the equivalent lower voltage motors. The motors have a flat design resulting in a higher torque output. This allows a gearbox with a reduced gear ratio to be used. A planetary gearbox with ratio 91:1 is used (Maxon GP 52 C). Its low ratio and good efficiency ($\approx$75%) allows the joint to be back-driven by the operator, even when the motor is providing torque to the joint. The maximum torque that can be actuated at each joint is 32 N.m, limited by the rated torque of the gearbox.

Motor controllers (Maxon DEC 70/10 4-Q-EC Amplifier) are used to operate the motors in current-control mode. The controllers are fed the desired motor current, which is calculated based on the desired joint torque and other factors such as the motor's torque/current constant, joint friction, and the ratio and efficiency of the gearbox.

E.2 Sensing

Sensing of the interaction between the robot, the human operator, and the environment is performed using force/torque sensors located at the end-effector of the robot. Two 6-axis ATI Nano25 sensors measure both force and torque in three axes each.

The joint position and velocity of the exoskeleton are measured using a combination of potentiometers and hall effect sensors. The brushless DC motors used to actuate each joint contain hall effect sensors for sensing the motor's position. A microcontroller utilises the hall effect sensor outputs as an encoder to monitor the position of the motor. The derivative of this signal is used to measure the velocity of each joint. When first powered on the robot is unable to determine its position from the hall effect

sensors themselves. Located at each joint are potentiometers which allows the robot to determine its absolute position when first powered.

E.3 xPC Target computer

The exoskeleton's control scheme is operated on a single board computer running the MATLAB xPC Target environment. The target computer operated with a Task-Execution-Time of 0.0015 seconds (666Hz). Specifications of the computer and its data acquisition capabilities are detailed in Table E.1.

Computer Specifications	
Manufacturer	Diamond Systems
Name	Poseidon
Processor	1.0GHz VIA Eden (single core)
RAM	512Mb DDR2
Data Acquisition Specifications	
Analog Inputs	32 single-ended or 16 differential channels
A\D resolution	16 bit
Max sample rate	250kHz

Table E.1: xPC Target computer specifications

F EMG Processing

EMG was measured using the Bagnoli sEMG system from Delsys. Analog output was measured using a 16-bit analog to digital convertor from National Instruments (USB-6210). Data was sampled at 10kHz using MATLAB to acquire and post process the signals. EMG was processed in the following order:

Notch filter A notch (bandstop) filter removed line noise. Two Chebyshev II IIR digital filters were cascaded to remove 50Hz and 100Hz noise. The 50Hz filter had pass and stop band frequencies set to 48/52Hz and 49.5/50.5Hz respectively. The 100Hz filter had pass and stop band frequencies set to 98/102Hz and 99.5/100.5Hz, respectively.

Highpass filter A Butterworth IIR highpass filter with a pass frequency of 20Hz removes DC bias and low frequency artifacts from the signal.

Rectify The signal is rectified and doubled. The doubling is performed to counter the attenuation effect which results from the lowpass filter which is applied afterwards.

Lowpass filter A Butterworth IIR lowpass filter with cutoff frequency of 5Hz smoothes the signal to produce a linear envelope. Zero-phase filtering by processing the signal in both the forward and reverse directions is used to achieve zero phase distortion. This can be performed since filtering is performed in post-processing and not required to be performed online.

F.1 Matlab code

The following is the EMG processing in MATLAB code. Lowpass filtering is performed using the function `filtfilthd` available from:
www.mathworks.com.au/matlabcentral/fileexchange/17061-filtfilthd.

```
% define DAQ frequency (Hz)
fs = 10000;

% 50Hz bandstop filter
d = fdesign.bandstop('Fp1,Fst1,Fst2,Fp2,Ap1,Ast,Ap2',48,49.5,50.5,52,1,60,1,fs);
Hdn1 = design(d,'cheby2');

% 100Hz bandstop filter
d = fdesign.bandstop('Fp1,Fst1,Fst2,Fp2,Ap1,Ast,Ap2',98,99.5,100.5,102,1,60,1,fs);
Hdn2 = design(d,'cheby2');

% 20Hz high pass filter
d = fdesign.highpass('Fst,Fp,Ast,Ap',15,20,30,1,fs);
Hdhp = design(d,'butter');

% 5Hz low pass filter
d = fdesign.lowpass('Fp,Fst,Ap,Ast',3,5,1,30,fs);
Hdlp = design(d,'butter');

% Combine 50Hz and 100Hz notch into single filter
Hdn = dfilt.cascade(Hdn1,Hdn2);


%% Apply processing to EMG data, stored as 'EMG0'
EMG0;                           % Raw EMG signals
EMG1 = filter(Hdn, EMG0);       % EMG after notch filtering
EMG2 = filter(Hdhp,EMG1);       % EMG after highpass filtering
EMG3 = 2*abs(EMG2);             % EMG after rectification
EMG4 = filtfilthd(Hdlp, EMG3);  % EMG after lowpass filtering
```

Bibliography

Ackland, D. C. and Pandy, M. G. (2009). 'Lines of action and stabilizing potential of the shoulder musculature.' *J Anat*, 215(2):184–197. [pp. 161]

Adee, S. (2008). 'Dean Kamen's "Luke arm" prosthesis readies for clinical trials'. *IEEE Spectrum*. [pp. 22]

Ambrose, R. and Diftler, M. (1998). 'The minimum form of strength in serial, parallel and bifurcated manipulators'. In *Robotics and Automation, 1998. Proceedings. 1998 IEEE International Conference on*, volume 2, pages 1334 –1339. [pp. 70]

Amell, T. (2004). 'Shoulder, elbow, and forearm strength'. In S. Kumar, editor, *Muscle Strength*, chapter 12, pages 227–246. CRC Press. [pp. 8, 84, 85, 106, 107, 110]

Amell, T., Kumar, S., Narayan, Y., and Coury, H. (2000). 'Effect of trunk rotation and arm position on gross upper extremity adduction strength and muscular activity'. *Ergonomics*, 43(4):512–27. [pp. 83]

Anderson, F. C. and Pandy, M. G. (2001). 'Dynamic optimization of human walking.' *J Biomech Eng*, 123(5):381–390. [pp. 49]

Arva, J., Buning, M. E., Ambrosio, F., Koontz, A., Cooper, R., and Souza, A. (2004). 'Strength and disability'. In S. Kumar, editor, *Muscle Strength*, chapter 21, pages 485–518. CRC Press. [pp. 8, 33, 88, 106, 114]

Australian Bureau of Statistics (2009). 'Future population growth and ageing'. [pp. 4, 5]

Bai, X., Wei, G., Ye, M., Wang, D., Hu, Y., Liu, Z., Nie, W., Zhang, L., Ji, W., Li, Y., and Wang, C. (2008). 'Finite element musculoskeletal modeling of mechanical virtual human of China'. In *Bioinformatics and Biomedical Engineering, 2008. ICBBE 2008. The 2nd International Conference on*, pages 1847 –1850. [pp. 39]

Baydal-Bertomeu, J. M., Garrido, D., and Mollá, F. (2008). 'Case study: A biomimetric, kinematically compliant knee joint modelled by a four bar linkage'. In J. L. Pons, editor, *Wearable Robots: Biomechatronic Exoskeletons*, pages 74 – 79. John Wiley and Sons, LTD. [pp. 46]

Bertrand, A. M., Mercier, C., Bourbonnais, D., Desrosiers, J., and Gravel, D. (2007). 'Reliability of maximal static strength measurements of the arms in subjects with hemiparesis.' *Clin Rehabil*, 21(3):248–257. [pp. 88]

Bicchi, A., Peshkin, M., and Colgate, J. E. (2008). 'Safety for physical human-robot interaction'. In B. Siciliano and O. Khatib, editors, *Handbook of Robotics*, chapter 57, pages 1335–1348. Springer, Berlin. [pp. 15, 25, 30]

Bicchi, A. and Tonietti, G. (2004). 'Fast and "soft-arm" tactics [robot arm design]'. *Robotics Automation Magazine, IEEE*, 11(2):22 – 33. [pp. 3]

Blemker, S. S., Teran, J., Sifakis, E., Fedkiw, R., and Delp, S. L. (2005). 'Fast 3D muscle simulations using a new quasistatic invertible finite-element algorithm'. *The 10th International Symposium on Computer Simulation in Biomechanics ISCSB*. [pp. 39]

Bohannon, R. W. and Andrews, A. W. (1987). 'Relative strength of seven upper extremity muscle groups in hemiparetic stroke patients'. *Neurorehabilitation and Neural Repair*, 1(4):161–165. [pp. 8, 33, 88, 89, 119, 120, 121, 180]

Brand, R. A., Pedersen, D. R., and Friederich, J. A. (1986). 'The sensitivity of muscle force predictions to changes in physiologic cross-sectional area.' *J Biomech*, 19(8):589–596. [pp. 49]

Brown, M., Tsagarakis, N., and Caldwell, D. (2003). 'Exoskeletons for human force augmentation'. *Industrial Robot: An International Journal*, 30(6):592–602. [pp. 4]

Buchanan, T. S., Lloyd, D. G., Manal, K., and Besier, T. F. (2005). 'Estimation of muscle forces and joint moments using a forward-inverse dynamics model.' *Med Sci Sports Exerc*, 37(11):1911–1916. [pp. 50, 106, 168]

Cai, L. L., Fong, A. J., Otoshi, C. K., Liang, Y., Burdick, J. W., Roy, R. R., and Edgerton, V. R. (2006). 'Implications of assist-as-needed robotic step training after a complete spinal cord injury on intrinsic strategies of motor learning.' *J Neurosci*, 26(41):10564–10568. [pp. 6]

Caldwell, L. S. (1959). 'The effect of the spatial position of a control on the strength of six linear hand movements.' *Rep US Army Med Res Lab*, pages 1–34. [pp. 110]

Canning, C. G., Ada, L., Adams, R., and O'Dwyer, N. J. (2004). 'Loss of strength contributes more to physical disability after stroke than loss of dexterity'. *Clinical Rehabilitation*, 18(3):300–308. [pp. 59]

Chaffin, D. B. and Andersson, G. B. J. (1999). *Occupational Biomechanics*. Wiley & Sons, New York. [pp. 84]

Chaffin, D. B. and Erig, M. (1991). 'Three-dimensional biomechanical static strength prediction model sensitivity to postural and anthropometric inaccuracies'. *IIE Transactions*, 23(3):215–227. [pp. 59, 84]

Chandler, R. F., Clauser, C. E., McConville, J. T., Reynolds, H. M., and Young, J. W. (1975). 'Investigation of inertial properties of the human body'. Technical report, U.S Department of Transportation. [pp. 69, 179]

Chao, E. Y. and Morrey, B. F. (1978). 'Three-dimensional rotation of the elbow.' *J Biomech*, 11(1-2):57–73. [pp. 46]

Chiaverini, S. and Sciavicco, L. (1993). 'The parallel approach to force/position control of robotic manipulators'. *Robotics and Automation, IEEE Transactions on*, 9(4):361 –373. [pp. 26]

Chung, W., Fu, L.-C., and Hsu, S.-H. (2008). 'Motion control'. In B. Siciliano and O. Khatib, editors, *Handbook of Robotics*, chapter 6, pages 133–159. Springer, Berlin. [pp. 25, 136]

Chéze, L., Gutierrez, C., Marcelino, R., and Dimnet, J. (1996). 'Biomechanics of the upper limb

using robotic techniques'. *Human Movement Science*, 15(3):477 – 496. [pp. 46]

Colgate, J., Peshkin, M., and Klostermeyer, S. (2003). 'Intelligent assist devices in industrial applications: a review'. In *Intelligent Robots and Systems, 2003. (IROS 2003). Proceedings. 2003 IEEE/RSJ International Conference on*, volume 3, pages 2516 – 2521 vol.3. [pp. 4, 15, 16, 29]

Collins, J. J. (1995). 'The redundant nature of locomotor optimization laws.' *J Biomech*, 28(3):251–267. [pp. 49]

Coote, S., Murphy, B., Harwin, W., and Stokes, E. (2008). 'The effect of the GENTLE/s robot-mediated therapy system on arm function after stroke.' *Clin Rehabil*, 22(5):395–405. [pp. 6]

Crowninshield, R. D., Johnston, R. C., Andrews, J. G., and Brand, R. A. (1978). 'A biomechanical investigation of the human hip.' *J Biomech*, 11(1-2):75–85. [pp. 49]

Das, B. and Forde, M. (1999). 'Isometric push-up and pull-down strengths of paraplegics in the workspace: 1. strength measurement profiles'. *Journal of Occupational Rehabilitation*, 9:277–289. [pp. 83]

Das, B. and Wang, Y. (2004). 'Isometric pull-push strengths in workspace: 1. strength profiles.' *Int J Occup Saf Ergon*, 10(1):43–58. [pp. 83]

de Groot, J. H. and Brand, R. (2001). 'A three-dimensional regression model of the shoulder rhythm'. *Clinical Biomechanics*, 16(9):735–743. [pp. 69]

De Luca, C. J. (1997). 'The use of surface electromyography in biomechanics'. *Journal of Applied Biomechanics*, 13(2):135 – 163. [pp. 148]

De Santis, A., Siciliano, B., Deluca, A., and Bicchi, A. (2008). 'An atlas of physical human-robot interaction'. *Mechanism and Machine Theory*, 43(3):253–270. [pp. 3, 25]

Delp, S., Anderson, F., Arnold, A., Loan, P., Habib, A., John, C., Guendelman, E., and Thelen, D. (2007). 'Opensim: Open-source software to create and analyze dynamic simulations of movement'. *Biomedical Engineering, IEEE Transactions on*, 54(11):1940–1950. [pp. 69, 73,

179]

Delp, S. L. and Loan, J. P. (1995). 'A graphics-based software system to develop and analyze models of musculoskeletal structures'. *Computers in Biology and Medicine*, 25(1):21–34. [pp. 44, 45, 46]

Dewald, J. P. and Beer, R. F. (2001). 'Abnormal joint torque patterns in the paretic upper limb of subjects with hemiparesis.' *Muscle Nerve*, 24(2):273–283. [pp. 88]

Dollar, A. and Herr, H. (2008). 'Lower extremity exoskeletons and active orthoses: Challenges and state-of-the-art'. *Robotics, IEEE Transactions on*, 24(1):144 –158. [pp. 4]

Emken, J., Bobrow, J., and Reinkensmeyer, D. (2005). 'Robotic movement training as an optimization problem: designing a controller that assists only as needed'. In *9th International Conference on Rehabilitation Robotics (ICORR), 2005*, pages 307 – 312. [pp. 8, 34, 35, 36, 38, 174]

Emken, J. L., Benitez, R., Sideris, A., Bobrow, J. E., and Reinkensmeyer, D. J. (2007). 'Motor adaptation as a greedy optimization of error and effort'. *Journal of Neurophysiology*, 97(6):3997–4006. [pp. 34, 35]

Engin, A. E. (1980). 'On the biomechanics of the shoulder complex'. *Journal of Biomechanics*, 13(7):575–90. [pp. 46]

Erdemir, A., McLean, S., Herzog, W., and van den Bogert, A. J. (2007). 'Model-based estimation of muscle forces exerted during movements.' *Clin Biomech (Bristol, Avon)*, 22(2):131–154. [pp. 50, 129]

Favre, P., Snedeker, J. G., and Gerber, C. (2009). 'Numerical modelling of the shoulder for clinical applications'. *Philosophical Transactions of the Royal Society A: Mathematical,Physical and Engineering Sciences*, 367(1895):2095–2118. [pp. 49, 161, 167]

Featherstone, R. and Orin, D. E. (2008). 'Dynamics'. In B. Siciliano and O. Khatib, editors, *Handbook of Robotics*, chapter 2, pages 35–65. Springer, Berlin. [pp. 47]

Flandorfer, P. (2012). 'Population ageing and socially assistive robots for elderly persons: The

importance of sociodemographic factors for user acceptance'. *International Journal of Population Research*, 2012:13. [pp. 4]

Flash, T. and Hogan, N. (1985). 'The coordination of arm movements: an experimentally confirmed mathematical model'. *The Journal of Neuroscience*, 5(7):1688–1703. [pp. 34]

Fleischer, C. and Hommel, G. (2008). 'A human–exoskeleton interface utilizing electromyography'. *Robotics, IEEE Transactions on*, 24(4):1552–3098. [pp. 29, 43, 51, 106, 168, 169]

Forster, E., Simon, U., Augat, P., and Claes, L. (2004). 'Extension of a state-of-the-art optimization criterion to predict co-contraction.' *J Biomech*, 37(4):577–581. [pp. 49]

Fregly, B. J., Boninger, M. L., and Reinkensmeyer, D. J. (2012). 'Personalized neuromusculoskeletal modeling to improve treatment of mobility impairments: a perspective from european research sites.' *J Neuroeng Rehabil*, 9:18. [pp. 170]

Fung, M., Kato, S., Barrance, P. J., Elias, J. J., McFarland, E. G., Nobuhara, K., and Chao, E. Y. (2001). 'Scapular and clavicular kinematics during humeral elevation: a study with cadavers.' *J Shoulder Elbow Surg*, 10(3):278–285. [pp. 46]

Gallagher, S., Moore, J. S., and Stobbe, T. J. (2004). 'Isometric, isoinertial, and psychophysical strength testing: Devices and protocols'. In S. Kumar, editor, *Muscle Strength*, chapter 8, pages 129–156. CRC Press. [pp. 96]

Garner, B. A. and Pandy, M. G. (2000). 'The obstacle-set method for representing muscle paths in musculoskeletal models'. *Computer Methods in Biomechanics and Biomedical Engineering*, 3:1–30. [pp. 44]

Garner, B. A. and Pandy, M. G. (2001). 'Musculoskeletal model of the upper limb based on the visible human male dataset'. *Computer Methods in Biomechanics and Biomedical Engineering*, 4(2):93–126. [pp. 68, 106]

Garner, B. A. and Pandy, M. G. (2003). 'Estimation of musculotendon properties in the human upper limb.' *Ann Biomed Eng*, 31(2):207–220. [pp. 168]

Gatti, C. J., Dickerson, C. R., Chadwick, E. K., Mell, A. G., and Hughes, R. E. (2007). 'Com-

parison of model-predicted and measured moment arms for the rotator cuff muscles'. *Clinical Biomechanics*, 22(6):639 – 644. [pp. 68, 82, 167]

Gordon, C. C., Churchill, T., Clauser, C. E., Bradtmiller, B., McConville, J. T., Tebbetts, I., and Walker, R. A. (1989). '1988 anthropometric survey of U.S. army personnel: Summary statistics interim report'. Technical report, United States Army Natick Research, Development and Engineering Centre, Yellow Springs, Ohio. [pp. 69, 179]

Guthart, G. and Salisbury, J., J.K. (2000). 'The Intuitive™ telesurgery system: overview and application'. In *Robotics and Automation, 2000. Proceedings. ICRA '00. IEEE International Conference on*, volume 1, pages 618 –621. [pp. 30, 31]

Hagberg, M., Silverstein, B., Wells, R., Smith, M. J., Hendrick, H. W., Carayon, P., and Pérusse, M. (1995). *Work Related Musculoskeletal Disorders (WMSDs): A Reference Book for Prevention*. Taylor and Francis, London. [pp. 84]

Hägele, M., Nilsson, K., and Pires, J. N. (2008). 'Industrial robotics'. In B. Siciliano and O. Khatib, editors, *Handbook of Robotics*, chapter 42, pages 963 – 986. Springer. [pp. 2, 25]

Happee, R. and der Helm, F. C. V. (1995). 'The control of shoulder muscles during goal directed movements, an inverse dynamic analysis.' *J Biomech*, 28(10):1179–1191. [pp. 49]

Hartsell, H. D., Hubbard, M., and Van Os, P. (1995). 'Isokinetic strength evaluation of wrist pronators and supinators: Implications for clinicians'. *Physiotherapy Canada*, 47(4):252–257. [pp. 84]

Heidenreich, P. A., Trogdon, J. G., Khavjou, O. A., Butler, J., Dracup, K., Ezekowitz, M. D., Finkelstein, E. A., Hong, Y., Johnston, S. C., Khera, A., Lloyd-Jones, D. M., Nelson, S. A., Nichol, G., Orenstein, D., Wilson, P. W. F., and Woo, Y. J. (2011). 'Forecasting the future of cardiovascular disease in the United States: a policy statement from the American Heart Association.' *Circulation*, 123(8):933–944. [pp. 6]

Hesse, S., Werner, C., Pohl, M., Rueckriem, S., Mehrholz, J., and Lingnau, M. L. (2005). 'Computerized arm training improves the motor control of the severely affected arm after stroke: a single-blinded randomized trial in two centers.' *Stroke*, 36(9):1960–1966. [pp. 6]

Hidler, J., Nichols, D., Pelliccio, M., Brady, K., Campbell, D. D., Kahn, J. H., and Hornby, T. G. (2009). 'Multicenter randomized clinical trial evaluating the effectiveness of the lokomat in subacute stroke.' *Neurorehabil Neural Repair*, 23(1):5–13. [pp. 6]

Hill, A. V. (1938). 'The heat of shortening and the dynamic constants of muscle'. In *Proceedings of the Royal Society of London. Series B, Biological Sciences*, volume 126, pages 136–195. [pp. 39]

Hirzinger, G., Albu-Schaffer, A., Hahnle, M., Schaefer, I., and Sporer, N. (2001). 'On a new generation of torque controlled light-weight robots'. In *Proceedings 2001 ICRA. IEEE International Conference on Robotics and Automation*, volume 4, pages 3356– 3363. Inst. of Robotics & Mechatronics, German Aerosp. Center, Wessling, Germany;. [pp. 3, 27]

Hirzinger, G., Sporer, N., Albu-Schaffer, A., Hahnle, M., Krenn, R., Pascucci, A., and Schedl, M. (2002). 'DLR's torque-controlled light weight robot III - are we reaching the technological limits now?' In *Robotics and Automation, 2002. Proceedings. ICRA '02. IEEE International Conference on*, volume 2, pages 1710 – 1716 vol.2. [pp. 3]

Hogan, N. (1985). 'Impedance control: An approach to manipulation: Part I - theory; part II - implementation; part III - applications'. *Journal of Dynamic Systems, Measurement, and Control*, 107(1):1–24. [pp. 26]

Hogan, N. and Krebs, H. I. (2004). 'Interactive robots for neuro-rehabilitation.' *Restor Neurol Neurosci*, 22(3-5):349–358. [pp. 6]

Hogan, N., Krebs, H. I., Rohrer, B., Palazzolo, J. J., Dipietro, L., Fasoli, S. E., Stein, J., Hughes, R., Frontera, W. R., Lynch, D., and Volpe, B. T. (2006). 'Motions or muscles? Some behavioral factors underlying robotic assistance of motor recovery.' *Journal of rehabilitation research and development*, 43(5):605–618. [pp. 7, 33, 59, 127, 169]

Holzbaur, K. R. S., Delp, S. L., Gold, G. E., and Murray, W. M. (2007a). 'Moment-generating capacity of upper limb muscles in healthy adults.' *J Biomech*, 40(11):2442–2449. [pp. 168]

Holzbaur, K. R. S., Murray, W. M., and Delp, S. L. (2005). 'A model of the upper extremity for simulating musculoskeletal surgery and analyzing neuromuscular control'. *Annals of Biomed-*

ical Engineering, 33(6):829–840. [pp. 39, 46, 68, 69, 82, 106, 115, 132, 141, 142, 143, 167, 168, 176, 177, 178, 179, 180]

Holzbaur, K. R. S., Murray, W. M., Gold, G. E., and Delp, S. L. (2007b). 'Upper limb muscle volumes in adult subjects.' *J Biomech*, 40(4):742–749. [pp. 168]

Honda (2009). 'Honda's prototype walking assist devices demonstrated in U.S.' http://www.honda.com/newsandviews/article.aspx?id=4987-en. [pp. 16]

Hornby, T. G., Campbell, D. D., Kahn, J. H., Demott, T., Moore, J. L., and Roth, H. R. (2008). 'Enhanced gait-related improvements after therapist- versus robotic-assisted locomotor training in subjects with chronic stroke: a randomized controlled study.' *Stroke*, 39(6):1786–1792. [pp. 6]

Housman, S. J., Scott, K. M., and Reinkensmeyer, D. J. (2009). 'A randomized controlled trial of gravity-supported, computer-enhanced arm exercise for individuals with severe hemiparesis.' *Neurorehabil Neural Repair*, 23(5):505–514. [pp. 6]

Hu, J., Edsinger, A., Lim, Y.-J., Donaldson, N., Solano, M., Solochek, A., and Marchessault, R. (2011a). 'An advanced medical robotic system augmenting healthcare capabilities - robotic nursing assistant'. In *Robotics and Automation (ICRA), 2011 IEEE International Conference on*, pages 6264 –6269. [pp. 4]

Hu, X., Murray, W. M., and Perreault, E. J. (2011b). 'Muscle short-range stiffness can be used to estimate the endpoint stiffness of the human arm'. *Journal of Neurophysiology*, 105(4):1633–1641. [pp. 68, 82, 167]

Huang, Z., Magnenat Thalmann, N., and Thalmann, D. (1994). 'Interactive human motion control using a closed-form of direct and inverse dynamics'. In *Proceedings of the second Pacific conference on Fundamentals of computer graphics*, Pacific Graphics '94, pages 243–255. World Scientific Publishing Co., Inc., River Edge, NJ, USA. [pp. 46]

Israel, J. F., Campbell, D. D., Kahn, J. H., and Hornby, T. G. (2006). 'Metabolic costs and muscle activity patterns during robotic- and therapist-assisted treadmill walking in individuals with incomplete spinal cord injury.' *Physical therapy*, 86(11):1466–1478. [pp. 34]

Jensen, R. and Davy, D. (1975). 'An investigation of muscle lines of action about the hip: A centroid line approach vs the straight line approach'. *Journal of Biomechanics*, 8(2):103–104, IN1, 105–110. [pp. 44]

Kavraki, L. E. and LaValle, S. M. (2008). 'Motion planning'. In B. Siciliano and O. Khatib, editors, *Handbook of Robotics*, chapter 5, pages 109–131. Springer, Berlin. [pp. 25]

Kawamoto, H., Lee, S., Kanbe, S., and Sankai, Y. (2003). 'Power assist method for HAL-3 using emg-based feedback controller'. In *Systems, Man and Cybernetics, 2003. IEEE International Conference on*, volume 2, pages 1648 – 1653 vol.2. [pp. 4, 18]

Kazerooni, H. (1990). 'Human-robot interaction via the transfer of power and information signals'. *Systems, Man and Cybernetics, IEEE Transactions on*, 20(2):450 –463. [pp. 57, 133]

Kazerooni, H. (1998). 'Human power extender: An example of human-machine interaction via the transfer of power and information signals'. [pp. 6, 28, 29, 30]

Kazerooni, H. (2008). 'Exoskeletons for human force augmentation'. In B. Siciliano and O. Khatib, editors, *Handbook of Robotics*, chapter 33, pages 773–793. Springer, Berlin. [pp. 28]

Kazerooni, H., Houpt, P., and Sheridan, T. (1986a). 'Robust compliant motion for manipulators, part II: Design method'. *Robotics and Automation, IEEE Journal of*, 2(2):93 – 105. [pp. 26]

Kazerooni, H., Sheridan, T., and Houpt, P. (1986b). 'Robust compliant motion for manipulators, part I: The fundamental concepts of compliant motion'. *Robotics and Automation, IEEE Journal of*, 2(2):83 – 92. [pp. 26]

Khatib, O., Warren, J., Sapio, V. D., and Sentis, L. (2004). 'Human-like motion from physiologically-based potential energies'. In J. Lenarčič and C. Galletti, editors, *On Advances in Robot Kinematics*, pages 149 – 163. Kluwer Academic Publishers. [pp. 50]

Kim, S. H., Banala, S. K., Brackbill, E. A., Agrawal, S. K., Krishnamoorthy, V., and Scholz, J. P. (2010). 'Robot-assisted modifications of gait in healthy individuals.' *Exp Brain Res*, 202(4):809–824. [pp. 174]

Koeslag, P. and Koeslag, J. (1993). 'The mechanics of bi-articular muscles'. *South African*

Journal of Science, 89:73–76. [pp. 82, 92]

Konrad, P. (2005). *The ABC of EMG*. Noraxon INC. USA. [pp. 146]

Koo, T. K. and Mak, A. F. (2006). 'A neuromusculoskeletal model to simulate the constant angular velocity elbow extension test of spasticity'. *Medical Engineering & Physics*, 28(1):60 – 69. [pp. 170]

Krebs, H., Hogan, N., Aisen, M., and Volpe, B. (1998). 'Robot-aided neurorehabilitation'. *Rehabilitation Engineering, IEEE Transactions on*, 6(1):75 –87. [pp. 20]

Krebs, H., Palazzolo, J., Dipietro, L., Ferraro, M., Krol, J., Rannekleiv, K., Volpe, B., and Hogan, N. (2003). 'Rehabilitation robotics: Performance-based progressive robot-assisted therapy'. *Autonomous Robots*, 15:7–20. [pp. 8, 20, 34, 35, 36, 37, 57, 77, 174]

Krebs, H., Volpe, B., Palazzolo, J., Fasoli, S., Ferraro, S., Edelstein, L., and Hogan, N. (2001). 'Disturbances of higher level neural control - robotic applications in stroke'. In *Engineering in Medicine and Biology Society, 2001. Proceedings of the 23rd Annual International Conference of the IEEE*, volume 4, pages 4069 – 4074. [pp. 34, 35]

Kumar, S. (2001). 'Theories of musculoskeletal injury causation'. *Ergonomics*, 44(1):17–47. [pp. 4]

Kumar, S. (2004). *Muscle Strength*. CRC Press. [pp. 58, 59, 84]

Kumar, S. and Garand, D. (1992). 'Static and dynamic lifting strength at different reach distances in symmetrical and asymmetrical planes'. *Ergonomics*, 35(7-8):861–880. [pp. 107, 110]

Lannersten, L., Harms-Ringdahl, K., Schüldt, K., and Ekholm, J. (1993). 'Isometric strength in flexors, abductors, and external rotators of the shoulder'. *Clinical Biomechanics*, 8(5):235 – 242. [pp. 84]

Lenarcic, J. and Umek, A. (1994). 'Simple model of human arm reachable workspace'. *Systems, Man and Cybernetics, IEEE Transactions on*, 24(8):1239 –1246. [pp. 46]

Liebesman, J. L. and Cafarelli, E. (1994). 'Physiology of range of motion in human joints: A critical review'. *Critical reviews in physical and rehabilitation medicine*, 6(2):131–160. [pp. 33]

Lin, H.-T., Nakamura, Y., Su, F.-C., Hashimoto, J., Nobuhara, K., and Chao, E. Y. S. (2005). 'Use of virtual, interactive, musculoskeletal system (VIMS) in modeling and analysis of shoulder throwing activity.' *J Biomech Eng*, 127(3):525–530. [pp. 46]

Lloyd-Jones, D., Adams, R. J., Brown, T. M., Carnethon, M., Dai, S., Simone, G. D., Ferguson, T. B., Ford, E., Furie, K., Gillespie, C., Go, A., Greenlund, K., Haase, N., Hailpern, S., Ho, P. M., Howard, V., Kissela, B., Kittner, S., Lackland, D., Lisabeth, L., Marelli, A., McDermott, M. M., Meigs, J., Mozaffarian, D., Mussolino, M., Nichol, G., Roger, V., Rosamond, W., Sacco, R., Sorlie, P., Stafford, R., Thom, T., Wasserthiel-Smoller, S., Wong, N. D., and Wylie-Rosett, J. (2009). 'Heart disease and stroke statistics–2010 update: a report from the American Heart Association'. *Circulation*. [pp. 6, 88]

Lum, P. S., Burgar, C. G., Shor, P. C., Majmundar, M., and der Loos, M. V. (2002). 'Robot-assisted movement training compared with conventional therapy techniques for the rehabilitation of upper-limb motor function after stroke'. *Arch. Phys. Med. Rehabil*, 83:952 – 959. [pp. 6]

Lynch, D., Ferraro, M., Krol, J., Trudell, C. M., Christos, P., and Volpe, B. T. (2005). 'Continuous passive motion improves shoulder joint integrity following stroke.' *Clinical Rehabilitation*, 19(6):594 – 599. [pp. 33]

Lynch, K. M., Liu, C., Sørensen, A., Kim, S., Peshkin, M., Colgate, J. E., Tickel, T., Hannon, D., and Shiels, K. (2002). 'Motion guides for assisted manipulation'. *The International Journal of Robotics Research*, 21(1):27–43. [pp. 7, 32]

Magermans, D., Chadwick, E., Veeger, H., Rozing, P., and van der Helm, F. (2004). 'Effectiveness of tendon transfers for massive rotator cuff tears: a simulation study'. *Clinical Biomechanics*, 19(2):116 – 122. [pp. 170, 172]

Makinson, B. J. (1971). 'Research and development prototype for machine augmentation of human strength and endurance. Hardiman I project'. Technical report, General Electric Company, Schenectady New York, Specialty Materials Handling Products Operation. [pp. 28,

29]

Manal, K. and Buchanan, T. S. (2004). 'Subject-specific estimates of tendon slack length: A numerical method.' *Journal of Applied Biomechanics*, 20(2):195 – 203. [pp. 106, 169]

Marchal-Crespo, L. and Reinkensmeyer, D. J. (2009). 'Review of control strategies for robotic movement training after neurologic injury'. *Journal of NeuroEngineering and Rehabilitation*, 6(1):20. [pp. 33]

Marley, R. J. and Thomson, M. R. (2000). 'Isokinetic strength characteristics in wrist flexion and extension'. *International Journal of Industrial Ergonomics*, 25(6):633–643. [pp. 84]

Martini, F. (2001). *Fundamentals of Anatomy and Physiology*, volume 7th. Prentice Hall. [pp. 39]

Matsumoto, Y., Nishida, Y., Motomura, Y., and Okawa, Y. (2011). 'A concept of needs-oriented design and evaluation of assistive robots based on ICF'. In *Rehabilitation Robotics (ICORR), 2011 IEEE International Conference on*, pages 1 –6. [pp. 58, 60, 71, 77]

Maurel, W. and Thalmann, D. (1999). 'A case study on human upper limb modelling for dynamic simulation'. *Computer Methods in Biomechanics and Biomedical Engineering*, 2(1):65–82. [pp. 39, 44, 46]

Maurel, W., Thalmann, D., Hoffmeyer, P., Beylot, P., Gingins, P., Kalra, P., and Thalmann, N. M. (1996). 'A biomechanical musculoskeletal model of human upper limb for dynamic simulation'. In *in Proceedings of the Eurographics Computer Animation and Simulation Workshop in Poitiers*, pages 121 – 136. Springer-Verlag. [pp. 46, 68]

Mayer, F., Horstmann, T., Röcker, K., Heitkamp, H. C., and Dickhuth, H. H. (1994). 'Normal values of isokinetic maximum strength, the strength/velocity curve, and the angle at peak torque of all degrees of freedom in the shoulder'. *International journal of sports medicine*, 15:S19–S25. [pp. 84]

McCormick, E. (1970). *Human factors engineering*. McGraw-Hill. [pp. 80, 81, 83, 107, 108, 109, 110, 112, 114, 127]

Menegaldo, L. L., de Toledo Fleury, A., and Weber, H. I. (2004). 'Moment arms and musculotendon lengths estimation for a three-dimensional lower-limb model.' *J Biomech*, 37(9):1447–1453. [pp. 171]

Meng, Q. and Lee, M. (2006). 'Design issues for assistive robotics for the elderly'. *Advanced Engineering Informatics*, 20(2):171 – 186. [pp. 4]

Mercier, C. and Bourbonnais, D. (2004). 'Relative shoulder flexor and handgrip strength is related to upper limb function after stroke'. *Clinical Rehabilitation*, 18(2):215–221. [pp. 8, 33, 59, 88, 89]

Morecki, A., Ekiel, J., and Fidelus, K. (1984). *Cybernetic Systems of Limb Movements in Man, Animals and Robots*. Prentice Hall. [pp. 49]

Morris, S. L., Dodd, K. J., and Morris, M. E. (2004). 'Outcomes of progressive resistance strength training following stroke: a systematic review.' *Clinical Rehabilitation*, 18(1):27–39. [pp. 59]

Morse, T., Fekieta, R., Rubenstein, H., Warren, N., Alexander, D., and Wawzyniecki, P. (2008). 'Doing the heavy lifting: health care workers take back their backs'. *New Solut*, 18(2):207–219. [pp. 4]

Nam, Y. and Uhm, H. W. (2011). 'Tendon slack length and its effect on muscle force-generation characteristics.' *Journal of Mechanics in Medicine & Biology*, 11(2):445 – 456. [pp. 106, 169]

National Research Council, Panel on Musculoskeletal Disorders and the Workplace, and Commission on Behavioral and Social Sciences and Education (2001). *Musculoskeletal Disorders and the Workplace : Low Back and Upper Extremities*. National Academies Press, Washington, DC. [pp. 4]

Nef, T., Mihelj, M., Colombo, G., and Riener, R. (2006). 'Armin - robot for rehabilitation of the upper extremities'. In *Robotics and Automation, 2006. ICRA 2006. Proceedings 2006 IEEE International Conference on*, pages 3152 –3157. [pp. 20]

Nieminen, H., Takala, E.-P., Niemi, J., and Viikari-Juntura, E. (1995). 'Muscular synergy in the

shoulder during a fatiguing static contraction.' *Clin Biomech (Bristol, Avon)*, 10(6):309–317. [pp. 49]

Ouellette, M. M., LeBrasseur, N. K., Bean, J. F., Phillips, E., Stein, J., Frontera, W. R., and Fielding, R. A. (2004). 'High-intensity resistance training improves muscle strength, self-reported function, and disability in long-term stroke survivors'. *Stroke*, 35(6):1404–1409. [pp. 59]

Pandy, M. G. (1999). 'Moment arm of a muscle force.' *Exerc Sport Sci Rev*, 27:79–118. [pp. 45, 99]

Patten, C., Dozono, J., Schmidt, S. G., Jue, M. E., and Lum, P. S. (2006). 'Combined functional task practice and dynamic high intensity resistance training promotes recovery of upper-extremity motor function in post-stroke hemiparesis: A case study'. *Journal of Neurologic Physical Therapy*, 30(3):99–115. [pp. 59]

Pedersen, D. R., Brand, R. A., and Davy, D. T. (1997). 'Pelvic muscle and acetabular contact forces during gait.' *J Biomech*, 30(9):959–965. [pp. 49]

Pentland, W., Lo, S., and Strauss, G. (1993). 'Reliability of upper extremity isokinetic torque measurements with the kin-com dynamometer'. *Isokinetics and Exercise Science*, 3(2):88–95. [pp. 84]

Peshkin, M. A., Colgate, J. E., Wannasuphoprasit, W., Moore, C. A., Gillespie, R. B., and Akella, P. (2001). 'Cobot architecture'. *Robotics and Automation, IEEE Transactions on*, 17(4):377–390. [pp. 30]

Pinter, I. J., Bobbert, M. F., van Soest, A. J. K., and Smeets, J. B. J. (2010). 'Isometric torque-angle relationships of the elbow flexors and extensors in the transverse plane.' *J Electromyogr Kinesiol*, 20(5):923–931. [pp. 84]

Pohl, M., Werner, C., Holzgraefe, M., Kroczek, G., Mehrholz, J., Wingendorf, I., Hoölig, G., Koch, R., and Hesse, S. (2007). 'Repetitive locomotor training and physiotherapy improve walking and basic activities of daily living after stroke: a single-blind, randomized multicentre trial (DEutsche GAngtrainerStudie, DEGAS).' *Clin Rehabil*, 21(1):17–27. [pp. 6]

Pons, J. L., editor (2008). *Wearable Robots: Biomechatronic Exoskeletons*. Wiley. [pp. 134, 135]

Pratt, G. and Williamson, M. (1995). 'Series elastic actuators'. In *Intelligent Robots and Systems 95. 'Human Robot Interaction and Cooperative Robots', Proceedings. 1995 IEEE/RSJ International Conference on*, volume 1, pages 399 –406 vol.1. [pp. 3]

Prilutsky, B. and Zatsiorsky, V. (2002). 'Optimization-based models of muscle coordination'. *Exerc Sport Sci Rev*, 30(1):32–8. [pp. 49, 129]

Raasch, C. C., Zajac, F. E., Ma, B., and Levine, W. S. (1997). 'Muscle coordination of maximum-speed pedaling.' *J Biomech*, 30(6):595–602. [pp. 50]

Raibert, M. H. and Craig, J. J. (1981). 'Hybrid position/force control of manipulators'. *Journal of Dynamic Systems, Measurement, and Control*, 103(2):126–133. [pp. 26]

Raikova, R. (1992). 'A general approach for modelling and mathematical investigation of the human upper limb.' *Journal of Biomechanics*, 25(8):857 – 867. [pp. 44]

Raytheon (2012). 'Big arm'. http://www.raytheon.com/businesses/rids/businesses/gis/strategic_solutions/robotics/bigarm/. Accessed: 8/11/2012. [pp. 31]

Riken (2011). 'RIBA-II, the next generation care-giving robot'. Technical report, RIKEN. [pp. 22]

Rocon, E., Belda-Lois, J., Ruiz, A., Manto, M., Moreno, J., and Pons, J. (2007). 'Design and validation of a rehabilitation robotic exoskeleton for tremor assessment and suppression'. *Neural Systems and Rehabilitation Engineering, IEEE Transactions on*, 15(3):367 –378. [pp. 30]

Roman-Liu, D. and Tokarski, T. (2005). 'Upper limb strength in relation to upper limb posture'. *International Journal of Industrial Ergonomics*, 35(1):19–31. [pp. 59, 83]

Rosati, G., Bobrow, J. E., and Reinkensmeyer, D. J. (2008). 'Compliant control of post-stroke rehabilitation robots: Using movement-specific models to improve controller performance'. *ASME Conference Proceedings*, 2008(48630):167–174. [pp. 37]

Rosen, J., Perry, J., Manning, N., Burns, S., and Hannaford, B. (2005). 'The human arm kine-

matics and dynamics during daily activities - toward a 7 dof upper limb powered exoskeleton'. In *Advanced Robotics, 2005. ICAR '05. Proceedings., 12th International Conference on*, pages 532–539. [pp. 61, 88, 91]

Salisbury, J. K. (1980). 'Active stiffness control of a manipulator in cartesian coordinates'. In *Decision and Control including the Symposium on Adaptive Processes, 1980 19th IEEE Conference on*, volume 19, pages 95 –100. [pp. 26]

Sankai, Y. (2011). 'HAL: Hybrid Assistive Limb based on cybernics'. In M. Kaneko and Y. Nakamura, editors, *Robotics Research*, volume 66 of *Springer Tracts in Advanced Robotics*, pages 25–34. Springer Berlin Heidelberg. [pp. 18]

Sapio, V. D., Warren, J., Khatib, O., and Delp, S. (2005). 'Simulating the task-level control of human motion: a methodology and framework for implementation'. *The Visual Computer*, 21(5):289–302. [pp. 43, 99]

Schutte, L., Rodgers, M., Zajac, F., and Glaser, R. (1993). 'Improving the efficacy of electrical stimulation-induced leg cycle ergometry: an analysis based on a dynamic musculoskeletal model'. *Rehabilitation Engineering, IEEE Transactions on*, 1(2):109–125. [pp. 39, 46, 48]

Secoli, R., Milot, M.-H., Rosati, G., and Reinkensmeyer, D. (2011). 'Effect of visual distraction and auditory feedback on patient effort during robot-assisted movement training after stroke'. *Journal of NeuroEngineering and Rehabilitation*, 8:1–10. [pp. 34]

Seireg, A. and Arvikar, R. (1989). *Biomedical Analysis of the Musculoskeletal Structure for Medicine and Sports*. Hemisphere Publishing Corporation. [pp. 39, 44]

Senes, S. (2006). *How We Manage Stroke in Australia*. Cardiovascular disease series. Australian Institute of Health and Welfare. [pp. 5]

Siciliano, B. and Villani, L. (1999). *Robot Force Control*. Kluwer Academic. [pp. 25, 26]

Sparrow, R. and Sparrow, L. (2006). 'In the hands of machines? the future of aged care'. *Minds and Machines*, 16:141–161. [pp. 4]

Steenbrink, F., de Groot, J., Veeger, H., van der Helm, F., and Rozing, P. (2009). 'Glenohumeral

stability in simulated rotator cuff tears'. *Journal of Biomechanics*, 42(11):1740 – 1745. [pp. 95, 161, 172]

Swan, W. (2010). *Australia to 2050: Future Challenges : the 2010 Intergenerational Report*. Intergenerational report. Commonwealth of Australia. [pp. 4]

Takahashi, C. D., Der-Yeghiaian, L., Le, V., Motiwala, R. R., and Cramer, S. C. (2008). 'Robot-based hand motor therapy after stroke.' *Brain*, 131(Pt 2):425–437. [pp. 6]

Taylor, R. H., Menciassi, A., Fichtinger, G., and Dario, P. (2008). 'Medical robotics and computer-integrated surgery'. In B. Siciliano and O. Khatib, editors, *Handbook of Robotics*, chapter 52, pages 1199–1222. Springer, Berlin. [pp. 30]

Thelen, D. G., Anderson, F. C., and Delp, S. L. (2003). 'Generating dynamic simulations of movement using computed muscle control'. *Journal of Biomechanics*, 36(3):321–328. [pp. 39, 48, 50]

Toshev, J. and Raikova, R. (1985). 'An estimation of the method of modeling the direction of muscle forces with straight lines'. In B. Jonsson, editor, *Biomechanics X-B: International Series on Biomechanics*, volume 6B, pages 1089–1093. Human Kinetics, Champaign, IL. [pp. 44]

Toyama, S. and Yamamoto, G. (2009). 'Development of wearable-agri-robot - mechanism for agricultural work'. In *Intelligent Robots and Systems, 2009. IROS 2009. IEEE/RSJ International Conference on*, pages 5801 –5806. [pp. 16]

Toyota (2011). 'TMC shows new nursing and healthcare robots in tokyo'. http://www2.toyota.co.jp/en/news/11/11/1101.html. [pp. 17, 18]

Tresch, M. C. and Jarc, A. (2009). 'The case for and against muscle synergies'. *Current Opinion in Neurobiology*, 19(6):601 – 607. [pp. 59]

Tsunoda, N., O'Hagan, F., Sale, D., and MacDougall, J. (1993). 'Elbow flexion strength curves in untrained men and women and male bodybuilders'. *European Journal of Applied Physiology and Occupational Physiology*, 66(3):235–9. [pp. 84]

Ueda, J., Ming, D., Krishnamoorthy, V., Shinohara, M., and Ogasawara, T. (2010). 'Individual

muscle control using an exoskeleton robot for muscle function testing'. *Neural Systems and Rehabilitation Engineering, IEEE Transactions on*, 18(4):339 –350. [pp. 51]

United Nations. Dept. of Economic and Social Affairs. Population Division (2002). *World Population Ageing, 1950-2050*. Number p. 81 in World Population Ageing, 1950-2050. UN. [pp. 4]

U.S. Department of Health and Human Services (1997). *Musculoskeletal Disorders and Workplace Factors*. 97B141. Cincinnati, OH. [pp. 4]

van der Helm, F. C. (1994). 'A finite element musculoskeletal model of the shoulder mechanism.' *J Biomech*, 27(5):551–569. [pp. 49]

van der Kooij, H., Veneman, J., and Ekkelenkamp, R. (2006). 'Compliant actuation of exoskeletons'. In A. Lazinica, editor, *Mobile Robots: towards New Applications*, chapter 7. InTech. [pp. 27]

van Drongelen, S., van der Woude, L., Janssen, T., Angenot, E., Chadwick, E., and Veeger, H. (2006). 'Glenohumeral joint loading in tetraplegia during weight relief lifting: A simulation study'. *Clinical Biomechanics*, 21(2):128 – 137. [pp. 90, 95, 127, 172]

van Zuylen, E., van Velzen, A., and van der Gon, J. (1988). 'A biomechanical model for flexion torques of human arm muscles as a function of elbow angle'. *Journal of Biomechanics*, 21(3):183 – 190. [pp. 44]

VanSwearingen, J. (1983). 'Measuring wrist muscle strength'. *Journal of Orthopaedic and Sports Physical Therapy*, 4(4):217–228. [pp. 84]

Villani, L. and Schutter, J. D. (2008). 'Force control'. In B. Siciliano and O. Khatib, editors, *Handbook of Robotics*, chapter 7, pages 161–185. Springer, Berlin. [pp. 26, 27]

Walmsley, R. P. and Dias, J. M. (1995). 'Intermachine reliability of isokinetic concentric measurements of shoulder internal and external peak torque'. *Isokinetics and Exercise Science*, 5:75–80. [pp. 84]

Weir, J. P., Wagner, L. L., Housh, T. J., and Johnson, G. O. (1992). 'Horizontal abduction and adduction strength at the shoulder of high school wrestlers across age'. *The Journal of*

orthopaedic and sports physical therapy, 15(4):183–186. [pp. 84]

Weiss, A., Suzuki, T., Bean, J., and Fielding, R. A. (2000). 'High intensity strength training improves strength and functional performance after stroke'. *American Journal of Physical Medicine & Rehabilitation*, 79(4):389–376. [pp. 59]

Whitney, D. E. (1977). 'Force feedback control of manipulator fine motions'. *Journal of Dynamic Systems, Measurement, and Control*, 99(2):91–97. [pp. 26]

Williams, P., Warwick, R., Dyson, M., and Bannister, L. (1989). *Gray's Anatomy*. Churchill Livingstone, Edinburgh. [pp. 92]

Winter, D. A. (1990). *Biomechanics and motor control of human movement*. A Wiley-Interscience publication, Ontario, Canada, 2nd edition. [pp. 69, 179]

Winters, J. M. and Kleweno, D. G. (1993). 'Effect of initial upper-limb alignment on muscle contributions to isometric strength curves.' *J Biomech*, 26(2):143–153. [pp. 84, 173]

Wolbrecht, E., Chan, V., Le, V., Cramer, S., Reinkensmeyer, D., and Bobrow, J. (2007). 'Real-time computer modeling of weakness following stroke optimizes robotic assistance for movement therapy'. In *Neural Engineering, 2007. CNE '07. 3rd International IEEE/EMBS Conference on*, pages 152 –158. [pp. 8, 35, 36, 37, 174]

Wolbrecht, E., Chan, V., Reinkensmeyer, D., and Bobrow, J. (2008). 'Optimizing compliant, model-based robotic assistance to promote neurorehabilitation'. *Neural Systems and Rehabilitation Engineering, IEEE Transactions on*, 16(3):286 –297. [pp. 8, 34, 35, 36, 71]

Yamaguchi, G. T. and Zajac, F. E. (1989). 'A planar model of the knee joint to characterize the knee extensor mechanism'. *Journal of Biomechanics*, 22(1):1 – 10. [pp. 46]

Yamamoto, K., Ishii, M., Noborisaka, H., and Hyodo, K. (2004). 'Stand alone wearable power assisting suit - sensing and control systems'. In *Robot and Human Interactive Communication, 2004. ROMAN 2004. 13th IEEE International Workshop on*, pages 661 – 666. [pp. 4]

Yanagawa, T., Pandy, M. G., Shelburne, K. B., Hawkins, R. J., and Torry, M. R. (2003). 'Estimation of muscle and joint reaction forces at the glenohumeral joint during arm abduction:

A musculoskeletal modeling approach'. In *Proceedings of the 2003 Summer Bioengineering Conference*. Key Biscayne, Florida. [pp. 161]

Yeong, C. F., Melendez-Calderon, A., Gassert, R., and Burdet, E. (2009). 'Reachman: a personal robot to train reaching and manipulation'. In *Intelligent Robots and Systems, 2009. IROS 2009. IEEE/RSJ International Conference on*, pages 4080 –4085. [pp. 79, 124]

Zajac, F. E. (1989). 'Muscle and tendon: properties, models, scaling, and application to biomechanics and motor control'. *Critical reviews in biomedical engineering*, 17(4):359–411. [pp. 39, 41, 42, 43, 48, 99]

Zinn, M., Roth, B., Khatib, O., and Salisbury, J. K. (2004). 'A new actuation approach for human friendly robot design'. *The International Journal of Robotics Research*, 23(4-5):379–398. [pp. 3]